Chiral Proton Catalysis: New Applications in Enantioselective Hetero-Diels-Alder Reactions, Amino Acid Synthesis, and Tetrahydroisoquinoline Alkaloid Synthesis

By

Daniel James Sprague

Dissertation

Submitted to the Faculty of the

Graduate School of Vanderbilt University

in partial fulfillment of the requirements

for the degree of

DOCTOR OF PHILOSOPHY
in

Chemistry

August, 2016
Nashville, Tennessee

Approved:

Jeffrey N. Johnston, Ph.D.
Timothy P. Hanusa, Ph.D.
Janet E. Macdonald, Ph.D.
Ned A. Porter, Ph.D.

To my family, with a multitude of love and an abundance of thanks.
Vita, Amor, et Scientia.

ACKNOWLEDGMENTS

The path to a Ph.D. cannot be traversed alone. It is also made up of more than just the five (or more) years spent in graduate school. It represents the culmination of one's journey through life up to that point, and it influences one's path for the future. With that in mind, there a lot of people who have been involved in the journey to this point, and they all deserve a word of mention and a word of thanks.

First and foremost, I have to thank my parents, Josh and Denise. I have been so fortunate to have them for parents. From a very young age, I had a strong work ethic instilled in me, and a "never-give-up" resilient attitude to go with it. This has paid infinite dividends throughout a sometimes frustrating graduate career, and it is owed directly to them. They've taught me how to succeed in life, and how to find my way and forge my own path in this world. For this, I can never repay them. Their support, to this day, has been a major factor in the completion of this work. I love them infinitely, and could never explain what their unwavering support means.

In the same breath, I have to thank my grandparents Josh and Dolores. Growing up, I spent a lot of time with them after school, and they had a major hand in raising me. I owe them an infinite amount of thanks for driving me to and from all of my music, sports, and science events in middle and high school; for always helping to make sure I had everything I could ever need, and for being a major part of my unwavering support system to help me through hard times. Britt, thank you for your support and love as well. Life would be a lot harder without you in it.

Mr. Brian Mai is owed many thanks, too. Brian was my high school biology teacher and is also a family friend. It was in Brian's class where I first became excited about science. He nurtured this excitement, mentored me through two science fair projects, and embedded the love of science in me for life. I always say that my love of science started because of how passionate he is about science and about learning for the sake of learning. He also is always up for a day-long excursion to Starbucks or Barnes and Noble when I'm back home in New Jersey, which is a nice break from life.

Continuing chronologically in my educational career, Dr. Norito Takenaka deserves to be mentioned here. It was in Norito's lab where I first got my feet wet with organic chemistry research. Norito took me under his wing as a junior in college and personally trained me in his lab. His enthusiasm for science and his enthusiasm for education were both infectious. I have always said that he can make anyone be interested, some way or somehow, in organic chemistry. He fostered my (newfound) love for organic chemistry, guided me toward some exciting and brand new science in his lab, and eventually he was the one who influenced me to go to graduate school in organic chemistry. Even now, years later, he is still a great mentor, colleague, and friend. Thanks Norito! My journey in organic chemistry started with you!

I have to thank my advisor Dr. Jeffrey N. Johnston. As an undergraduate, I was planning on attending Vanderbilt for graduate school in pharmacology. When I mentioned this to Norito, he literally took out a pile of Jeff's papers from his filing cabinet, and told me to go read them. I was visiting Nashville my senior year of college for something completely unrelated, and thought I'd try to meet with Jeff and use the trip to kill two birds with one stone. Jeff wasn't available during the week, but asked me for my cell phone number. He called me when he returned on Saturday from his trip to find out what hotel I was staying in, and then met me in the hotel lobby to introduce himself, talk chemistry, and let me learn about his lab. From that moment forward, I was sold – I had to work for Jeff. Throughout the 5 years I have spent at Vanderbilt, I could not have asked for a better advisor. I am not the easiest person in the world to work with, and he has been extremely patient with me. I'm not the most organized person in the world – he has spent every last ounce of effort he has trying to reverse that (sorry Jeff!).But most importantly, the education he has provided me is priceless. Jeff has a keen eye for small details, a very creative mind filled with an enormous amount of science, and an infectious, unwavering enthusiasm for chemistry. This has rubbed off on me, and I thank you for imparting some of your wisdom on me. You have helped shaped me not only into the chemist I am today, but also in to the person I've become over the last five years. When I finally decided I wanted to go to medical school, I was worried to tell him. When I finally did, I was honestly shocked at the amount of support he had for me following that dream.

Your compassion and your friendship which you offer, perfectly complementing your role as a PI, has been invaluable. Thank you for everything Jeff.

Likewise, I am very grateful for the Johnston group members with whom I've worked with through the years. Dr. Mark Dobish helped welcome me in to the lab and get me started on everything. Tom Struble, thanks for being a sounding-board for all of my terribly crazy ideas in lab, and thanks for always being willing to talk chemistry. I'm truly envious of the knowledge of, and the creativity and eye you have for, chemical transformations. Thanks for helping to make graduate school great! Mike Danneman, I don't even know what I can say here. Thanks for everything over the years we overlapped. You were always a great comic relief which helped lighten the mood. More than that, your work ethic and attention to detail made you a wonderful role model for an incoming graduate student such as myself. I appreciate everything from our time in the lab together to your four years as coach. I'll never forget bringing home all of our championships! Brandon Vara, thanks for helping make grad school enjoyable by sharing in my love of baseball, football, Diels-Alder reactions, and fluorine. I enjoyed working with you and enjoyed the friendship we built. Suzanne Batiste, you're spirit and enthusiasm helps to brighten up the lab, and to make tough times feel a little bit less overbearing. Thank you for the last 4 years of friendship, support, coffee trips, and hilariousness. I'm going to miss you when I leave. Matt Knowe, thanks for our numerous conversations, scientific and not, and thank you for always being on my team in soccer – I'm too out of shape to be on the other team!

I've made some other amazing friends in Nashville, too. Noah Orfield, if our stipend could have been paid to the Flying Saucer, I feel as though it would have been just as effective! Thanks for always being up for a beer, some baseball, and other debauchery. Shane Finn, thanks for being there from the beginning of grad school. It's been great going through the process being in the same class; thanks for always being for grabbing a beer or filling a hole in softball! Mike Goodman, I wish we would have started hanging out sooner, but I'm glad we finally started grabbing beers together. Thanks for all of our great conversations over good beer and sports!

I'd like to thank my committee members, Drs. Timothy Hanusa, Janet Macdonald, and Ned Porter, for taking time out of their schedules to be a significant part of my educational career, and for all of their advice and intellectual contributions they have provided over the last 5 years. They always bring a refreshing angle with which to view my chemistry or ideas – normally one I hadn't even considered beforehand. My Ph.D. career has been better off because of them – thank you!

Finally, Drs. Don Stec and Markus Voehler are due thanks for their upkeep of our wonderful NMR facilities. They are invaluable resources to any practicing organic chemist such as myself. In the same sense, many thanks go out to the NIH and NSF as well as the D. Stanley and Ann T. Tarbell endowment and Vanderbilt Institute of Chemical Biology for funding support over the years.

TABLE OF CONTENTS

Page

LIST OF FIGURES

Page

LIST OF SCHEMES

Page

LIST OF TABLES

Page

Chapter 1. An Introduction to Asymmetric Hydrogen bonding Catalysis

1.1 Introduction

The field of asymmetric organocatalysis, that is, the use of metal free organic molecules to catalyze enantioselective transformations, has witnessed an explosion of development over the past two decades. Although chemical transformations utilizing organocatalysis have been reported intermittently over the past century (the Hajos-Parrish reaction[1] and peptide catalysis as an example),[2] it was not until the late 1990s that the field of organocatalysis was born around a small number of articles which inspired the field to be what it is today. Between 1999 and 2016, there have been 12,817 published documents containing the concept of 'organocatalysis'.[3] This is a staggering number when you think about the fact that from 1990-1998 a cursory search shows that there were *zero* papers published containing the term of organocatalysis.[4] Obviously, organocatalysis has become an indispensable tool in the organic chemist's arsenal. Organocatalysis is a complementary field of catalysis compared to the more traditional Lewis acid catalysis and has the potential for savings in cost, simplified experimental procedures, and reduction in waste and byproducts. These benefits are observed in the fact that most organocatalysts are generally insensitive to oxygen and moisture in the atmosphere, and that a wide variety of organic reagents are available in enantiopure form. Lastly, small organic molecules are typically nontoxic (by acute exposure), environmentally friendly relative to some Lewis acids, and easily removed. This helps to increase the safety of catalysis in chemical research across both industrial and academic research.

Much of the success in this field can be attributed to the identification of a few general modes of activation, asymmetric induction, and reactivity of the catalysts. This generality and consistency of catalysts within different catalyst classes allows for predictability in the development of reactions –after generic modes of activation have been established they can be used as a platform for designing new enantioselective reactions. This is useful to chemists because it leads to the development of catalyst families composed of similar structure and/or functionality that are useful for a wide range of reactions. Useful modes of activation have included iminium catalysis, enamine catalysis, SOMO catalysis, counteranion catalysis, and hydrogen bonding catalysis, just to name a few. It is hydrogen bonding catalysis that will be discussed in depth in the coming chapters, and therefore will be covered for the rest of the introduction.

1.2 The History and Development of Hydrogen bonding Catalysis[5]

The use of small-molecule chiral, non-racemic, hydrogen bond donors has become a frontier of research within the broad field of organocatalysis.[6] Early in the literature, it was discovered that several catalytic asymmetric

---

[1] Hajos, Z. G.; Parrish, D. R. *J. Org. Chem.* **1974**, *39*, 1615.

[2] Hydrogen-bonding derived from proline catalysis is less relevant to the manuscript as a whole and as such will not be discussed further in this overview. For a review of the topic see: Albrecht, L.; Jiang, H.; Jorgensen, K. A. *Chemistry* **2014**, *20*, 358.

[3] This number was obtained *via* a SciFinder search of the topic "organocatalysis" and refining the results to the years 1999-2016.

[4] As in footnote 3, this number was obtained *via* a SciFinder search of the topic "organocatalysis" and refining the results to the years 1990-1998.

[5] For one early review see: Taylor, M. S.; Jacobsen, E. N. *Angew. Chem. Int. Ed.* **2006**, *45*, 1520.

[6] It should be noted that Etter and coworkers recognized early that electron-deficent diaryl ureas formed cocrystals with Lewis bases: Etter, M. C. *Acc. Chem. Res.* **1990**, *23*, 120; Etter, M. C.; Urbanczyklipkowska, Z.; Ziaebrahimi, M.; Panunto, T. W. *J. Am. Chem. Soc.* **1990**, *112*, 8415; Etter, M. C. *J. Phys. Chem.* **1991**, *95*, 4601. These studies along with others provided the basis for the

processes could be the result of the activation of a substrate and the organization of the transition state *via* well-defined hydrogen bonding interactions.[7] However, these results were dismissed at the time, as it was the generally held belief in the field that hydrogen bonding was too insufficient for the activation of substrates and for inducing asymmetry to have any general use in asymmetric catalysis. This was shown to not be the case by Jacobsen (1998) and Corey (1999); in fact hydrogen bonding catalysis could now be claimed to organize transition states (almost, if not completely) as well as covalent catalysis.

Scheme 1. An Example of Jacobsen's Enantioselective Strecker Reaction

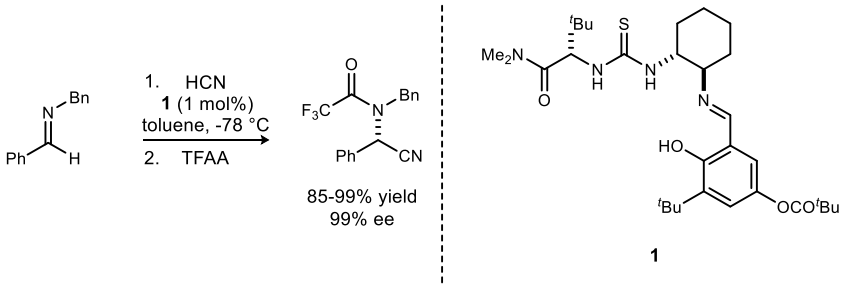

Independently, Jacobsen[8] **(Scheme 1**) and Corey[9] (**Scheme 2**) reported an asymmetric version of the Strecker reaction using hydrogen bonding organocatalysts to activate imines toward nucleophilic attack. Jacobsen later developed these thioureas for use in other reactions. In doing so, it could be considered that Jacobsen demonstrated the notion that indeed the generic use of hydrogen bonding catalysis could be a fruitful area. This activation mode has become the foundation of a quite dynamic area of research, as many new asymmetric reactions have been developed on this simple principle of electrostatic interactions.

Scheme 2. An Example of Corey's Guanidine Catalyzed Enantioselective Strecker Reaction

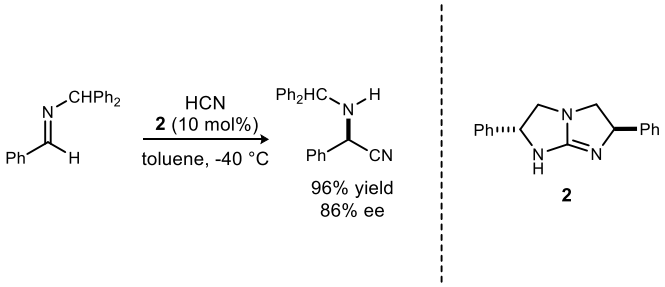

Many of the hydrogen bond catalysts to date possess a wide range of structural backbones and differ widely in their acidities, spanning over 20 pK_a units. However, all of the catalysts share a fundamental design feature: a single or dual hydrogen bond donor site, also containing sites with the ability to have secondary interactions with

development of achiral (thio)urea-derived hydrogen-bond donor catalysts; obviously these achiral catalysts were the precursors to asymmetric hydrogen-bonding catalysis.

[7] Selected examples of early asymmetric catalysis *via* hydrogen-bonding: Hiemstra, H.; Wynberg, H. *J. Am. Chem. Soc.* **1981**, *103*, 417; Oku, J. I.; Inoue, S. *J Chem Soc Chem Comm* **1981**, 229; Dolling, U. H.; Davis, P.; Grabowski, E. J. J. *J. Am. Chem. Soc.* **1984**, *106*, 446.

[8] Sigman, M. S.; Jacobsen, E. N. *J. Am. Chem. Soc.* **1998**, *120*, 4901; Sigman, M. S.; Vachal, P.; Jacobsen, E. N. *Angew. Chem., Int. Ed. Engl.* **2000**, *39*, 1279; Vachal, P.; Jacobsen, E. N. *Org. Lett.* **2000**, *2*, 867.

[9] Corey, E. J.; Grogan, M. J. *Org. Lett.* **1999**, *1*, 157.

the substrates. The following subsections are not by any means meant to be an all-inclusive review of the field, however, they are meant to give an overview of the different types of catalysts reported in the literature and some of the varying types of reactions they catalyze.

1.2.1 Hydrogen bond Catalyzed Asymmetric Aldol Reactions

Hydrogen bond-donating catalysts, such as TADDOL (**3a, Figure 1**) and its derivatives along with other chiral biphenols have been demonstrated to be remarkably effective as enantioselective catalysts in the activation of aldehydes and ketones toward nucleophilic attack. Early in development, Rawal and coworkers reported a

Figure 1. The Structure of TADDOL and a Derivative

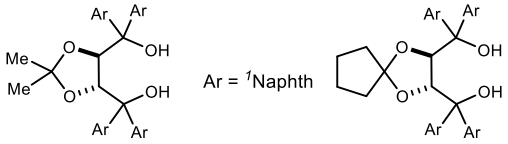

vinylogous Mukaiyama aldol reaction of dienol ethers with aldehydes catalyzed by **3a**.[10] Only highly reactive aldehydes were competent electrophiles in this report (**Scheme 3**, eq 1). However, when electron-rich *N,O*-acetals are employed, the scope of possible aldehydes usable in the Mukaiyama aldol reaction is considerably greater (**Scheme 3**, eq 2).[11] This advance in the reaction shows tolerance toward electron-rich and electron-poor aromatic aldehydes, along with aliphatic aldehydes, providing the products in high diastereo- and enantioselectivity. These products were then converted to β-hydroxy aldehydes while retaining enrichment.

Scheme 3. An Example of Rawal's Enantioselective Vinylogous Mukaiyama Aldol Reactions

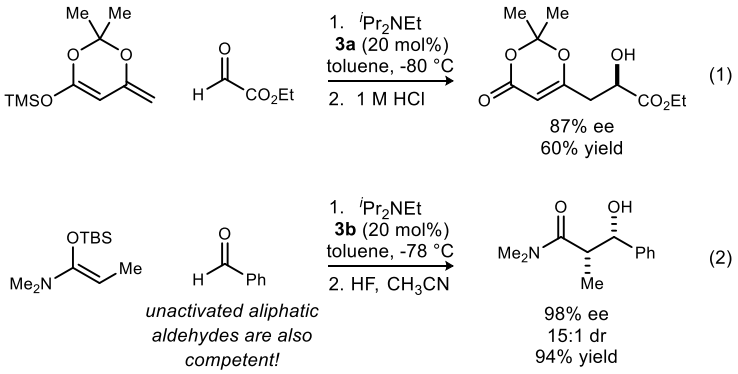

Rawal continued to advance the field of Mukaiyama aldol reactions. In 2010, he reported the first example of hydrogen bond mediated *N,O*-ketene acetals with less reactive *ketones* which proceed in high enantio- and diastereoselectivity (**Scheme 4**).[12] One drawback of this methodology is that the ketones must be highly activated, such as pyruvates or benzoyl formates. However, it does provide highly functionalized molecules in short fashion.

---

[10] Gondi, V. B.; Gravel, M.; Rawal, V. H. *Org. Lett.* **2005**, *7*, 5657.
[11] McGilvra, J. D.; Unni, A. K.; Modi, K.; Rawal, V. H. *Angew. Chem., Int. Ed. Engl.* **2006**, *45*, 6130.
[12] Gondi, V. B.; Hagihara, K.; Rawal, V. H. *Chem Commun (Camb)* **2010**, *46*, 904.

A significant development in the field, in 2009 Terada and coworkers reported the direct aldol reaction of azlactones via protonation of vinyl ethers (**Scheme 5**).[13] Their chiral phosphoric acid catalyst was able to protonate vinyl ethers to generate an oxocarbenium ion, which can then bind to the chiral phosphate in order to effect the asymmetric transformation. Significantly, this reaction produced α-quaternary β-hydroxy-α-amino acid derivatives which are of interest in the pharmaceutical industry among other areas of study.

Scheme 4. An Example of Rawal's Enantioselective Vinylogous Mukaiyama Aldol Reactions: Activated Ketone Electrophiles

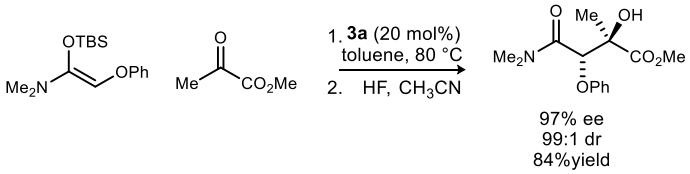

Scheme 5. An Example of Terada's Direct Aldol Reaction *via* Protonation of Vinyl Ethers

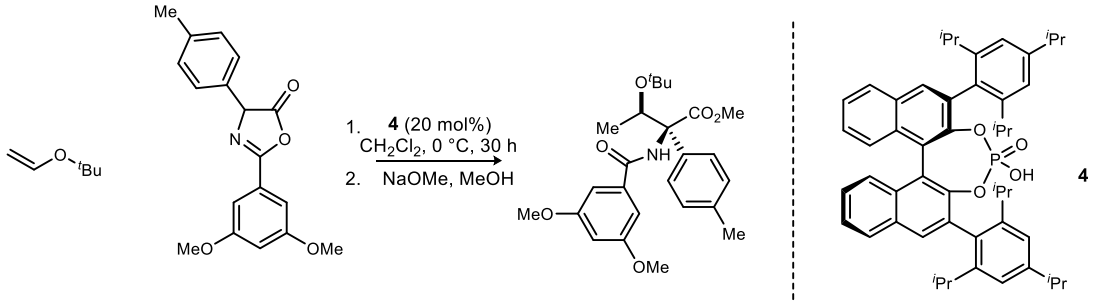

1.2.2 Hydrogen bond Catalyzed Asymmetric Hetero-Diels-Alder Reactions

Arguably one of the most useful reactions in organic chemistry is the Diels-Alder reaction – a [4+2] cycloaddition between electron rich dienes and electron poor dienophiles, providing structurally and stereochemically complex products in a single reaction. Continuing with the discussion of chiral hydrogen bond donor catalysts, many different small molecules have proven effective in catalyzing hetero-Diels-Alder (HDA) reactions. TADDOL derivatives were first introduced, again by the Rawal group, as chiral hydrogen bond donor catalysts in an HDA.[14] Initially, they discovered that protic solvents accelerated the HDA reaction of unactivated aldehydes and ketones. Following this lead, they explored the use of chiral alcohols as catalysts to attempt to induce asymmetry in the products, and indeed were successful (**Scheme 6**).

Scheme 6. Rawal's TADDOL-Catalyzed Asymmetric Hetero-Diels-Alder Reaction

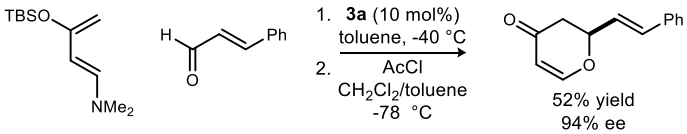

[13] Terada, M.; Tanaka, H.; Sorimachi, K. *J. Am. Chem. Soc.* **2009**, *131*, 3430.
[14] Huang, Y.; Unni, A. K.; Thadani, A. N.; Rawal, V. H. *Nature* **2003**, *424*, 146.

BAMOL, a novel axially-chiral diol catalyst related to **3a**, was effective in this reaction as well. Hydrogen bonding (at least in the solid state) was observed *via* crystal structure analysis which suggested a BAMOL-benzaldehyde complex and demonstrated that the catalyst and dienophile associate to form a chiral pocket for the reaction *via* a single hydrogen bond, and that, interestingly, there is an intramolecular hydrogen bond between the two hydroxyl groups in the chiral catalyst (*not shown*, see ref 14). This suggests that hydrogen bonding biphenol derivatives can play a key role in a mechanistically distinct class of reactions different than aldol reactions. This reaction is notable because it is an example of the same type of catalyst being applied across two mechanistically unrelated reactions, demonstrating the usefulness of being able to develop a family of catalysts based on hydrogen bonding principles.

Mikami and Tonoi reported quite a different hydrogen bond donor as a catalyst for a similar HDA reaction. They discovered that bis(triflamide) **5** promotes the HDA of Danishefsky's diene derivatives with glyoxylates and phenylglyoxals to afford dihydropyrones in moderate enantioselection and good yields (**Scheme 7**).[15] The limitation of their methodology to glyoxalates probably suggests that two-point activation by the catalyst is necessary in order to activate the dienophiles to stereochemically controlled nucleophilic attack.

Scheme 7. Triflamide Catalyzed Hetero-Diels Alder Reaction of Glyoxalates

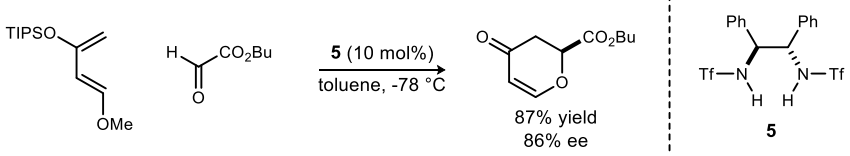

Similarly, Sigman and Rajaram have shown that simple aromatic aldehydes can be dienophiles for HDA reactions *via* sulfonylamide **6** (**Scheme 8**).[16] They designed this catalyst to present two hydrogen bond donors within a rigid oxazoline scaffold. In the presence of this catalyst, a wide range of aryl aldehydes undergo cyclization to afford dihydropyrones with moderate to good enantioselection.

Scheme 8. Sigman's Sulfonamide-Catalyzed Hetero-Diels-Alder Reaction

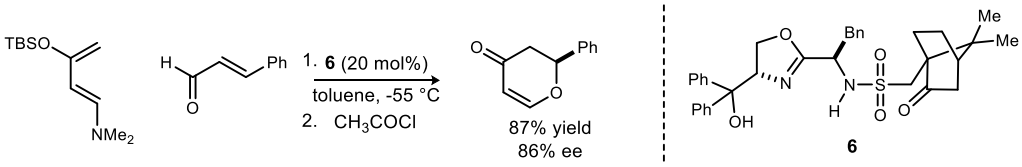

The groups of Ricci,[17] He,[18] and Bolm[19] have also contributed to the field of asymmetric HDA reactions *via* hydrogen bonding catalysis. The asymmetric HDA reaction has had numerous variants of hydrogen bonding

[15] Tonoi, T.; Mikami, K. *Tetrahedron Lett.* **2005**, *46*, 6355.
[16] Rajaram, S.; Sigman, M. S. *Org. Lett.* **2005**, *7*, 5473.
[17] Gioia, C.; Bernardi, L.; Ricci, A. *Synthesis* **2010**, *2010*, 161.
[18] Lin, Y. J.; Du, L. N.; Kang, T. R.; Liu, Q. Z.; Chen, Z. Q.; He, L. *Chemistry* **2015**, *21*, 11773.
[19] Beemelmanns, C.; Husmann, R.; Whelligan, D. K.; Ozcubukcu, S.; Bolm, C. *Eur. J. Org. Chem.* **2012**, *2012*, 3373.

catalysis applied to it; notably, there are multiple types of catalysts that can catalyze the same types of reaction, showing the broad applicability of this method of activation in organocatalysis.

1.2.3 Hydrogen bond Catalyzed Asymmetric (carbo)-Diels-Alder Reactions

As mentioned above for the hetero-Diels-Alder reaction, the Diels-Alder reaction, too, is an indispensable tool in the synthetic chemist's toolbox. The reaction provides stereochemically complex cyclohexenes with up to four new stereocenters formed in one reaction. Historically, the majority of success seen in developing asymmetric catalysts to promote Diels-Alder reactions has come in the form of metal-derived Lewis acid catalysis. However, recently more focus on hydrogen bonding catalysts has shown that indeed it is a viable option for promoting asymmetric Diels-Alder reactions. In fact, it was known as far back as 1942 that hydrogen bond donors could promote these types of reactions.[20]

Continuing with their development of chiral diol catalysts, Rawal and coworkers successfully applied **3a** to the traditional Diels-Alder reactions between aminodienes and acroleins (**Scheme 9**).[21] Uniformly high yields and enantioselection were observed when employing α-alkyl substituted aldehydes, generating functionalized cyclohexanone products.

Scheme 9. Rawal's TADDOL-Catalyzed Asymmetric Diels-Alder Reaction

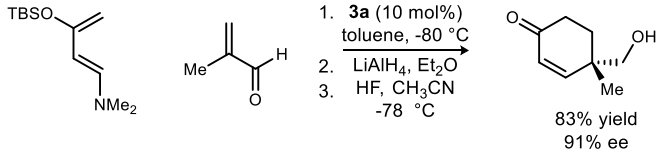

More recently, chiral phosphoric acids have emerged as an important class of hydrogen bond donor catalysts. Yamamoto and coworkers discovered that the relatively acidic *N*-triflyl phosphoramide **7** promotes the [4+2] cycloaddition albeit with a limited set of dienes, with high stereoselection (**Scheme 10**).[22] Notably, this increased acidity afforded by the triflyl groups is necessary; Terada's phosphoric acid catalyst **4** is inactive under similar conditions.

Scheme 10. Yamamoto's *N*-Triflylphosphoramide Catalyzed Asymmetric Diels-Alder Reaction

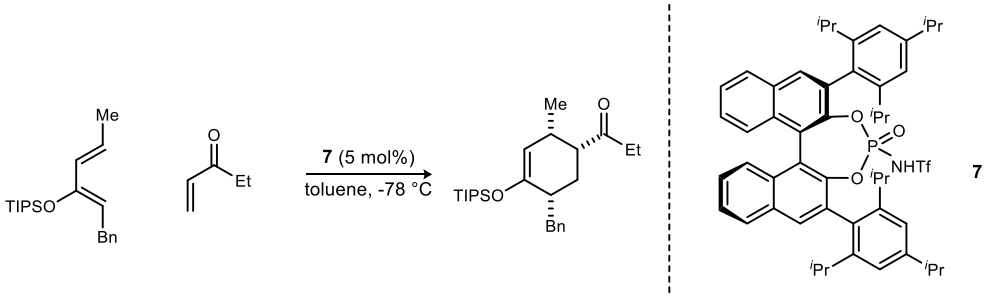

A unique reaction in Diels-Alder chemistry is that of utilizing nitroolefins as dienophiles. Nitroalkenes typically behave as dienes due to the double bond character of the N-O bond in the nitro group when coordinated

[20] Wassermann, A. *J. Chem. Soc.* **1942**, 623; Wassermann, A. *J. Chem. Soc.* **1942**, 618.
[21] Thadani, A. N.; Stankovic, A. R.; Rawal, V. H. *Proc. Natl. Acad. Sci. U. S. A.* **2004**, *101*, 5846.
[22] Nakashima, D.; Yamamoto, H. *J. Am. Chem. Soc.* **2006**, *128*, 9626.

to a Lewis Acid. This causes them to participate in hetero-Diels-Alder reactions with competent dienophiles. The Takenaka group reported the use of a bidentate helical-chiral hydrogen bond donor **8** to solve this problem (**Scheme 11**).[23] The protonated catalyst is able to coordinate both oxygens of the nitro group equally. This electrostatically removes the double bond character, leaving only a single π-system to react. The wall-like characteristics of the helical backbone biases one face of the π-bond to react with the incoming cyclopentadiene derivatives, which allows for nitroethene to participate in the first reported asymmetric nitroalkene Diels-Alder reaction.

Scheme 11. Takenaka's Helicene-Catalyzed Asymmetric Nitroalkene-Diels-Alder Reaction

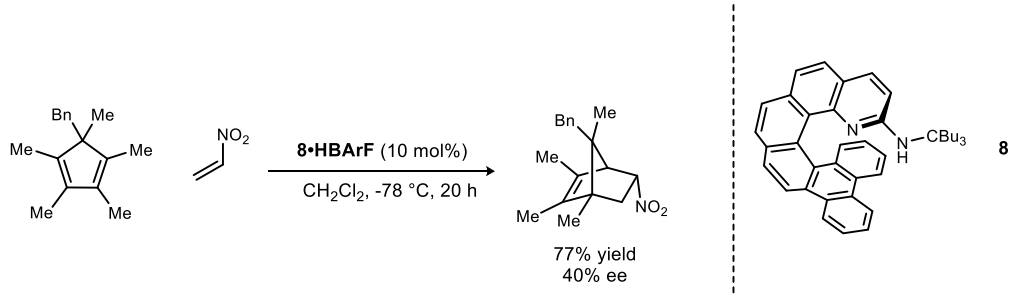

1.2.4 Hydrogen bond Catalyzed Asymmetric Henry Reactions

The Henry reaction, or the nitroaldol reaction, also has enantioselective variants catalyzed by small-molecule hydrogen bond donors. In 2006 Hiemstra and coworkers reported that cinchona alkaloid **9**, substituted at the 6' position by a thiourea, served as an enantioselective catalyst for the addition of nitromethane to aldehydes (**Scheme 12**).[24] The group previously discovered that Deng's catalyst **10**, a bifunctional catalyst containing both a phenolic moiety and a quinuclidine moiety promoted the reaction with benzaldehyde with low stereoselectivity. Replacing the phenol with a thiourea led to an improved catalyst for the Henry reaction; high enantioselection was observed when using 10 mol% of **9**.

Scheme 12. An Example of Hiemstra's Asymmetric Henry Reaction

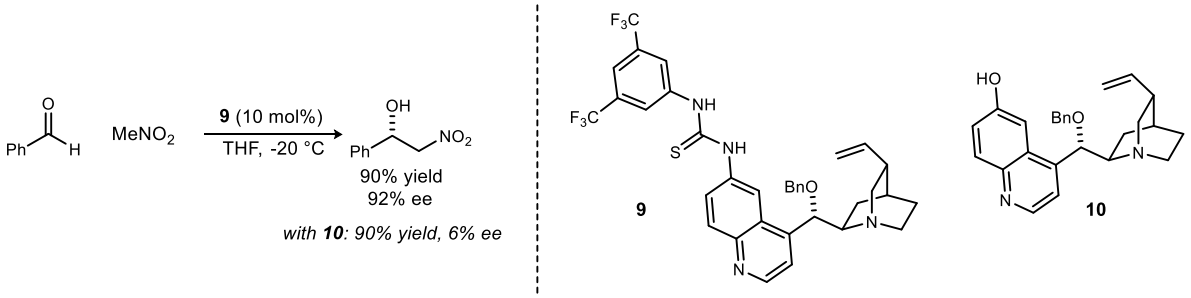

[23] Narcis, M. J.; Sprague, D. J.; Captain, B.; Takenaka, N. *Org. Biomol. Chem.* **2012**, *10*, 9134.
[24] Marcelli, T.; van der Haas, R. N.; van Maarseveen, J. H.; Hiemstra, H. *Angew. Chem., Int. Ed. Engl.* **2006**, *45*, 929.

Deng and coworkers demonstrated that **11** is an excellent catalyst for the reaction of α-ketoesters with nitromethane (**Scheme 13**).[25] The enriched products from the Henry reaction can be elaborated to a variety of useful compounds such as aziridines, β-lactams, and α-alkylcysteines.

Scheme 13. Deng's Henry Reaction Using α-Ketoesters as Electrophiles

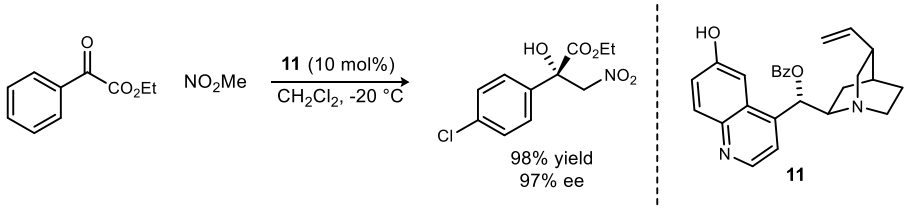

In 2009, Terada and coworkers reported a Henry reaction catalyzed by axially-chiral guanidine **12** (**Scheme 14**).[26] They propose a bidentate activation of the reaction complex is responsible for the diastereoselection and enantioselection they observe in their addition of various nitroalkanes to various aldehydes. In their manuscript, they also advance a full stereochemical model for their reaction. Unfortunately, only moderate yields and

Scheme 14. An Asymmteric Henry Reaction Catalyzed by a Chiral Guanidine

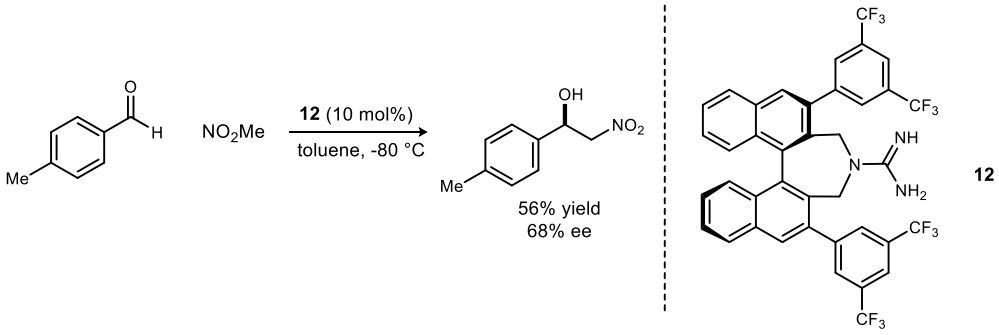

stereoselection were observed.

In 2013, the Kitagaki group contributed novel catalyst **13** to the field – a bis(thiourea) attached to a planar chiral paracyclophane backbone (**Scheme 15**).[27] They combined their catalyst with an exogenous amine base and the reaction is tolerant to various nitroalkanes and aromatic aldehydes to effect the Henry reaction, arriving at

Scheme 15. Kitagaki's Paracyclophane Hydrogen bond Donor Catalyst

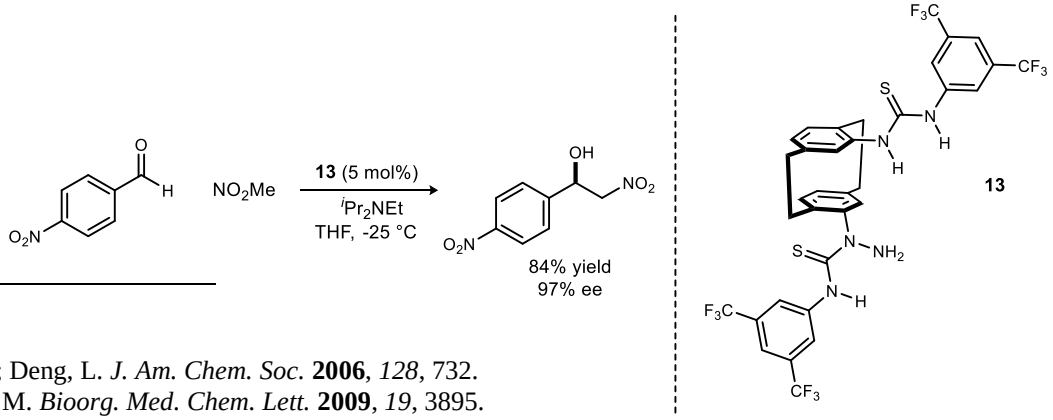

[25] Li, H.; Wang, B.; Deng, L. *J. Am. Chem. Soc.* **2006**, *128*, 732.
[26] Ube, H.; Terada, M. *Bioorg. Med. Chem. Lett.* **2009**, *19*, 3895.
[27] Kitagaki, S.; Ueda, T.; Mukai, C. *Chem Commun (Camb)* **2013**, *49*, 4030.

stereochemically enriched β-hydroxy nitroalkanes in good yields and with good enantioselection. Limiting the generality of their development of this reaction is the fact that very little diastereoselection is seen when α-substituted nitroalkanes are employed.

1.2.5 Other Developments in Hydrogen bonding Catalysis

There are applications of hydrogen bonding catalysis related to a wide variety of other types of reactions. Relevant advances in the aza-Henry (nitro-Mannich) reaction will be discussed in Section 1.3, and throughout the text. Those described above are intended to give a broad overview of some of the synthetic power inherent to the still burgeoning field of asymmetric hydrogen bonding catalysis. For further description of some of the numerous catalyzed reactions and catalysts in the field, see a review from the Jacobsen group.[28]

Thus far, only polar *covalent* hydrogen bonds have been discussed – that is, the activating hydrogen bond is polarized, but covalently bonded to its chiral backbone. Another class of hydrogen bonding catalysts are polar *ionic* hydrogen bond donors, which will be described in Section 1.3.

1.3 Chiral Proton Catalysis: The Johnston Group's Development of a Chiral Polar Ionic Hydrogen Bond Catalyst

The proton (H^+) is arguably the most common Lewis acid found in nature and can exist in two forms based on the type of hydrogen bond resulting from the Lewis acid-Lewis base interaction present: polar covalent and polar ionic hydrogen bonds. Due to this, it comes as no surprise that enzymes utilize hydrogen bonding for substrate activation quite frequently. Much more recently than nature, chemists have learned how to harvest hydrogen bond activation for synthetically useful asymmetric transformations. Already discussed extensively in the previous sections are advances in asymmetric hydrogen bonding catalysts based on polar covalent hydrogen bonds (**Figure 2a**); these types of catalysts are ubiquitous in the literature. More elusive is the analogous use of a polar *ionic* hydrogen bond for enantioselective transformations (**Figure 2b**). For a long time, this was thought to not be feasible *via* small-molecule catalysis because the proton's empty *1s* orbital challenges the design of a discrete coordination complex and because it was thought that attempts to implement the chiral molecule would fail kinetically because the solvent would coordinate the proton, and ultimately the reaction would succumb to achiral catalysis *via* a solvated Brønsted acid rather than a discrete chiral proton complex.

Figure 2. A Comparison of Polar Covalent Hydrogen Bonding and Polar Ionic Hydrogen Bonding

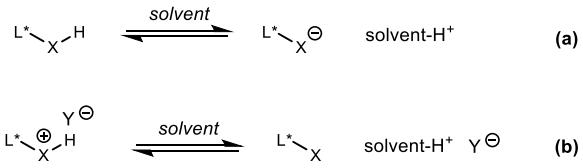

In 2004, the Johnston group demonstrated that this problem can be solved by employing structurally distinct monoprotonated bis(amidine) salts as bifunctional catalysts.[29] These catalysts provide a bidentate amidinium ion, the source of a *polar ionic hydrogen bond* used to activate an electrophile, and a free Brønsted basic moiety

[28] Doyle, A. G.; Jacobsen, E. N. *Chem. Rev.* **2007**, *107*, 5713.
[29] Nugent, B. M.; Yoder, R. A.; Johnston, J. N. *J. Am. Chem. Soc.* **2004**, *126*, 3418.

provided by the other amidine which can be used to activate a pronucleophile for nucleophilic addition to this activated electrophile. Working in tandem, the two arms of the bifunctional catalyst can then not only activate, but also orient the substrates for reaction within the chiral pocket resulting in enantioenriched products.

The initial manuscript described the development of a direct aza-Henry (nitro-Mannich) reaction of aryl *N*-Boc aldimines with nitromethane or nitroethane (as the solvent) catalyzed by H,Quin-BAM•HOTf (**14•HOTf**) (**Scheme 16**). The resulting products were obtained in synthetically useful yields with moderate to good enantioselectivity. Notably, neither exogenous base nor preactivation of the nucleophile were necessary. The protonated catalyst was necessary for stereoselection, however, as the free base gave unsatisfactory results. Most importantly, this was the first example of asymmetric catalysis utilizing a polar *ionic* hydrogen bond and a discovery whose study continues to the present.

Scheme 16. The First Report of Asymmetric Polar Ionic Hydrogen Bond Catalysis: H,Quin-BAM

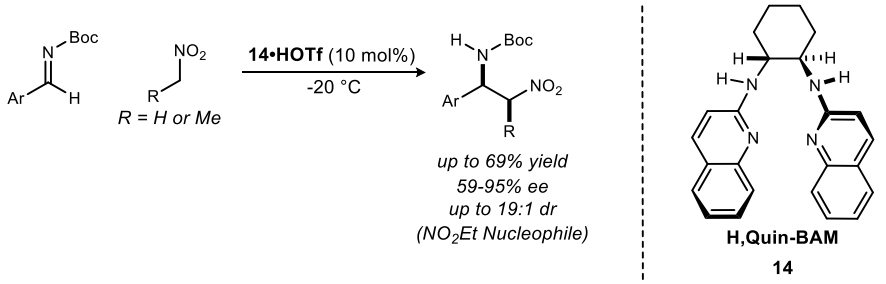

In 2007, the group applied the technology to the synthesis of α,β-diamino acid derivatives *via* the addition of *tert*-butyl nitroacetate to various aromatic aldimines with high stereochemical control (**Scheme 17**).[30] Key to successfully achieving high diastereoselection when employing the nitroacetate was altering the catalyst structure to **15•HOTf**; H,Quin-BAM•HOTf afforded moderate enantioselection but delivered no diastereocontrol.

Scheme 17. The Synthesis of Masked α,β-Diamino Acid Derivatives

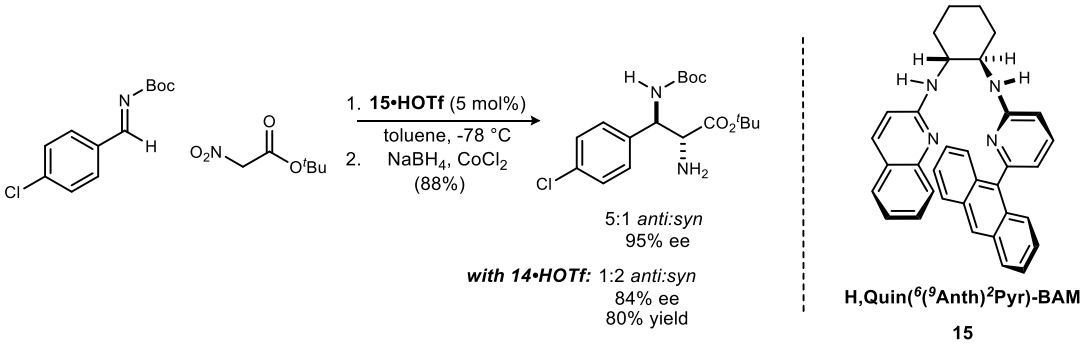

Subsequent studies allowed the addition of α-substituted nitroacetates to aldimines.[31] This provided α-quaternary α,β-diamino acids in good yield and excellent stereoselectivity. Essential to achieving good stereoselectivity and reactivity in this case was the interplay of **16•HOTf**, a more electron-rich variant of catalyst **15,** and a bulky ester on the nucleophile (**Scheme 19**). This will be discussed further in Chapter 4.

---

[30] Singh, A.; Yoder, R. A.; Shen, B.; Johnston, J. N. *J. Am. Chem. Soc.* **2007**, *129*, 3466.
[31] Singh, A.; Johnston, J. N. *J. Am. Chem. Soc.* **2008**, *130*, 5866.

Scheme 18. BAM-Catalyzed Synthesis of Stereochemically Enriched *syn*-α,β-Diamino Acids

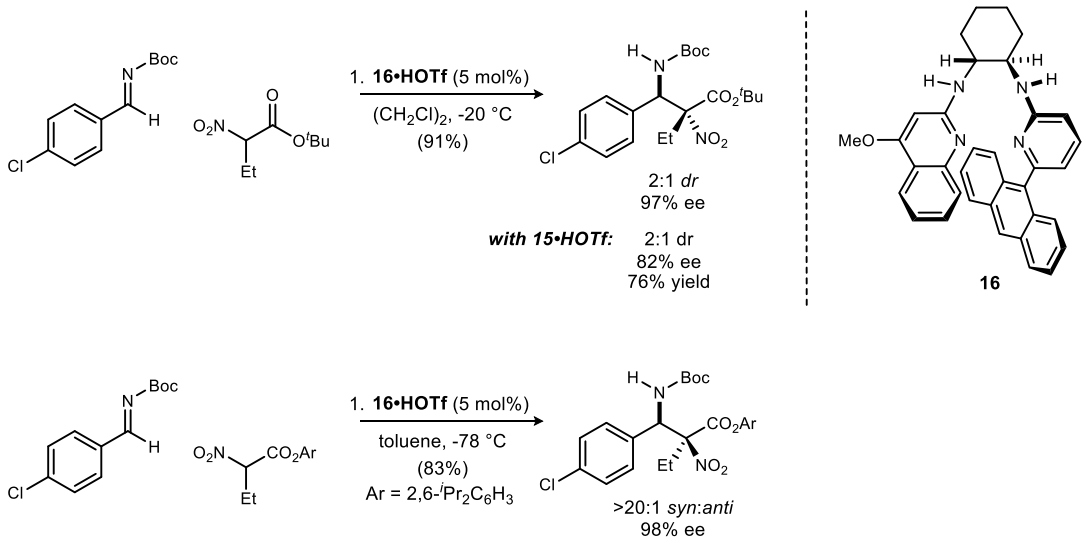

In 2010, the group reported the catalyst dubbed PBAM (**17**), and demonstrated that increased Brønsted basicity of the catalyst can increase the reactivity of a chiral Brønsted acid.[32] In other words, the better Brønsted acid is derived from, and is itself, the better Brønsted base. The manuscript demonstrated that the increase in the Brønsted basicity of the catalyst affected the overall efficiency of the aza-Henry reaction, and in doing so, the nucleophile

Scheme 19. PBAM is a More Electron Rich, More Active Chiral Proton Catalyst

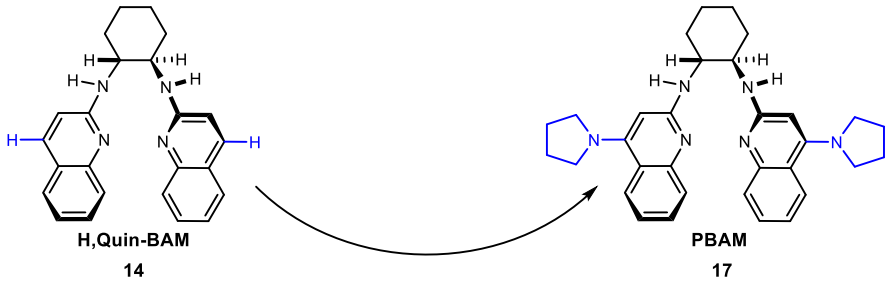

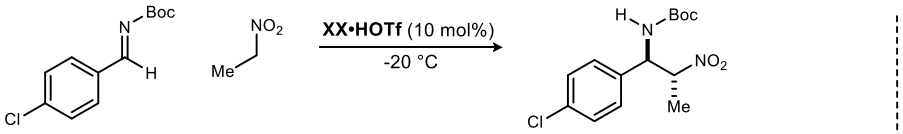

catalyst	dr (anti:syn)	ee (%)	yield (%)	
14•HOTf	8:1	87	29	(*NO_2Et as solvent, 56 equiv.*)
18•HOTf	13:1	73	52	(*NO_2Et as solvent, 56 equiv.*)
17•HOTf	7:1	90	78	(*in toluene, 1.5 equiv. NO_2Et*)

the increase basicity increases the overall reactivity and selectivity of the catalyst

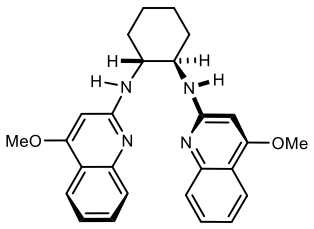

[32] Davis, T. A.; Wilt, J. C.; Johnston, J. N. *J. Am. Chem. Soc.* **2010**, *132*, 2880.

no longer had to be used as a solvent (**Scheme 19**). Since then, PBAM is now commercially available,[33] and also amenable to straightforward large scale two-step synthesis from commercially available compounds.[34]

Using PBAM derivative **19**, Davis and coworkers were able to add phenylnitromethane derivatives into *N*-Boc aldimines with high stereoselection (**Scheme 20**).[35] This new methodology was applied to the synthesis of anticancer compound Nutlin-3 which was later accomplished efficiently on decagram scale.[36] This is also the first time that the free base of the catalyst was effective in affording high stereoselection in the aza-Henry and related reactions.

Scheme 20. Davis's Synthesis of (-)-Nutlin 3 *via* a Chiral Proton-Catalyzed aza-Henry Reaction

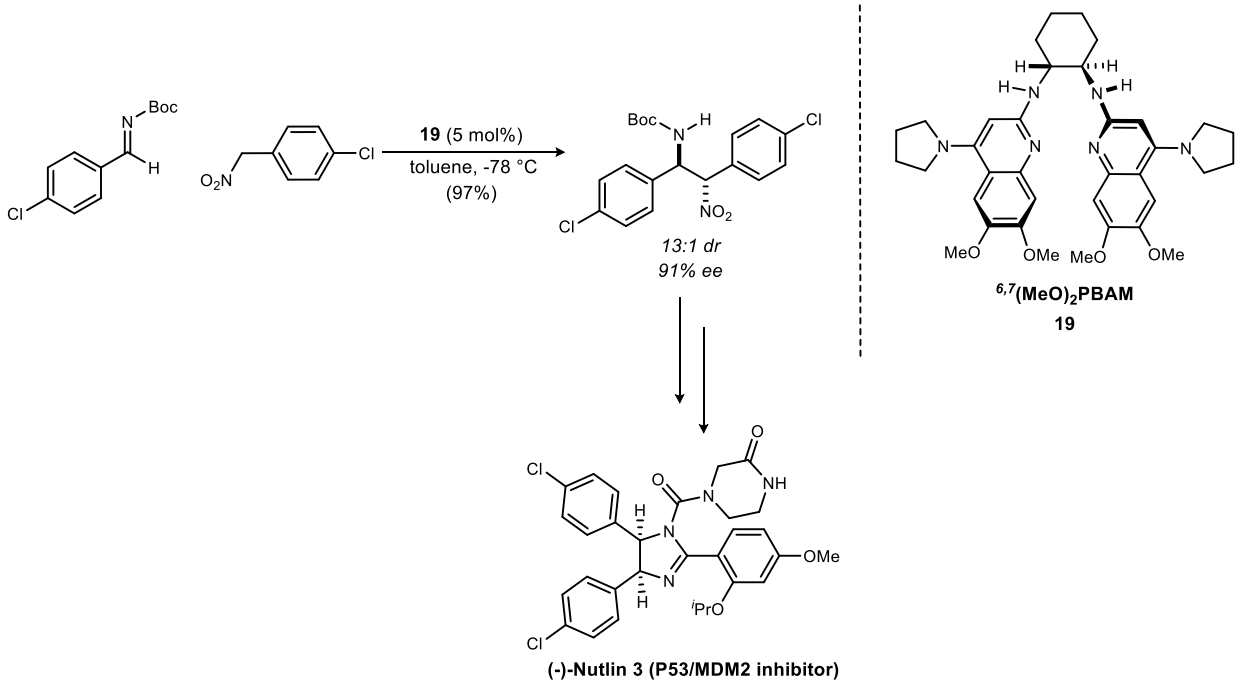

Finally, the Johnston group has used PBAM to synthesize β-amino-α-bromonitroalkanes which are substrates for iterative umpolung amide synthesis (UmAS).[37] UmAS allows a mechanistically unique reaction to occur. In the transformation, amides are formed from α-bromonitroalkanes (carboxylic acid surrogates), and electrophilic haloamines in an umpolung (reversed polarity) fashion, mechanistically avoiding the possibility for epimerization at the α-position of the newly formed amide – a noted problem in conventional amide synthesis due to electrophilic/acidic active ester intermediates.[38]

In addition to the aza-Henry reaction, chiral proton catalysis has been useful in a few reactions which are completely different mechanistically from the aza-Henry reaction. Dobish and coworkers reported an enantioselective halolactonization where StilbPBAM•$HNTf_2$ (**20•$HNTf_2$**) delivered 6-*exo* iodolactones in good yield with high enantioselectivity (**Scheme 21**).[39] Interestingly, the group discovered that the enantioselectivity

[33] Sigma-Aldrich catalog #799599
[34] Davis, T. A.; Dobish, M. C.; Schwieter, K. E.; Chun, A. C.; Johnston, J. N. *Organic syntheses; an annual publication of satisfactory methods for the preparation of organic chemicals* **2012**, *89*, 380.
[35] Davis, T. A.; Johnston, J. N. *Chem Sci* **2011**, *2*, 1076.
[36] Davis, T. A.; Vilgelm, A. E.; Richmond, A.; Johnston, J. N. *J. Org. Chem.* **2013**, *78*, 10605.
[37] Shen, B.; Makley, D. M.; Johnston, J. N. *Nature* **2010**, *465*, 1027.
[38] Lim, V. *Org. Synth.* **2016**, *93*, 88; Makley, D. M.; Johnston, J. N. *Org. Lett.* **2014**, *16*, 3146.
[39] Dobish, M. C.; Johnston, J. N. *J. Am. Chem. Soc.* **2012**, *134*, 6068.

observed was influenced by the pocket formed by the *achiral* counteranion of the catalyst-salt complex. Triflimidic acid provided the best results.

Scheme 21. Dobish's Enantioselective Iodolactonization

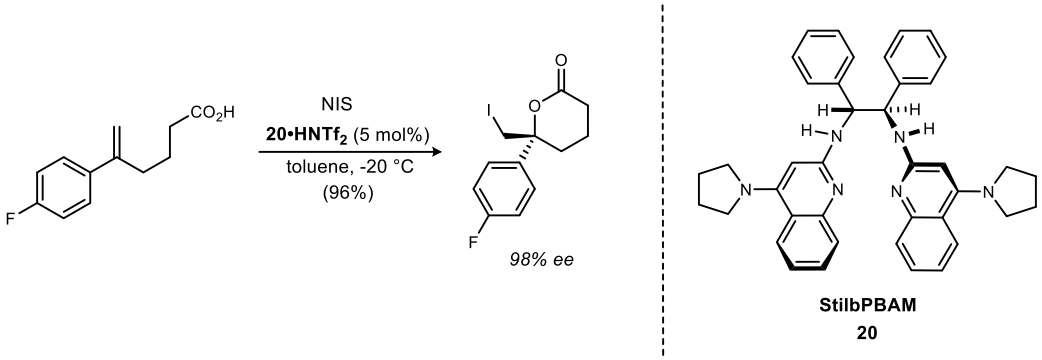

Most recently, the group reported an enantioselective organocatalyzed iodocarbonation *via* CO_2 capture and cyclization of the intermediate to form iodocarbonates in good yields with excellent enantiocontrol using **20•HNTf2** (**Scheme 22**).[40] In this reaction, StilbPBAM•$HNTf_2$ helps to not only activate the substrate, but also stabilize the transient alkylcarbonic acid to allow the reaction to occur.

Scheme 22. Vara and Coworkers' Enantioselective Iodocarbonation Reaction

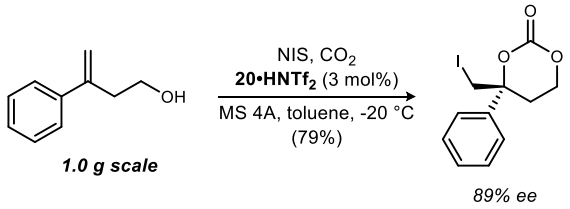

By demonstrating success in catalyzing mechanistically different reactions, it can be suggested that optimization of the catalyst in different situations can make chiral proton catalysis a useful tool to synthesize stereochemically complex molecules.

Most notably, there were only minor changes made to each BAM ligand above to make them amenable to each reaction. This is one of the characteristics of this class of catalysts that make them quite amenable to general use in organic chemistry. They are easily synthesized *via* well-established chemistry (**Scheme 23**). Stemming from this facile synthesis, it is possible to straightforwardly alter the steric environment *via* substitutions on the

Scheme 23. Representative BAM-catalyst Synthesis: PBAM

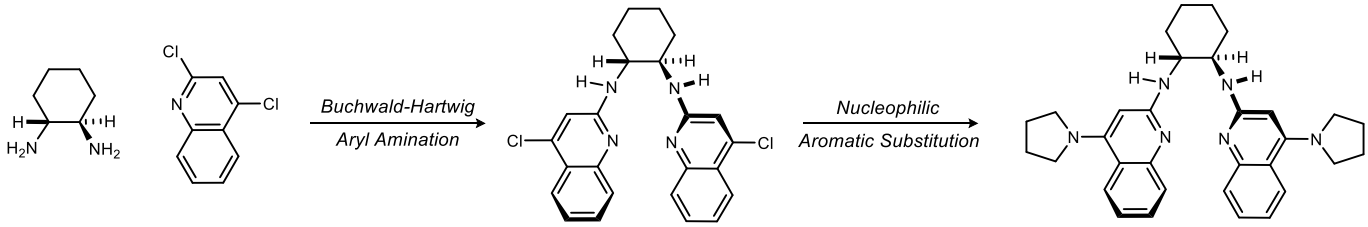

[40] Vara, B. A.; Struble, T. J.; Wang, W.; Dobish, M. C.; Johnston, J. N. *J. Am. Chem. Soc.* **2015**, *137*, 7302.

quinoline rings, or by changing the structure of the diamine backbone. Finally, it is possible to alter the electronics of the quinoline rings based on the introduction of electron donating or withdrawing substituents at specific positions on the quinoline rings. These modifications lend themselves to the ability to develop an endless number of different chiral ligands for the proton.

The remainder of this dissertation will discuss new developments and applications of chiral proton catalysis. These include a chiral proton catalyzed biomimetic aza-Diels-Alder reaction, the synthesis of important amino acid derivatives, and aza-Henry reactions employed toward the synthesis of tetrahydroisoquinoline alkaloids and their analogues.

Chapter 2. The Enantioselective Synthesis of α,β-Diamino Acids

2.1. Introduction and Background

Chiral, non-racemic vicinal diamines form an important class of compounds which are relevant for both their biological activity and for the interesting effects they have in structural biology. They also have emerged as one of the driving forces behind the explosive growth of organocatalysis seen in the past few decades.[41]

A subset of chiral vicinal diamines are the α,β-diamino acids. These compounds are atypical, nonproteinogenic amino acids which have been used as building blocks for the synthesis of amino acid surrogates to modulate their structural profile and biological behavior. Examples of free α,β-diamino acids in nature include the simplest member, α,β-diaminopropionic acid (**21**) which is found in protein-free extracts from Bombyx insects.[42] Some α,β-diamino acids found in plants display neurotoxic activity toward animals, and may even be linked to neurodegenerative diseases such as ALS, Alzheimer's disease, and Parkinsonism dementia (**Figure 3**).[43]

Figure 3. Some Simple Free α,β-Diamino Acids Found in Nature.

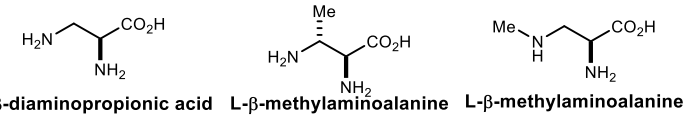

21 **22** **23**

In addition to the free α,β-diamino acids mentioned thus far, many complex natural products have been isolated which contain the diamino acid functionality in slightly modified form. Among the most useful of these, perhaps, is the bleomycin family of antitumor agents (**Figure 4**). The bleomycins were isolated from *Streptomyces verticillus* and are clinically used for the treatment of Hodgkin's lymphoma, testicular cancer, and head, neck, and skin carcinomas. Peplomycin, another member of this family, is less toxic and displays a wide antitumor spectrum.[44]

Figure 4. The Structure of Bleomycin and Peplomycin.

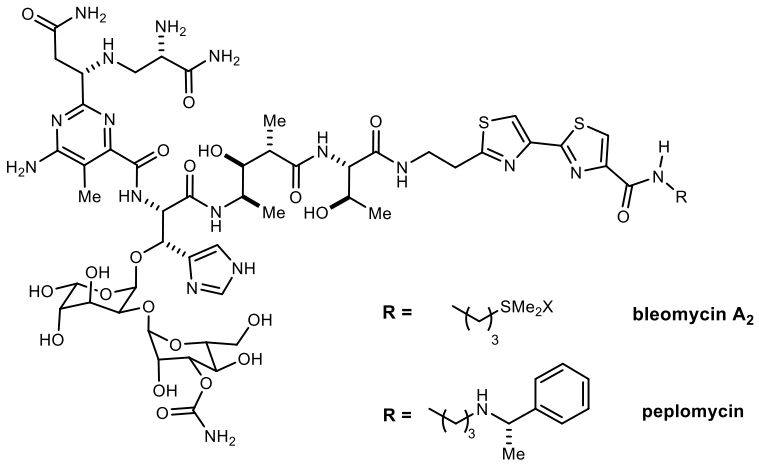

[41] Noyori, R.; Hashiguchi, S. *Acc. Chem. Res.* **1997**, *30*, 97. Trost, B. M.; Xie, J. *J. Am. Chem. Soc.* **2006**, *128*, 6044. Yoon, T. P.; Jacobsen, E. N. *Angew. Chem., Int. Ed. Engl.* **2005**, *44*, 466. Saito, B.; Fu, G. C. *J. Am. Chem. Soc.* **2008**, *130*, 6694; Nugent, B. M.; Yoder, R. A.; Johnston, J. N. *J. Am. Chem. Soc.* **2004**, *126*, 3418.

[42] Corrigan, J. J.; Srinivasan, N. G. *Biochemistry* **1966**, *5*, 1185.

[43] Cox, P. A.; Banack, S. A.; Murch, S. J. *Proc. Natl. Acad. Sci. U. S. A.* **2003**, *100*, 13380.

[44] Galm, U.; Hager, M. H.; Van Lanen, S. G.; Ju, J.; Thorson, J. S.; Shen, B. *Chem. Rev.* **2005**, *105*, 739.

Adding α-substitution to these α,β-diamino acids and their derivatives have attracted the attention of scientists in biochemistry due to their ability to destabilize membranes, and impart helix-inducing properties in small peptides.[45] They have attracted the attention of drug discovery scientists due to their ability to enhance the resistance of constituent peptides toward chemical and enzymatic degradation. Finally, they have interested synthetic organic chemists due to the difficulty in generating a densely functionalized carbon core, containing vicinal stereocenters.

Because of the widespread interest of these versatile building blocks throughout the scientific community, many efforts have been devoted toward their synthesis. These simple, polyfunctional molecules represent a significant synthetic challenge owing to the presence of contiguous stereocenters in a flexible, acyclic molecule. When a sterically hindered quaternary stereocenter is generated, the synthetic difficulties are even greater. These synthetic approaches can be broadly grouped into two categories: 1) reactions which create the carbon backbone, and 2) reactions that introduce nitrogen atoms, starting with the carbon center already assembled.

2.2 Previous Syntheses of α,β-Diamino Acids.[46]

2.2.1 Synthetic Approaches Toward Stereochemically Enriched α,α-Disubstituted α,β-Diamino Acids: C-N Bond Formation

While there are plenty of approaches to synthesize α-*unsubstituted* α,β-diamino acid derivatves *via* C-N bond formation,[46] approaches to access α-tetrasubstituted α,β-diamino acids by applying C-N bond forming reactions have seen relatively little success in the literature. 2-Cyanopropanoates have been subjected to electrophilic amination leading to α,β-diamino acids (**Scheme 24**).[47] Cativiela has reported that 2-alkyl- and 2-benzyl-2-cyano propanoates containing chiral isonorbornyloxy auxiliary **24** can be converted into chiral, nonracemic 2-amino-2-cyanopropanoates in moderate diastereoselectivity. Separation of the diastereomers, followed by hydrogenation and hydrolysis leads to the enantiopure diamino acid. While a useful proof of principal, this method suffers from the use of a stoichiometric chiral auxiliary, and imperfect stereoselectivity.

Scheme 24. Cativiela's Approach to α-Substituted α,β-Diamino Acids Using a Chiral Auxiliary

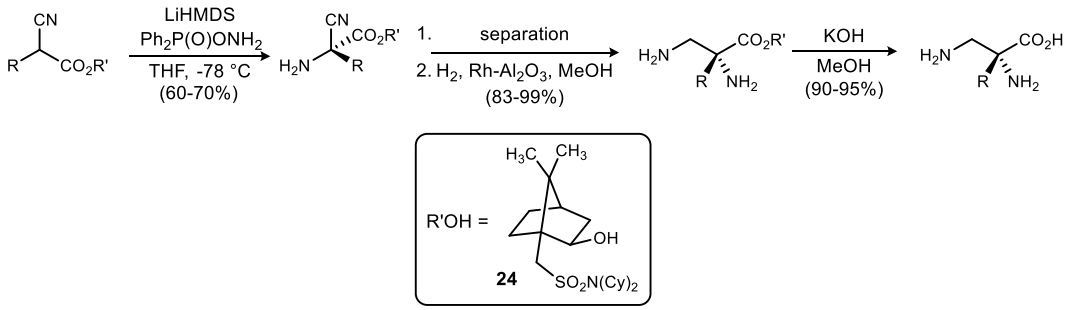

[45] Degenkolb, T.; Berg, A.; Gams, W.; Schlegel, B.; Grafe, U. *J. Pept. Sci.* **2003**, *9*, 666.
[46] For a fantastic, recently written, review see: Viso, A.; Fernandez de la Pradilla, R.; Tortosa, M.; Garcia, A.; Flores, A. *Chem. Rev.* **2011**, *111*, PR1.
[47] Badorrey, R.; Cativiela, C.; Diaz-de-Villegas, M. D.; Gálvez, J. *Tetrahedron: Asymmetry* **1995**, *6*, 2787.

The strategy of electrophilic amination has been applied to the synthesis of (-)-dysibetaine.[48] Wardrop's route to this target is shown in **Scheme 25**. Beginning with unsaturated ester **25**, enantiopure α-silyloxy methoxyamide **26** is obtained in 4 steps, utilizing Sharpless asymmetric dihydroxylation as a key step. Hypervalent iodine promotes the formation of spirodienone **27** as an epimeric mixture (9:1) at C-5. Ozonolysis, formyl group reduction, and cleavage of the N-O bond results in pyrrolidinone **28**. Mesylation of the primary alcohol followed by S_N2 displacement with azide sets the stage for the endgame synthesis of the molecule. Deprotection, methylation, and ester hydrolysis afforded the desired molecule **30**.

Scheme 25. Wardrop's Synthesis of (-)-Dysibetaine.

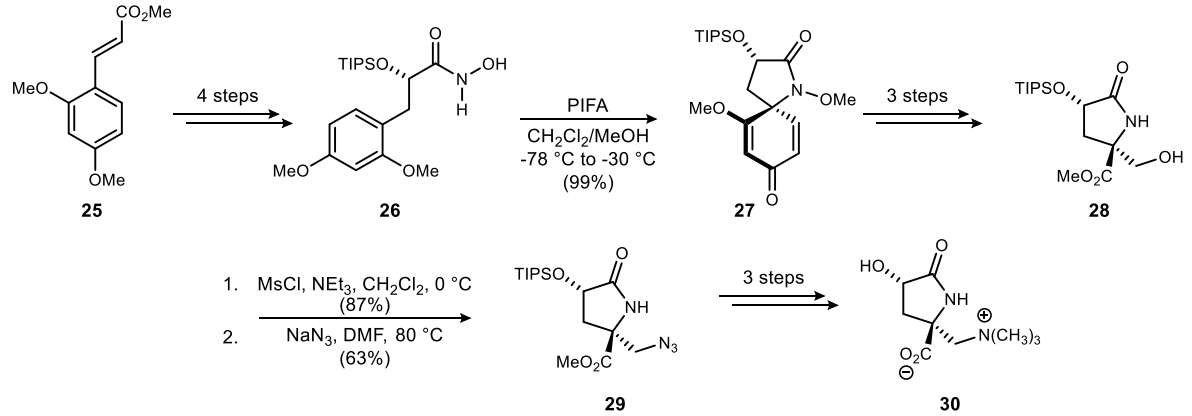

Finally, Du Bois and coworkers have reported the rhodium-catalyzed amination of sulfamate **32**, which was easily synthesized from Roche ester **31** under Mitsunobu reaction conditions (**Scheme 26**).[49] They show that treatment of **32** with $Rh_2(oct)_4$ in the presence of magnesium oxide and iodosobenzene afforded the oxidative cyclization product 33. Du Bois points out that the use of the *p*-methoxybenzenesulfonyl (Mbs) group was advantageous for the transformation, facilitating the cyclization by reducing the sp^2 character of the nitrogen center relative to an *N*-Boc or *N*-formyl protecting group. Reduction of the N-O bond with a Zn(Cu), followed by treatment with methanolic HCl liberates monoprotected α-tetrasubstituted α,β-diamino acid **34**.

Scheme 26. Du Bois's Rhodium-Catalyzed Amination.

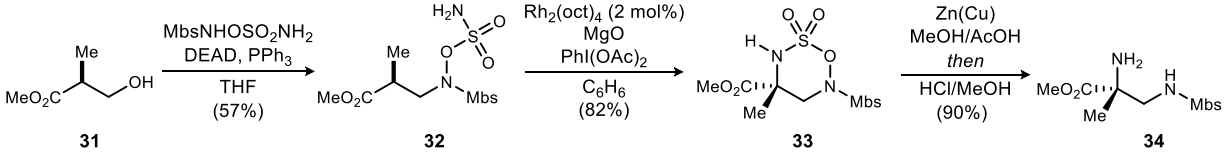

It's important to note that common to all of these routes is that they are unable to provide compounds with vicinal diamino stereocenters – the β-carbon is a primary amine.

[48] Wardrop, D. J.; Burge, M. S. *Chem Commun (Camb)* **2004**, 1230.
[49] Olson, D. E.; Du Bois, J. *J. Am. Chem. Soc.* **2008**, *130*, 11248.

2.2.2 Synthetic Approaches Toward Stereochemically Enriched α,β-Diamino Acids: Building the Carbon Skeleton

Unlike using C-N bond formation as discussed previously, building the carbon skeleton to access stereochemically enriched α,β-diamino acids has proven much more fruitful. Addition to chiral, non-racemic sulfinimines represents one successful approach to the synthesis of α-tetrasubstituted α,β-diamino acids.[50] In this approach, an imino ester is deprotonated to form the enolate. Treatment of the resultant intermediate with BF_3•Et_2O affords an imidazoline. Manipulation of the resultant aminal provides the diamino acid derivative in useful yields of the *syn*-diastereomer (**Scheme 27**). However, the use of a stoichiometric chiral auxiliary is necessary.

Scheme 27. Arriving at Stereoenriched α-Substituted α,β-Diamino Acids via Enolate Addition to Chiral, Non-Racemic Sulfinimines

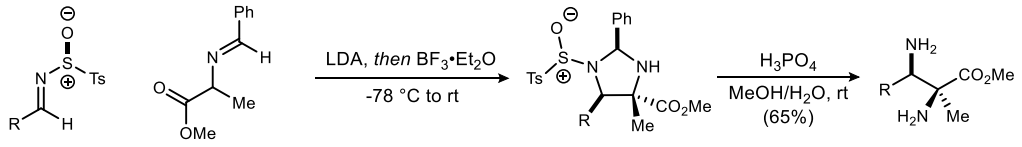

Mittendorf and co-workers have reported the diastereoselective alkylation of bislactam ether **35** with CH_2Br_2, followed by S_N2 displacement by NaN_3 (**Scheme 28**).[51] The azide was then reduced and after a six-step sequence, enantiopure α-methyl-α,β diamino acid **38** was obtained as the hydrochloride salt. Unfortunately this group is limited to an α-methyl substituent, and *vicinal*-diamino stereocenters cannot be accessed, as the β-carbon is only a methine.

Scheme 28. Mittendorf's Alkylation Approach to Access α-Substituted α,β-Diamino Acids

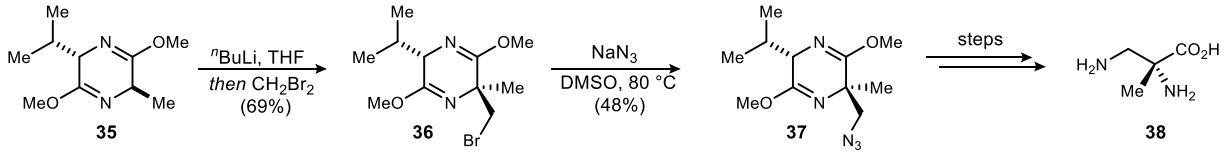

The alkylation of glycinates is another well-studied method for the synthesis of α,β-diamino acids. Carretero and coworkers have demonstrated a very nice catalytic asymmetric approach toward *anti*-α,β-diamino esters (Scheme 29).[52] They show that by using a highly engineered substrate combined with a Cu^I and a planar chiral phosphine ligand, they are able to produce α-unsubstituted- or α-methyl-diamino esters in both high enantio- and diastereoselectivity. One advance claimed in the publication is the group's ability to produce α-tetrasubstitued α,β-diamino ester derivatives, although their substrate scope is severely limited in that the only examples are α-methyl substituents. Instead, more notably, they are able to produce *vicinal* diamino stereocenters, unlike many other methodologies mentioned in this section.

[50] Viso, A.; Fernandez de la Pradilla, R.; Lopez-Rodriguez, M. L.; Garcia, A.; Flores, A.; Alonso, M. *J. Org. Chem.* **2004**, *69*, 1542; Viso, A.; de la Pradilla, R. F.; Garcia, A.; Alonso, M.; Guerrero-Strachan, C.; Fonseca, I. *Synlett* **1999**, *1999*, 1543.
[51] Hartwig, W.; Mittendorf, J. *Synthesis* **1991**, *1991*, 939.
[52] Hernandez-Toribio, J.; Gomez Arrayas, R.; Carretero, J. C. *J. Am. Chem. Soc.* **2008**, *130*, 16150.

Scheme 29. Carretero's Approach to Accessing α,β-Diamino Acids.

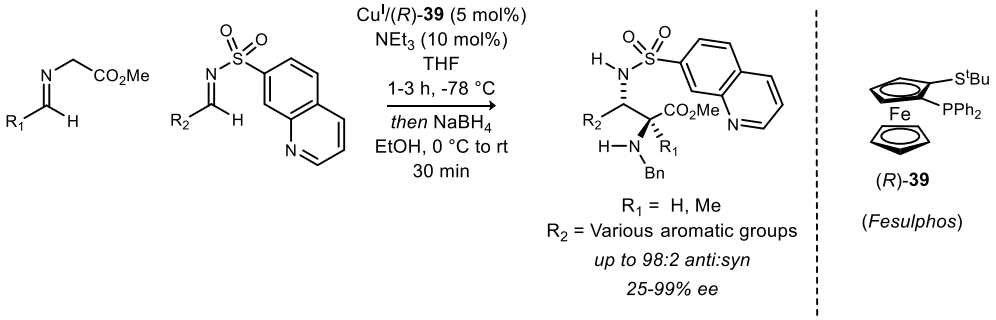

Lambert also has contributed to the Mannich reactions of glycinates with *N*-Boc imines.[53] Over the years, the Lambert group is known for its work in the area of asymmetric catalysis utilizing chiral, non-racemic cyclopropenimines as their catalyst and source of asymmetric induction. This contribution to the literature is no different. In a very elegant fashion, they are able to utilize catalyst **40** (which is now commercially available) to deliver *anti*-α,β-diamino acid derivatives (Scheme 30). Although they do not access molecules that are α-tetrasubstituted, they are able to utilize aliphatic imines, which is a notable advance in asymmetric organocatalysis when using imine electrophiles. Additionally, they showcase the utility of their methodology with a number of transformations of the product: they are able to access enantiopure *trans*-imidazolines, enantioenriched β-lactams, and peptides, among others. Impressively, they can access these types of molecules on gram-scale (>25 g of product) using 1 mol% catalyst and producing the products with high stereochemical purity.

Scheme 30. Lambert's Cyclopropenimine Catalysis: Accessing Stereochemically Differentially Protected α,β-Diamino Acids.

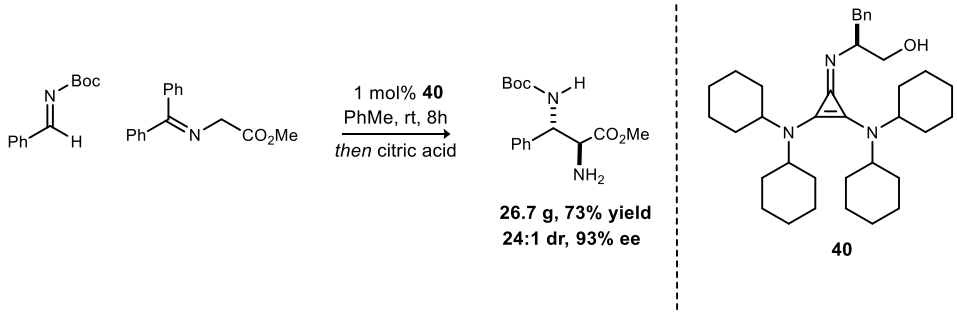

The Strecker reaction has been employed for the total synthesis of (*S*)-dysibetaine, a cyclic α-tetrasubstituted α,β-diamino acid (**Scheme 31**).[54] The requisite iminium ion, poised for the addition of TMSCN, was generated from enantiopure lactam **41**. A diastereoselective Strecker reaction provided **42** which was further transformed to **43** in a highly diastereoselective fashion. Hydrogenolysis, hydrolysis, and esterification furnished the hydroxymethyl lactam **44**. Subsequent mesylation, followed by S_N2 substitution of the mesylate by sodium azide provided compound **45** which was then subjected to reduction and deprotection leading to the synthesis of **46**.

[53] Bandar, J. S.; Lambert, T. H. *J. Am. Chem. Soc.* **2013**, *135*, 11799.
[54] Langlois, N.; Le Nguyen, B. K. *J. Org. Chem.* **2004**, *69*, 7558.

Scheme 31. A Strecker Reaction Toward the Total Synthesis of (*S*)-Dysibetaine.

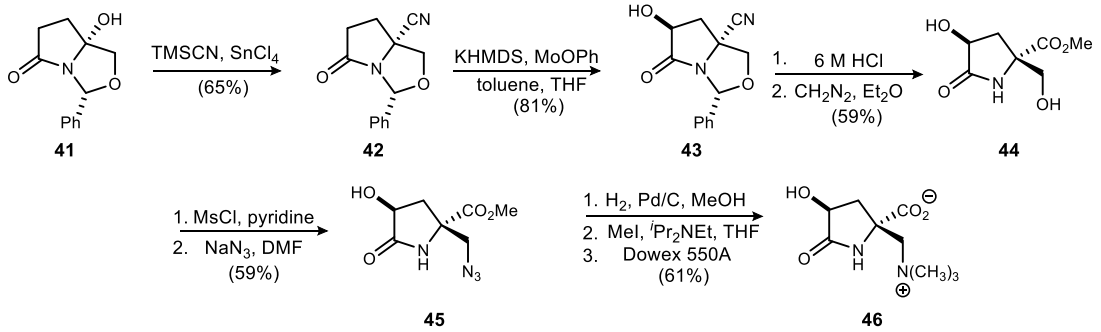

One of the less explored, but potentially just as useful, carbon-carbon bond forming methods is the stereoselective introduction of new substituents on a diamine backbone. This method was applied by Juriasti to the synthesis of α-alkyl-α,β-diamino acids (**Scheme 32**).[55] Their route relies on the optically pure pyrimidine **47** which is available from the chiral pool (5 steps from asparagine). This intermediate is then subjected to alkylation using LDA and alkyl halides, though the alkylation occurred with low diastereoselectivity. Electrophilic amination with DBAD afforded **49** in a highly diastereoselective fashion. After a three-step deprotection sequence, the free diamino acid **50** was obtained. Unfortunately, this route cannot provide vicinal diamino stereocenters.

Scheme 32. Juriasti's Approach: The Installation of New Substituents on a Diamine Backbone.

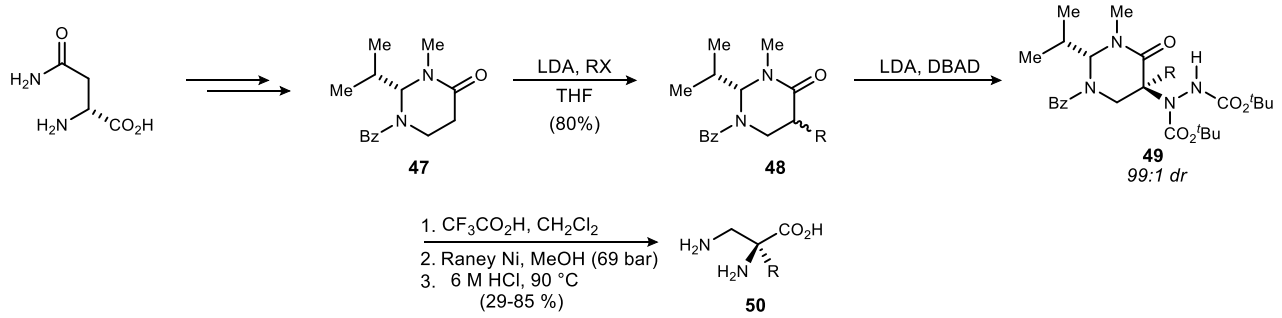

The Chin group introduced a novel method for accessing *anti*- or *syn*-α,β-diamino acids in high stereochemical purity utilizing a diaza-Cope rearrangement (**Scheme 33**).[56] This reaction is stereospecific, rather than stereoselective, with complete transfer of chirality observed. Notably this was the first 1,4-diaza-Cope rearrangement using a ketone. This reaction can be used to install α-quaternary centers with high stereoselectivity. However, the substrate scope of the α-quaternary substituent is limited, as only an α-methyl group is reported. Additionally this reaction suffers from being forced to use a stoichiometric amount of chiral auxiliary.

[55] Castellanos, E.; Reyes-Rangel, G.; Juaristi, E. *Helv. Chim. Acta* **2004**, *87*, 1016.
[56] Kim, H.; Chin, J. *Org. Lett.* **2009**, *11*, 5258.

Scheme 33. Chin's Stereospecific Diaza-Cope Rearrangement to Access α,β-Diamino Acids.

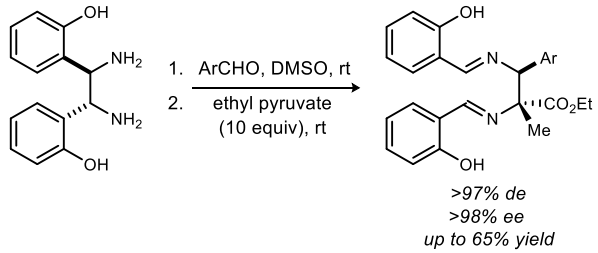

Other groups have contributed to this area as well; for further reading see ref. 57. Common to some of the carbon-carbon bond forming methods mentioned thus far is the use of stoichiometric auxiliaries, the separation of a mixture of stereoisomers, or chiral pool materials followed by (sometimes poor) diastereoselective reactions. Many of the methodologies discussed in this section suffer from the lack of ability to provide vicinal diamino stereocenters at all (providing only a methine carbon at the β-position). The groups that do utilize organocatalytic reactions from simple, achiral starting materials typically suffer from being able to create an α-tetrasubstitued stereocenter in the product α,β-diamino acids; those that can accomplish this typically suffer from poor substrate scope regarding the nucleophile and its substituents. Inherently, these routes are plagued by many steps and suffer from inefficiency while attempting to generate chiral nonracemic α-substituted α,β-diamino acids. Due to the increasing interest in these molecules around the scientific community, a more practical methodology to access them would be quite useful.

2.3 The aza-Henry Reaction in the Synthesis of α-Substituted α,β-Diamino Acids

Methodology that employs simple starting materials to quickly build molecular complexity, ideally diastereo- and enantioselectively under catalytic conditions, would be more conducive to the efficient synthesis of these molecules discussed thus far in Chapter 3. *The aza-Henry reaction lends itself to being developed for such a purpose*. If effective, the reaction has the potential to yield stereochemically enriched vicinal diamines – particularly α-quaternary β-tertiary compounds – interesting in both chemistry, biology, and pharmacology (*vide supra*).[58]

The aza-Henry reaction was first applied to the synthesis of precursors to α-tetrasubstituted α,β-diamino acids by Jørgenson who demonstrated that nitroacetate **51** can be added to a glyoxal imine **52** to give the *syn* masked

Scheme 34. Jørgenson's aza-Henry Reaction Utilizing α-Substituted Nitroacetates.

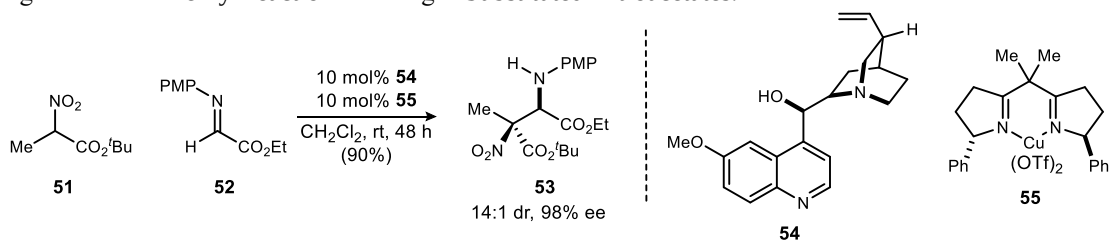

[57] Saha, N.; Chatterjee, B.; Chattopadhyay, S. K. *J. Org. Chem.* **2015**, *80*, 1896. Jiang, Y.; Chen, X.; Hu, X.-Y.; Shu, C.; Zhang, Y.-H.; Zheng, Y.-S.; Lian, C.-X.; Yuan, W.-C.; Zhang, X.-M. *Adv. Synth. Catal.* **2013**, *355*, 1931. Viso, A.; Fernandez de la Pradilla, R.; Lopez-Rodriguez, M. L.; Garcia, A.; Flores, A.; Alonso, M. *J. Org. Chem.* **2004**, *69*, 1542. Shi, S. H.; Huang, F. P.; Zhu, P.; Dong, Z. W.; Hui, X. P. *Org. Lett.* **2012**, *14*, 2010. Liu, X.; Deng, L.; Jiang, X.; Yan, W.; Liu, C.; Wang, R. *Org. Lett.* **2010**, *12*, 876.
[58] Noble, A.; Anderson, J. C. *Chem. Rev.* **2013**, *113*, 2887.

diamine **53** in 14:1 dr and 98% ee (**Scheme 34**).[59] The catalysis was performed by a two-component system: a Cu(II)-bisoxazoline complex **55** was used to activate the electrophile, and cinchona alkaloid catalysts such as **54** were used to activate the pendant nucleophile. Unfortunately, the group only published one example, and so this was not established as a general methodology.

Chen and coworkers reported the use of thiourea catalysts containing a secondary amine for the enantioselective addition of α-substituted nitroacetates to *N*-Boc imines (**Scheme 35**).[60] *syn*-Adducts were obtained in moderate to good dr, with high enantioselection. In this work, it was found that catalysts derived from 1,2-diphenylethylene diamine were most efficient, and that a secondary amine moiety was critical to obtain high diastereo- and enantioselection.

Scheme 35. Chen's Synthesis of α-tetrasubstituted α,β-diamino acids Using a Thiourea Catalyst.

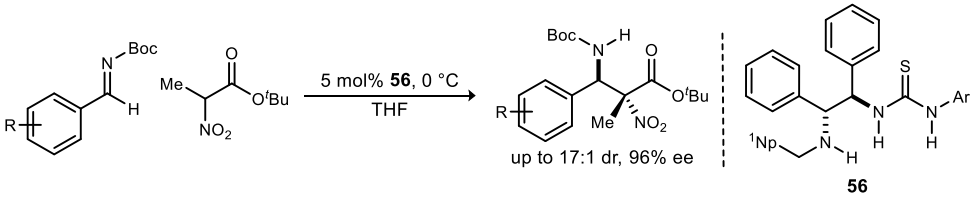

Shibisaki has reported a very elegant method for the addition of α-substituted nitroacetates to *N*-Boc imines using a homodinuclear Ni(II)-Schiff base complex (**57**) (**Scheme 36**).[61] This method affords the *anti*-diamine adducts with high diastereomeric and enantiomeric purity. Notably three examples of enolizable alkyl imines also underwent the reaction procedure to produce products in high diastereo- and enantioselection.

Scheme 36. Shibiskai's Reaction Utilizing a Dinuclear Ni(II)-Schiff Base Complex.

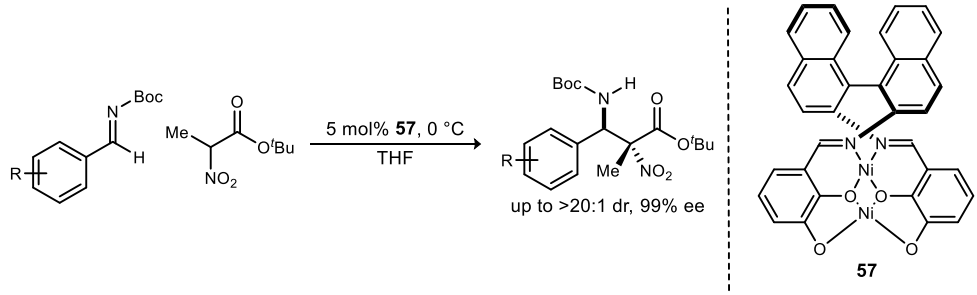

For a few more examples of utilizing the aza-Henry reaction to synthesize α-tetrasubstituted α,β-diamino acids see publications from the Ooi group,[62] and Rueping group.[63] Our group has also ventured into utilizing the aza-Henry reaction toward the stereoselective synthesis of both α-trisubstitued and α-tetrasubstitued α,β-diamino acids. The next section will be devoted to further discussion of the synthetic development of this reaction.

2.4 The Johnston Group's Synthetic Approach Toward α,β-Diamino Acid Derivatives

As discussed in Chapter 1, our group had previous success with BAM•HOTf ligands catalyzing the addition of α-unsubstituted nitroacetates to azomethines (**Scheme 37**). This success suggested that it may be possible to

[59] Knudsen, K. R.; Risgaard, T.; Nishiwaki, N.; Gothelf, K. V.; Jørgensen, K. A. *J. Am. Chem. Soc.* **2001**, *123*, 5843.
[60] Han, B.; Liu, Q. P.; Li, R.; Tian, X.; Xiong, X. F.; Deng, J. G.; Chen, Y. C. *Chemistry* **2008**, *14*, 8094.
[61] Chen, Z.; Morimoto, H.; Matsunaga, S.; Shibasaki, M. *J. Am. Chem. Soc.* **2008**, *130*, 2170.
[62] Uraguchi, D.; Koshimoto, K.; Ooi, T. *J. Am. Chem. Soc.* **2008**, *130*, 10878.
[63] Rueping, M.; Antonchick, A. P. *Org. Lett.* **2008**, *10*, 1731.

add α-substituted α-nitroacetates to azomethines, although the use of more sterically hindered nucleophiles would be expected to decrease reactivity. Besides hindering reactivity, the substitution of a hydrogen atom with an alkyl group can be expected to decrease stereoselection (**Figure 5**) since the distinction in the steric bulk of the groups being differentiated (ester and alkyl) would be diminished (compared to ester and H).

Figure 5 Hypothesis for the Expected Erosion of Diastereoselection when Employing α-Substituted Nitroacetates Compared to their *Un*substituted Analogues

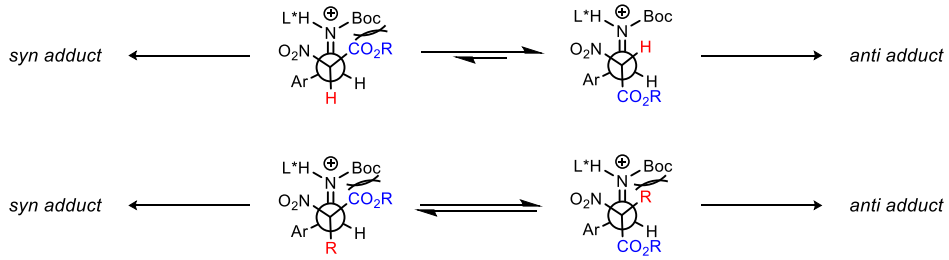

With these concerns in mind, Singh began to investigate this reaction by adding α-methyl *tert*-butyl nitroacetate to an aldimines using H,Quin-BAM•HOTf (**14•HOTf**). The reaction led to product formation, albeit with low reactivity and stereoselectivity (**Scheme 37**).[64] The low reactivity and stereoselectivity confirmed the hypothesis about the change in reactivity an α-substituent would bring about.

Scheme 37. Singh's Initial Exploration of α-Substituted Nitroacetate Nucleophiles

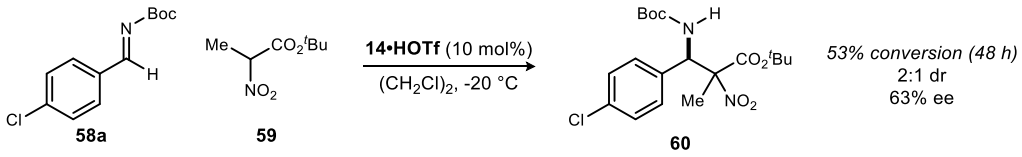

The general rate enhancement afforded by BAM•HOTf complexes is a combined effect of two orthogonal modes of reactivity. The Brønsted acidic nature of these catalysts serves to activate the electrophilic imine while the Brønsted basic property serves to deprotonate and orient the pronucleophinic nitro-compound prior to the aza-Henry reaction. What this means is that in order to increase the concentration of the active nucleophile in solution, and consequently the reaction rate, either the acidity of the pronucleophile needs to be increased or the basicity of the catalyst needs to be enhanced. From previous studies, it was known that the 4-position of our BAM catalysts has very little effect on stereoselection. So, it was suggested that an electron-donating substituent at the 4-position of the quinoline should increase the electron density of the quinoline ring, and consequently the Brønsted basicity of the catalyst; this seemed like the simplest way to modify the complex to increase the rate of reaction without affecting stereoselectivity in the reaction. Gratifyingly, bis(methoxy) catalyst **18•HOTf** provided a considerable increase in conversion and a slight increase in enantioselection, however the reaction still lacked diastereoselection – as such, the results were not optimal (**Scheme 38**).

[64] Singh, A., Vanderbilt University, 2009.

Scheme 38. Increased Quinoline Electron Density Increases Catalyst Activating Ability

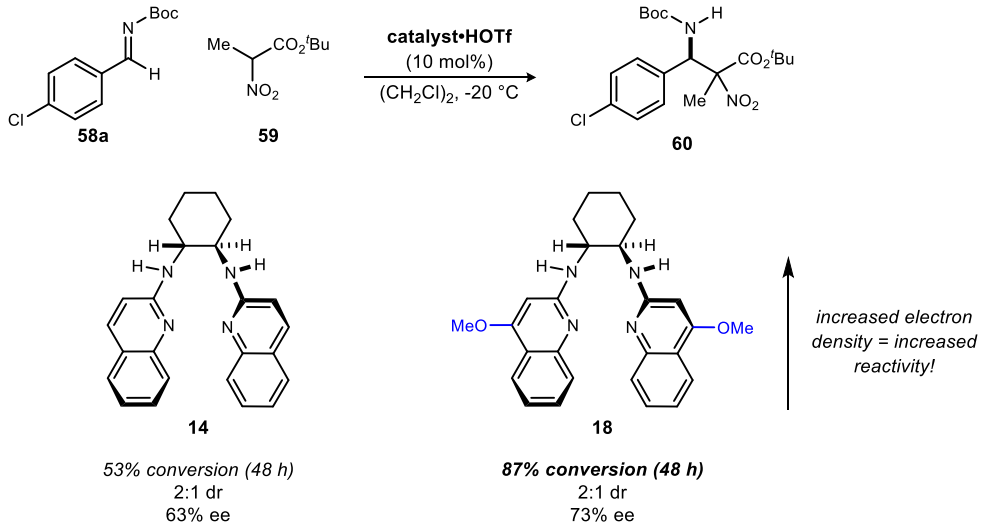

In reactions studied using α-*unsubstituted* α-nitroacetates, unsymmetrical catalysts containing a hindered substrate binding pocket provided higher enantioselection than symmetrical catalysts did. We wondered whether the same increase could be translated to reactions with *α-substituted* nitroacetate pronucleophiles. Indeed, this was the case that unsymmetrical catalyst **15•HOTf** afforded an increase in enantioselection while maintaining an acceptable rate of reaction (*vide infra*).[65] Interestingly, this means that two very different catalysts provided distinct advantages over utilizing H,QuinBAM•HOTf: an increased reaction rate tracked with electron donating quinoline substituents, and increased enantioselectivity was obtained by using an unsymmetrical catalyst. Essentially, a single new catalyst design was needed that would combine both an increase in reactivity and an increase in enantioselectivity. **Figure 6** demonstrates the algorithm Singh took to rationally develop this catalyst.[66]

[65] The unsymmetrical catalyst increased reactivity moderately as well, though to a lesser degree than **18•HOTf.** Preliminary, this could be explained from a proximity effect, wherein the bulkier catalyst brings the electrophile and nucleophile closer together, increasing conversion *via* increasing the concentration of the active catalyst.
[66] Figure adapted from ref. 64.

Figure 6. Singh's Algorithm for the Design of an Optimal Catalyst for the Addition of α-Alkyl Nitroacetates to Imines

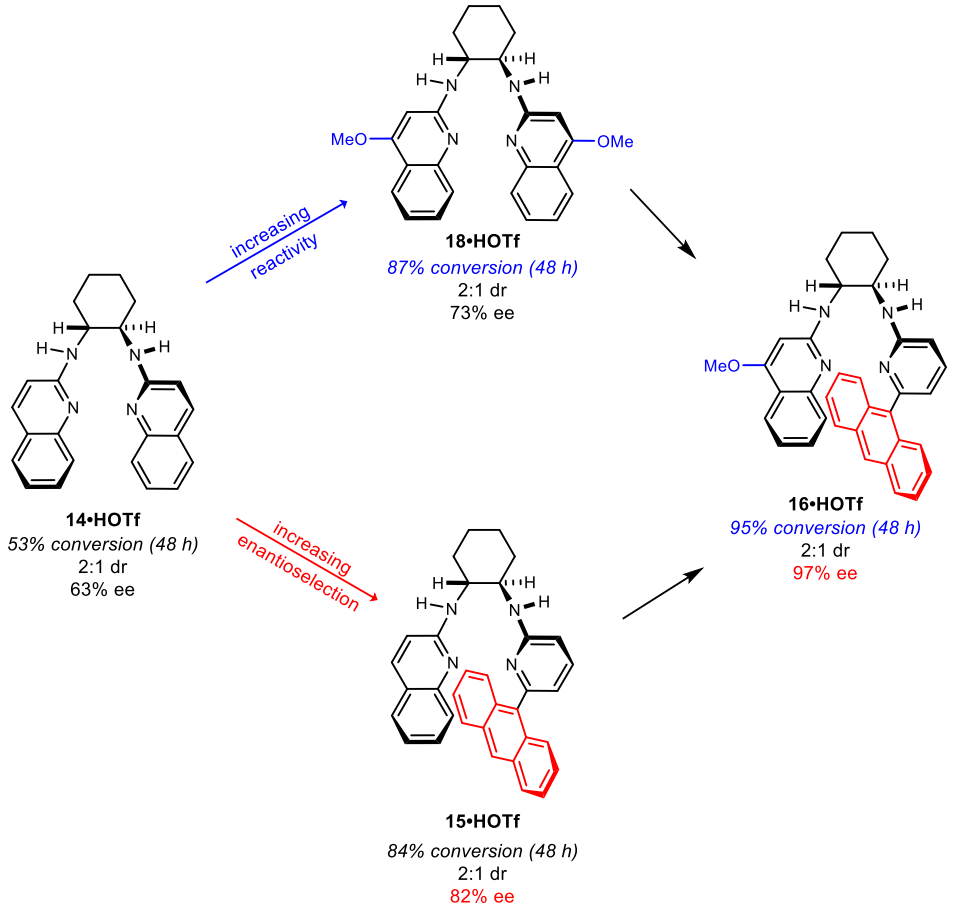

Impressively and gratifyingly the rational catalyst design was effective. Unfortunately, diastereoselectivity was still low. It was hypothesized that the steric nature of the ester in combination with the hindered binding pocket may be able to influence diastereoselectivity. Singh investigated esters with varying steric bulk and revealed this hypothesis to be correct (**Scheme 39**).[64] The use of the propofolate **59d** afforded high diastereoselection while maintaining reactivity and high enantioselection. This reaction had a wide substrate scope.[31]

Scheme 39. Modulation of Diastereoselection *via* Ester Size Modification

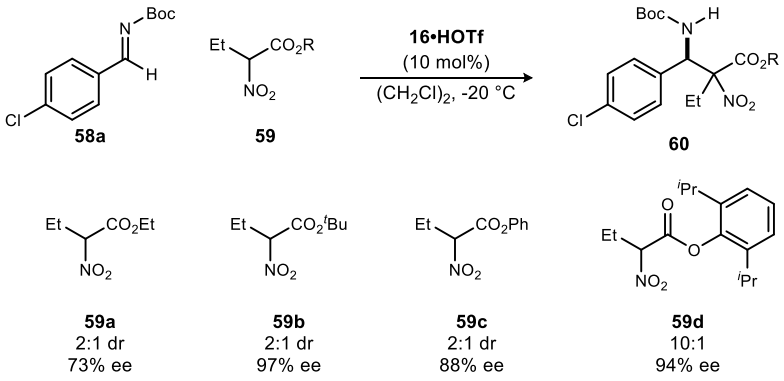

The absolute stereochemistry at the benzylic carbon was the expected outcome based on previous chemistry. Perhaps most interestingly, X-ray diffraction showed that the *syn*-diastereomer was synthesized from these

additions. The production of the *syn*-diastereomer as the major product was somewhat unexpected since until this point, chiral proton catalyzed additions of nitroalkanes, α-unsubstituted nitroacetates, and nitrophosphonates afforded *anti*-adducts. While the source of s*yn*-diastereoslectivity at this point is not completely understood, differences in catalyst/nucleophile structure might shed some light on this outcome.

In the case of nitrophosphonates, high *anti*-diastereoselection was achieved by using bulky nitrophosphonates with either H,Quin-BAM•HOTf or H,^{4}OMeQuin-BAM•HOTf. **Figure 7** shows the rationale for the observed *anti*-selectivity along with an analogous hypothesis for the addition of α-nitro acetates. The important difference in the addition of the nitroacetates is that of the structure of the catalyst and the nature of the ester. It could be hypothesized that the combination of a bulky (anthracene containing) catalyst and the bulky propofol ester help to stabilize the hydrogen bonding of the ester to the catalyst proton (*or* destabilize a NO_2-catalyst hydrogen bonding interaction) thus promoting formation of the observed *syn*-diastereomer.

Figure 7. Newman Projection Modeling of Diastereoselection in the aza-Henry Reaction Using Chiral Proton Catalysis.

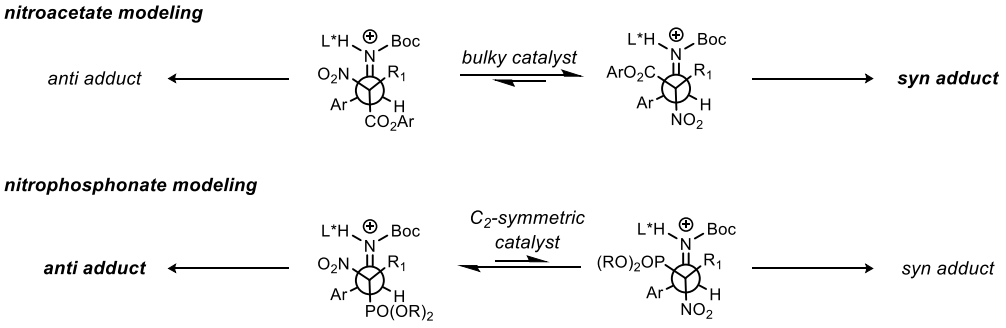

To evaluate our model for internal consistency, and also to evaluate the role of the bulky catalyst, it was hypothesized that maintaining a bulky propofolate ester, but using a less bulky catalyst such as **18** would restore the ability of an NO_2-catalyst interaction and/or take away any stability afforded by the more sterically demanding catalyst, and in doing so, the *anti*-diastereomer would be favored. Chapter 4 will be devoted to discussing this hypothesis.

2.5 The Discovery of a Chiral Proton Catalyzed Diastereodivergent Synthesis of anti α-Substituted α,β-Diamino Acids

As discussed in Chapter 3, the production of the *syn*-diastereomer as the major product is an interesting result since until this point chiral proton catalyzed additions of α-nitro compounds to azomethines had only produced the *anti*-adduct. The employment of H,[4]MeOQuin-BAM•HOTf, a less hindered C_2-symmetrical catalyst, was made in order to examine the impact of a less congested binding pocket on selectivity of the optimized reaction. Encouragingly, the use of the less hindered catalyst does support our hypothesis and lead to the *anti*-diastereomer as the major product. Although the diastereoselection is only moderate at best, enantioselection remained consistently high. Hoping to develop an efficient, synthesis of *anti*-α-substituted-α,β-diamino acids, complementary to our previous work on the *syn* compounds, conditions were sought for a catalyst to provide optimal diastereoselectivity while maintaining high enantioselectivity. This would provide on-demand organocatalytic synthesis of all 4 stereoisomers of α-quaternary α,β-diamino acids simply by choosing the proper

Scheme 40. Discovery of Catalyst-Controlled Reversal of Diastereoselectivity.

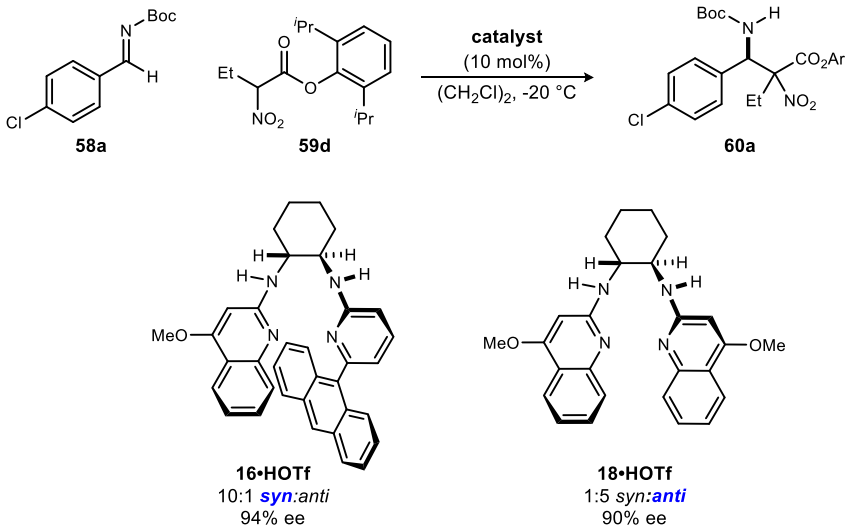

chiral proton catalyst.

We began by investigating the addition of nitroacetate **127d** to aldimine **124a** using ^{4}OMeQuin-BAM•HOTf (**18•HOTf**) in dichloroethane at -20 °C. This afforded the *anti* adduct in a 5:1 ratio, and 90% ee (**Scheme 40**). Optimization of the solvent from dichloroethane to toluene increased both diastereoselection (to 14:1 dr) and enantioselection (from 90% ee to 96% ee). Switching of the chiral catalyst to PBAM, which maintains the Brønsted basicity needed for nucleophile activation, again increased selectivity to 17:1 dr and 97% ee. Finally, optimization of the achiral counteranion to triflimide provided the aza-Henry adduct in 37:1 dr while still maintaining enantioselectivity at 97% ee (**Figure 8**). Again, the propfolate was the optimal ester for *anti*-selectivity.

Having identified optimal reaction conditions and ester/catalyst combination to produce high *anti*-selectivity and enantioselection, we turned to an evaluation of the substrate scope. The effect of the size of the alkyl substituent presented by the hindered nitroester was probed first by increasing chain length, while using ^{p}Cl-phenyl aldimine **58a** as a standard electrophile (**Table 1**). The steric model of selectivity advanced in **Figure 7** projects the nitroester substituent (R^1) in a gauche relationship with the Boc group and aldimine hydrogen. α-Nitro propionate **59e**, butanoate **59d**, pentanoate **59f**, and hexanoate **59g** each afforded product in good yield with excellent diastereoselection (11:1→20:1 dr) and uniformly high enantioselection (96-99% ee) (**Table 1**, entries 1-4). As the α-substituent is changed further only those with sp^2-hybridization resulted in lower diastereoselection (4:1 at the lowest). Branching alkyl substituents, however, returned selectivity to greater than 15:1 dr. α-Cyclopropyl nitroacetate **59j** afforded product in 68% isolated yield with 15:1 dr and 98% ee (**Table 1**, entry 7), and α-isopropyl nitroacetate **59k** afforded product in 66% isolated yield with >20:1 dr and 93% ee (**Table 1**, entry 8). α-Cyclohexyl nitroacetate **59l** gave the desired diamine derivative in >20:1 dr and 87% ee, albeit in a lower isolated yield (46%) (**Table 1**, entry 9). The lower conversion, and consequently lower isolated yield, reflects the

Figure 8. Optimization of Reaction Conditions Providing the *anti*-aza-Henry Adduct.

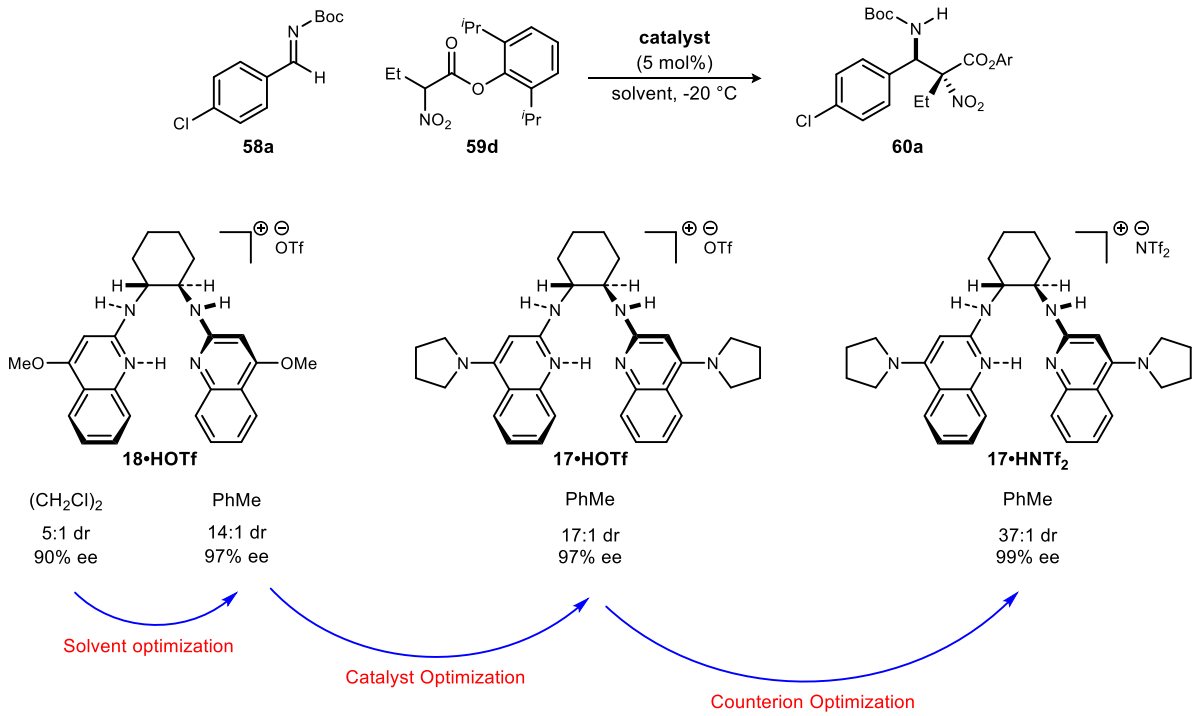

increased steric bulk surrounding the nucleophilic carbon. Nevertheless, synthetically useful amounts of stereoenriched product **60i** can be obtained under the reaction conditions. An allyl group was incorporated at the

α-position in good isolated yield, dr, and high ee (**Table 1**, entry 5). This installs a handle for further synthetic manipulations.

Table 1. *anti*-Selective Chiral Proton-Catalyzed Additions of α-Alkyl α-Nitroesters to Azomethines: Nucleophile Scope

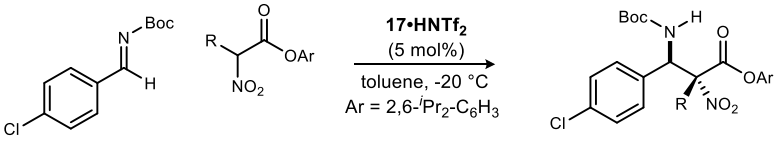

58a **59** **60**

entry[a]	R	**60**	dr[b]	ee[c]	yield[d]
1	Me (**59e**)	**b**	>20:1	99	70
2	Et (**59d**)	**a**	>20:1	99	66
3	^{n}Pr (**59f**)	**c**	>20:1	96	72
4	^{n}Bu (**59g**)	**d**	11:1	97	64
5	allyl (**59h**)	**e**	9:1	97	71
6	Bn (**59i**)	**f**	4:1	83	65
7	^{c}Pr (**59j**)	**g**	15:1	98	68
8	^{i}Pr (**59k**)	**h**	>20:1	93	66
9	^{c}Hex (**59l**)	**i**	>20:1	87	46

[a]All reactions were 0.7 M in imine, used 1.1 equiv. of the α-nitroester, and had a standard 48 h reaction time. [b]Diastereomeric ratios measured using ^{1}H NMR. [c]Enantiomeric excess (%) measured using HPLC and a chiral stationary phase. [d]Yields (%) are those of isolated, analytically pure adduct.

After exploring the scope of the nucleophile employed in this reaction, we turned our attention toward investigating the scope of the electrophile (**Table 2**). α-Nitro butanoate **59d** was employed as a standard pronucleophile. Electronically neutral aldimines resulted in good isolated yield (54-76%), high diastereoselection (12:1→20:1 dr) and high enantioselection (96-99% ee) (**Table 2**). Notably, sterically demanding 1-naphthylbenzaldimine **58i** (**Table 2**, entry 9**)** and *para*-phenylbenzaldimine **58m** (**Table 2**, entry 13) were well tolerated with high stereoselection. Electron deficient aldimines were also competent electrophiles. Trifluoromethylphenyl substituted imine **58l** afforded the adduct in 74% isolated yield with 15:1 dr and 97% ee (**Table 2**, entry 12). Both chloro- and bromo-substituted imines afforded the adduct in good yield with excellent diastereoselection (>20:1) and enantioselection (99%) (**Table 2**, entries 2 and 3). Thiophenyl and pyridyl aldimines were equally amenable to addition (**Table 2**, entries 8 and 11). Electron rich rings afforded the aza-Henry adduct in good yields with notably lower diastereoselectivity, though enantioselectivity was generally maintained (**Table 2**, entries 5-7). The erosion of diastereoselection may be attributed to a less electrophilic azomethine, leading to a longer electrophile-nucleophile distance in the bond-forming step, or a diminished secondary interaction between the nitro compound and the azomethine. Unfortunately, *N*-Boc ketimines exhibited their typical unreactive nature in this system, likely due to the severe steric congestion, despite stirring at room temperature for 7 days.

Table 2. *anti*-Selective Chiral Proton-Catalyzed Additions of α-Alkyl α-Nitroesters to Azomethines: Electrophile Scope

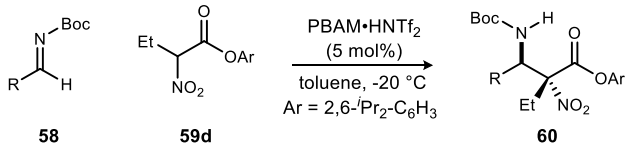

58 59d 60

entry[a]	R	60	dr[b]	ee[c]	yield[d]
1	C_6H_5 (**58b**)	**j**	>20:1	96	76
2	^{4}Cl-C_6H_4 (**58a**)	**a**	>20:1	99	66
3	^{4}Br-C_6H_4 (**58c**)	**k**	>20:1	99	71
4	^{3}Me-C_6H_4 (**58d**)	**l**	12:1	97	71
5	^{3}MeO-C_6H_4 (**58e**)	**m**	5:1	96	71
6	^{4}MeO-C_6H_4 (**58f**)	**n**	5:1	78	68
7	^{2}furyl (**58g**)	**o**	4:1	91	63
8	^{2}thiophenyl (**58h**)	**p**	>20:1	97	63
9	^{1}naphthyl (**58i**)	**q**	15:1	99	54
10	^{2}naphthyl (**58j**)	**r**	>20:1	96	70
11	^{3}pyridyl (**58k**)	**s**	9:1	96	48
12	$^4CF_3$-C_6H_4 (**58l**)	**t**	15:1	97	74
13	^{4}Ph-C_6H_4 (**58m**)	**u**	>20:1	99	73

[a]All reactions were 0.7 M in imine, used 1.1 equiv. of the α-nitroester, and had a standard 48 h reaction time. [b]Diastereomeric ratios measured using ^{1}H NMR. [c]Enantiomeric excess measured using HPLC and a chiral stationary phase. [d]Yields are those of isolated, analytically pure adduct.

The absolute and relative stereochemical assignment of adduct **60** was assigned *via* chemical correlation to known compound **62**. (*S*,*S*)-**62** was reported to have a rotation of +44.[67] Synthetic **62**, arising from derivatization of aza-Henry adduct **60** provided by **17•HNTf2**, exhibited a measured rotation of -39. Therefore, the adducts produced by (*R*,*R*)-PBAM•$HNTf_2$ have the configuration of (*R*,*R*) as depicted in **Scheme 41**, and the rest of the adducts were assigned *via* analogy.

Scheme 41. Determination of the Absolute Stereochemistry of the aza-Henry Adducts *via* Chemical Correlation.

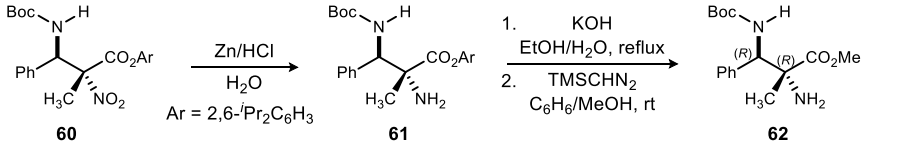

60 61 62

observed: -39 (c 0.34, EtOH)
lit. (*S*,*S*): +44 (c 0.34, EtOH)

2.6 The Development of a Stereochemical Model: A Computationally Guided Exploration

Our interest in the development of the aza-Henry reaction of α-nitro esters stemmed from the need for an alternative to enantioselective α-amino acid synthesis based on glycine Schiff base reagents (e.g. O'Donnell's enantioselective phase transfer catalyzed alkylations). α-Nitro esters require, in principle, far less basic conditions for activation by a Brønsted base. Furthermore, Mannich reactions of glycine Schiff base pronucleophiles have numerous solutions. Finally, discovering diastereodivergent conditions based upon similar chiral proton catalyst

[67] Han, B.; Huang, W.; Xu, Z. R.; Dong, X. P. *Chin. Chem. Lett.* **2011**, *22*, 923.

schemes provides the opportunity for easily synthesizing all four (biologically and synthetically useful) stereoisomers of α-substituted α,β-diamino acids.

Catalysts **16•HOTf** and **17•HNTf$_2$** behaved similarly from the standpoint of reactivity and enantioselectivity, but favored opposite diastereomers. This provides a unique opportunity for stereochemical analysis by using a modest change in catalyst structure as a single variable to consider. The key difference between these catalysts is the increased crowding in the quinolinium binding pocket of unsymmetrical catalyst **16•HOTf**.

Our development of a computationally-driven model for enantioselection in the aza-Henry reaction of nitromethane to *N*-Boc imines is based on a hydrogen bond donor-acceptor interaction between the catalyst and *N*-Boc carbonyl oxygen, respectively, leading (*R,R*)-catalysts to produce *R*-configured benzylic amines. This catalyst-benzylic amine correlation of configuration is conserved across all BAM-catalyzed aza-Henry reactions to date. That is, it is the rule, not the exception, for diastereomeric aza-Henry products from BAM catalysis to be homochiral at the benzylic amine carbon. This regularity with which benzylic amine carbon and catalyst antipode correlate suggests a robust catalyst-electrophile complexation.

Recent investigation by Dudding produced a detailed depiction of catalyst-substrate interactions using computational analysis. He advanced a hydrogen bond donor-acceptor interaction between the quinolinium and Boc-imine, respectively, that leads to *Si*-face selectivity when using the (*R,R*)-cyclohexane diamine catalyst backbone. This analysis became a launching point for our hypothesis that this coordination complex is conserved in the transition states leading to each diastereomer, owing to the homochirality of the benzylic amine carbon. A second hydrogen bond donor-acceptor interaction might be a key determinant of aza-Henry reactions exhibiting low diastereoselection, one that must be minimized in order to return to high diastereoselection. In the case of nitro esters, the ester is presented as a hydrogen bond acceptor that might compete with the nitro group for a hydrogen bond donor, or provide a nitro-group surrogate for a dipole-dipole interaction in the transition state.

Following this reasoning, complexes exhibiting a crowded imine-binding pocket would be more selective toward the preferred hydrogen bond acceptor (i.e. the nitro functionality). Moreover, the ester carbonyl in our studies was sterically deterred as a hydrogen bond acceptor by increasing the size of the ester substituent, a change that would also increase the steric penalty of its role as an opposing dipole. In this section, we provide computational insight into this model.

2.6.1 Computational Analysis/Mechanistic Analysis

Computational investigation of the BAM-catalyzed aza-Henry reaction is limited to a single pair of recent reports focusing on the H,Quin-BAM•HOTf catalyzed addition of nitromethane to *N*-Boc imines.[68] These studies by the Dudding group provided analysis that favored: 1) a synclinal arrangement between the NO_2 of the nitronate and Boc-imine nitrogen, attributed to secondary orbital overlap and 2) two point hydrogen bond contact between the amidinium and *N*-Boc imine, favoring polar ionic hydrogen bond:nitrogen and polar covalent hydrogen bond:oxygen regioselection. This study also supported that the rate-limiting step of the reaction is nitroalkane activation by the Brønsted base character of the catalyst. This selective orientation of the *N*-Boc imine electrophile

[68] Belding, L.; Taimoory, S. M.; Dudding, T. *ACS Catalysis* **2015**, *5*, 343; Taimoory, S. M.; Dudding, T. *J. Org. Chem.* **2016**, *81*, 3286.

and coordinated nitromethane-derived nitronate delivery combined to result computationally in the experimentally observed enantioselection as delivered by the chiral cyclohexane diamine backbone.

This picture dovetails with our hypothesis that both diastereomers evolve from very similar catalyst-imine complexes. What this suggests is that high diastereoselectivity is achieved by effecting differences in catalyst-nitronate binding and consequently the delivery of the nucleophile to the *N*-Boc azomethine. Dudding's work provided a picture and rationale for stereoselection using the C_2-symmetric H,Quin-BAM based Brønsted acid catalyst. Additional catalysts, such as those utilized in our studies, must be examined by analogy.

Using the assumption that catalyst-imine binding is a generally conserved feature, we wanted to better understand the catalyst-nitroalkane interactions that might exist in competing transition states. First, we investigated α-nitroester deprotonation by modeling the structure of the salt formed from deprotonating **59e** with 2-aminoquinoline (which functioned to serve as a truncated form of a typical BAM catalyst) (**Figure 9**). Since it has been shown experimentally that the 4-methoxy or 4-pyrrolidinyl substituents affect *reactivity* substantially,

Figure 9. Computational Analysis of α-Nitroester Conjugate Base Orientations Relative to the Amidinium Ion Modeled After **17** and **18**

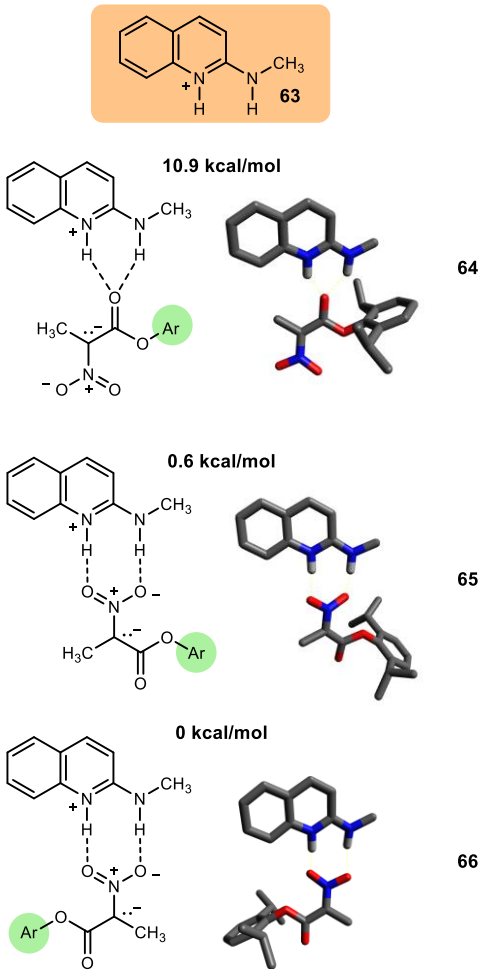

with little impact on *selectivity*, we reasoned that this simple quinoline, unsubstituted at the 4-position, was sufficient to use for these initial studies on selectivity and binding modes. The hindered ester **59e** was chosen to represent hindered α-nitro esters, and its conjugate base was modeled in complexation with quinolinium **63**. The salt presents a delocalized nitroalkane conjugate base wherein one or both anion stabilizing groups can engage in a hydrogen bonding interaction with the catalyst when in the *Z*-configuration. The lowest energy orientation

between α-nitroester and amidinium are those involving nitronate binding (**65** and **66**). When compared to amidinium binding to the enolate oxygen, for which a urea-like two-point binding complex was located, nitronate binding through both oxygens of the nitro group was favored by over 10 kcal/mol (**64**). The difference in energy between **65** and **66** was much lower at 0.6 kcal/mol, with the large ester favored in a *syn* relationship to the quinoline ring. Isomer **65** would be expected to be much higher in energy when considering the chiral catalyst where the cyclohexane diamine backbone replaces the methyl of the methylamine in **65**.

The same interactions were probed using a truncated version of anthracenyl catalyst **16**, in which 6-(1-anthracenyl)-2-methylaminoquinoline **(67**) was modeled (**Figure 10**). The binding of the carbonyl oxygen was once again >11 kcal/mol higher in energy than the corresponding binding of the catalyst to the nitronate (**68**). This high relative energy is also observed when replacing the bulky aryl ester with a methyl ester (still >10 kcal/mol higher in energy, figure not shown). The energy difference between rotamers **69** and **70** in this case was

Figure 10. Computational Analysis of α-Nitroester Conjugate Base Orientations Relative to the Amidinium Ion Modeled After **16**

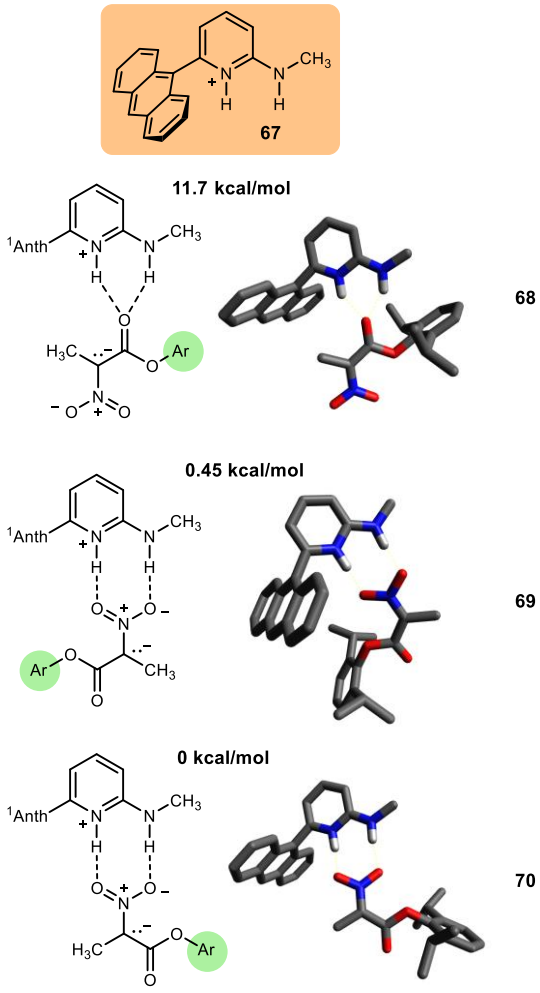

similar, but favored that in which the ester is in a *syn* relationship with the methylamino group. As noted above, this isomer would be expected to be significantly raised in energy when the full catalyst is modeled.

We then returned to the initial assumption that imine binding to the catalyst is relatively conserved, leading to high selectivity for diastereomers homochiral at the benzylic amine carbon, with the proposition that this might be explored by modeling the individual diastereomers with and without each catalyst (**Figure 11**). In the absence

of catalyst, using **60** as a representative example, *syn*-**60** was found to be lower in energy than *anti*-**60** by 1.64 kcal/mol. This behavior is consistent with all of our past work, in which thermodynamic conditions that establish either reversible aza-Henry reaction at ambient temperature or reversible nitronate formation, led to maximal *syn*:*anti* ratios of 2-3:1.

Figure 11. Computational Analysis: *syn*-**60** is 1.6 kcal/mol Lower in Energy than *anti*-**60**

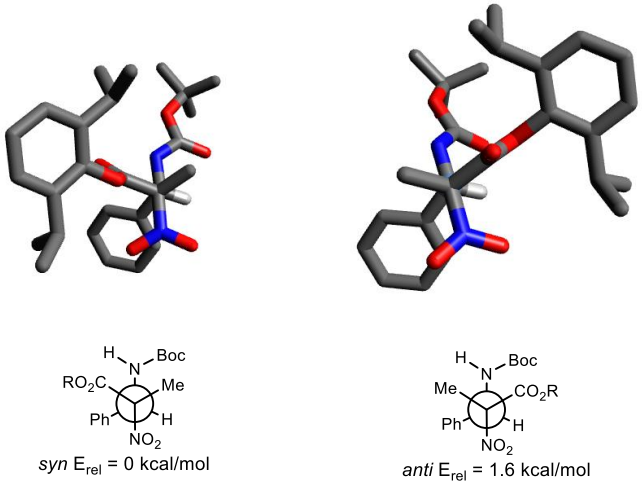

Dudding has advanced a bidentate amidinium complexed with the *N*-Boc imine in which both nitrogen and carbamate oxygen serve as hydrogen bond acceptors. There are two possible orientations for the *N*-Boc imine, for which the Boc-oxygen receives a hydrogen bond from the exocyclic *N*-H bond, resulting in bidentate binding. This is observed in our models using **63** (truncated **17**/**18**) as well. A conformation search of the analogous complex using the truncated anthracenyl pyridine **67** was performed, but a different relative arrangement was observed. Unlike the coplanar orientation with **63**, a single-point binding of amidinium to the Boc-nitrogen is favored, allowing the large planar surface of the imine to situate coplanar with the anthracenyl ring. Since the anthracene ring is perpendicular to the pyridine ring, the overall orientation of the imine is quite unique.

Thus far, the data have shown the preferred regioselection for the nitroester binding to the catalyst: the *syn*-adduct is slightly lower in energy. These properties are inherent to the nitroacetate and will be the same regardless of the catalyst. We then modeled binding conformations on truncated catalysts, and found two different conformations for substrate binding. We wondered if these results would translate when investigating with the full catalyst structure.

The denticity of the Boc-imine binding to the catalyst and low-energy conformation of the nitronate binding were examined next with the full catalyst structure. In the absence of substrates, symmetrical, less hindered catalyst **17** favors a conformation in which the cyclohexane diamine is *trans*-diequatorial. As expected, hindered, non-symmetrical **16** also exists as a *trans*-diequatorial conformer in the absence of substrates. Upon binding to the imine and nitronate, the preference inverts in favor of a *trans*-diaxial conformation. This effect is attributed to the inherent congestion of the binding pocket in **16** which is magnified even further upon the substrates binding. Interestingly, the strain also appears to favor a single-point hydrogen bond between the aminopyridinium moiety and the oxygen of the Boc group. A benefit of the *trans*-diaxial conformation is the enlargement of the binding pocket, which is then able to better accommodate the protonated aminoquinoline-nitronate ion pair as well.

Despite induced change to single-point Boc-oxygen hydrogen bonding and the enlarged pocket, the anthracene moiety rescues control of imine facial differentiation by acting as a shelf on which the imine lies flat. The minimized structures containing this hypothesized conformation maintain addition to the s*i*-face of the azomethine – the selectivity experimentally confirmed in every case. While the *Si*-face selectivity of the azomethine is preserved, facial control of the nitronate is reversed upon changing between catalysts **17•HNTf$_2$** (*anti*-selectivity) and **16•HOTf** (*syn*-selectivity). *The bound nitroester's orientation is dictated by sterics between two main interactions in each catalyst:* 1) ester steric interactions with the cyclohexane diamine backbone and 2) steric interactions of the large ester with the azomethine substituent in the binding pocket. In other words, it seems in these cases that *the complex organizes to minimize sterically unfavorable interactions*. What changes is *where* the steric bulk is concentrated within the complex.

When using PBAM•HNTf$_2$ (**17•HNTf$_2$**), the imine binds parallel to the amidine. This binding creates a congested pocket that is between the two quinolines. As a result, the incoming nitronate will orient in such a way that the bulky ester projects away from this congested pocket. Secondary to this, the nitronate also approaches in a way to minimize the steric interactions between the azomethine carbamate and the ester. The facial selectivity of the imine remains such that the resulting benzylic stereocenter is the *R*-configuration when using (*R*,*R*)-PBAM•HNTf$_2$ (**Figure 12**).

Figure 12. Binding Orientation for the Symmetric Catalyst **17** Arises from Avoiding Congested Pocket Between the Quinolines

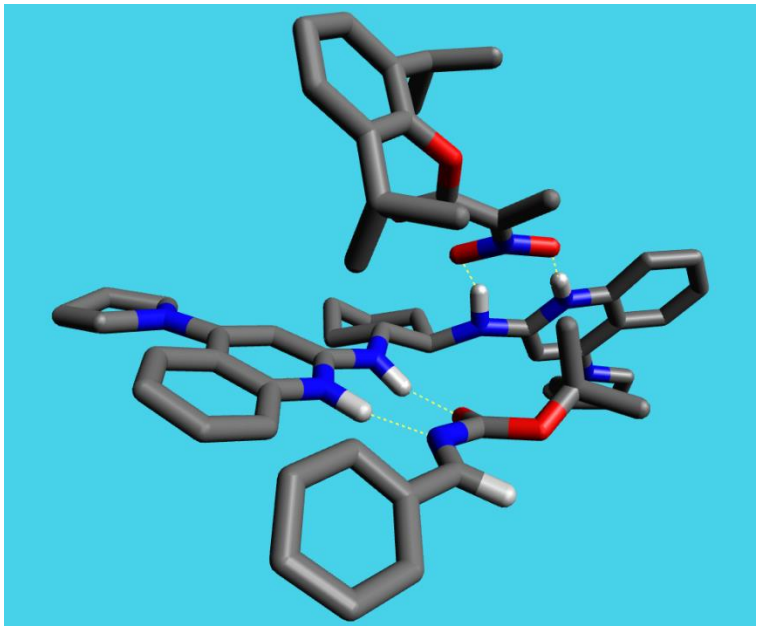

When using the anthracenyl derived catalyst (**16•HOTf**), the derived model suggests that the imine lays planar against the anthracenyl ring; this controls the facial selectivity for addition to the *N*-Boc imine. In doing so, this creates the most hindered pocket near the *backbone* of the catalyst. Therefore, to avoid unfavorable steric interactions, the nitronate approaches from the open face of the imine, biasing diastereoselectivity by minimizing interactions between the sterically demanding ester and the congested diaminocyclohexane backbone. As before, a secondary interaction orients the pendant nucleophile in such a way as to avoid clashing between the ester and the carbamate of the imine (**Figure 13**).

Figure 13. Binding Orientation for the Nonsymmetric Catalyst **16** Arises from Avoiding Congested Area Near Diamine Backbone

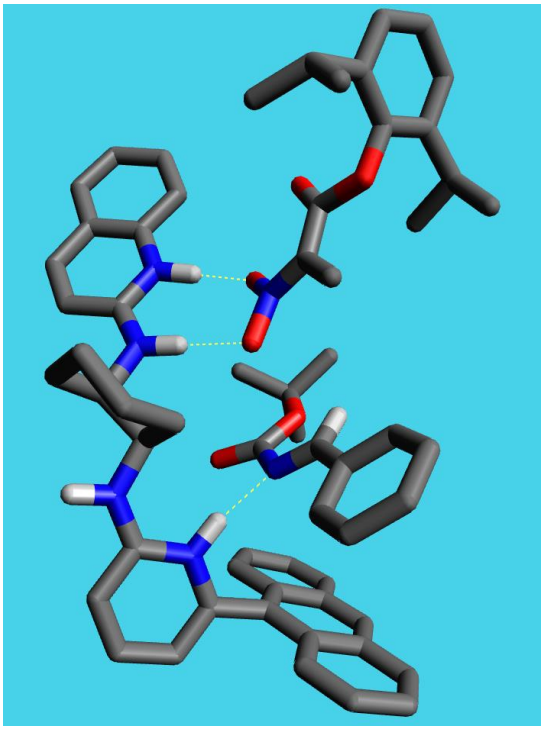

To recapitulate, the following key interactions have been highlighted: 1) the *s-trans* nitroester configuration is energetically disfavored when unbound, but when bound to the catalyst allows for hydrogen bond contacts, and is therefore lower in energy, and 2) the nitrogen on the imine binds to the polar ionic hydrogen bond while the carbonyl binds to the covalent hydrogen bond of the backbone. In doing so pockets are created which have bulkiness in different areas of the chiral environment. 3) The incoming nitronate orients in such a way to avoid unfavorable steric interactions between the bulky ester and the bulky areas of the chiral pocket.

So far, we have been able to propose the preliminary models described above for the observed BAM catalyst-controlled reversal of diastereoselectivity we see experimentally in the addition of α-quaternary nitroacetates to aldimines. Further studies at a higher level of theory are underway. Additional studies will include modeling and computationally observing the *transition states* leading to the experimentally observed diastereodivergence. This data will allow for the development of a complete model of catalysis for these unique aza-Henry reactions. To our knowledge, this catalyst system may be the first to deliver nitroester additions with a high degree of diastereocontrol, utilizing catalyst symmetry properties to selectively manipulate the configuration at the α-nitro ester carbon.

2.7 Synthesis of a Human Proteasome Inhibitor

NF-κB is a mammalian transcription factor responsible for the regulation of more than 150 genes and impacts virtually every aspect of cellular adaptation. In normal, non-stimulated cells, NF-κB is sequestered in the cytoplasm by another protein. Upon stimulation by pro-inflammatory cytokines, the pathway becomes activated; NF-κB is released and rapidly translocated into the nucleus. Once in the nucleus, it binds to DNA and initiates the transcription of a host of pro-inflammatory signaling genes. As such, deregulation of this NF-κB pathway has been implicated in the pathogenesis of inflammatory diseases such as rheumatoid arthritis, inflammatory bowel

disease, multiple sclerosis, and asthma. Given the critical role of NF-κB mediated expression of cytokines, this transcription factor has been actively pursued as a target for these types of inflammatory disorders.[69]

For example, cytokines IL-1, IL-2, IL-6, and TNF-α are expressed by NF-κB and induce the amplification of inflammatory signals. IL-6 and TNF-α have been identified as key targets in rheumatoid arthritis and other inflammatory disorders. Pharmacological intervention of rheumatoid arthritis was improved drastically with the advent of biologicals that specifically target either of these two cytokines. Unfortunately, these treatments suffer from high costs, and from variable responses to the drugs, and they also lack data pertaining to their long-term safety, tolerability, and sustained efficacy.

The Tepe lab at Michigan State University has developed imidazoline scaffolds as potent inhibitors of cytokine precursor NF-κB. They were found to inhibit both NF-κB mediated transcription in cell culture and cytokine production in stimulated human blood (**Figure 14**). These imidazolines were found to not be cytotoxic at a concentration up to 10 μM, and proved to be preliminarily effective as a treatment after the stimulation of inflammation. In other words, they could be used as a *reactive* treatment, not just prophylaxis in at-risk populations.[69]

Figure 14. An Example of Tepe's Imidazoline-Based Proteasome Inhibitors

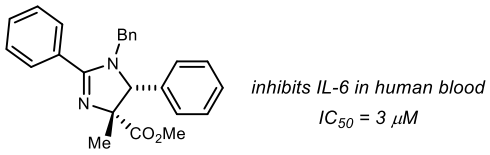

71

The proteasome has emerged recently as a chemotherapeutic treatment of certain cancers. Despite the promise of these types of drugs, all proteasome inhibitors currently in the clinic elicit their activity through the same mechanism – by covalently binding the *N*-terminal threonine residue on the proteasome. This blocks total proteasome-dependent proteolysis, ultimately leading to cell death. Through this mechanism, most patients become resistant or intolerant to the treatment within a few years, after which survival is typically less than one year. Through further studies, it was found that Tepe's imidazolines bind to the human proteasome in an allosteric, noncompetitive fashion, effectively just modulating the activity of the complex.[70] Aside from overcoming acquired resistance to active-site inhibitors, this type of specific interaction may limit toxicity through limiting off-target effects. Important structure-activity relationship studies revealed that the enantiopure *trans*-configuration in the imidazoline is important for activity; the *cis*-isomer has a greatly diminished efficacy, and one enantiomer in most cases is much more potent than its antipode.[70]

Scheme 42. Tepe's Representative Synthesis of Bioactive Imidazolines.

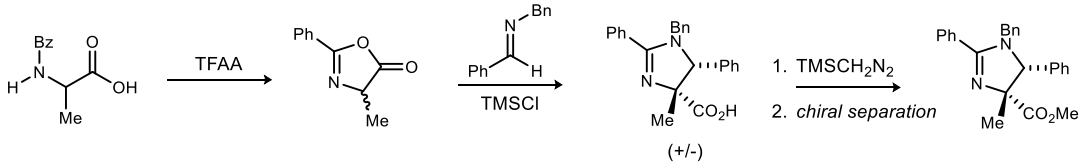

[69] Kahlon, D. K.; Lansdell, T. A.; Fisk, J. S.; Tepe, J. J. *Bioorg. Med. Chem.* **2009**, *17*, 3093.
[70] Azevedo, L. M.; Lansdell, T. A.; Ludwig, J. R.; Mosey, R. A.; Woloch, D. K.; Cogan, D. P.; Patten, G. P.; Kuszpit, M. R.; Fisk, J. S.; Tepe, J. J. *J. Med. Chem.* **2013**, *56*, 5974.

Despite the impetus for the development of stereoselective syntheses of these *trans*-imidazolines, Tepe's synthesis involves a diastereoselective synthesis of a racemic mixture, which is then separated into its constituent enantiomers *via* chiral chromatography (**Scheme 42**).[71] The methodology also employs TMSCl as a Lewis acid, which is not compatible with many functionalities if other sensitive derivatives were to be examined.

We envisioned that our mild, newly developed chiral proton catalyzed synthesis of *anti*-α,β-diamino acids would allow entrance into a single stereoisomer of these biologically important molecules in an efficient fashion. Retrosynthetically, imidazoline **70** would come from a chemoselective dehydration followed by a transesterification of **72**. This compound could come from a Boc-deprotection followed by a reductive amination of **73**. Finally, the monoprotected diamine could come from our stereoselective aza-Henry reaction followed by the reduction of the nitro group in compound **74** (**Scheme 43**). **Scheme 44** describes this synthesis in the forward direction.

Scheme 43. Retrosynthesis of Imidazoline **70**.

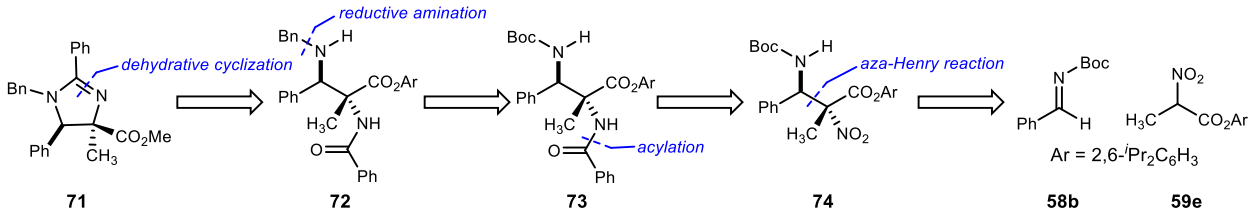

The chiral proton catalyzed aza-Henry reaction afforded adduct **74** on gram-scale with reduced catalyst loading. Notably, yield (70%), diastereo- and enantioselection (>20:1 dr, 99% ee) were maintained in this reaction, and the reaction was amenable to scale up. It had been reported that the combination of $NiCl_2$ and $NaBH_4$ was effective to reduce these types of nitro groups to amines.[60] However, in our hands the nickel promoted reduction only afforded the hydroxylamine – presumably a product of a stalled reaction. Using the same conditions with $CoCl_2$[36] only afforded decomposition. Neither heating nor alternate reaction conditions were able to successfully push the reaction any further toward completion. Likewise, it had been reported that employing catalytic Pd/C in the presence of ammonium formate as the reductant afforded α-amino esters from α-nitro esters However, this too only resulted in quantitative conversion to the hydroxylamine.

Scheme 44. Synthesis of Human Proteasome Inhibitor **71** Using the *anti*-Selective Synthesis of α-Methyl β-Amino Ester **74**

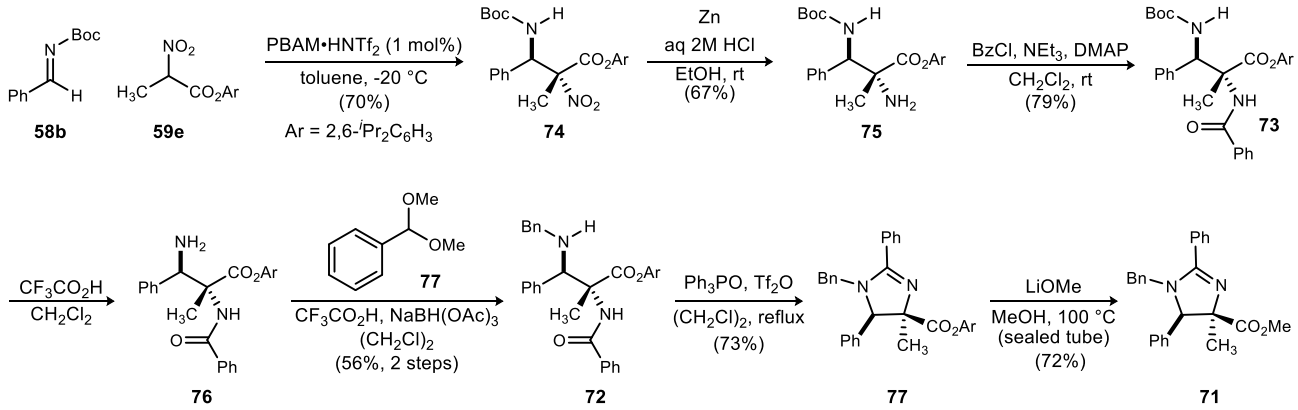

[71] Kahlon, D. K.; Lansdell, T. A.; Fisk, J. S.; Hupp, C. D.; Friebe, T. L.; Hovde, S.; Jones, A. D.; Dyer, R. D.; Henry, R. W.; Tepe, J. J. *J. Med. Chem.* **2009**, *52*, 1302.

Turning toward other reducing agents, the combination of freshly washed Zn^0 in aqueous HCl cleanly reduced the nitro group to amine **75** on gram-scale without affecting the Boc protecting group. Subsequent acylation with benzoyl chloride afforded **73** in good yield. Amine deprotection with trifluoroacetic acid in dichloromethane, followed by reductive amination with benzaldehyde dimethyl acetal (**77**), afforded benzyl amine **72** as a colorless solid. Standard reductive amination with benzaldehyde or attempts at preforming the imine prior to reduction were both unsuccessful. Presumably, using the acetal provided the C-O bond in an energetically favorable form for the reaction by beginning with the π-bond already broken.

Dehydrative cyclization using Hendrickson's reagent provided no conversion in refluxing dichloromethane. However, changing the solvent to 1,2-dichloroethane to allow refluxing at a higher temperature (70 °C) provided enough energy to transverse the activation barrier, and the reaction proceeded smoothly and cleanly to afford *trans*-imidazoline **77**.

The last step in the synthesis was the transesterification of the bulky 2,6-dialkylphenyl ester to a methyl ester. Although it has been reported that the transesterification and cleavage of this bulky ester is rare and quite difficult,[72] we were successful in clearing this hurdle. Freshly prepared LiOMe in refluxing methanol provided no conversion, and starting material was recovered quantitatively. However, heating the same solution to 100-110 °C in a sealed tube afforded clean conversion to the target imidazoline **71** in good yield.

To our knowledge, this represents the first synthesis of this biologically active molecule in both a diastereo-***and*** enantioselective fashion. Key to this synthesis was the development of a general synthesis of α-substituted *anti*-α,β-diamino acid derivatives (*vide supra*). The mild conditions provided by this route should allow access to many analogues of the skeleton which could be used for further biological studies.

[72] Romanski, J.; Nowak, P.; Kosinski, K.; Jurczak, J. *Tetrahedron Lett.* **2012**, *53*, 5287.

Chapter 3. A Chiral Proton Catalyzed Biomimetic Hetero-Diels-Alder Reaction

3.1 The Brevianamides

First isolated in 1969 from *Penicillium brevicompactum* by Birch and Wright, the brevianamide class of natural products possess a structurally interesting, and rather rare, diazabicyclo[2.2.2]octane core (Figure 15).[73] Over the years, this core has stimulated interest in the biosynthetic pathway of these compounds as well as their total chemical synthesis.

Figure 15. Representative Examples of the Brevianamide Family of Natural Products

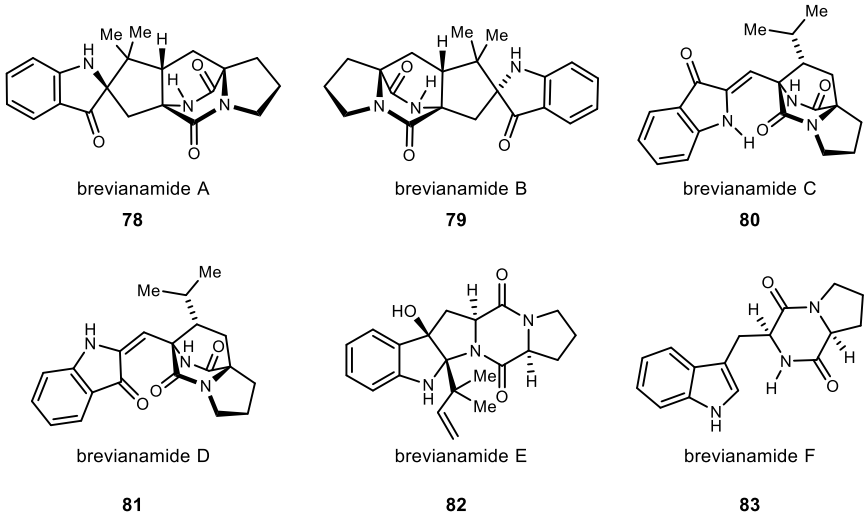

Initial structural elucidation of brevianamide A revealed both a bicyclic diketopiperazine moiety, and a spiroindoxyl center. X-Ray analysis of a semisynthetic derivative by Coetzer and coworkers confirmed the proposed structure, and established its relative and absolute stereochemistry.[74] It should be noted that the brevianamides are not unique in possessing the diazabicyclo[2.2.2]octane core – most notably the paraherquamides, avrainvillamide, and stephacidin B all contain the core as well. However, the brevianamides are distinguished from others in the class with respect to the relative stereochemistry at C19 (*brevianamide numbering*). The configuration is either *syn* or *anti* with respect to the relationship between the carbon containing the *gem*-dimethyl substitution (C18) and the pyrrolidine nitrogen (Figure 16). The brevianamides exhibit the *anti* configuration at this center, while all other members of this class to date possess the epimeric *syn* configuration.

As investigations continued, minor metabolites were also isolated from the same *Penicillium* species, and were named brevianamides B-F.[75] Brevianamides C and D were later found to be an artifact of culture conditions, and

Figure 16. Nomenclature for Brevianamide C19 Center

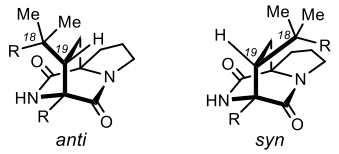

[73] (a) Birch, A. J.; Wright, J. J. *Journal of the Chemical Society D: Chemical Communications* **1969**, 644b. (b) Birch, A. J.; Wright, J. J. *Tetrahedron* **1970**, *26*, 2329. (c) Birch, A. J. *J. Agric. Food Chem.* **1971**, *19*, 1088.
[74] Coetzer, J. *Acta Crystallographica Section B Structural Crystallography and Crystal Chemistry* **1974**, *30*, 2254.
[75] Birch, A. J.; Russell, R. A. *Tetrahedron* **1972**, *28*, 2999.

brevianamide E and F were later confirmed to not be biosynthetic precursors of brevianamide A through labeled feeding studies involving isotopically-labeled compounds. Of these other metabolites, however, brevianamide B proved to be the most interesting.

The structure of brevianamide B was originally hypothesized to be epimeric to brevianamide A at the C2 spirocyclic center. However, in 1988, Williams and coworkers completed the total synthesis of brevianamide which revealed its proper stereochemistry.[76] Unexpectedly, brevianamides A and B possess *identical configurations* at the spiroindoxyl center, and are *enantiomorphic* with respect to their diazabicyclo[2.2.2]octane core. This discovery had major implications on the ensuing debate of the biosynthesis of these natural products.

Shortly after the structures were published, Sammes and Porter put forth a provocative hypothesis for the bicyclo[2.2.2]pyrazinedione core: it is the product of an intramolecular [4+2] cycloaddition of a hydroxypyrazinone moiety and a tethered prenyl group.[77] At the time, Diels-Alder reactions on these systems were unknown; however, they also supported the feasibility of this proposal with experimental results on model pyrazine systems

Figure 17. Sammes' Diels-Alder Proposal Leading to Brevianamides A and B

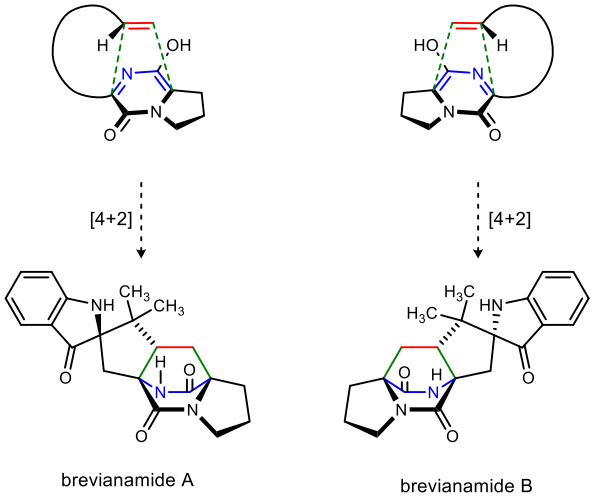

The proposal of a biological Diels-Alder reaction allowed one to account for the formation of both enantiomers of the bicyclic core. Approach of the prenyl dienophile from one face of the planar, prochiral diene would produce the core of brevianamide A, whereas approach from the opposite face would produce the core of brevianamide B (Figure 17).

Combining Sammes' proposal with the absolute stereochemistry of brevianamide B, Williams hypothesized a biosynthetic route toward these molecules (Scheme 45).[78] In this proposal, two-electron oxidation of deoxybrevianamide E (**84**) forms the achiral pyrazinone which serves as the diene in this reaction. Then, approach of the dienophile from either face furnishes products **85** or **86**. Oxidation at the 3-position of the indole produces

[76] Williams, R. M.; Glinka, T.; Kwast, E. *J. Am. Chem. Soc.* **1988**, *110*, 5927.
[77] Porter, A. E. A.; Sammes, P. G. *JSC Chem Comm.* **1970**, *0*, 1103a.
[78] Williams, R. M.; Kwast, E.; Coffman, H.; Glinka, T. *J. Am. Chem. Soc.* **1989**, *111*, 3064.

Scheme 45. Williams' Initial Biosynthetic Proposal for Brevianamide A and B

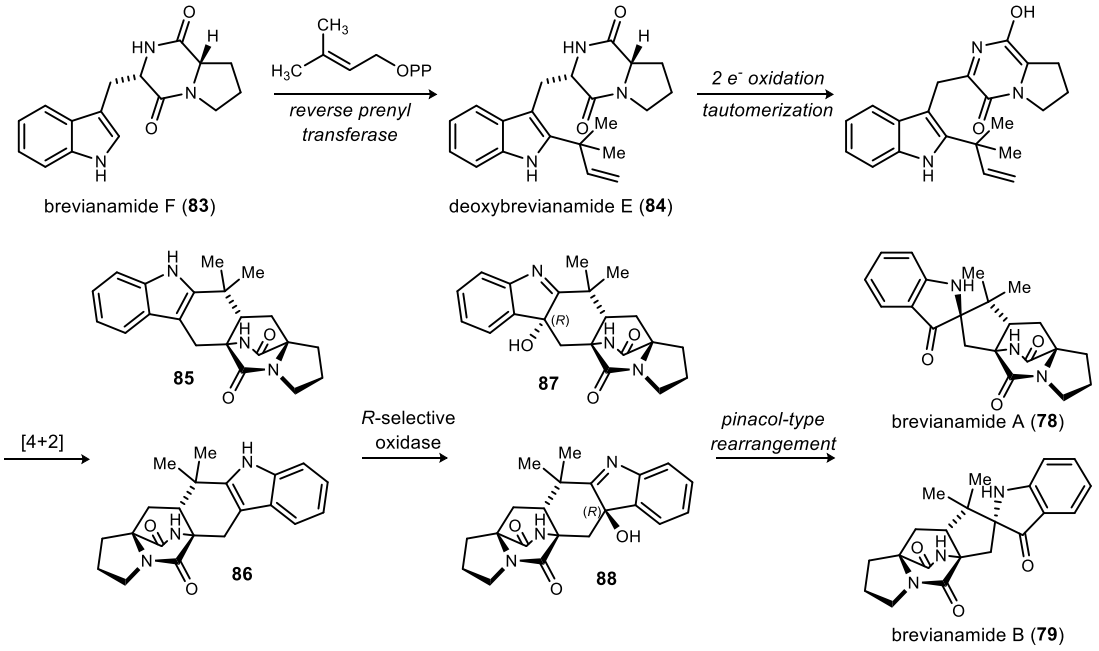

87 and **88** which undergo a stereospecific Pinacol rearrangement to furnish both naturally occurring brevianamides A (**78**) and B (**79**). The implications of this biosynthetic proposal have not gone unnoticed.

Brevianamide A is produced in a quantity ~20-fold greater than brevianamide B. Thus, either the Diels-Alder reaction produces **85** and **86** in unequal, nonracemic form favoring **85**, or a kinetic resolution takes place in the oxidation of racemic mixture of **85** and **86**. If the former were true, intervention of an enzyme (a Diels-Alderase) would be necessary. Moreover, this Diels-Alderase would explain the complete diastereoselectivity observed in the biosynthesis. Only the *anti*-C19 configuration is produced; this is the minor diastereomer produced in the thermal Diels-Alder reaction.

Second, since both brevianamides A and B share the same (*R*) stereochemistry at the indoxyl spirocenter, the oxidation of **88** would take place from the less hindered face to form brevianamide B and the *more hindered face* of **89** for brevianamide A. The preferred facial selectivity of this oxidation has been established in the semisynthesis of brevianamide B from A. An (*R*)-selective oxidase has been proposed to explain the diastereoselectivity of the oxidation step, however, no enzyme responsible for mediating the Diels-Alder reaction *or* indole oxidation has been characterized to date in *Pencillium brevicompactum.*

In later feeding experiments, it was shown that radiolabeled brevianamide F was not incorporated into brevianamide A or B.[79] As a result, a revised biosynthetic pathway was proposed (Scheme 46).[80] In this pathway, deoxybevianamide E (**84**) is first diastereoselectively oxidized by an (*R*)-selective indole oxidase, producing hydroxyindolenine **89**. This intermediate can then undergo nucleophilic addition to form brevianamide E (**82**); alternatively, **89** could undergo a stereospecific pinacol rearrangement to form **90**. **90** must then undergo a 2-electron oxidation to give the putative hydroxypyrazinone **91** which can then participate in the hetero-Diels-Alder reaction. This revised route was supported by feeding experiments, and at the same time, brevianamide E was

[79] Sanz-Cervera, J. F.; Glinka, T.; Williams, R. M. *Tetrahedron* **1993**, *49*, 8471.
[80] Sanz-Cervera, J. F.; Glinka, T.; Williams, R. M. *J. Am. Chem. Soc.* **1993**, *115*, 347.

recognized as a shunt metabolite which is not an intermediate in brevianamide A or B biosynthesis. To the best of our knowledge, attempts to synthesize **91** for feeding experiments to validate this pathway have been unsuccessful.

Scheme 46. Williams' Revised Biosynthetic Proposal

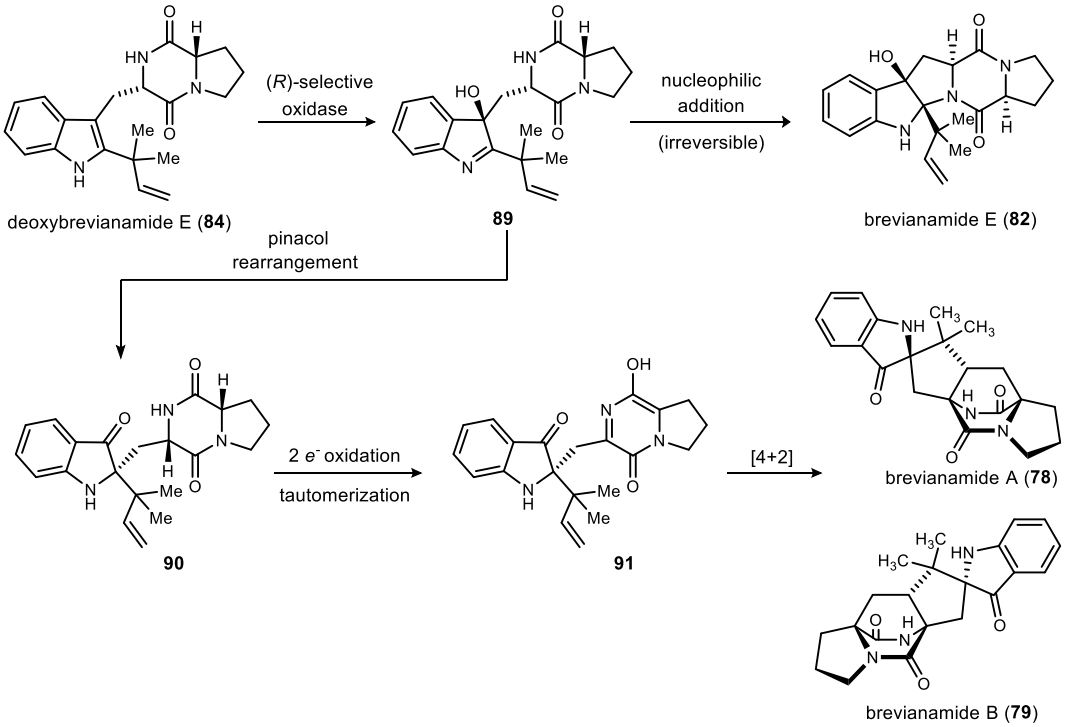

3.2 Previous Syntheses within the Brevianamide Class of Molecules

As part of their in-depth study on the brevianamides, Williams and coworkers were the first to synthesize (-)-brevianamide B.[76] They accomplished this synthesis by making use of a stereoselective $S_N2`$ cyclization to form the bicyclo[2.2.2]diazaoctane core (Scheme 47).

Beginning with aminal **92**, treatment with **93** formed amide **94**. *N*-Acylation of the proline ring followed by alkylative ring closure afforded **95**. Ozonolysis of the terminal olefin, Wittig olefination of the resulting aldehyde, and then alkylation afforded **96**. After considerable effort, they discovered that treatment of **97** with NaH in THF with several equivalents of 18-crown-6 afforded **97**, which containined the desired bicyclic core, in 4.9:1 dr. Subsequent treatment of **97** with HCl gave ring closure and concomitant Boc-deprotection to afford **98**. Oxidation of **98** afforded a single diastereomer of **99**. Finally, treatment of **99** with methanolic NaOMe induced a stereospecific pinacol rearrangement to (-)-brevianamide B (**79**). The relative stereochemistry was confirmed by X-ray crystallographic analysis.

Ten years later, the Williams group utilized a biomimetic intramolecular hetero-Diels-Alder reaction to synthesize racemic C19-epi-brevianamide A and brevianamide B (**Scheme 47**).[81] Treatment of epi-deoxybrevianamide E[82] with Meerwein's salt produced imino ether **100**. Oxidation with DDQ then afforded diene **100**. Upon exposure of **101** to KOH, the desired Diels-Alder precursor, achiral azadiene **102**, was produced.

---

[81] Williams, R. M.; Sanz-Cervera, J. F.; Sancenon, F.; Marco, J. A.; Halligan, K. M. *Bioorg. Med. Chem.* **1998**, *6*, 1233.
[82] As synthesized *via* Kametani's route (*vide infra*)

Azadiene **102** spontaneously cyclized to afford **103** as a 2:1 mixture of diastereomers. The major diastereomer was carried forward to the non-natural C19-epi-brevianamide A, and the minor diastereomer was used to form brevianamide B. Notably, this study demonstrated the chemical feasibility of an intramolecular Diels-Alder reaction of a hydroxypyrazinone intermediate in the biosynthesis of the bicyclo[2.2.2]diazaoctane portion of the brevianamides.

Scheme 47. Williams' Total Synthesis of (-)-Brevianamide B

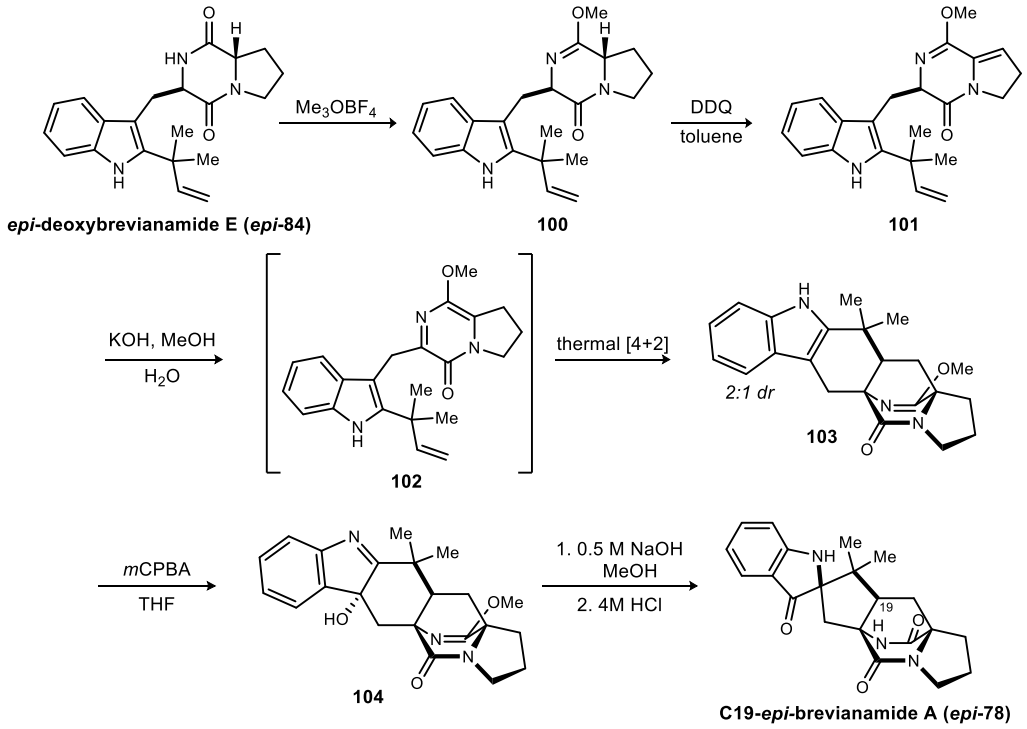

It should be noted that many groups have also studied routes toward the synthesis of this core and the total synthesis of related natural products.[83] While the routes are interesting and innovative, they are mostly outside the scope of this dissertation, and will not be discussed further.

3.3 The Development of a Chiral Proton Catalyzed Hetero-Diels-Alder Reaction[84]

3.3.1 Synthetic Strategy

The proton (H^+) is arguably the most common Lewis acid found in nature, and many enzymes use hydrogen bonds (X-H or $[X\text{-}H]^+$) to carry out asymmetric transformations with awe-inspiring selectivity. These "natural" acid catalysts have served over the years as an inspiration to synthetic chemists for the development of both reagent-controlled regioselective and stereoselective biomimetic bond-forming transformations.[85]

Over the past decade, the Johnston group has been dedicated to investigating what we term "chiral proton catalysis" (*vide supra*). As mentioned previously, chiral bis(amidine) acid salts have found notable success in

[83] For a comprehensive review see: Miller, K. A.; Williams, R. M. *Chem. Soc. Rev.* **2009**, *38*, 3160.
[84] Sprague, D. J.; Nugent, B. M.; Yoder, R. A.; Vara, B. A.; Johnston, J. N. *Org. Lett.* **2015**, *17*, 880.
[85] Kirschning, A.; Hahn, F. *Angew. Chem., Int. Ed. Engl.* **2012**, *51*, 4012.

promoting asymmetric aza-Henry (nitro-Mannich) reactions, nitroalkane alkylations, enantioselective halolactonizations, and most recently asymmetric iodocarbonations *via* the capture of CO_2 by homoallylic alcohols. These successes have established the foundation for chiral proton catalysis in asymmetric reaction development, and have also provided the opportunity to explore mechanistically distinct transformations utilizing the same basic scaffold design (bis(amidines) and their salts), showing that, indeed, chiral proton catalysis can be a general tool for asymmetric catalysis. Based on this, we turned our attention to the application of chiral proton catalysis in natural product synthesis.

Inspired by nature, we were intrigued by the notion that a chiral proton complex might emulate the role of an enzyme in a biomimetic reaction – one in which the small molecule ligand uses the same chemical functionality to achieve activation and stereocontrol much like its larger enzymatic counterpart. The recent success the field has seen suggests that molecules as large as proteins may not be necessary to achieve the high levels of stereoselectivity exhibited in enzyme-mediated reactions.

The Diels-Alder reaction ([4+2] cycloaddition) is one of the most powerful transformations in synthetic organic chemistry, allowing for the rapid generation of complex six-membered rings with multiple stereocenters in a single step. The growing number of naturally occurring compounds with structures resembling Diels-Alder adducts have stimulated numerous biosynthetic proposals involving enzyme-mediated [4+2] cycloadditions.[86] At least two potential Diels-Alderases have been characterized,[87,88] a definite enzyme mediated [4+2] cycloaddition has just been discovered,[89] and the mechanistic details of another standalone natural Diels-Alderase has very recently been reported.[90,91]

As described earlier, a biological Diels-Alder reaction was proposed by both Sammes and Williams to be responsible for the formation of the brevianamide diazabicyclo[2.2.2]octane core. That this hypothesis is plausible was further supported by both synthetic and biological studies. Furthermore, the intervention of a Diels-Alderase has been suggested to account for the selective formation of the major metabolite, brevianamide A, as well as the exclusive *anti* diastereoselectivity seen in these natural products (*vide supra*). Although brevianamide B has been previously synthesized in enantioenriched form, to the best of our knowledge *there has been no attempt to carry out the proposed biosynthetic Diels-Alder reaction enantioselectively*. Therefore, this hypothetical cycloaddition seemed like a good inspiration from which to develop a synthetic "Diels-Alderase".

---

[86] For a recent, very insightful review on the field: Klas, K.; Tsukamoto, S.; Sherman, D. H.; Williams, R. M. *J. Org. Chem.* **2015**, *80*, 11672.

[87] Auclair, K.; Sutherland, A.; Kennedy, J.; Witter, D. J.; Van den Heever, J. P.; Hutchinson, C. R.; Vederas, J. C. *J. Am. Chem. Soc.* **2000**, *122*, 11519.

[88] Watanabe, K.; Mie, T.; Ichihara, A.; Oikawa, H.; Honma, M. *J. Biol. Chem.* **2000**, *275*, 38393.

[89] Zheng, Q.; Guo, Y.; Yang, L.; Zhao, Z.; Wu, Z.; Zhang, H.; Liu, J.; Cheng, X.; Wu, J.; Yang, H.; Jiang, H.; Pan, L.; Liu, W. *Cell Chem Biol* **2016**, *23*, 352.

[90] Byrne, M. J.; Lees, N. R.; Han, L. C.; van der Kamp, M. W.; Mulholland, A. J.; Stach, J. E.; Willis, C. L.; Race, P. R. *J. Am. Chem. Soc.* **2016**, *138*, 6095.

[91] Minami, A.; Oikawa, H. *The Journal of antibiotics* **2016**. doi: 10.1038/ja.2016.67.

Based on the knowledge gained throughout the lab from our continuous studies on the aza-Henry reaction, the putative brevianamide Diels-Alder intermediate (in **Figure 17**) was thought to be a feasible candidate for catalysis with BAM ligand-protic acid complexes. Therefore, we had hoped to investigate a [4+2] cycloaddition in the context of a very specific system – that which would lead to the diazabicyclic core. The relative planarity of the 2-hydroxypyrazinone moiety, analogous to the *N*-Boc imines, was envisioned to permit access to the sterically congested BAM chiral pocket (**Figure 18**). This intermediate also offers multiple Lewis basic sites for proton binding, a prerequisite for high enantioselectivity in the catalyzed aza-Henry reaction. With these characteristics

Figure 18. Lateral Application of Bis(Amidine) Catalyst Design Features to the Hetero-Diels-Alder Reaction

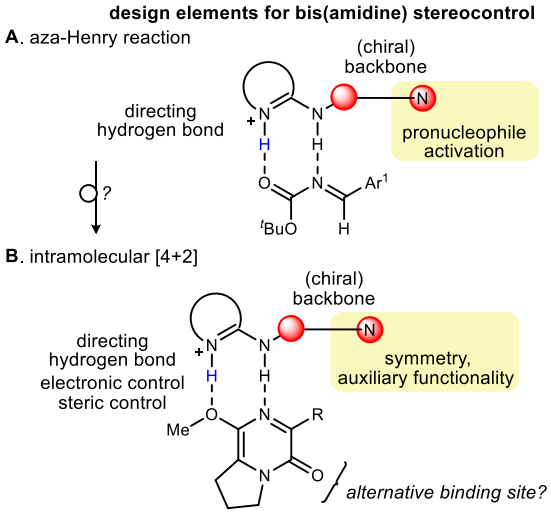

in mind, the synthesis of the enantioenriched core of the brevianamides seemed to be a real possibility.

In order to efficiently synthesize the bicyclooctane core, the chiral proton catalyst must be able to direct both enantio- and diastereocontrol of the hetero-Diels-Alder reaction. Chelation of the pyrazinone amidate to the BAM-acid complex is envisioned to occur in a bidentate manner, analogous to the stereochemical model developed for *N*-Boc imines that was adopted for the aza-Henry reaction. The BAM ligand must then effectively destabilize the transition state formed by approach of the tethered dienophile from one face of the planar pyrazinone relative to the opposite face in order to give enantioselection (Figure 19). If facial discrimination is accomplished, then the use of the opposite enantiomer of the BAM catalyst would also furnish the opposite enantiomer of the Diels-Alder adduct, providing access to the cores of both brevianamide A and B.

Figure 19. BAM•HX:Azadiene Complex – Diene Facial Discrimination Leads to Opposite Enantiomers of the Core.

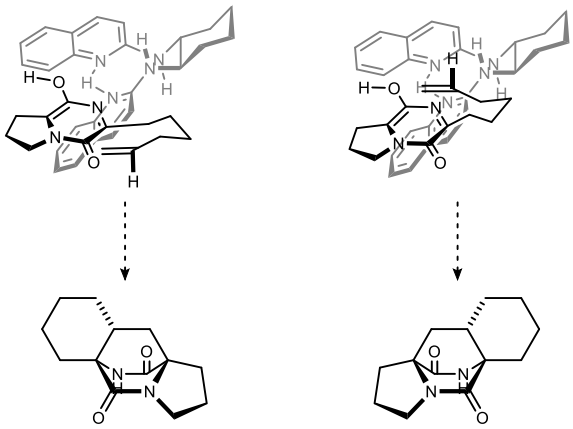

The diastereoselectivity of the reaction also must be considered, and is determined by the preference for the *endo* or *exo* orientation of the prenyl olefin in the transition state of the reaction (Figure 20). The *endo* transition state is favored in the thermal variant of this reaction (*vide supra*), which produces the *syn* configuration at C19 (see Figure 16 for nomenclature). Therefore, the catalyst will be called upon not to enhance, but rather *completely reverse* the *endo*:*exo* relationship from the thermal reaction. To allow access to the brevianamide core, this is critical. However, in the presence of high enantioselection for the core, and high ***syn*** selectivity, this would prove useful to synthesizing other related alkaloids which are postulated to be synthesized biologically in the same way.

Figure 20. Model for *endo vs. exo* Selectivity

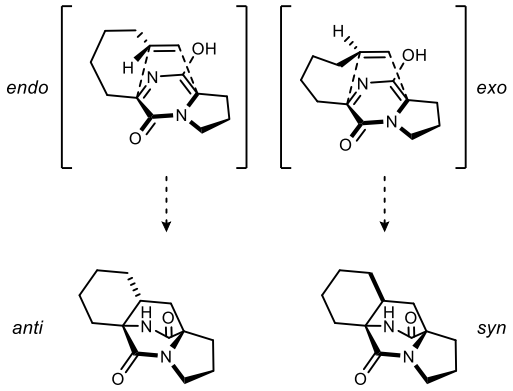

Utilization of a chiral proton complex to catalyze this Diels-Alder reaction would not only provide the first enantioselective *biomimetic* synthesis of this class of natural products, but would also support the chemical feasibility of this relatively unknown biological [4+2] reaction. It should be noted that we are not suggesting that the demonstration of a chiral proton catalyzed [4+2] cycloaddition to form the core unequivocally proves the existence of a Diels-Alderase in nature, but rather would shed additional light onto the biosynthesis of this inspiring, and structurally intriguing family of alkaloids. Furthermore, it would provide a compelling basis to further explore the biosynthesis of these natural products. In addition to the intriguing biosynthetic possibilities that would result from these studies, the work has intrinsic synthetic value too. That is, if successful, this would be a rare example of an enantioselective hydrogen bond-mediated inverse electron demand aza-Diels-Alder reaction.

3.3.2 Synthesis and Scale-Up of the aza-Diene Precursor

In order to efficiently and effectively develop this reaction, a substantial supply of the (known) substrate was necessary. We were able to increase the scale and cost effectiveness of the synthesis by combining methods developed by Danishefsky**Error! Bookmark not defined.** and Perrin[92] (Scheme 48).

The amine nitrogen of tryptophan was phthaloyl-protected smoothly on 382 mmol scale. The resulting *N*-phthaloyl tryptophan was converted to methyl ester **76** upon heating with methanolic acetyl chloride at 65 °C. It should be noted that this reaction is extremely sensitive to heating conditions; an increase of temperature to 75 °C reproducibly resulted in dramatically decreased yields. Installation of the reverse prenyl group proceeded exceedingly well on scale. Purification of the resulting solid proved challenging, as excess cyclooctadiene and boron byproducts were frequently seen. However, these impurities seemed to have no effect on the phthalate deprotection, which provided the free amine in 53% yield over the two step procedure. Attempts to optimize the deprotection by heating or using excess hydrazine resulted in dimerization of the desired product to afford the dipeptide.

Scheme 48. Large Scale Synthesis of the Azadiene Precursor

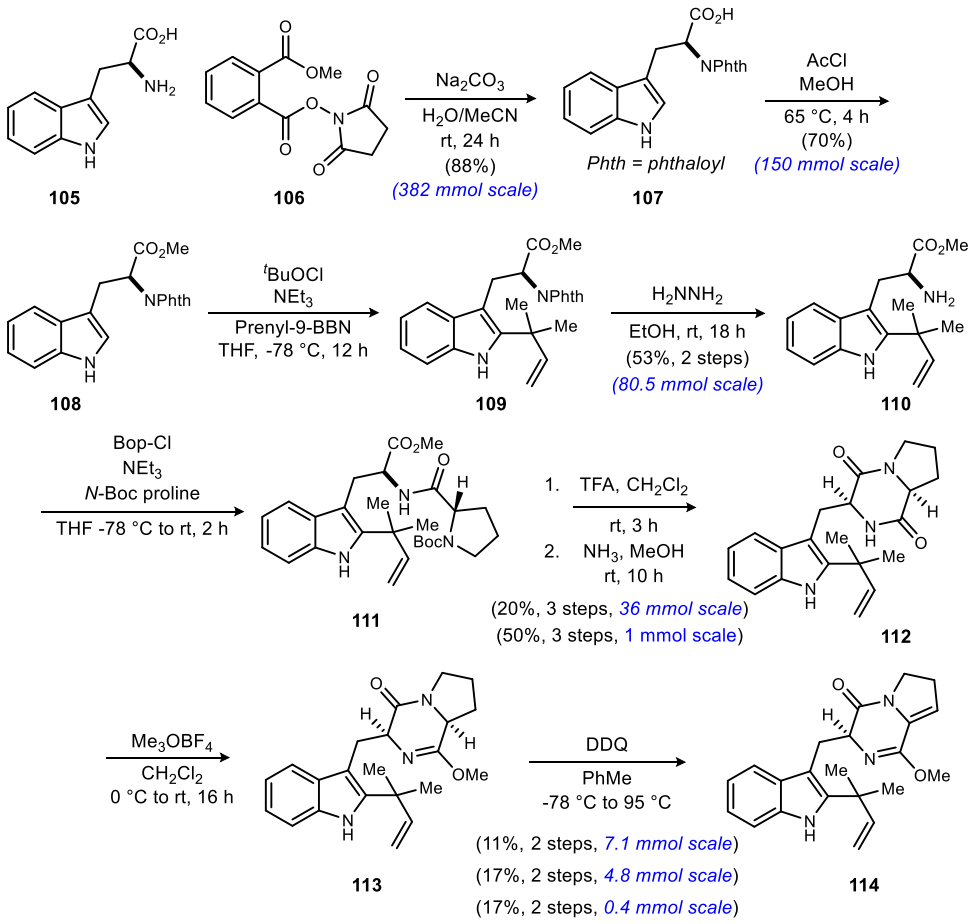

[92] Zhao, L.; May, J. P.; Huang, J.; Perrin, D. M. *Org. Lett.* **2012**, *14*, 90.

With **110** in hand, we undertook the endgame of the synthesis. Coupling of *N*-Boc proline, followed by Boc deprotection afforded a crude purple residue which was dissolved in methanolic ammonia and stirred to promote the cyclization to **112**. On 1 mmol scale, this procedure worked well. Unfortunately, upon scaling up we were only able to obtain up to 20% yield reproducibly. Nevertheless, **112** was treated with the methyl version of Meerwein's reagent to produce the imino ether which was then oxidized by DDQ. This provided **113** in 10-20% yields over the 2 steps. Despite the poor yields late in the synthesis, a review of the literature suggests that this was not to be unexpected.[93] Thus, over 10 steps (5 purifications) we were able to obtain sufficient amounts of the desired azadiene precursor in order to investigate the BAM-chaperoned hetero-Diels-Alder reaction. The diene was stored as compound **114**, and then isomerized directly before the experiment, as it spontaneously undergoes cycloaddition in the conjugated *s-cis* conformation.

3.3.3 Development of the Reaction Conditions and Catalyst Optimization – The First Chiral Proton-Controlled Hetero-Diels-Alder Reaction

With the requisite material in hand, attempts were made to optimize the isomerization of the stored compound (**114**) to the reactive intermediate (**115**) with the goal being to drive the reaction as far to completion as possible while simultaneously not allowing any cycloaddition (to **116**) to occur before chiral ligand is added to the mixture (Table 3). Optimal conditions were to treat **114** with aqueous KOH in methanol for 45 minutes at 0 °C, and then 45 minutes at ambient temperature before workup and catalyst addition. This led to 90% conversion to the azadiene without any cycloaddition occurring (Table 3, entry 2).

Table 3. Optimization of KOH-Induced Cyclization to *s-cis* Azadiene

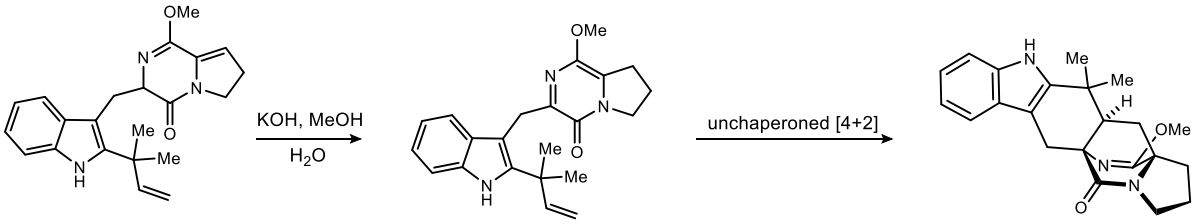

114 **115** **116**

entry	time, 0 °C (min)	time, rt (min)	ratio of 82:83:84
1	30	30	40:60:0
2	45	45	10:90:0
3	60	60	0:90:10
4	30	240	0:60:40

[93] There are very few methods that efficiently accomplish this type of oxidation.

With conditions to the azadiene optimized, we next examined the rate of the [4+2] cycloaddition. This was accomplished by sampling the reaction to determine conversion by ^{1}H NMR spectroscopy (Figure 21). The kinetics of cyclization are consistent with a unimolecular reaction, leading to full conversion at 43 hours (25 °C). Knowing more precisely the time to completion, we established 48 hours as the standard experiment time, since any conversion of unreacted diene during the workup procedure would lead to racemic product, thereby thwarting our efforts toward a stereoselective reaction.

Figure 21. Preparation of **83**, and ^{1}H NMR Study of its Thermal (25 °C) Cycloaddition Rate to **116**.

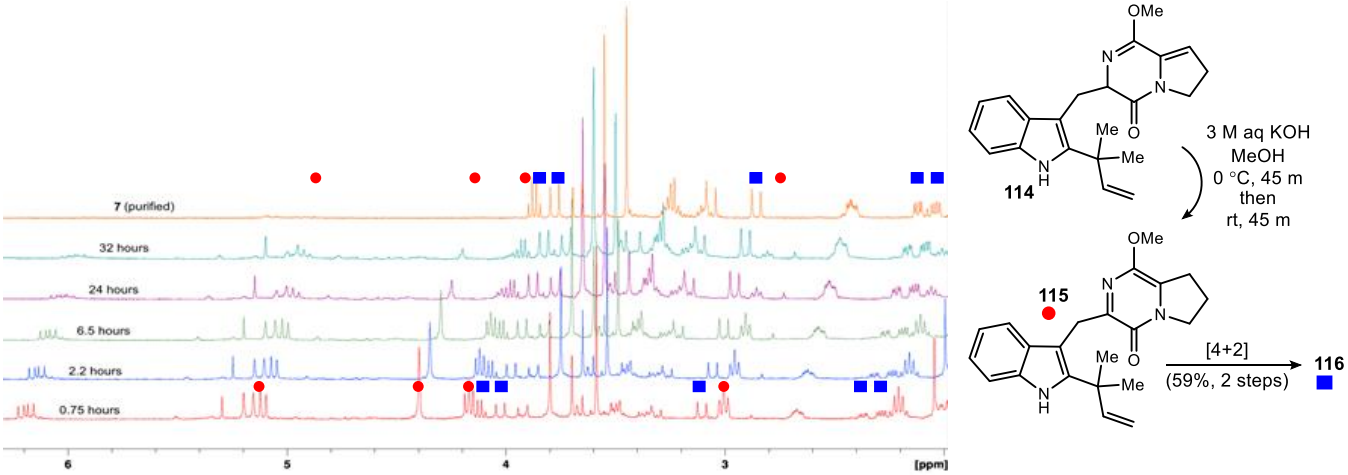

[a]Isomerization of purified **114** was effected as in described in Table 3 (See Supporting Information for full details). Time: t = 0 established as time of first analysis by ^{1}H NMR for this experiment. Selected peaks labeled for **115** (●) and **116** (■). Residual CH_2Cl_2 (5.3 ppm) used as an internal standard and reference point. [b]Composition calculated using integrations of **115** and **116**, defined as **116**/(**115**+**116**).

After we determined a standard reaction time, numerous attempts were initially made to chaperone the cycloaddition in solution in the presence of a chiral Brønsted acid such as **14**. These experiments uniformly provided racemic cycloadduct. We hypothesized that perhaps the chaperone:substrate interaction is a fairly weak one, and therefore solvation may be inhibiting this interaction from happening in any stereoselective manner. Since the solvent is merely a matter of convenience in reaction setup and analysis, a protocol was developed that involved the preparation of **115** at low temperature, division of a batch into 2-4 separate experiments, addition of chaperone and solvent, mixing, and then solvent removal *in vacuo*, all at low temperature. The resulting film containing a 1:1 mixture of **115**:chaperone was maintained at ambient temperature for 48 h prior to workup and analysis. This allowed an equimolar mixture of substrate and organocatalyst to convert to product as a neat residue. This protocol resulted in two distinct outcomes: (1) the expected formation of the cycloadduct **116** along with the organocatalyst, or (2) a complex mixture of products sometimes devoid of the desired cycloaddition product. Table 4 shows the results from a wide variety of chaperones and the discovery of the optimal chaperone. For a complete summary of ligands examined and the corresponding results, see Appendix A.

The parent bis(amidine), H,Quin-BAM (**14**), contains two potential polar covalent hydrogen bond donors for stereocontrol, but it provided results identical to the thermal cycloaddition (Table 4, entries 1 and 2). Use of its triflic acid complex (installing a polar-ionic hydrogen bond donor) revealed a subtle, but detectable, increase in both diastereomeric and enantiomeric ratios (Table 4, entry 3). On the basis of the similarity in size between the catalyst and substrate and the assumption that the substrate-binding site would be at the aminopyridinium ion,

Table 4. Application of Chiral Hydrogen bonding Small Molecules to the Intramolecular Hetero-Diels-Alder Cycloaddition of Azadiene **83**

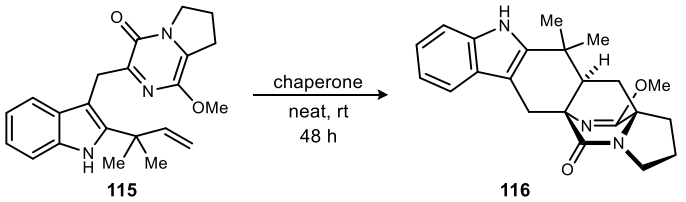

entry[a,b]	chaperone	dr[c]	er[d]
1	none	1.3:1	50:50
2	H,Quin-BAM	2:1	50:50
3	H,Quin-BAM•HOTf	2.8:1	54:46
4	H,^{5}Me-BAM•HOTf	1.3:1	53:47
5	H,$^{4}CF_3$Quin-BAM•HOTf	1.9:1	54:46
6	PBAM•HOTf	1.6:1	53:47
7	H,^{8}MeO-PBAM•HOTf	1.7:1	54:46
8	(*S,S*)-StilbPBAM•HOTf	2:1	49:51
9	(*S,S*)-^{4}MeOStilbBAM•HOTf	1:1.1	43:57
10	H,^{3}Quin-BAM•HOTf	3.5:1	64:36
11	H,Quinox-BAM•HOTf	3.5:1	67:33
12	H,Quin-BAMide•HOTf	2.1:1	72:28
13	H,^{3}Quin-BAM	1.3:1	45:55
14	*ent*-H,^{3}Quin-BAM•HOTf	4.2:1	38:62
15	H,^{3}Quin-BAM•HO_2CCF_3	1.9:1	50:40
16	H,^{3}Quin-BAM•HCl	2.5:1	57:43
17	H,^{3}Quin-BAM•HBF_4	2.7:1	59:41
18	H,^{3}Quin-BAM•$HSbF_6$	2.9:1	66:34

[a]The substrate was prepared as described in Table 3, combined with the chaperone in dichloromethane, and concentrated to a neat film, all at 0 °C or below until final warming to room temperature for the chaperoned reaction. Isolated yields generally ranged from 50% to 70%. Absolute configuration as depicted is arbitrary, relative stereochemistry reported as *syn:anti*. [b]Results are reported as an average of reactions. [c]Determined by relative integration of MeO methyl (^{1}H NMR of crude reaction mixture). [d]Determined by HPLC using Chiralcel OD-H stationary phase.

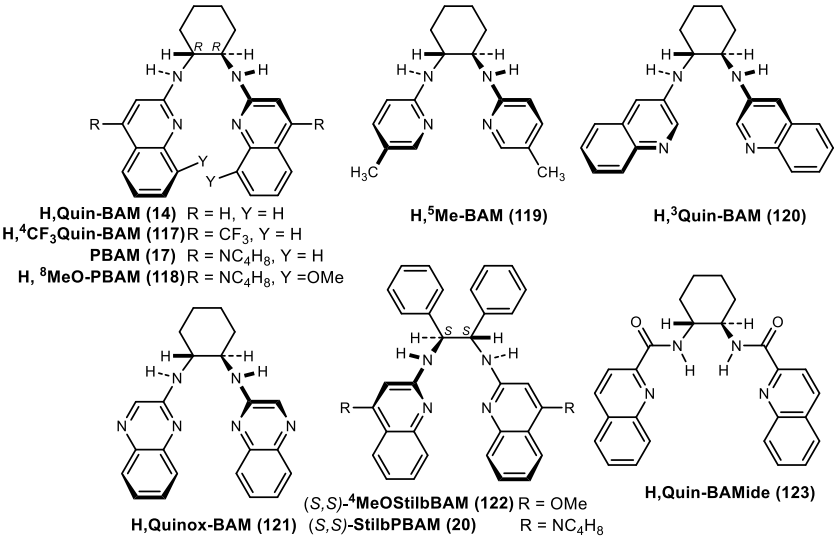

H,^{5}Me-BAM•HOTf was evaluated for its more open binding area. Unfortunately, this led to nearly racemic product (Table 4, entry 4).

Attempts to modulate the polarity of the hydrogen bond by substitution of the aminoquinoline at the 4-position with electron-withdrawing (trifluoromethyl) or –donating (pyrrolidine) groups led to equally nonselective reactions (Table 4, entries 5 and 6). Utilizing H,^{8}MeO-PBAM•HOTf represented an attempt to affect the coordination chemistry of the key hydrogen bond by a proximal oxygen. Failing to affect the coordination chemistry in a productive fashion, this chaperone produced a product with similar selectivity to the thermal reaction (Table 4, entry 7).

Another attempt to rationally and modestly change the angles within the binding pocket involved the use of the stilbene diamine backbone alternative to cyclohexane diamine. StilbPBAM•HOTf delivered product with results comparable to its counterpart PBAM•HOTf (Table 4, entry 8). However, the 4-methoxy-substituted variant effected an interesting change in diastereoselection, with a small preference for the minor diastereomer produced under all conditions to this point (Table 4, entry 9).

Significant improvement in selectivity was ultimately achieved by more profound changes in ligand structure, if even less rational in overall design.[94] Regioisomeric chaperone H,^{3}Quin-BAM•HOTf, in which the diamine is connected *via* C3 of the quinoline rather than C2 led to as high as 3.5:1 dr and 64:36 er (Table 4, entry 10). The hydrogen bond donating ability of this aminoquinoline regioisomer is quite different, and the possibility of intramolecular hydrogen bonding is limited. A quinoxaline ligand, H,Quinox-BAM•HOTf, was next examined, as it combined both the 2- and 3-aminoquinoline substructures. This chaperone was even more selective, at 3.5:1 dr and 68:32 er (Table 4, entry 11). Ultimately, a ligand that combined both quinolinium and amide functional groups provided the maximum enantioselection observed during these studies: H,Quin-BAMide. This chaperone afforded the cycloadduct in 2.1:1 dr and 72:28 er (44% ee) (Table 4, entry 12).

After the discovery of H,Quin-BAMide, we set out to optimize the binding pocket around the bis(amide) functionality. However, multiple attempts at structure modifications did not afford any improvement from the parent compound (Appendix A).

With no improvement *via* structure modification, a final study was undertaken to more clearly establish the influence of the polar ionic hydrogen bond on the observed stereoselectivity. A series of acid salts prepared from H,^{3}Quin-BAM were deployed in parallel experiments.[95] Compared to the free base which exhibited low selectivity for the opposite enantiomer normally observed (Table 4, entry 13), use of acid salts bearing increasingly less-coordinating character displayed a trend of increasing selectivity, in the order: HO_2CCF_3, HCl, HBF_4, HOTf, $HSbF_6$ (Table 4, entries 10, 14-18). The diastereomeric ratios also tracked higher along this order. This behavior might be interpreted to further highlight the importance of the proton's coordination sphere for its influence on both relative and absolute stereocontrol.[96] Increasing *syn* diastereoselection that tracks with

[94] See the Supporting Information for a bar graph visually depicting increasing enantioselection as a function of the chiral chaperone employed.

[95] The effect of the counterion on selectivity was best demonstrated using this free base. Attempts at deploying salts of H,Quin-BAMide unfortunately resulted in significant decomposition and intractable mixtures.

[96] The influence of an achiral counteranion on enantioselection has been demonstrated in chiral proton catalysis: Dobish, M. C.; Johnston, J. N. *J. Am. Chem. Soc.* **2012**, *134*, 6068.

increasing enantioselection is consistent with the binding hypothesis depicted in Figure 18. The catalyst binding as shown would be expected to sterically disfavor the formation of the *anti* diastereomer.

In conclusion, we were able to demonstrate that a chiral polar ionic hydrogen bond can induce enantioselectivity in a hetero-Diels-Alder reaction which produces the core of the brevianamide natural products. Collectively, these studies establish the ability to modulate diastereo- and enantioselectivity using a collection of small molecule chaperones functioning solely by the principles of hydrogen bond donor/acceptor interactions. It was not possible to determine whether these chaperones accelerated the rate of cycloaddition relative to thermal energy alone,[97] but their ability to control stereoselection using hydrogen bonding at ambient temperature does provide a discrete chemical context for the proposal that certain enzymes chaperone [4+2] cycloadditions.[98] Notably, *this catalyst class can now be considered a basis for rendering Williams' total synthesis enantioselective.*

Further improvements in enantioselection might be achieved by increasing the size of the chaperone. In principle tools are in place to achieve this using short peptide catalysis,[99] enzyme evolution techniques,[100] or the tools of calculation *in silico* and the strategy of enzyme repurposing.[101,102]

The *chemical feasibility* of an enantioselective Brønsted acid catalyzed hetero-Diels-Alder reaction for brevianamide synthesis is established for the first time through our studies. There is great potential in the development of a small molecule Diels-Alderase and its application in a biosynthesis-inspired natural-product total synthesis whether or not a brevianamide-class Diels-Alderase is ever discovered.

---

[97] Neither a direct analysis of the neat reaction mixture using spectroscopic methods nor a low-temperature analysis/workup that removes the contribution of unchaperoned cyclization was possible.

[98] Unfortunately, the absolute configuration of these cycloadducts could not be determined. As a result, it is not yet possible to propose stereochemical models for the observed enantioselectivity.

[99] Miller, S. J. *Acc. Chem. Res.* **2004**, *37*, 601.

[100] Birmingham, W. R.; Starbird, C. A.; Panosian, T. D.; Nannemann, D. P.; Iverson, T. M.; Bachmann, B. O. *Nat. Chem. Biol.* **2014**, *10*, 392.

[101] Linder, M.; Johansson, A. J.; Manta, B.; Olsson, P.; Brinck, T. *Chem Commun (Camb)* **2012**, *48*, 5665.

[102] Reetz, M. T. *Chem. Rec.* **2012**, *12*, 391.

Chapter 4. Progress Toward The Synthesis of Morphine-Related Tetrahydroisoquinoline Derviatives

4.1 A Brief Introduction to Morphine

Morphine (**124**) has a fascinating history,[103] with pharmacological, societal, and historical impact on humans. The isolation of morphine precedes Wöhler's synthesis of urea (the 'beginning of organic chemistry') by 25 years. It was isolated from opium by Sertürner in 1805, but the structure was not confirmed for another century. Sertürner was also the first person to perform human and animal trials with morphine.[104]

Morphine and its cogeners codeine, thebaine, and oripavine are opioids derived from the poppy plant and are of great importance to both the medical and chemical communities (**Figure 22**). Academically, the total synthesis of these alkaloids began in 1952 with Gates' seminal publications[105] and continues to this day. Medicine requires a constant supply of morphine and other structurally related analgesics for basic pain control. All of the unnatural derivatives are obtained *via* semisynthesis starting from the naturally occurring alkaloids which are primarily harvested in Asia and Tasmania for legal consumption. It is difficult to accurately estimate the worldwide requirements for these compounds. In 2007, it was estimated that the world consumption of oxymorphone was

Figure 22. Morphine and Some Opioid Derivied Agonists and Antagonists

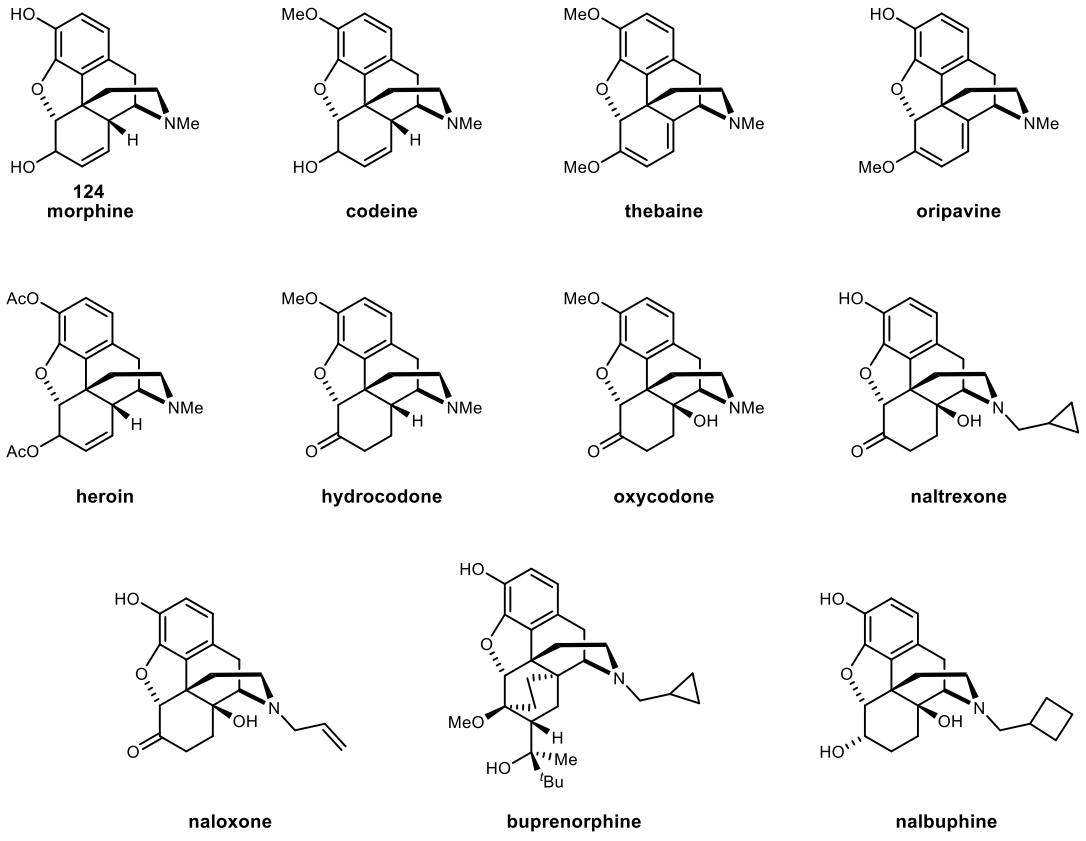

[103] Booth, M. *Opium: A History*; St. Martin's Press: New York, 1998; L.D., K. *Opium Poppy: Botany, Chemistry, and Pharmacology*; Food Products Press: New York, 1995.
[104] Klockgether-Radke, A. P. *Anästhesiol Intensivmed Notfallmed Schmerzther* **2002**, *37*, 244.
[105] Gates, M.; Tschudi, G. *J. Am. Chem. Soc.* **1952**, *74*, 1109; Gates, M.; Tschudi, G. *J. Am. Chem. Soc.* **1956**, *78*, 1380.

16.8 tons. Likewise, estimates for global consumption of naltrexone and naloxone combined may be as high as 10 tons. Unsurprisingly, to date there is no practical source of morphine, either by chemical synthesis or through fermentation, which would compete with the cost of isolation (~$400-700/kg).

Despite the multitude of advances in synthetic organic chemistry, the synthesis of morphine remains challenging. The formal synthesis by Rice and coworkers[106] is still its most efficient chemical preparation (**Scheme 49**). There have been plenty of other creative syntheses in the literature, which should be noted, however they all lack pharmaceutical practicality except for Rice's synthesis, which could have potential for scale-up processes.[107] To date, the only process that could conceivably come close to the cost effectiveness of isolation would be fermentation, unfortunately, there is no effective, efficient fermentation process in existence.

Scheme 49. Rice's Formal Synthesis of Morphine

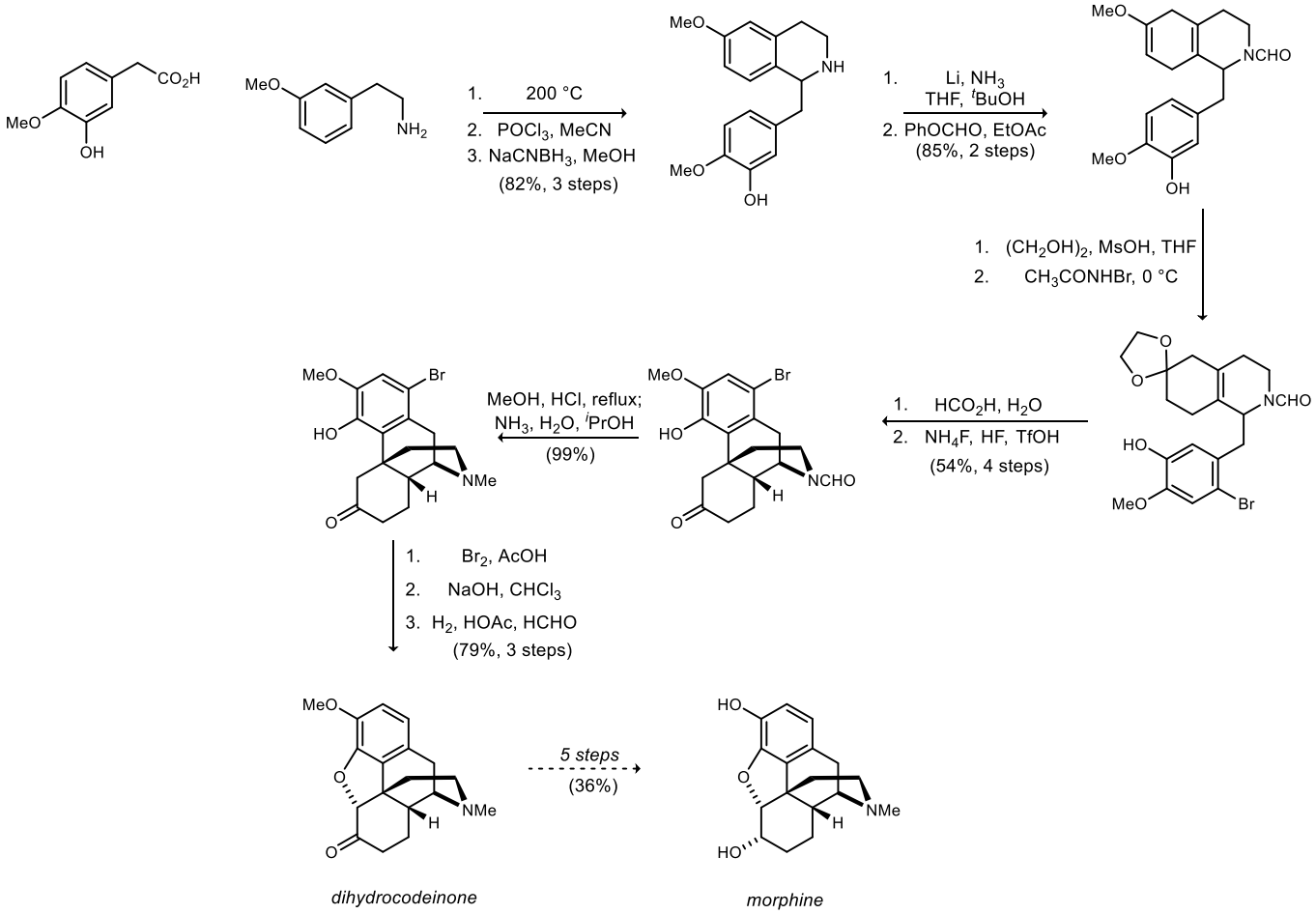

Recently, pieces of the biosynthetic pathway from glucose to morphine have been reconstituted in yeast (**Scheme 50**). It is possible to synthesize (*S*)-reticuline from glucose[108] and morphine from (*R*)-reticuline.[109]

[106] Rice, K. C. *J. Org. Chem.* **1980**, *45*, 3135.
[107] Rinner, U.; Hudlicky, T. *Top. Curr. Chem.* **2012**, *309*, 33.
[108] DeLoache, W. C.; Russ, Z. N.; Narcross, L.; Gonzales, A. M.; Martin, V. J.; Dueber, J. E. *Nat. Chem. Biol.* **2015**, *11*, 465.
[109] Fossati, E.; Narcross, L.; Ekins, A.; Falgueyret, J. P.; Martin, V. J. *PLoS One* **2015**, *10*, e0124459.

Missing from this process is the ability to convert (*S*)-reticuline to (*R*)-reticuline.[110] Once this enzymatic step is reconstituted in yeast, it will be possible to produce morphine from glucose *via* fermentation. This would be a significant advance in the preparation of morphine, and also a significant accomplishment in bioengineering, however it probably will still not outcompete the cost-effectiveness of isolation of the natural product from the natural sources.

Scheme 50. A Depiction of the Morphine Biosynthetic Pathway Reconstituted in Yeast Cells

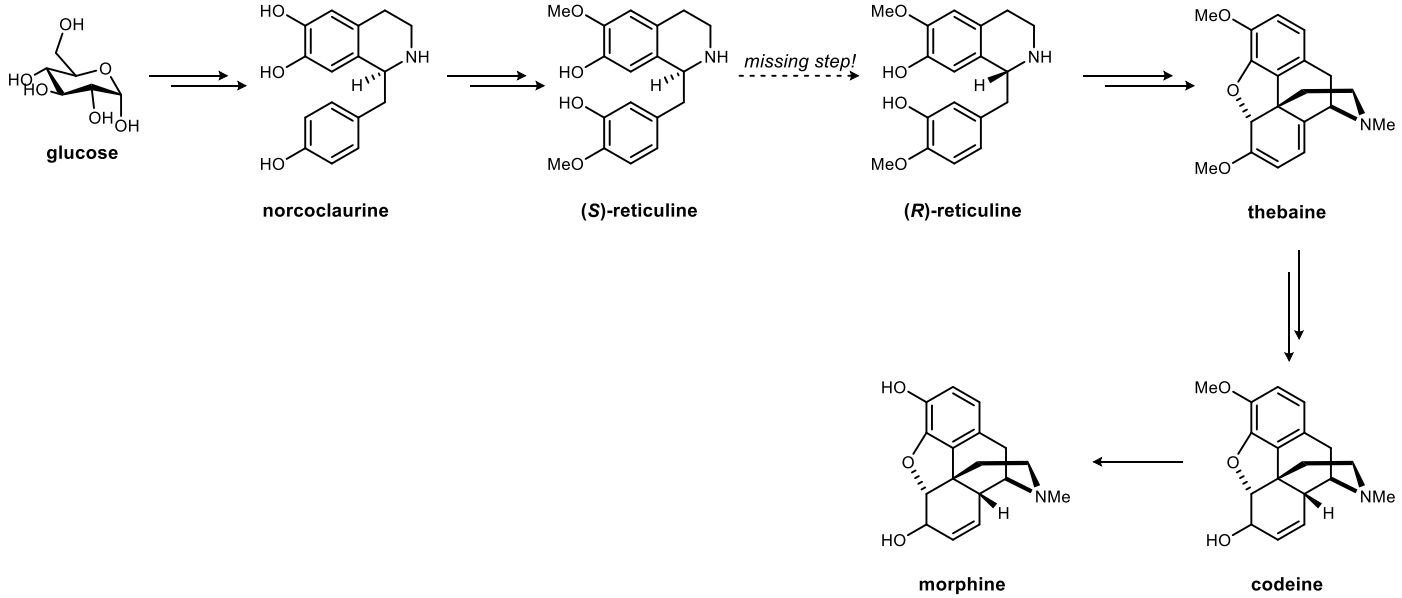

More interesting would be to harness the power of bioengineering and fermentation to synthesize unnatural analogues of morphine on scale.[111] We wondered if we would be able to chemically synthesize analogues of norcoclaurine and (*R*)-reticuline which could be fed into the biosynthetic pathway to ultimately synthesize morphine analogues with interesting biological activities. If so, microbial synthesis could be a powerful alternative to ineffective or impractical chemical syntheses of interesting morphine analogues which could then be used in biological studies. The following sections will discuss our design of and progress toward investigating this idea.

4.2 A Brief Introduction to Fluorine and Fluorine Containing Compounds

The fluorine atom possesses many unique properties which make it significant in pharmaceutical, agrochemical, and materials sciences.[112] Industrial sources estimate that as many as 30-40% of agrochemicals and 20% of pharmaceuticals on the market contain fluorine.[113] These numbers are expected to continue to increase in the coming years given recent advances in fluorine chemistry in concurrence with favorable data from previous fluorinated molecules.

---

[110] This enzyme in poppy plants has recently been identified: Winzer, T.; Kern, M.; King, A. J.; Larson, T. R.; Teodor, R. I.; Donninger, S. L.; Li, Y.; Dowle, A. A.; Cartwright, J.; Bates, R.; Ashford, D.; Thomas, J.; Walker, C.; Bowser, T. A.; Graham, I. A. *Science* **2015**, *349*, 309. Alternatively, another group has discovered a fusion protein which can accomplish the same task – effectively completing the pathway: Galanie, S.; Thodey, K.; Trenchard, I. J.; Filsinger Interrante, M.; Smolke, C. D. *Science* **2015**, *349*, 1095.
[111] It's already been observed that some of the enzymes in this pathway are rather promiscuous.
[112] Hiyama, T. In *Organofluorine Compounds: Chemistry and Applications*; Yamamoto, H., Ed.; Springer: New York, 2000.
[113] Purser, S.; Moore, P. R.; Swallow, S.; Gouverneur, V. *Chem. Soc. Rev.* **2008**, *37*, 320.

Fluorine arguably retains the most unique physiochemical properties of elements employed in synthetic organic chemistry. The small covalent radius of fluorine (C-F, F radius = 1.47 Å) along with its high electronegativity contribute to the atom's unique characteristics – handling, stability, and incorporation of the element into small molecules is challenging using traditional synthetic techniques.[114] Interestingly, naturally occurring fluorinated molecules are rare (fluoroacetic acid is one example)[115] and have no known biological activity, but a number of important pharmaceutical agents contain at least one fluorine atom. Collectively, fluorine substituents impart numerous chemical properties to their molecules, including lipophilicity, metabolic stability, and bioavailability.

Marketed by Hoffmann-LaRoche beginning in 1957, the antineoplastic compound 5-fluorouracil was the earliest reported fluorinated pharmaceutical agent (**Figure 23**).[116] It effects its anticancer activity by inhibiting thymidylate synthase, which in turn prevents the cellular synthesis of thymidine. This simple addition of fluorine to the nucleobase uracil significantly enhanced its desirable biological properties, and can be considered the grandfather of the modern interest seen in fluorine medicinal chemistry. Fluoxetine (Prozac, an antidepressant), fulvestrant (an anticancer agent), and the combination therapy efavirenz (an antiviral agent) are three other drugs, spanning a range of diseases and mechanisms of action, benefitting from the addition of the fluorine atom.

Prozac is one of the more well-known antidepressants, and was a blockbuster for Eli Lilly, with sales approaching $1B annually at its peak. The inclusion of a trifluoromethyl group in the *para*-position of the phenolic ring increases the potency for inhibiting serotonin uptake sixfold compared to the non-fluorinated parent compound.[117]

Efavirenz, an antiretroviral cocktail from Gilead and Bristol-Myers-Squibb, includes two structurally diverse fluorinated compounds. Structure-activity relationship studies showed the presence of the trifluoromethyl group in efavirenz improved drug potency by lowering the pK_a of the cyclic carbamate; this carbamate makes a key hydrogen bond contact with the HIV-1 protein. The trifluoromethyl group also acts to improve allosteric binding to HIV-1, altering the enzyme's conformation and inhibiting its activity.

Figure 23. Diverse, Fluorine-Containing Parmaceutical Agents

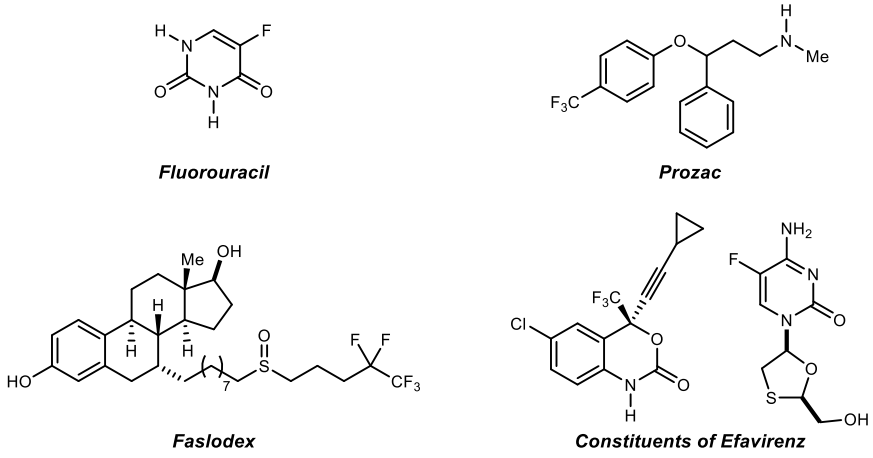

[114] O'Hagan, D. *Chem. Soc. Rev.* **2008**, *37*, 308.
[115] Vartiainen, T.; Kauranen, P. *Anal. Chim. Acta* **1984**, *157*, 91.
[116] Heidelberger, C.; Chaudhuri, N. K.; Danneberg, P.; Mooren, D.; Griesbach, L.; Duschinsky, R.; Schnitzer, R. J.; Pleven, E.; Scheiner, J. *Nature* **1957**, *179*, 663.
[117] Wong, D. T.; Bymaster, F. P.; Engleman, E. A. *Life Sci.* **1995**, *57*, 411.

β-Fluoroamines are a unique class of fluorinated compounds[118] that display remarkable CNS-penetrant properties (**Figure 24**). The most illustrious pharmaceutical agent with such a scaffold is arguably sofosbuvir, which is an RNA polymerase inhibitor responsible for recent high cure rates of the hepatitis C virus.[119] In addition to the success of sofosbuvir, there are recent examples of BACE and PIM kinase inhibitors which are clinical candidates containing β-fluoroamines for use in treatment of Alzheimer's dementia and leukemia. Furthermore, β-fluoroamines exhibit decreased amine basicity and enhanced binding interactions similar to the fluorinated motifs discussed earlier.[120] Understandably, the β-fluoroamine motif is a desirable functionality when targeting a wide array of disease states; notably, it improves biological efficacy in compounds with widely differing mechanisms of action. Despite this, from a synthetic standpoint there is a lack of direct methods to access both chiral, racemic *or* chiral, non-racemic β-fluoroamines.

Figure 24. Some β-Fluoroamine-Containing Pharmaceutical Agents

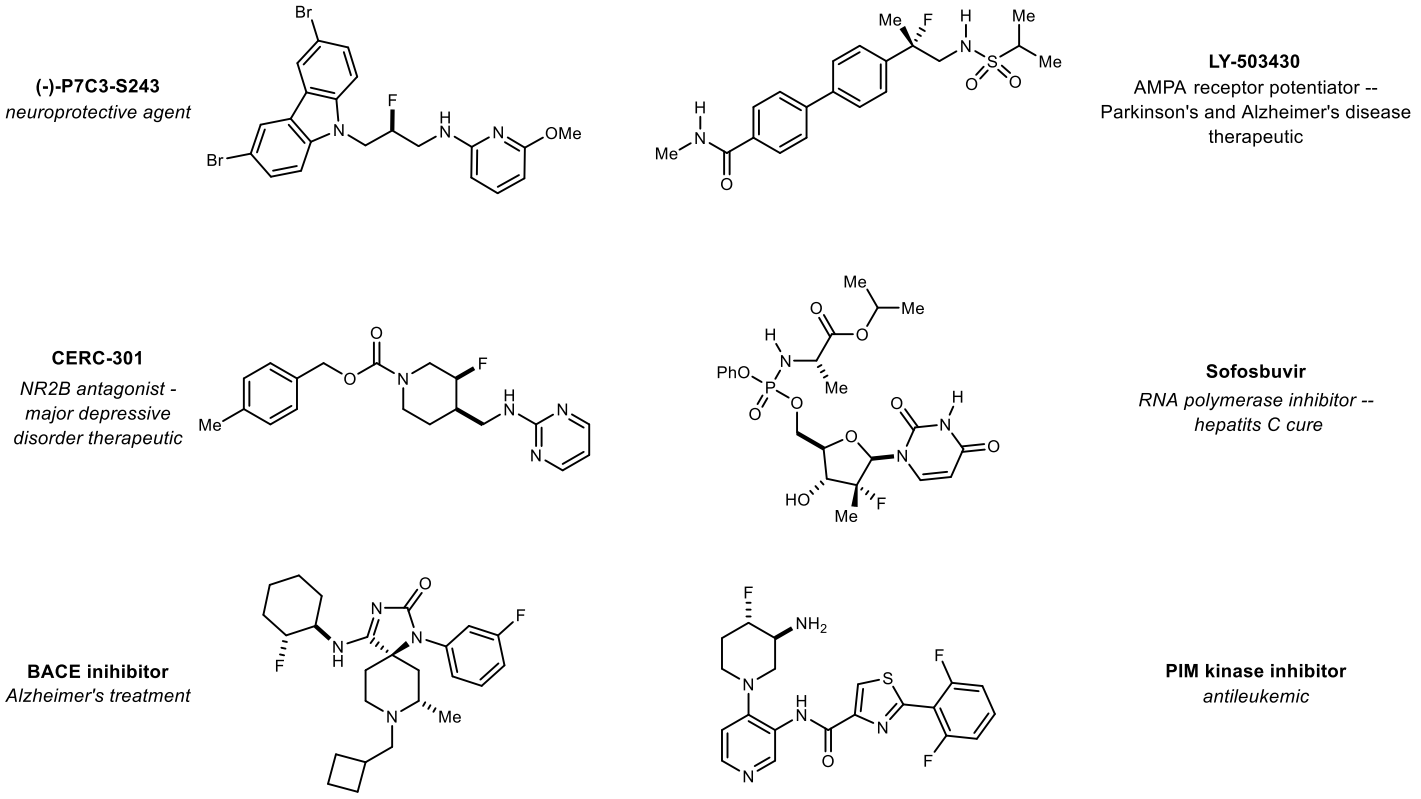

While the number of enantioselective fluorination reactions has grown tremendously in the recent literature, the majority of the transformations still require rigorous setup conditions, prefunctionalized substrates and specially tuned catalysts to deliver the fluorine atom in an enantioselective manner in order to construct β-fluoroamines. Recently developed in our group is a chiral proton-catalyzed direct aza-Henry reaction between α-fluoronitroalkanes and readily accessible imines. These adducts provide access to β-fluoro-β-nitroamines in good

[118] Percy, J. M. *Sci. Synth.* **2005**, *34*, 379.
[119] Clark, J. L.; Hollecker, L.; Mason, J. C.; Stuyver, L. J.; Tharnish, P. M.; Lostia, S.; McBrayer, T. R.; Schinazi, R. F.; Watanabe, K. A.; Otto, M. J.; Furman, P. A.; Stec, W. J.; Patterson, S. E.; Pankiewicz, K. W. *J. Med. Chem.* **2005**, *48*, 5504.
[120] Morgenthaler, M.; Schweizer, E.; Hoffmann-Roder, A.; Benini, F.; Martin, R. E.; Jaeschke, G.; Wagner, B.; Fischer, H.; Bendels, S.; Zimmerli, D.; Schneider, J.; Diederich, F.; Kansy, M.; Muller, K. *ChemMedChem* **2007**, *2*, 1100.

synthetic yield and high enantioselectivity. Subsequent stannane-mediated radical denitration of the aza-Henry adduct affords the β-fluoroamine motif in good yield *via* synthetically practical procedures (**Scheme 51**).[121] While these β-fluoroamines are inherently valuable by themselves, the ability to transform them into biologically relevant compounds would be especially noteworthy. β-Fluoroamines are known to have dramatic influences on blood-brain barrier penetrant small molecules. With the multitude of data on the pharmaceutical benefits of fluorine, and the specific effect fluorine has on blood-brain barrier penetrance, we wondered what effect adding a fluorine atom β to the amine would have on the properties of morphine.

Scheme 51. Vara's Synthesis of β-Fluoroamines

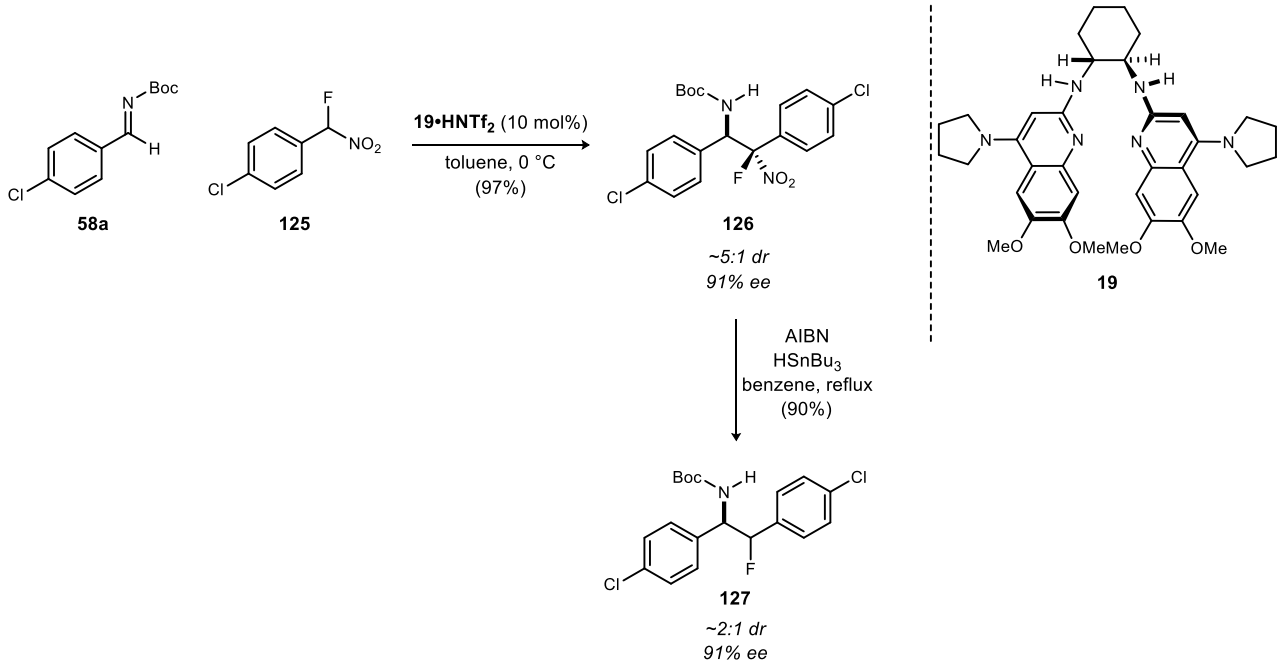

In order for morphine to be active, it must cross the blood-brain barrier to access opioid receptors. To interact with these receptors, the amine must be protonated. However, the molecule must be the free base to transverse the blood-brain barrier. We hypothesized that a fluorinated morphine molecule would be more lipophilic than its parent molecule, thereby helping to facilitate the transversing of the blood-brain barrier. The amine should still be basic enough to be reversibly protonated at physiological pH, however, and therefore be active *once inside* the blood-brain barrier. In other words, we thought that fluorinated morphine may have increased beneficial properties.

We established the goal to synthesize four molecules related to morphine. The first target was a stereoenriched fluorinated intermediate within Rice's route to morphine, which could eventually be carried through toward a complete chemical synthesis of fluorinated morphine. Since Rice's route is arguably the most efficient route in the literature, we reasoned that intercepting the route could also lead to a concise synthesis of a fluorinated morphine. We also targeted fluorinated norcoclaurine and fluorinated reticuline in order to submit them to the biosynthetic opioid pathway in yeast with hopes to probe the promiscuity of the enzymatic machinery and produce fluorinated opioid derivatives. If it becomes possible to produce them *via* fermentation instead of chemical

[121] Vara, B.A.; Johnston, J.N. *Manuscript Submitted*.

synthesis, the opportunity to easily perform biological studies on the analogues will be greatly enhanced. Finally, we targeted Rice's (unfluorinated) tetrahydroisoquinoline intermediate, as its preparation in enantioenriched form would constitute an *enantioselective* formal synthesis of morphine; Rice's route only produced the racemate – but we know that only one stereoisomer of the opioid has its famed and desired biological activity.

4.3 The Synthesis of a Fluorinated Analogue en route to Fluorinated Morphine

To synthesize fluorinated morphine, fluorinated tetrahydroisoquinoline **128** was targeted as an analogue that could participate in a (modified) route similar to Rice's endgame-synthesis of morphine (*vide supra*). Our retrosynthetic planning is detailed in **Scheme 52**. The target compound **128** could come from saponification of acetate **129**. **129** in turn could be formed from a reductive amination of aminoaldehyde **130**. The aldehyde would be installed from alkene cleavage of **131** *via* ozonolysis or a Johnson-Lemieux type oxidation. Alkene **131** would come from a radical denitration, followed by acidic deprotection of the *N*-Boc amine **132**. Finally, **132** could come from a BAM-catalyzed aza-Henry reaction between imine **133** and α-fluoronitroalkane **134**.

Scheme 52. Initial Retrosynthesis of the Fluorinated Intermediate **128**

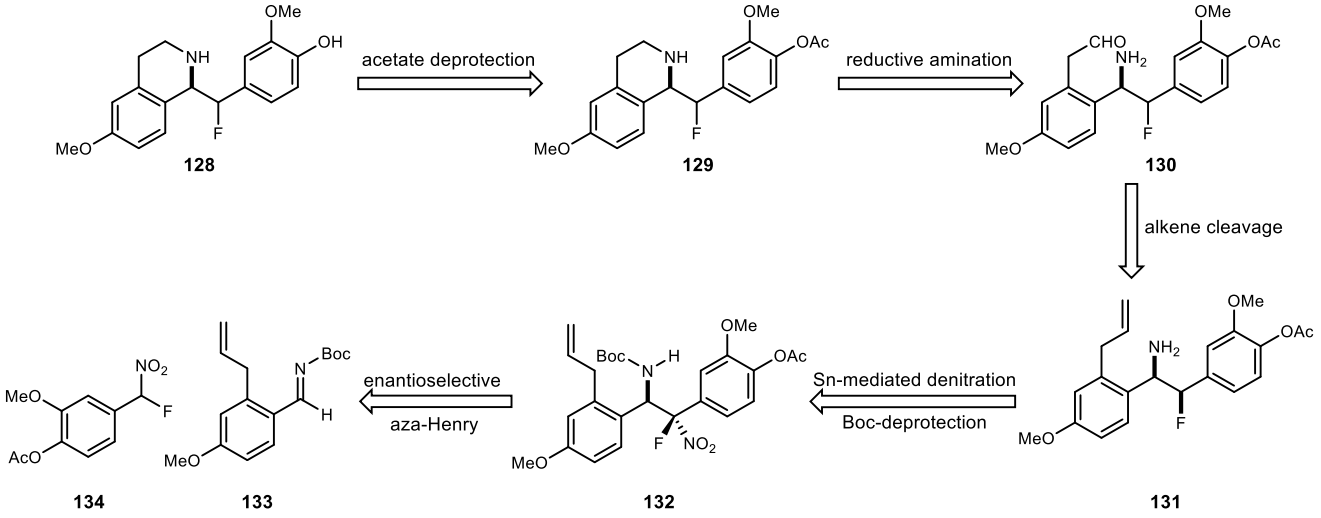

With this sequence in mind, we then had to develop efficient, practical routes to both nitroalkane **134** and imine **133**. It was envisioned that the α-fluoronitroalkane would be synthesized uneventfully from the parent nitroalkane **137** *via* quenching of the derived potassium nitronate with Selectfluor®. The challenge in this route lays in accessing the parent phenylnitromethane. A two-step sequence from inexpensive vanillin acetate should provide the desired intermediate. **(Scheme 53**).

Scheme 53. Initial Retrosynthesis of Phenylnitromethane **156**

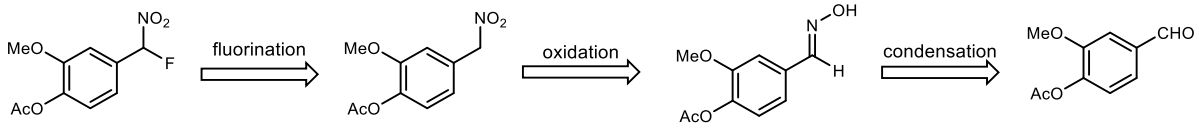

Unfortunately, multiple attempts at oxidizing the oxime to the nitroalkane proceeded in ~13% yield at best (**Scheme 54**). Presumably, the acetate was also being oxidized in a Baeyer-Villiger fashion, leading to decomposition pathways for the molecule. Kornblum chemistry was similarly ineffective. These two routes were not going to be suitable for a multi-step reaction sequence toward a target. Therefore, a different methodology was sought.

Scheme 54. Ineffective Synthesis of the Nitroalkane from Vanillin Acetate.

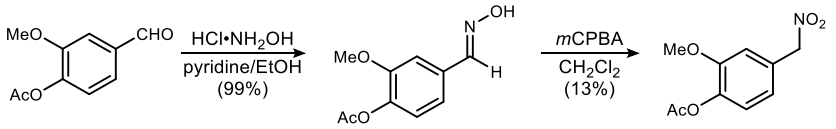

The Kozlowski group has developed a very nice palladium mediated cross-coupling of nitromethane with aryl halides.[122] This seemed like a straightforward method to synthesize our desired phenylnitromethane. First, we needed to synthesize the aryl halide. Commercially available 3-bromoguaiacol was protected as the toluenesulfonate (which will be more stable in future steps than the acetate used in the previous two schemes) in good yield affording aryl bromide **136**. This was successfully coupled with nitromethane to afford the desired nitroalkane in good yields on small to medium scale (**Scheme 55**). Upon scaling up, the reaction became unpredictable: yields were variable and irreproducible despite best attempts at optimization.[123] While Kozlowski's methodology (and swap to the sulfonate protecting group) was an improvement on the aldehyde oxidation chemistry when employing the acetyl protecting group, this route was also not projected to be amenable to producing material on scale for a multistep synthesis due to reproducibility issues, safety concerns, and palladium cost.

Scheme 55. Synthesis of Phenylnitromethane **137** utilizing Kozlowski's Methodology.

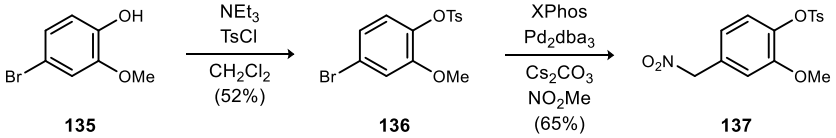

Having settled on using the more stable sulfonate-protected aryl ring, we turned back to synthesizing the nitroalkane *via* oxidation of the corresponding oxime precursor. Beginning from inexpensive, readily available vanillin, tosyl protection proceeded quantitatively, as did oxime formation in the second step (**Scheme 56**). Unlike with the acetate protecting group, MCPBA oxidation was reasonably efficient in this case, affording the desired nitroalkane in 45% yield over 3 steps. Notably, this reaction sequence was amenable to scale-up, as the route described above was performed on 38-gram scale. Additionally, this sequence only requires one chromatographic separation.[124] Fluorination proceeded uneventfully in 56-75% yield to afford the pronucleophile for the aza-Henry

Scheme 56. Practical, Efficient Synthesis of the Nitroalkane Precursor.

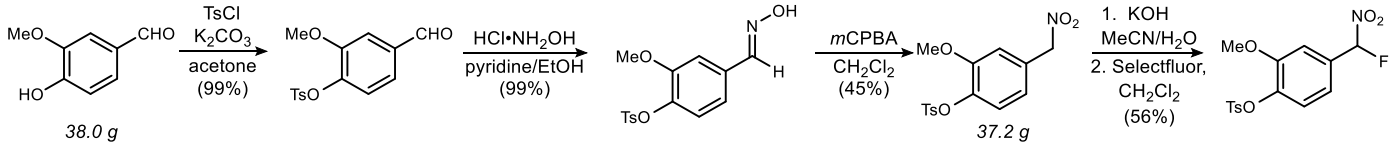

[122] Walvoord, R. R.; Kozlowski, M. C. *J. Org. Chem.* **2013**, *78*, 8859; Walvoord, R. R.; Berritt, S.; Kozlowski, M. C. *Org. Lett.* **2012**, *14*, 4086.

[123] Notably, one time (after being monitored to be stable) the reaction unpredictably became violent, popped the septum off of the flask, and coated the fume hood in chemicals.

[124] The nitroalkane could most likely be recrystallized, removing chromatographic separations, however effective recrystallization conditions were not found.

reaction. This route was deemed to be efficient enough to carry forward, and with this material in hand, we next turned our focus to synthesizing the imine needed for the aza-Henry reaction.

Substitution of commercially available benzyl bromide **138**[125] with vinylmagnesium bromide afforded aryl bromide **139** (**Scheme 57**). Subsequent lithium/halogen exchange followed by quenching with DMF yielded aldehyde **140** in synthetically useful yields. Unfortunately, all attempts to convert the aldehyde to the corresponding sulfone (**141**) *en route* to the imine were unsuccessful. Perhaps this was due to the pendant sulfone being too soluble to precipitate from the reaction and drive the reaction forward.

Scheme 57. Attempts to Synthesize Imine **155**

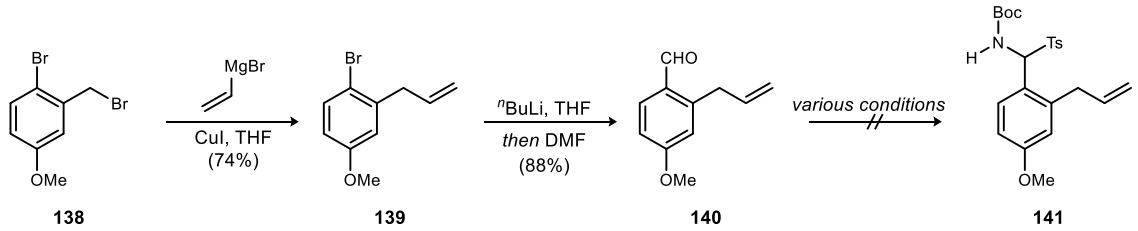

Not to be deterred, we reasoned that we could use our same planned route, but install the allyl group later in the synthesis *via* cross-coupling methodology. Therefore, our second generation plan was to utilize imine **167**, with a bromine handle in the 2-position. Aldehyde **143** is commercially available, however it's fairly expensive. Therefore, we chose to synthesize **143** from inexpensive aldehyde **142** and NaOMe utilizing a simple S_NAr reaction which proceeded very nicely on scale (**Scheme 58**). With the aldehyde in hand, initial attempts at sulfone formation in a mixture of methanol and water as solvent proved ineffective. However, switching to a mixture of toluene and water as solvent proved to be a better choice, providing the sulfone in 71% yield on up to 20 g scale. Elimination of the sulfone to the imine occurred unremarkably, affording the required electrophile for the key aza-Henry reaction.

Scheme 58. Synthesis of 2-Bromo-4-Methoxyimine from Commercial Materials

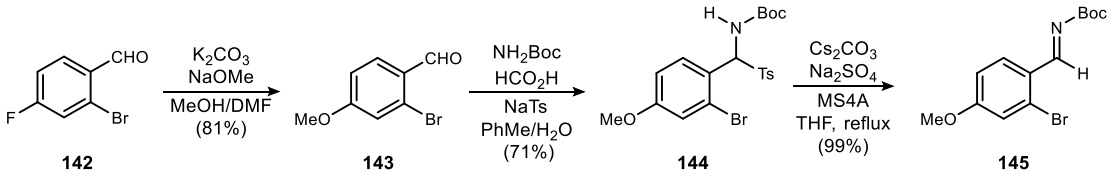

Now that successful routes to both the fluoronitroalkane and imine were developed, we turned our attention toward the key enantioselective aza-Henry reaction. Applying Vara's conditions for this type of aza-Henry reaction, **19•HNTf$_2$** afforded the aza-Henry adduct as a single diastereomer after column chromatography in 71% yield and 97% ee (**Scheme 59**).

The next step was to subject the aza-Henry adduct to a stannane-mediated denitration reaction. Unfortunately, this was unsuccessful. Denitration was competitive with radical debromination of the aryl ring. Analysis of a reaction stopped prior to full conversion revealed that debromination was faster than denitration, as there was

[125] CAUTION! This compound is an extremely potent lachrymator, and causes severe burns. All efforts must be made to handle this compound properly.

evidence of debrominated starting material, with the nitro group still intact. Therefore, it would not be possible to isolate high yields of the denitrated material with the bromine still attached.[126]

Scheme 59. Initial Attempts Toward **150**

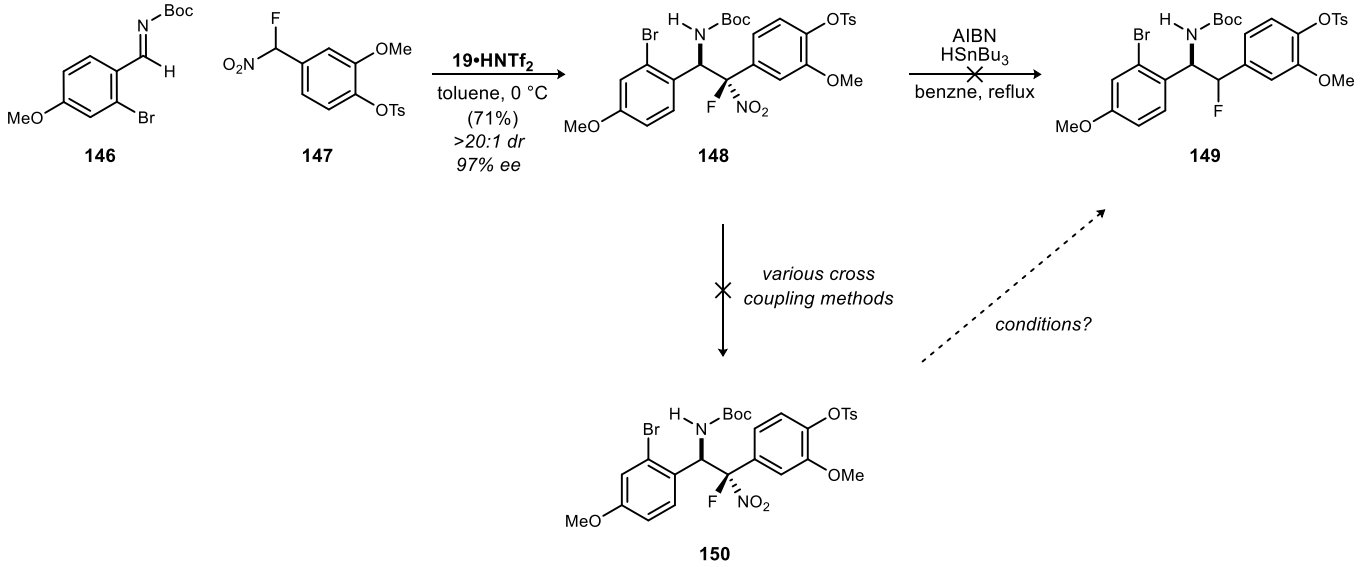

Undeterred, instead of denitrating immediately after the aza-Henry reaction, it was planned to install the allyl group to the aromatic ring first, and denitrate the compound after the offending bromide was no longer part of the molecule. Initial attempts were made to install the allyl group *via* a Stille coupling of allyltributylstannane and **169**[127] using $Pd(PPh_3)_4$ as a catalyst. This yielded no discernable product, and an intractable mixture of compounds. Upon switching to a more active catalyst, $Pd(P^tBu_3)_2$, there was no sign of product, and the majority of the reaction mixture was imine (resulting from retro-aza-Henry reaction) and aldehyde (from hydrolysis of the imine). Likewise, Kumada[128] and Negishi couplings were attempted, but both of these also resulted in general decomposition alongside retro-aza-Henry reaction. Another attempt was made to turn the aryl ring on the aza-Henry adduct into a pinacolatoboronate, which could then serve as a cross-coupling partner. The only products observed from that reaction were again from a retro-aza-Henry reaction. At this point, it seemed as though the aryl bromide was not going to yield any useful cross-coupled product, so we decided to move on to a different strategy.

Since attempts to selectively denitrate the aryl bromide were unsuccessful, we reasoned that installing a chlorine instead of a bromine *ortho* to the imine may allow us to denitrate the resulting aza-Henry adduct under

Scheme 60. Synthesis of 2-Chloro-4-Methoxyimine from Commercial Materials

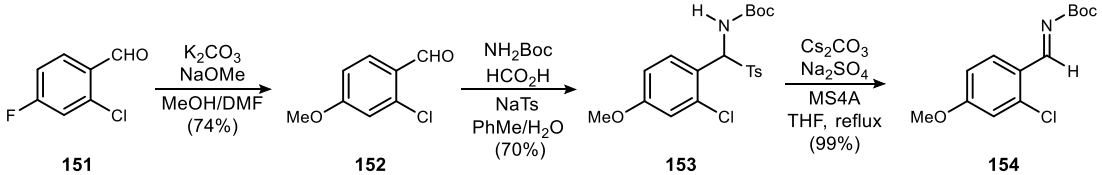

[126] Other methods for denitration were investigated including: Fessard, T. C.; Motoyoshi, H.; Carreira, E. M. *Angew. Chem., Int. Ed. Engl.* **2007**, *46*, 2078; Kornblum, N.; Carlson, S. C.; Smith, R. G. *J. Am. Chem. Soc.* **1979**, *101*, 647. These, too, proved fruitless.
[127] Littke, A. F.; Schwarz, L.; Fu, G. C. *J. Am. Chem. Soc.* **2002**, *124*, 6343.
[128] Safronov, A. V.; Shlyakhtina, N. I.; Everett, T. A.; VanGordon, M. R.; Sevryugina, Y. V.; Jalisatgi, S. S.; Hawthorne, M. F. *Inorg. Chem.* **2014**, *53*, 10045.

radical conditions without dehalogenating the aryl ring. By denitrating before cross-coupling, it would lessen the risk of the retro-aza-Henry reaction occurring during the cross-coupling step. The imine was synthesized in a manner analogous to synthesis of **146** (**Scheme 60**).

Imine **154** was competent in the enantioselective aza-Henry reaction (**Scheme 61**). The desired adduct was isolated as a single diastereomer in 77% yield and 98% ee. The adduct was subjected to radical denitration conditions with $HSnBu_3$ and AIBN, and gratifyingly this afforded the denitrated product **156** in 80% yield on 6-gram scale with the chlorine still intact! Unfortunately, though not unexpectedly, the reaction takes place via a stereochemically labile carbon radical intermediate, and therefore the stereochemistry at the fluorine stereocenter reverts to an epimeric mixture; the denitrated compound was isolated in ~1.5:1 dr. Use of other denitration methods or bulkier stannane reagents did not alter the final ratio of diastereomers.

Scheme 61. Attempts **157** Using Imine **154**

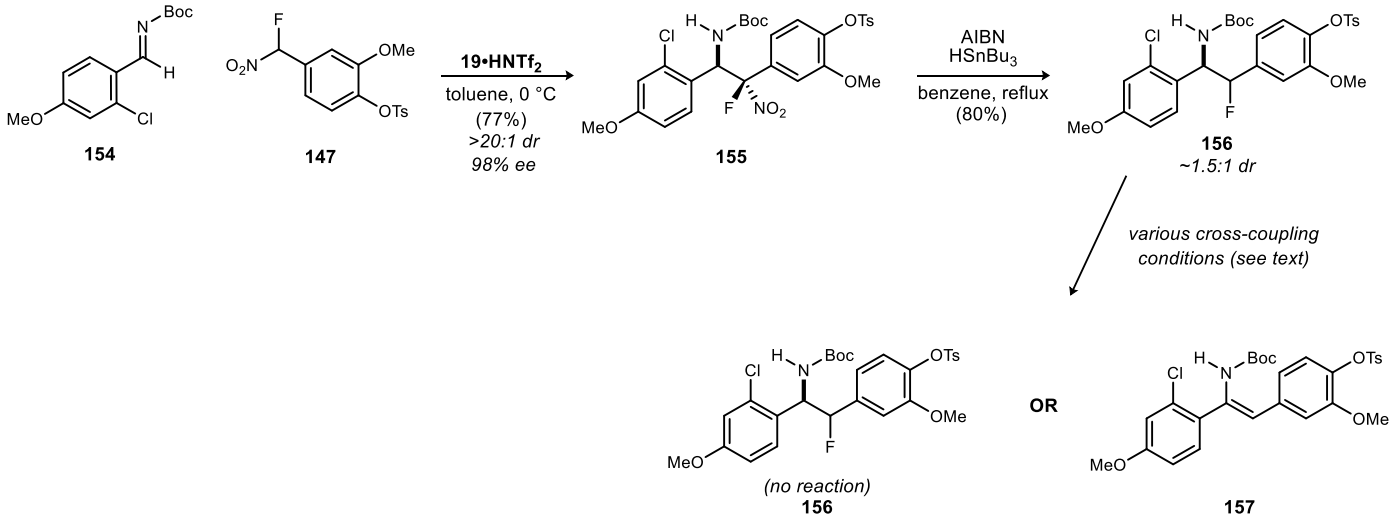

Next, we attempted to install the allyl group *via* a Stille coupling – no reaction took place, and 95% of the starting material was recovered. Stille coupling with the more reactive Fu catalyst, in the presence of CsF as a promoter of transmetalation did not provide desired coupled product, but rather resulted in elimination of fluorine across the backbone of the molecule (**157**). Evidently, this fluoride is prone to a facile elimination pathway (**Scheme 61**). Despite extensive experimentation, we were never able to install the allyl group on this aza-Henry adduct.

After these unsuccessful routes, it became obvious that a different bond disconnection strategy would be necessary to complete our target molecule. This is depicted in **Scheme 62**. In this new strategy, we decided to form the tetrahydroisoquinoline ring *via* reduction of the corresponding lactam **180**. **180** would be accessed from intramolecular cyclization of amine **181**. Amine **181** would come from stannane-mediated denitration and subsequent Boc-deprotection of aza-Henry adduct **182**. aza-Henry adduct **182** was planned to come from imine **183** and fluoronitroalkane **168**.

Scheme 62. Revised Retrosynthesis of the Fluorinated Analogue of Rice's Intermediate

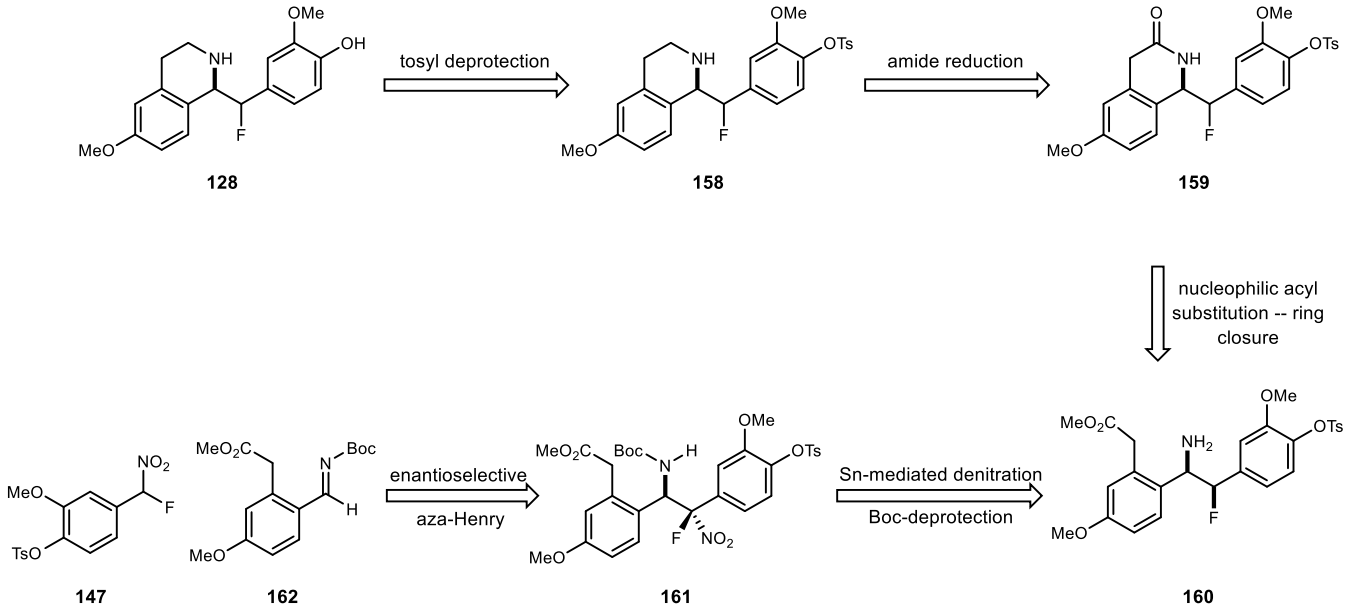

In order to make this a possibility, we needed to develop an efficient route to imine **162**. Aldehyde **165** was synthesized by the reaction of 3-methoxyphenyl acetic acid and formalin under acidic conditions, followed by CAN mediated oxidation *via* known literature procedures (**Scheme 63**). With the aldehyde in hand, we turned our attention to the synthesis of the desired sulfone (imine precursor). Standard reaction conditions[129] in MeOH/H_2O, PhMe/H_2O, THF, or Et_2O all failed to produce even trace amounts of sulfone. Reasoning that perhaps in this case a stronger acid than formic acid was needed to promote the reaction, trichloroacetic acid was added to the reaction, and gratifyingly this was successful. As shown in **Scheme 63**, sulfone **166** was isolated in 75% yield as a colorless powder. Optimization of reaction conditions to produce the imine led us to discover that this sulfone is sensitive to both base used and temperature used for the reaction. It was found that gently heating the sulfone with K_2CO_3 in THF overnight fully converts the sulfone to the imine in quantitative yield.

Scheme 63. Synthesis of 3rd Generation Imine **162**

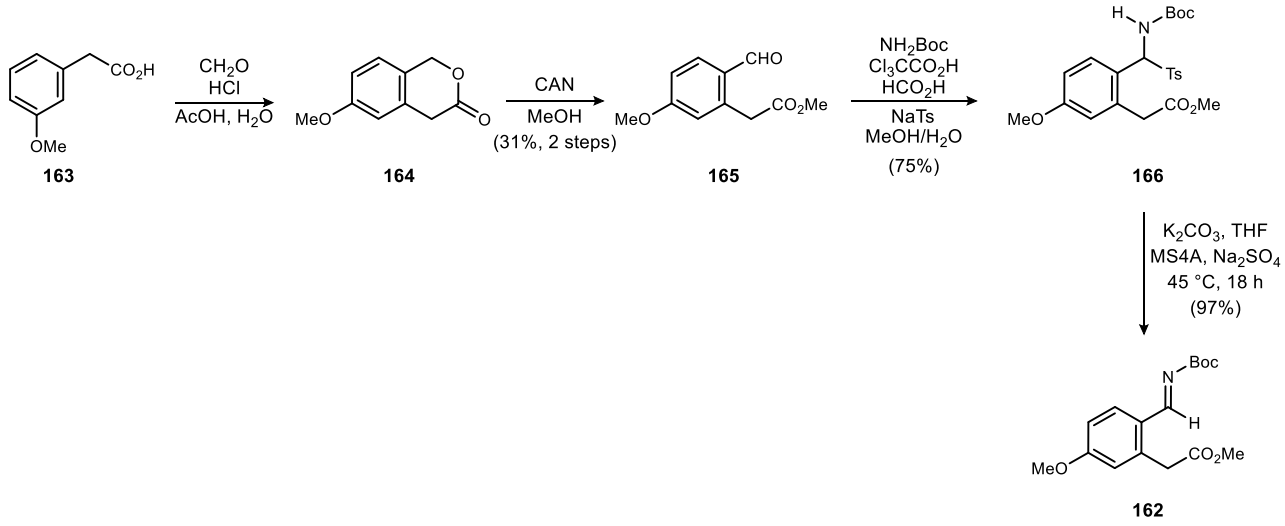

[129] Vara, B. A.; Mayasundari, A.; Tellis, J. C.; Danneman, M. W.; Arredondo, V.; Davis, T. A.; Min, J.; Finch, K.; Guy, R. K.; Johnston, J. N. *J. Org. Chem.* **2014**, *79*, 6913.

With both fluoronitroalkane **147** and imine **162** in hand, the stage was set to attempt the 3rd generation aza-Henry reaction toward our target molecule. **19•HNTf$_2$** was used to catalyzed the reaction, as before, and the aza-Henry adduct was isolated as a 6:1 mixture of diastereomers in 60% yield and 89% ee (**Scheme 64**). This adduct was then submitted to stannane-mediated denitration conditions, and the protected β-fluoroamine **160** was isolated in 71% yield.

Continuing on to form the tetrahydroisoquinoline ring, carbamate **160** was heated in a solution of HCl in dioxane. This deprotected the Boc group *in situ* and also promoted the cyclization to fluorinated lactam **159** in 97% yield.

Scheme 64. 3rd Generation Synthesis of **150**

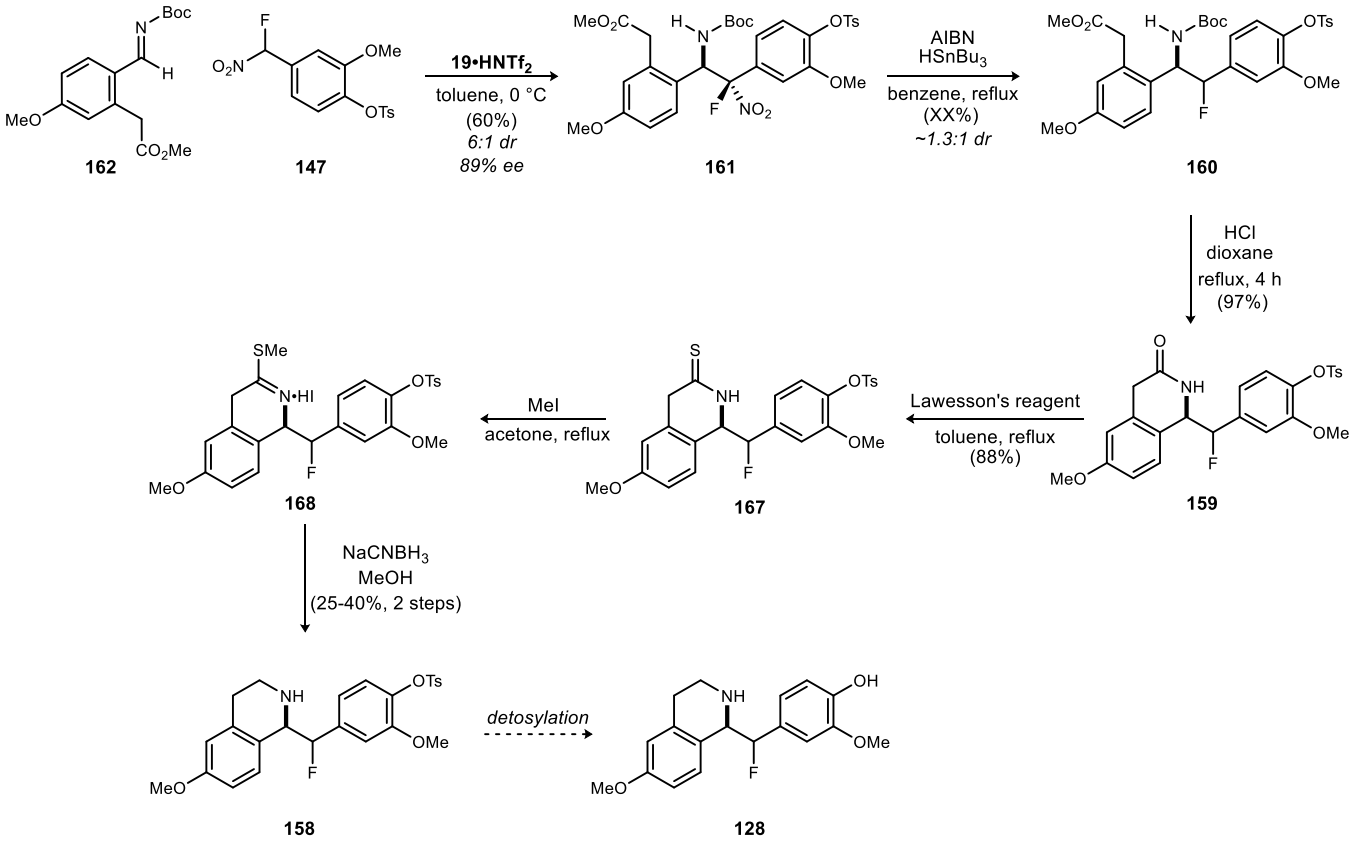

Subsequent reduction of this lactam to the tetrahydroisoquinoline ring proved rather challenging. Typical conditions employing $LiAlH_4$ at 0 °C resulted in defluorination of the molecule. Reasoning that less basic conditions may be necessary, BH_3•THF was employed as a reductant. Analysis of the resulting reaction showed a similar reaction profile to $LiAlH_4$; DIBAL-H did as well. Refluxing the lactam in THF in the presence of $NaBH_4$ unsurprisingly failed to produce any appreciable reaction. Attempts at reducing the molecule with Red-Al at chilled temperatures only resulted in an intractable tar and complete decomposition of the starting material. Attempts to make the imino ether using triflic anhydride, followed by reduction, also proved fruitless – only decomposition was obtained. As all of the aforementioned standard reduction methods failed, Brookhart's iridium catalyzed reduction of amides and lactams, which uses Et_2SiH_2 as a reductant, seemed like a good reaction to attempt.[130] Unfortunately, and somewhat surprisingly, this set of mild conditions *also* gave the same reactivity

[130] Cheng, C.; Brookhart, M. *J. Am. Chem. Soc.* **2012**, *134*, 11304.

profile as seen with $LiAlH_4$. Finally, the decision was made to convert the amide to a thionamide using Lawesson's reagent. This reaction proceeded smoothly, affording **167** in 88% yield. Treatment of **167** with MeI in acetone afforded imidate **168**. Subjecting **168** to $NaCNBH_3$ in MeOH afforded the desired tetrahydroisoquinoline **158**, albeit in low (25-40%) yield over the two steps.

Removal of the tosyl group will provide the fluorinated version of a compound which could intercept a modified version of Rice's route toward morphine. Future directions include pushing the synthetic route to completion in order to arrive at fluorinated morphine. Once in hand, efforts will be made in order to evaluate its biological activity and compare the results to the natural compound. These experiments are ongoing in the laboratory.

4.4 Progress Toward the Synthesis of Fluorinated (S)-Reticuline

As discussed above, we hoped to access fluorinated (*S*)-reticuline to investigate its possibility to act as a biosynthetic precursor to fluorinated morphine. We envisioned the retrosynthesis as shown in **Scheme 65**. **169** will come from detosylation and amine methylation of **170**. Amine **170** can be envisioned to come from a reduction of lactam **171** which is a result of the acid-catalyzed cyclization of carbamate **172**. Carbamate **172** is the product of a stannane-mediated denitration of aza-Henry adduct **173**. Fluoronitroalkane **173** can come from nitroalkane **174** and imine **175** in a reaction catalyzed by (*S,S*)-**19•HNTf$_2$.**

Scheme 65. Retrosynthesis of Fluorinated (*S*)-Reticuline

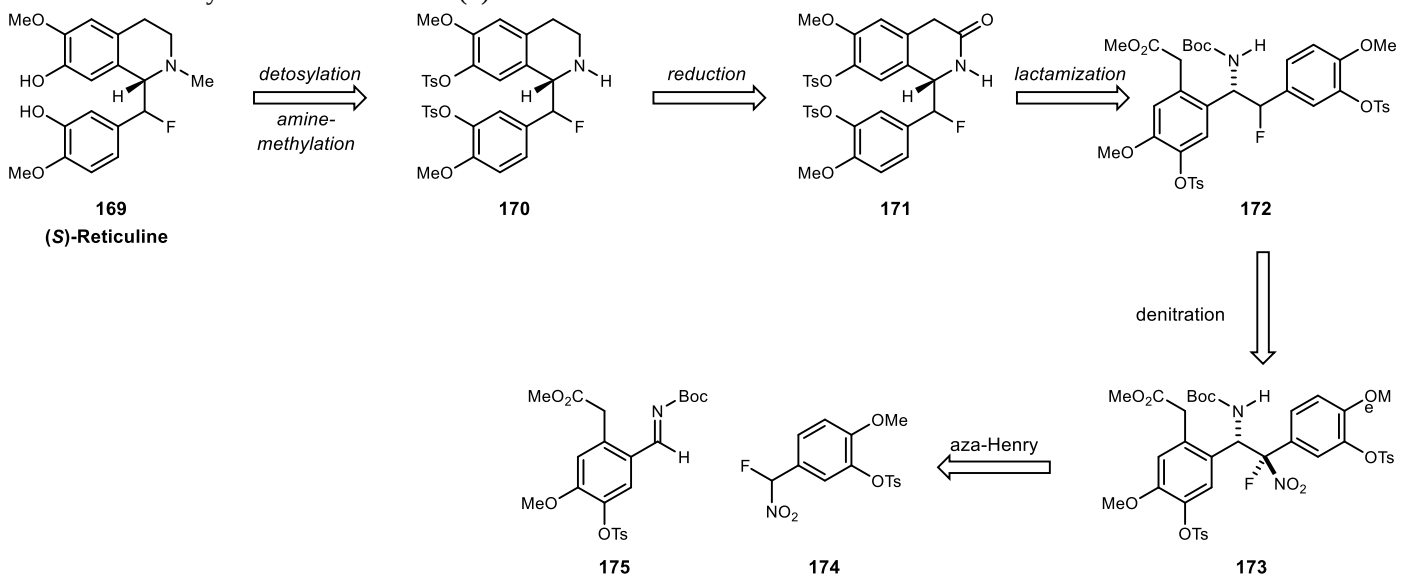

The requisite fluoronitroalkane can be envisioned to come from inexpensive isovanillin (**Scheme 66**). Nitroalkane **174** is envisioned to come from quenching of the nitronate of **176** with Selectfluor®. **176** will be synthesized *via* peracid oxidation of oxime **177**. Oxime **177** can come from the condensation of hydroxylamine on aldehyde **178**. Aldehyde **178** is tosylate-protected isovanillin **179**.

Scheme 66. Retrosynthesis of the Required Fluoronitroalkane to Synthesize Fluorinated (*S*)-Reticuline

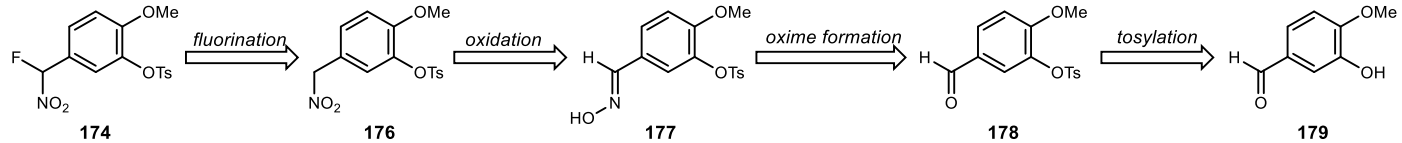

In the forward direction, isovanillin was protected in quantitative yield to afford aldehyde **178**. **178** was condensed with hydroxylamine hydrochloride, synthesizing oxime **177**. The crude reaction mixture was then oxidized with *m*CPBA to give the nitroalkane **176** in 32% yield over 2 steps. The nitronate of **176** was formed by treating it with KOH, and then the reaction was quenched with Selectfluor® to give the desired fluoronitroalkane **174** in 67% yield (**Scheme 67**).

Scheme 67. The Synthesis of Fluoronitroalkane **194**

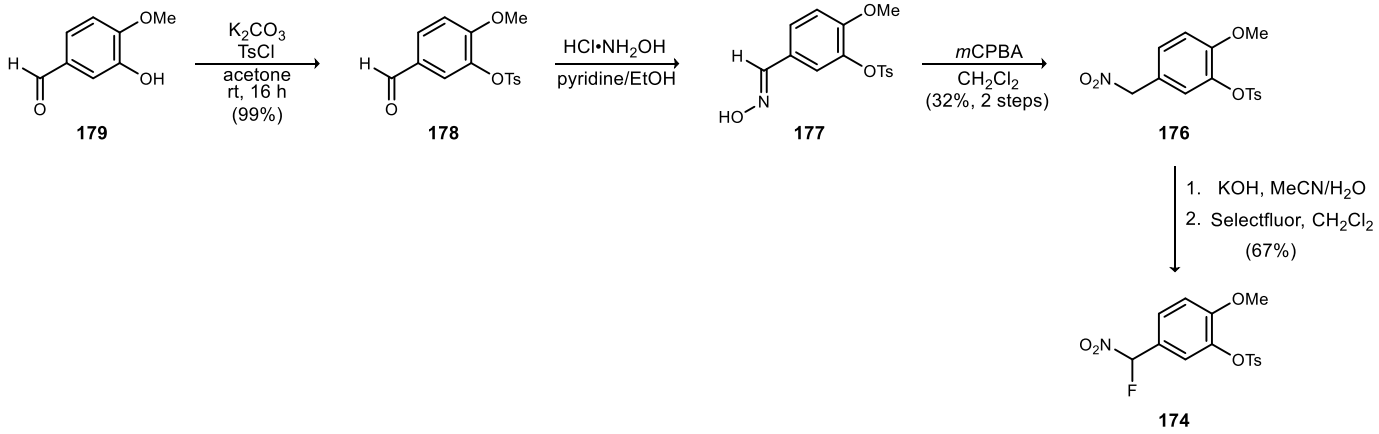

With the required nucleophile in hand, the next step was to synthesize the necessary imine electrophile **175** for the transformation. We envisioned **175** to come from homovanillic acid (**180**) in a 5 step sequence (**Scheme 68**). The imine would come from the elimination of sulfone **181**. The sulfone would be formed *via* general methodology from aldehyde **182**. The aldehyde would be accessed *via* a Friedel-Crafts acylation of ester **183**, which is two steps from homovanillic acid **184**.

Scheme 68. The Retrosynthesis of Imine **185**

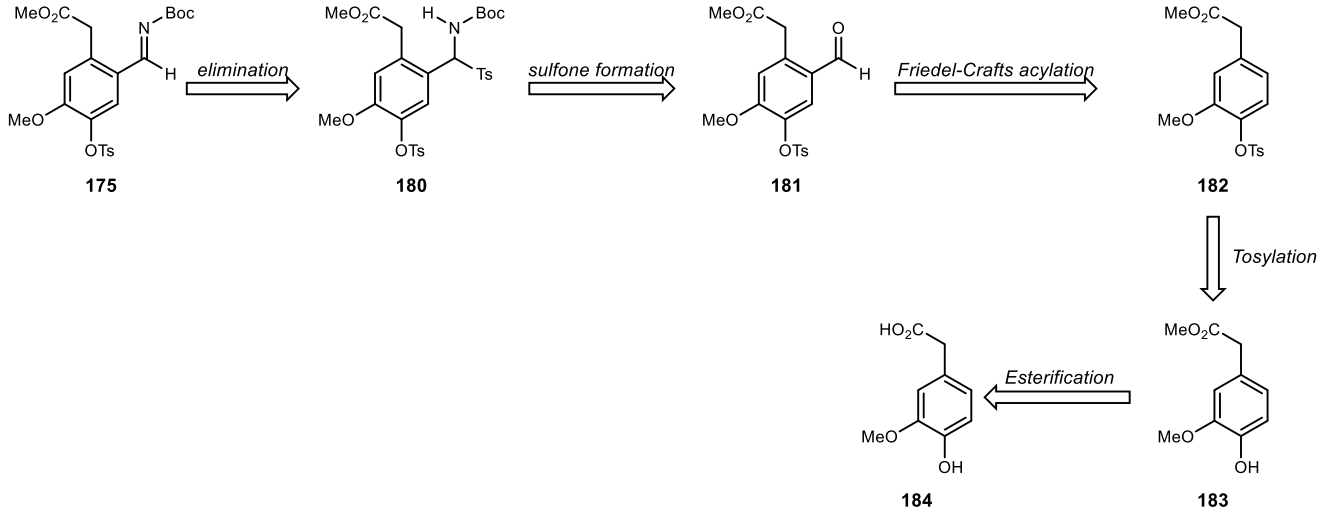

Unfortunately, in the forward direction, the formation of this imine was not this straightforward (**Scheme 69**). Esterification to give ester **183** proceeds quantitatively to afford the phenol as a viscous colorless to pale yellow oil. Tosylation also proceeds quantitatively to afford **182** as a colorless solid. After considerable experimentation, $SnCl_4$ was found to promote the Friedel-Crafts reaction rather cleanly, providing aldehyde **181** in 96% yield on scale. Unfortunately, despite extensive solvent investigation, aldehyde **181** was found to be insoluble in nearly all conditions – every time a reaction was set-up to form sulfone, the result observed was simply recrystallized aldehyde from the solution (or the aldehyde was never solubilized). The aldehyde *was* soluble in chlorinated

solvents, but Petrini's sulfone formation method did not work for this aldehyde. Reasoning that perhaps the tosylate protecting group is influencing the (lack of) solubility of this aldehyde, we decided to investigate other protecting groups on the aldehyde.

Scheme 69. First Generation Synthesis of Imine **175** – Unsuccessful

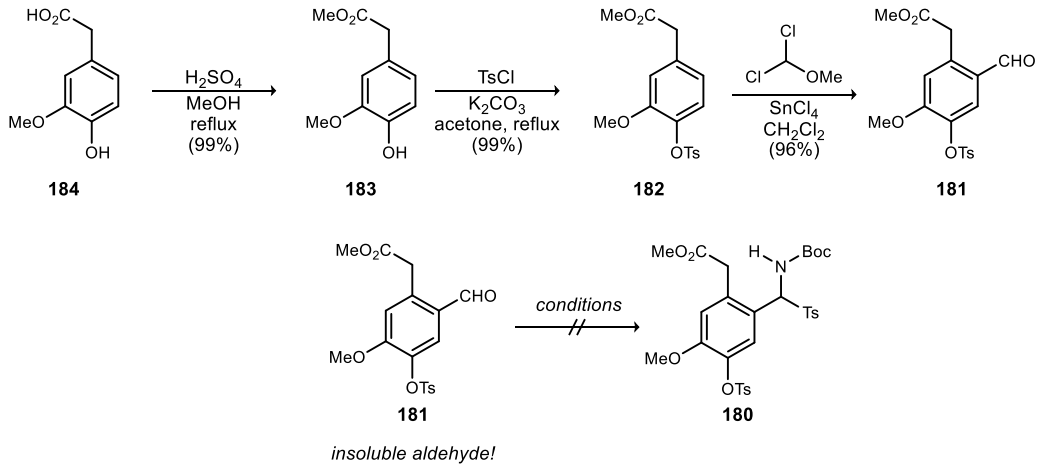

Attracted to the stability of a sulfonyl group, we elected to replace the tosyl with a triflyl group. The protection proceeded cleanly and quantitatively. Unfortunately, the electron withdrawing nature of the triflate was too much to overcome, and the ester was not sufficiently nucleophilic to participate in a Friedel-Crafts acylation reaction, despite extensive heating (**Scheme 70**).

Scheme 70. Attempts at Using a Triflyl Protected Phenol – Unsuccessful

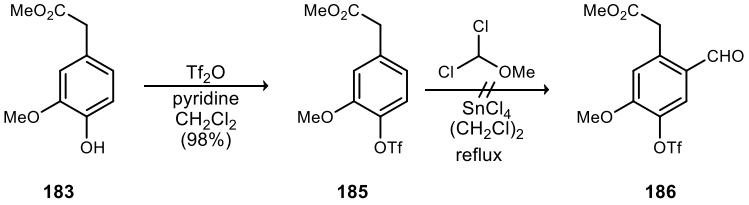

Next, a benzoyl protecting group was investigated. Again, the protection was quantitative, affording ester **187** as a colorless solid after chromatography. Ester **187** was easily formylated in 78% yield to afford the desired aldehyde, **188**. Unfortunately, just like the case was with tosylated aldehyde **181**, **188** is insoluble in a mixture of methanol and water, even after extensive heating. Aldehyde **188** was soluble in a mixture of toluene and water (conditions known to support sulfone formation), however sulfone formation was never observed for this aldehyde (**Scheme 71**).

Scheme 71. Attempts at Using a Benzoyl Protected Phenol – Unsuccessful

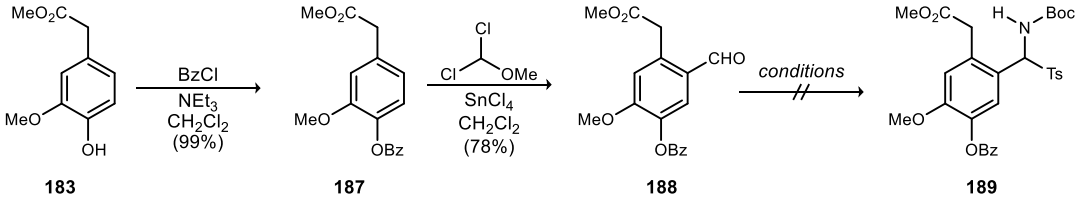

Attempting to find a different protecting group suitable for this synthesis, we settled on an allyl group. Protection of the phenol was quantitative. Unfortunately, the unsaturation was unstable to formylation conditions

(**Scheme 73**). Though the product was never isolated, it appeared as though HCl added across the olefin. Nonetheless, it was apparent the allyl protecting group would not be suitable for our route.

Scheme 72. Attempts at Using an Allyl Protecting Group – Unsuccessful

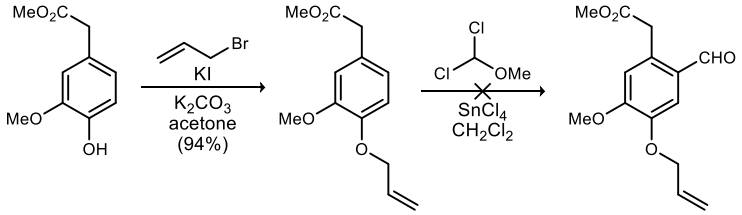

183 **190** **191**

Failing here, we then investigated a benzyl protected phenol. Protection went well, affording the benzylated phenol in 87% yield. Unfortunately, attempts to synthesize the aldehyde from this compound were unsuccessful (**Scheme 73**).

Scheme 73. Attempts at Using a Benzyl Protecting Group – Unsuccessful

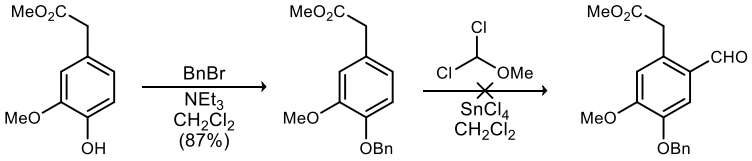

183 **192** **193**

Understanding that the aldehyde forms easily from the benzoyl-protected phenol, we reasoned that an acyl protecting group should allow us to synthesize the corresponding aldehyde. The benzoyl-protected phenol was insoluble, though. Therefore, we hypothesized that a more lipophilic protecting group may provide a compound with the right properties to be able to synthesize the sulfone necessary to carry this route forward. At the present time, this is being investigated by way of protecting the ring with a pivalate group.

4.5 Progress Toward the Synthesis of Fluorinated Norcoclaurine

We also hoped to access a fluorinated analogue of norcoclaurine in order to see if it would be competent in the biosynthetic pathway toward morphine which was reconstituted in yeast (*vide supra*). To do so, we pictured a retrosynthesis similar to those previously discussed, and as shown in **Scheme 74**. Compound **194** could come from BBr_3-mediated demethylation of amine **195**. **195** can be envisioned to come from reduction of lactam **196,** which comes from acid-catalyzed cyclization of **197**. **197** is the product of a stannane-mediated denitration of aza-Henry adduct **198**. **198** is planned to be synthesized *via* a chiral proton-catalyzed aza-Henry reaction between known fluoronitroalkane **199** and imine **200**. Since the nucleophile is a known compound in this case, the main focus was spent on synthesizing the imine.

The imine is envisioned to be synthesized from aldehyde **202** as depicted in **Scheme 75**. Aldehyde **202** is a known compound, synthesized from 3,4-dimethoxyphenylacetic acid (**204**). Unfortunately, as in the case for (*S*)-reticuline in the previous section, aldehyde **202** is not very soluble under some of the sulfone-forming conditions investigated so far (**Scheme 76**). Further investigation is underway, and the methoxy groups will be altered if necessary for a better solubility profile. Once this problem is solved, the synthesis will be continued.

Scheme 74. Retrosynthesis of Fluorinated Norcoclaurine

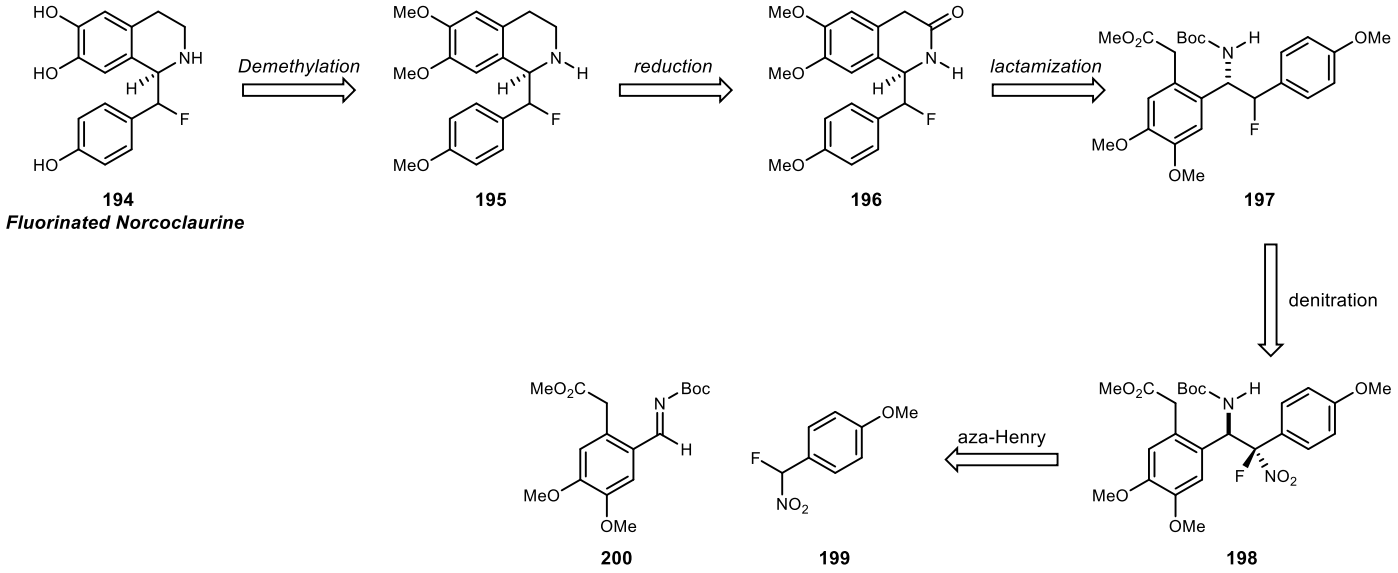

Scheme 75. Retrosynthesis of Imine **220**

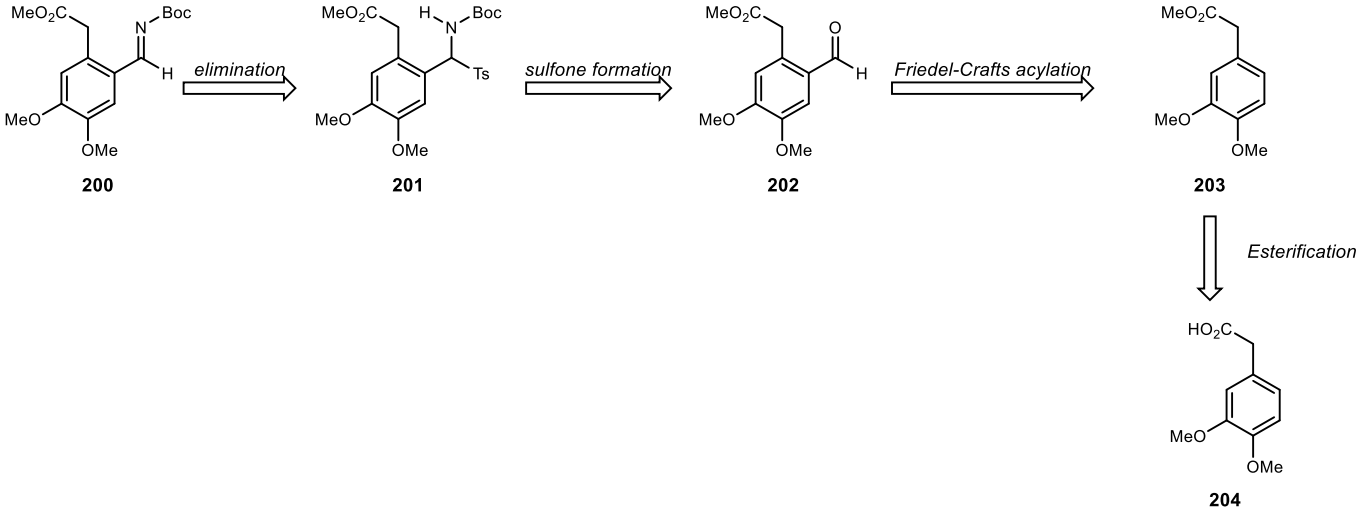

Scheme 76. Forward Synthesis of Imine **220**

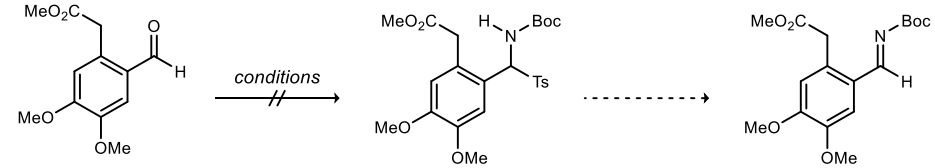

Chapter 5. Conclusion

In summary, my graduate researchhas examined the development and application of chiral proton catalysis to three different reactions. First, we were able to detail the first chiral proton-catalyzed asymmetric hetero-Diels-Alder reaction to construct the core of the brevianamide class of [2.2.2]bicyclooctane natural products (**Scheme 77**). Key to this finding was that the reaction needed to be run solvent-free as a film, with 100 mol% of chiral ligand. One equivalent of ligand was used in order to provide the greatest opportunity for the otherwise spontaneous reaction to occur in a chiral environment. Evidently, the hydrogen bonding between the ligand and substrate is a fairly weak interaction; running the reactions solventless helped to influence this interaction between the chiral proton and substrate by minimizing other possible interactions. Finally, the best enantioselectivity was observed when a more rigid bis(amide) catalyst, H,Quin-BAMide•HOTf, was employed instead of our more

Scheme 77. A Chiral Proton-Catalyzed Diels-Alder Reaction Toward the Brevianamides

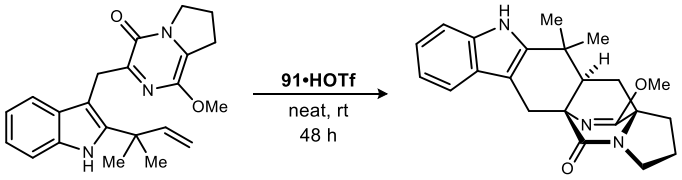

traditional bis(amidine) ligands.

The *anti*-selective aza-Henry reaction between α-substituted nitroacetates and aldimines, catalyzed by bis(amidine) **17•HNTf$_2$**, was also developed (**Scheme 78**). Utilizing a very bulky ester combined with a C_2-symmetric catalyst successfully afforded the *anti*-α,β-diamino acid derivative. Notably, this diastereomer is the opposite of what is observed when bulky unsymmetrical catalyst **16•HOTf** was used. A computational model was advanced in Section 4.2 to help explain this interesting catalyst-controlled diastereodivergence. This methodology is noteworthy because by choosing the correct BAM-catalyst, it is possible to easily prepare all four stereoisomers of α-substituted α,β-diamino acid derivatives. To the best of our knowledge, this is rare in the literature, and this is the first time it has been observed in the catalysis of aza-Henry reactions. This methodology was then applied to the first diastereo- and enantioselective synthesis of Tepe's imidazoline proteasome inhibitor.

Scheme 78. A Chiral Proton-Catalyzed Synthesis of *anti* α-Quaternary α,β-Diamino Acid Derivatives

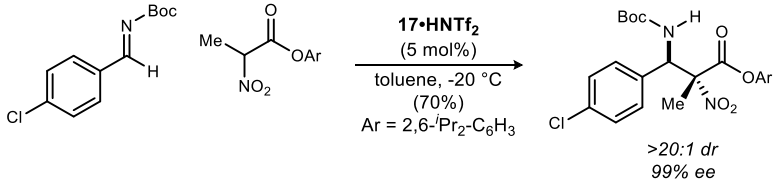

Finally, chiral proton catalysis was applied toward the synthesis of fluorinated variants of morphine-related alkaloids (as described in Chapter 5). These routes are works in progress, and therefore more data will be reported in the future as results are obtained. Overall, these findings contribute to the growing applications of polar-ionic hydrogen bond catalysis which can now be added to the synthetic chemist's toolbox.

Appendix A

A Comprehensive Look at Ligands Investigated in the Hetero-Diels-Alder Reaction

Figure 25. Ligands Investigated in the Hetero-Diels-Alder Reaction - I[131]

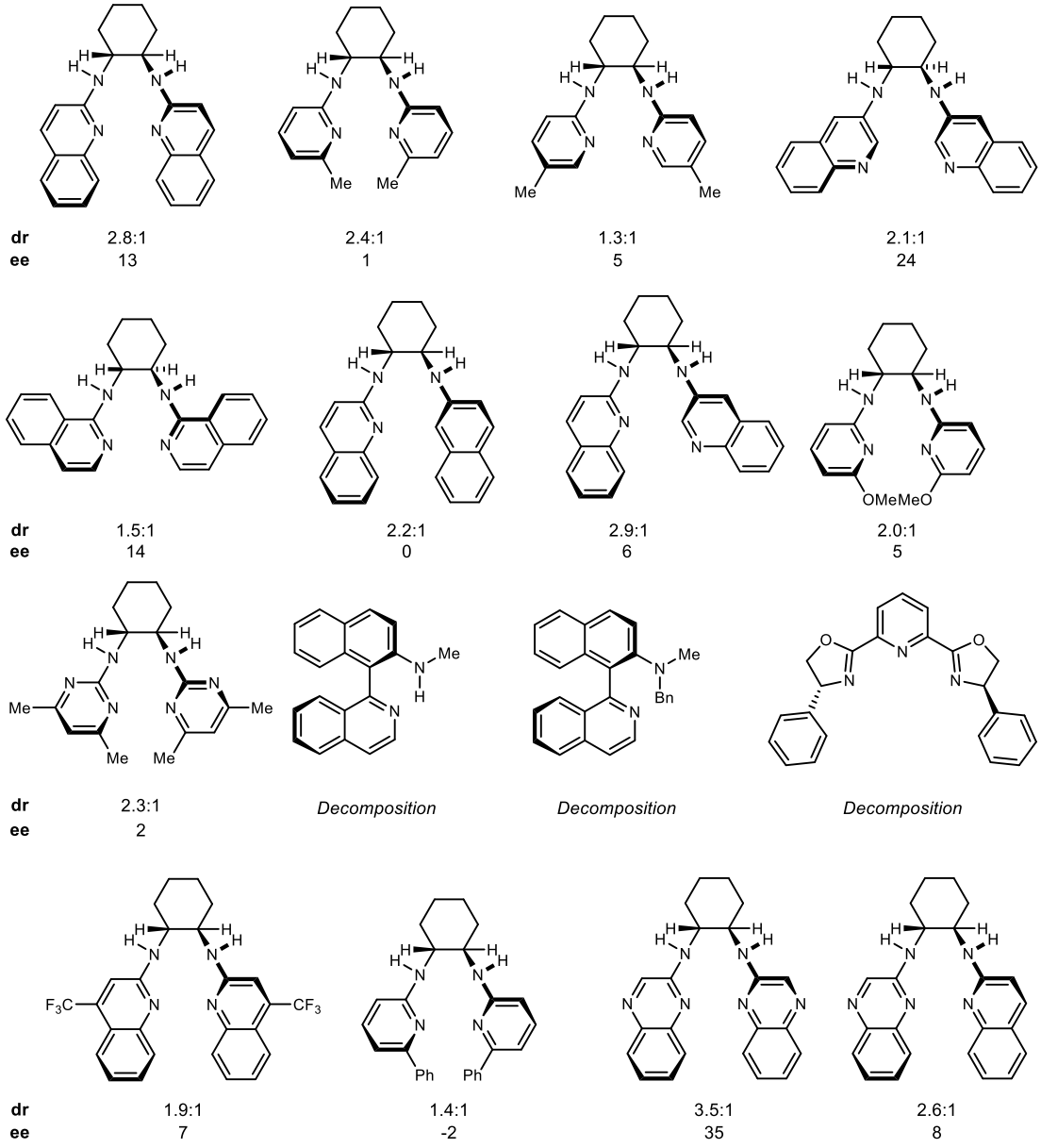

[131] Diastereomeric ratios are reported as a ratio measured *via* ^{1}H NMR. Enantiomeric Excess is reported as (%) and was measured *via* HPLC.

Figure 26. Ligands Investigated in the Hetero-Diels-Alder Reaction - II[131]

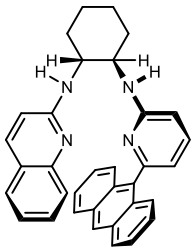

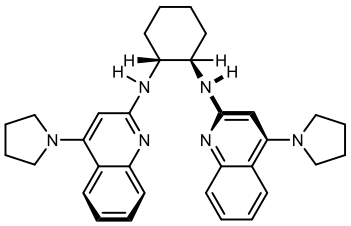

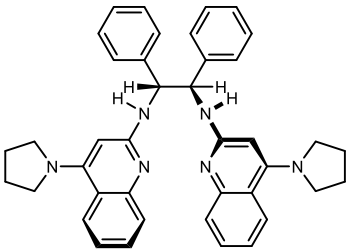

d.r.	2.6:1	1.6:1	2.0:1
e.e.	15	5	0

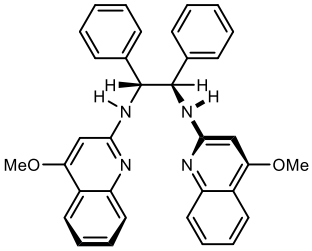

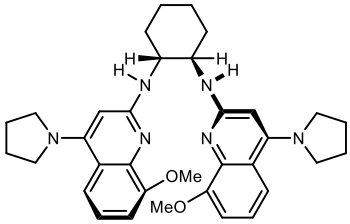

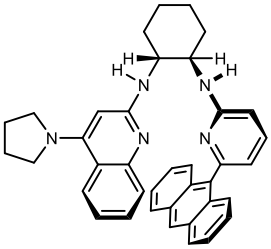

d.r.	-1.1:1	1.8:1	1.2:1
e.e.	14	8	11

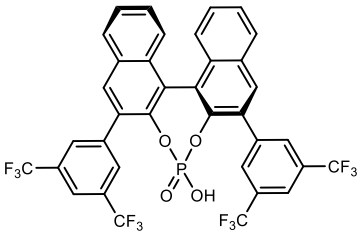

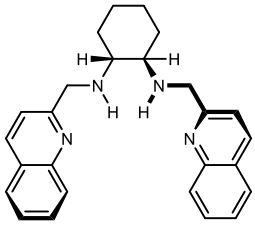

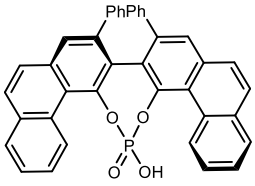

d.r.	*Decomposition*	2.6:1	1.8:1
e.e.		8	0

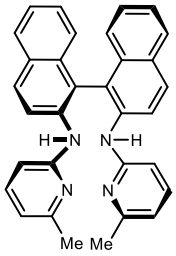

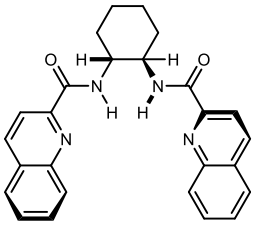

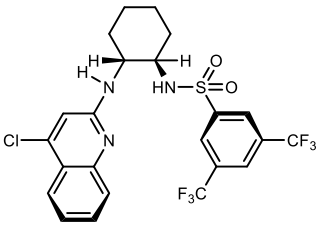

d.r.	3:1	2.1 : 1	3:1
e.e.	22	43	0

Figure 27. Ligands Investigated in the Hetero-Diels-Alder Reaction - III[131]

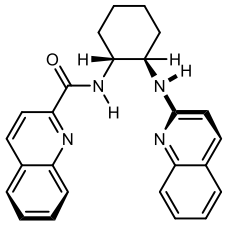

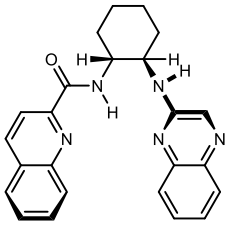

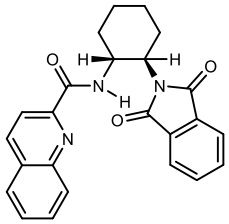

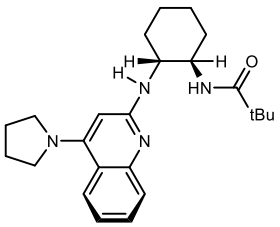

d.r.	2.2:1	2.7:1	-2.1:1	1.2:1
e.e.	0	0	-7	13

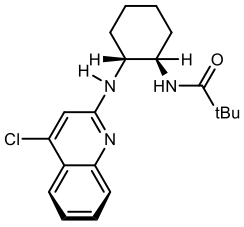

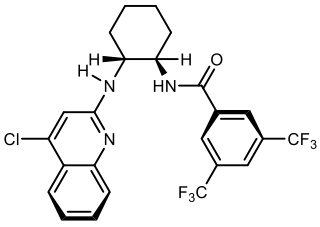

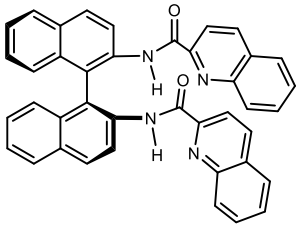

d.r.	2.2:1	2:1	1:1.6
e.e.	7	10	19

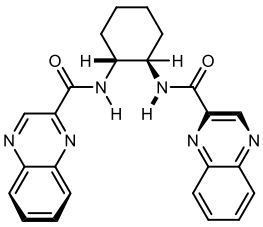

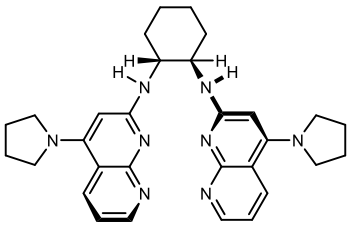

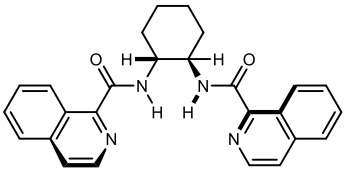

d.r.	1.7:1	1.8:1	2.2:1
e.e.	23	16	0

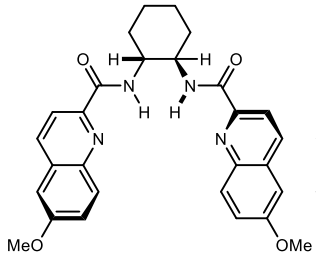

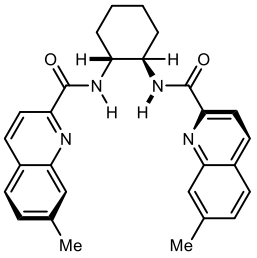

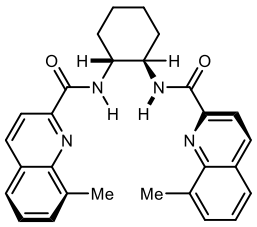

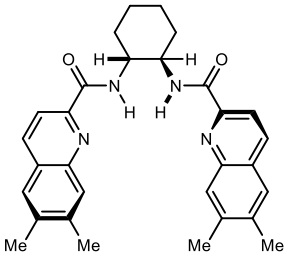

Decomposition	*Decomposition*	*Decomposition*	*Decomposition*

Figure 28. Ligands Investigated in the Hetero-Diels-Alder Reaction - IV[131]

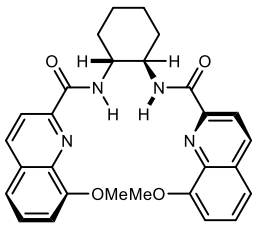

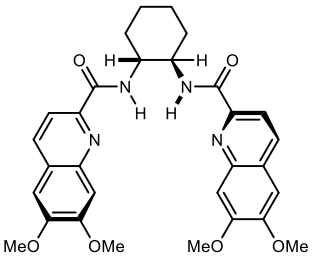

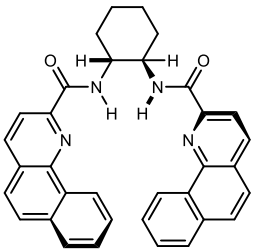

d.r.
e.e.

Decomposition

Decomposition

1.8 : 1
2

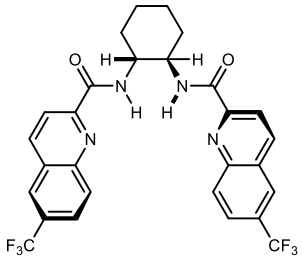

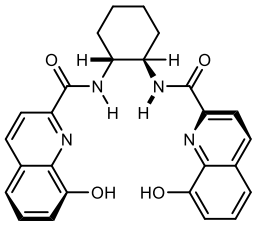

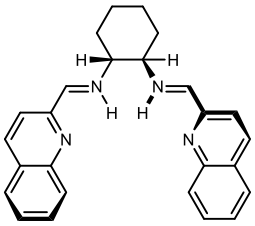

d.r.
e.e.

Decomp

1.6 : 1
8

1.7:1
-1

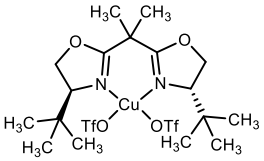

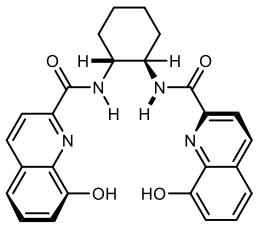

$Cu(OTf)_2$

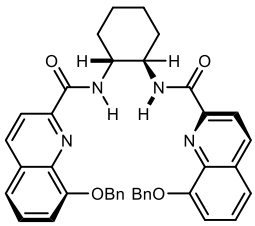

Decomposition

Decomposition

Decomposition

Appendix B

SI-I

All reagents and solvents were commercial grade and purified prior to use when necessary. Toluene and tetrahydrofuran, dichloromethane, and benzene were dried by passage through a column of activated alumina as described by Grubbs.[132] When noted, activated molecular sieves (4Å) were used. Thin layer chromatography (TLC) was performed using glass-backed silica gel (250 μm) plates and flash chromatography utilized 230–400 mesh silica gel from Sorbent Technologies. UV light, and/or the use of potassium iodoplatinate and potassium permanganate solutions were used to visualize products.

Nuclear magnetic resonance spectra (NMR) were acquired on a Bruker AV-400 (400 MHz), Bruker DRX-500 (500 MHz) or Bruker AV-II-600 (600 MHz) spectrometer. Chemical shifts were measured relative to residual solvent peaks as an internal standard set to δ 7.26 and δ 77.0 ($CDCl_3$). IR spectra were recorded on a Thermo Nicolet IR100 spectrophotometer and are reported in wave numbers (cm^{-1}). Compounds were analyzed as neat films on a NaCl plate (transmission). Mass spectra were recorded on a Waters LCT spectrometer by use of the ionization method noted. A post acquisition gain correction was applied using sodium formate or sodium iodide as the lock mass. Optical rotations were measured on a Perkin Elmer-341 polarimeter.

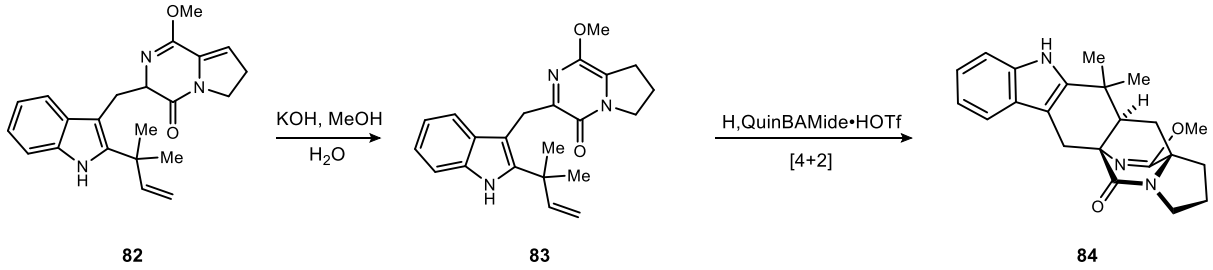

82 **83** **84**

Representative Procedure for the hetero-Diels-Alder Reaction: To a solution of amidate **82** (10.0 mg, 27.5 μmol) in methanol (1.25 mL) at 0 ºC was added 3 M aq KOH (55 μL, 165 μmol). The solution was stirred at 0 ºC for 45 min, then warmed to room temperature for an additional 45 min, monitoring by TLC to confirm consumption of amidate. The solution was concentrated quickly at rt, extracted with cold dichloromethane, and the organic layers were dried (Na_2SO_4), filtered, and concentrated to give crude azadiene **83**.[133] The residue was dissolved in dichloromethane (150 μL), and H,QuinBAMide•HOTf (15.8 mg, 27.5 μmol) was added. The solution was concentrated to remove all solvent, and the neat film was allowed to stand at 25 °C for ~48 h, until the azadiene was fully consumed (verified by ^{1}H NMR). The residue was directly purified by flash column chromatography (SiO_2, 60-75% ethyl acetate in hexanes) to afford the cycloadduct **84** (5.4 mg, 54% yield) as an inseparable mixture of two diastereomers (2.1:1, *syn*:*anti*). The major diastereomer was determined to have an enantiomeric ratio of 72:28 by chiral HPLC analysis (Chiralcel OD-H, 80:20 hexanes: ^{i}PrOH, 1 mL/min, t_r(*anti*,

[132] Pangborn, A. B.; Giardello, M. A.; Grubbs, R. H.; Rosen, R. K.; Timmers, F. J. *Organometallics* **1996**, *15*, 1518-1520.
[133] Solutions were chilled (-20 °C or below) during the extraction, drying, and concentration steps to minimize the amount of conversion to the [4+2] product prior to the intentional hetero-Diels-Alder step. However, it is possible that some conversion occurred during this time.

major) = 7.2 min, t_r(*syn*, major) = 8.9 min, t_r(*syn*, minor) = 12.9 min, t_r(*anti*, minor) = 15.5 min; R_f (**84**) = 0.20 (75% EtOAc/hexanes); R_f (**83**) = 0.63 (75% EtOAc/hexanes).[134]

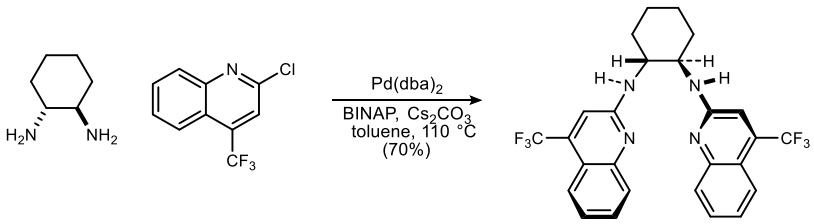

H,^{4}CF3-BAM (85). $Pd(dba)_2$ (25.3 mg, 44.0 µmol), BINAP (54.8 mg, 88.0 µmol), and Cs_2CO_3 (863 mg, 2.65 mmol) were combined in a round-bottomed flask in a glove box. Toluene (1.7 mL) was added to the mixture, followed by 1,2-(*R*,*R*)-*trans*-diaminocyclohexane (48.0 mg, 442 µmol) and 2-chloro-4-trifluoromethylquinoline (325 mg, 972 µmol). The reaction was stirred at 110 °C for 15 h then cooled to room temperature and filtered through Celite. The filtrate was concentrated, and the dark orange residue was purified by flash chromatography (SiO_2, 8-25% diethyl ether in hexanes) to provide the desired diamine as a colorless solid (157 mg, 70%); $[\alpha]_D^{25}$ +46 (*c* 0.24, $CHCl_3$); mp = 206-207 °C; R_f = 0.18 (10% EtOAc/hexanes); IR (neat) 3283, 2858, 1633, 1546 cm^{-1}; ^{1}H NMR (400 MHz, $CDCl_3$) δ 7.73 (d, *J* = 8.4 Hz, 1H), 7.69 (d, *J* = 8.8 Hz, 1H), 7.52 (dd, *J* = 7.8, 1.2 Hz, 1H), 7.20 (dd, *J* = 7.6, 0.8 Hz, 1H), 6.50 (s, 1H), 5.92 (br s, 1H), 4.08 (br m, 1H), 2.30 (d, *J* = 11.2 Hz, 1H), 1.79 (br d, *J* = 7.2 Hz, 1H), 1.50-1.35 (br m, 2H); ^{13}C NMR (100 MHz, $CDCl_3$) ppm 155.5, 148.7, 135.3 (q, $^2J_{CF}$ = 32 Hz), 130.3, 126.6, 124.1, 123.1, 123.0 (q, $^1J_{CF}$ = 273 Hz), 117.7, 111.0 (q, $^3J_{CF}$ = 6 Hz), 56.4, 32.7, 24.9; HRMS (EI): Exact mass calcd for $C_{26}H_{23}F_6N_4$ $[M+H]^+$ 505.1827, found 505.1813.

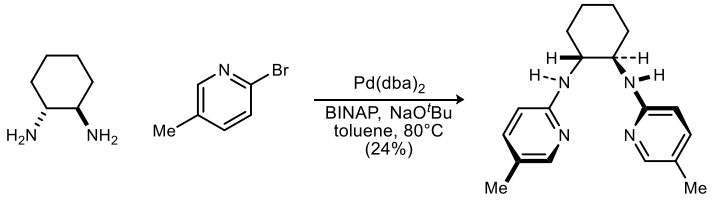

H,^{5}Me-BAM (87). $Pd(dba)_2$ (14.4 mg, 50.0 µmol), BINAP (31.1 mg, 50.0 µmol), and NaO^{t}Bu (288 mg, 3.00 mmol) were combined in a round-bottomed flask in a glove box. Toluene (10 mL) was added to the mixture, followed by 1,2-(*R*,*R*)-*trans*-diaminocyclohexane (114 mg, 1.00 mmol) and 2-bromo-5-methylpyridine (344 mg, 2.00 mmol). The reaction was stirred at 80 °C until TLC indicated complete conversion. The reaction was cooled to room temperature, concentrated, and purified by flash chromatography (SiO_2, 25% ethyl acetate in hexanes) to provide the desired diamine as a colorless solid (70 mg, 24%); $[\alpha]_D^{25}$ +590 (*c* 0.50, $CHCl_3$); mp = 126-128 °C; R_f = 0.33 (40% EtOAc/hexanes); IR (neat) 3283, 3006, 2928, 2858, 1616, 1500 cm^{-1}; ^{1}H NMR (400 MHz, $CDCl_3$) δ 7.85 (s, 1H), 7.09 (dd, *J* = 8.4, 2.0 Hz, 1H), 6.16 (d, *J* = 8.4 Hz, 1H), 4.96 (br s, 1H), 3.76-3.63 (m, 1H), 2.21 (br d, *J* = 12.8 Hz, 1H), 2.12 (s, 3H), 1.74 (br d, *J* = 7.2 Hz, 1H), 1.49-1.20 (series of br m, 2H); ^{13}C NMR (100

[134] Characterization data is reported in Williams, R. M.; Sanz-Cervera, J. F.; Sancenon, F.; Marco, J. A.; Halligan, K. M. *Bioorg. Med. Chem.* **1998**, *6*, 1233.

MHz, $CDCl_3$) ppm 156.9, 146.8, 138.1, 120.8, 108.2, 56.0, 33.0, 24.8, 17.3; HRMS (EI): Exact mass calcd for $C_{18}H_{25}N_4$ $[M+H]^+$ 297.2074, found 297.2079.

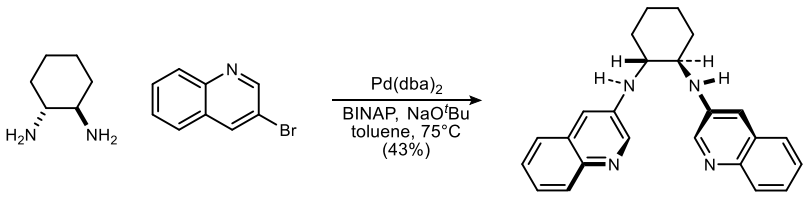

H,^{3}Quin-BAM (88). $Pd(dba)_2$ (14.4 mg, 25.0 µmol), BINAP (31.1 mg, 50.0 µmol), and NaO^tBu (288 mg, 3.00 mmol) were loaded into a round bottom flask in a glove box. Toluene (10 mL) was added to the mixture followed by the 1,2-(*R*,*R*)-*trans*-diaminocyclohexane (114 mg, 1.00 mmol). 3-bromoquinoline (268 µL, 2.00 mmol) was added and the reaction was allowed to stir at 80 °C and monitored by TLC. The reaction was then cooled to room temperature, concentrated, and purified by flash chromatography (SiO_2, 25% ethyl acetate in hexanes) affording the desired diamine as a colorless solid (158 mg, 43%); mp = 128-130 °C; R_f = 0.15 (50% EtOAc/hexanes); $[\alpha]_D^{25}$ +20 (*c* 0.74, $CHCl_3$); IR (film) 3259, 3048, 2935, 2851, 1608, 1538, 1487, 1392, 1221 cm^{-1}; ^1H NMR (400 MHz, $CDCl_3$) δ 8.43 (br s, 1H), 7.89 (br d, *J* = 6.6 Hz, 1H), 7.48-7.32 (series of m, 3H), 6.71 (s, 1H), 4.78 (br s, 1H), 3.20 (br s, 1H), 2.36 (br d, *J* = 13.3 Hz, 1H), 1.83 (br d, *J* = 8.1 Hz, 1H), 1.43 (dd, *J* = 9.5, 9.3 Hz, 1H), 1.33-1.17 (br m, 1H); ^{13}C NMR (100 MHz, $CDCl_3$) ppm 143.9, 141.9, 141.2, 129.8, 129.0, 127.0, 126.3, 124.9, 109.7, 56.4, 31.8, 24.8; HRMS (ESI): Exact mass calcd for $C_{24}H_{25}N_4$ $[M+H]^+$ 369.2079, found 369.2071.

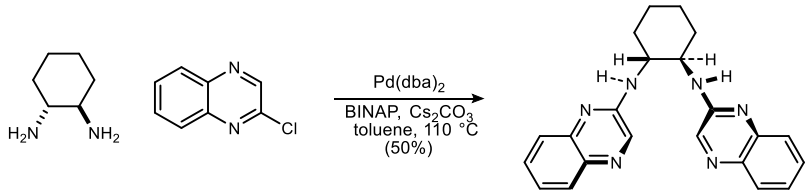

H,Quinox-BAM (89). $Pd(dba)_2$ (47.7 mg, 83.0 µmol), BINAP (103 mg, 165 µmol), and Cs_2CO_3 (1.62 g, 4.96 mmol) were combined in a round-bottomed flask in a glove box. Toluene (3.3 mL) was added to the mixture, followed by 1,2-(*R*,*R*)-*trans*-diaminocyclohexane (94.4 mg, 827 µmol) and 2-chloroquinoxaline (300 mg, 1.82 mmol). The reaction was stirred at 110 °C for 15 h then cooled to room temperature and filtered through Celite. The filtrate was concentrated, and the dark orange residue was purified by flash chromatography (SiO_2, 50-100% diethyl ether in hexanes) to provide the desired diamine as a colorless solid (153 mg, 50%); mp = 176-178 °C; R_f = 0.28 (100% diethyl ether); $[\alpha]_D^{25}$ +49 (*c* 0.48 $CHCl_3$); IR (film) 3265, 1586, 1545, 759; ^1H NMR (500 MHz, $CDCl_3$) δ 7.92 (s, 1H), 7.79 (d, *J* = 8.0 Hz, 1H), 7.70 (d, *J* = 8.5 Hz, 1H), 7.56 (dd, *J* = 8.0, 8.0 Hz, 1H), 7.34 (dd, *J* = 8.0, 8.0 Hz, 1H), 6.15 (br s, 1H), 4.12 (br s, 1H), 2.38 (br d, *J* = 10.5 Hz, 1H), 1.87 (br d, *J* = 7.0 Hz, 1H), 1.58-1.38 (br m, 2H); ^{13}C NMR (125 MHz, $CDCl_3$) ppm 151.9, 141.3, 139.1, 137.0, 130.1, 128.9, 125.7, 124.2, 56.2, 32.6, 24.7; HRMS (ESI): Exact mass calcd for $C_{22}H_{23}N_6$ $[M+H]^+$ 371.1984, found 371.1974.

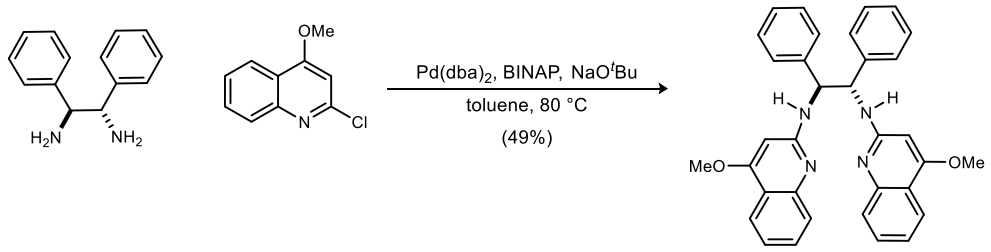

(S,S)-^{4}MeOStilbBAM (90). $Pd(dba)_2$ (54 mg, 94 µmol), *rac*-BINAP (117 mg, 188 µmol) and sodium *tert*-butoxide (1.35 g, 14.1 mmol) were loaded into a vial in a glove box. (1*S*,2*S*)-1,2-diphenylethane-1,2-diamine (1.00 g, 4.70 mmol) and 2-chloro-4-methoxyquinoline (1.81 g, 9.40mmol) were loaded into a flask. The contents of the vial were transferred into the flask and toluene (45 mL) was added. The reaction was allowed to stir at 80 ˚C under argon for 1.5 h. Upon completion as judged by TLC, the reaction mixture was cooled to room temperature, diluted with ethyl acetate and filtered through Celite. Flash column chromatography (SiO_2, 1-3-5-10% methanol in dichloromethane) afforded the desired compound as a yellow foam (1.21 g, 49%). R_f = 0.45 (5% MeOH/CH_2Cl_2); $[\alpha]_D^{20}$ -80 (*c* 0.45, $CHCl_3$); IR (film) 3238, 2985, 2871, 1620 cm^{-1}; ^{1}H NMR (600 MHz, DMSO-d_6) δ 7.77 (d, *J* = 8.0 Hz, 1H), 7.71 (d, *J* = 4.9 Hz, 1H), 7.44-7.41 (m, 2H), 7.39 (d, *J* = 7.6 Hz, 2H), 7.17 (t, *J* = 7.7 Hz, 2H), 7.10-7.06 (m, 2H), 6.23 (s, 1H), 5.69 (br s, 1H), 3.85 (s, 3H); ^{13}C NMR (150 MHz, DMSO) ppm 161.7, 158.3, 148.8, 142.7, 129.9, 128.17, 128.15, 126.9, 126.0, 121.6, 121.1, 117.5, 59.9, 55.8; HRMS (ESI): Exact mass calcd for $C_{34}H_{31}N_4O_2$ $[M+H]^+$ 527.2447, found 527.2435.

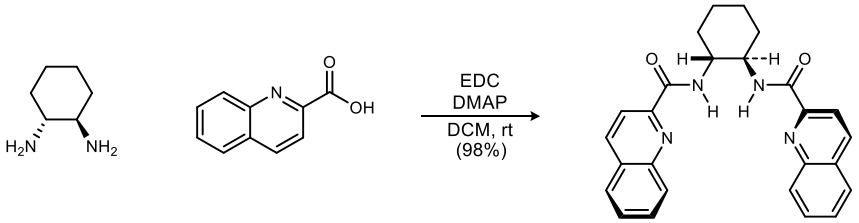

H,Quin-BAMide (91). A flask was charged with the diamine (553 mg, 4.84 mmol), acid (2.09 g, 12.1 mmol), and CH_2Cl_2 (25.0 mL). To the resulting solution was added EDC•HCl (3.07 g, 16.0 mmol) and DMAP (60 mg, 484 µmol). The reaction was stirred for 15 h, quenched with 1 M HCl, and extracted with CH_2Cl_2. The organic layers were combined, washed with 1 M NaOH, brine, dried, and then concentrated to yield analytically pure material as a fluffy, colorless solid (2.00 g, 98%). R_f = 0.53 (50% EtOAc/hexanes); $[\alpha]_D^{20}$ -420 (*c* 0.70, $CHCl_3$); IR (film) 3371, 2936, 1669, 1563, 1521, 1501 cm^{-1}; ^{1}H NMR (400 MHz, $CDCl_3$) δ 8.51 (br d, *J* = 7.2 Hz, 1H), 8.18 (d, *J* = 8.4 Hz, 1H), 8.17 (s, 1H), 8.14 (d, *J* = 8.4 Hz, 1H), 7.83 (d, *J* = 8.4 Hz, 1H), 7.73 (ddd, *J* = 6.8, 6.8, 1.2 Hz, 1H), 7.56 (dd, *J* = 7.2, 7.2 Hz, 1H), 4.21-4.17 (m, 1H), 2.32 (d, *J* = 10.58 Hz, 1H), 1.90 (d, *J* = 7.2 Hz, 1H), 1.59-1.53 (m, 2H); ^{13}C NMR (100 MHz, $CDCl_3$) ppm 164.8, 149.5, 146.3, 137.0, 129.8, 129.7, 129.0, 127.6, 127.4, 118.6, 53.4, 32.7, 24.8; HRMS (ESI): Exact mass calcd for $C_{26}H_{25}N_4O_2$ $[M+H]^+$ 425.1978, found 425.1998.

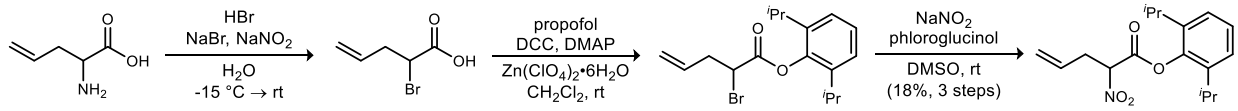

2,6-Diisopropylphenyl 2-nitropent-4-enoate (127h). The α-bromo carboxylic acid was prepared according to literature procedure.[135] The carboxylic acid (7.77 g, 43.4 mmol) was dissolved in dichloromethane (217 mL) and chilled to 0 °C. To the resulting solution was added propofol (7.5 mL, 39 mmol), $Zn(ClO_4)_2•6H_2O$ (2.0 g, 5.2 mmol), DMAP (1.1 g, 8.7 mmol) and DCC (10.7 g, 52.1 mmol). The resulting mixture was warmed to ambient temperature and stirred for 24 h. Diethyl ether (250 mL) was added and the reaction mixture was filtered through Celite. The filtrate was washed with 1 M NaOH, 1 M HCl, and brine, and then dried and concentrated. The resulting dark brown oil was passed through a short pad of silica gel (5% ethyl acetate in hexanes) and concentrated to a pale yellow oil.

The oil was dissolved in DMSO (180 mL) and $NaNO_2$ (4.3 g, 62 mmol) and phloroglucinol (4.7 g, 37.2 mmol) were added. The deep red solution was stirred for 24 h and then poured over ice. The ice mixture was warmed to ambient temperature and extracted with Et_2O. The combined organic layers were washed with brine, dried, and concentrated to a dark red oil. Flash column chromatography (SiO_2, 0.5-3% diethyl ether in hexanes) afforded an orange oil contaminated by propofol. This mixture was then subjected to bulb-to-bulb distillation (150 °C, 0.35 torr) which removed further impurities, leaving behind the desired α-nitro ester[136] (4.3 g, 18% yield over 3 steps). R_f = 0.25 (2% Et_2O/Hexanes); IR (film) 3573, 3070, 2963, 2872, 1772, 1645, 1566, 1463, 1365, 794, 749 cm^{-1}; ^1H NMR (400 MHz, $CDCl_3$) δ 7.26 (br dd, *J* = 8.4, 8.4 Hz, 1H), 7.17 (br d, *J* = 7.8 Hz, 2H), 5.85 (dddd, *J* = 13.1, 10.2, 6.7, 6.7 Hz, 1H), 5.46 (dd, *J* = 9.9, 5.4 Hz, 1H), 5.34 (dddd, *J* = 17.0, 1.3, 1.3, 1.3 Hz, 1H), 5.29 (dddd, *J* = 10.2, 1.1, 1.1, 1.1 Hz, 1H), 3.24-3.03 M, 2H), 2.95-2.78 (br m, 1H), 1.19 (br d, *J* = 6.9 Hz, 12H); ^{13}C NMR (100 MHz, $CDCl_3$) ppm 162.8, 144.7, 140.0, 133.6, 129.9, 127.4, 124.2, 123.4, 120.8, 87.2, 34.4, 27.4, 27.1, 23.6, 22.7 (br, 3C); HRMS (ESI): Exact mass calcd for $C_{17}H_{24}NO_4$ $[M+H]^+$ 306.1700, found 306.1702.

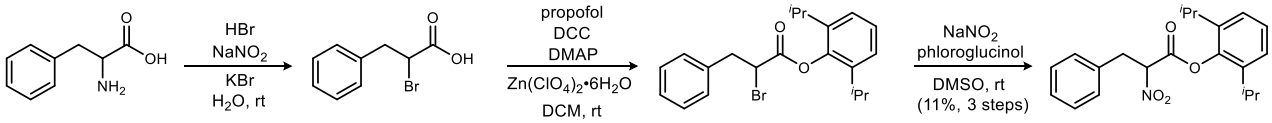

2,6-Diisopropylphenyl 2-nitro-3-phenylpropanoate (127i). According to a known procedure,[137] DL-phenylalanine (2.15 g, 13.0 mmol), $NaNO_2$ (1.88 g, 27.3 mmol), aq HBr (48%, 9.4 mL), and KBr (6.2 g, 52.0 mmol) in H_2O (27 mL) afforded the α-bromo acid as a yellow oil which was used without further purification.

The α-bromo acid was dissolved in CH_2Cl_2 (50 mL) and chilled to 0 °C. To this was added propofol (1.61 mL, 8.67 mmol), $Zn(ClO_4)_2•6H_2O$ (323 mg, 867 μmol), DMAP (159 mg, 1.30 mmol), and DCC (2.67 g, 13.0 mmol). The resulting solution was warmed to ambient temperature and stirred for 24 h. The reaction was diluted with Et_2O, filtered through Celite, and concentrated. The residue was dissolved in Et_2O, and washed with 1 N NaOH, 1 N HCl, and brine, and then dried and concentrated. The residue was subjected to MPLC (SiO_2, 0-3% ethyl acetate in hexanes) to afford the α-bromo ester as a pale yellow oil contaminated with 10% of propofol[138] (2.33 g).

---

[135] {Guthrie, 2009 #75}
[136] The α-nitro ester was contaminated by 8% propofol. Further attempts at purification proved unsuccessful.
[137] {Kudelko, 2012 #12}
[138] At this scale, further separation was not attempted. Purification was more straightforward after nitration.

This α-bromo ester was dissolved in DMSO (24.0 mL), treated with $NaNO_2$ (711 mg, 10.3 mmol) and phloroglucinol (792 mg, 6.28 mmol), and stirred at ambient temperature for 16 h. The resulting solution was poured over ice, and warmed to ambient temperature. The aqueous layer was extracted with Et_2O, dried, and concentrated. The residue was subjected to flash column chromatography (SiO_2, 0.5-2.0% diethyl ether in hexanes) to afford the desired α-nitro ester as a colorless oil (348 mg, 11% yield over 3 steps). R_f = 0.10, $KMnO_4$ (3% Et_2O/hexanes); IR (film) 2968, 1769, 1562, 1161, 1144 cm^{-1}; ^1H NMR (500 MHz, $CDCl_3$) δ 7.40-7.28 (series of br m, 5H), 7.24 (br dd, *J* = 8.0, 8.0 Hz, 1H), 7.16 (br s, 2H), 5.67 (dd, *J* = 7.1, 7.1 Hz, 1H), 3.75 (dd, *J* = 14.4, 8.9 Hz, 1H), 3.65 (dd, *J* = 14.4, 6.6 Hz, 1H), 2.91 (br s, 1H), 2.48 (br s, 1H), 1.25-1.00 (br m, 12H); ^{13}C NMR (125 MHz, $CDCl_3$) ppm 162.7, 144.7, 140.0 (br), 133.7, 129.1, 129.0, 127.9, 127.4, 124.2, 88.8, 36.3, 27.3, 23.7, 22.7 (2C); HRMS (CI): Exact mass calcd for $C_{21}H_{26}NO_4$ $[M+H]^+$ 356.1856, found 356.1848.

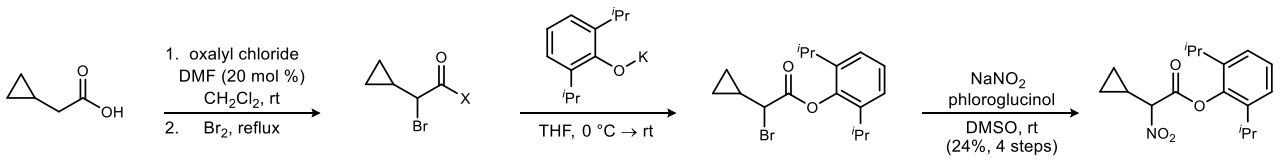

2,6-Diisopropylphenyl 2-cyclopropyl-2-nitroacetate (127j). According to Fu's procedure,[139] a flame-dried flask was charged with the carboxylic acid (1.40 mL, 15.0 mmol), DMF (230 µL, 3.00 mmol), and CH_2Cl_2 (60 mL) and chilled to 0 °C. Oxalyl chloride (1.4 mL, 16 mmol) was added dropwise as gas evolved. The solution was warmed to ambient temperature and stirred for 12 h. Short path distillation of the yellow solution (bath temperature = 75 °C) removed excess oxalyl chloride and solvent, leaving behind the acid chloride in crude form.

Bromine (845 µL, 16.5 mmol) was added to the acid chloride and the mixture was refluxed for 4 h. Short path distillation (as above, to remove excess bromine) left behind a mixture of acid halides[140] which were subsequently esterified without further purification or analysis.

A flame-dried flask was charged with KHMDS (2.51 g, 12.6 mmol) and THF (40 mL) and chilled to 0 °C. Propofol (2.22 mL, 12.0 mmol) was added, and the mixture was stirred at 0 °C for 1 h. The mixture of acid halides in THF (50 mL) was added dropwise to the resulting phenolate solution, warmed to ambient temperature and stirred for 12 h. The resulting brown mixture was poured into H_2O and extracted with CH_2Cl_2. The combined organic layers were washed with satd aq $Na_2S_2O_3$, 1 N NaOH, H_2O, and brine. The organic layer was then dried and concentrated. The residue was subjected to MPLC (SiO_2, 0-3% ethyl acetate in hexanes, 80 mL/min) to afford a mixture of α-bromo ester and phenol (3.18 g).138

The α-bromo ester was dissolved in DMSO (37.0 mL) and treated with $NaNO_2$ (1.12 g, 16.2 mmol) and phloroglucinol (1.30 g, 10.3 mmol). The mixture was stirred at ambient temperature for 12 h. The resulting dark red solution was poured over ice, warmed to ambient temperature, and extracted with Et_2O. The combined organic layers were washed with brine, dried, and concentrated to yield the crude nitroester as a red oil. Flash column chromatography (SiO_2, 0.5-3% diethyl ether in hexanes) afforded the title compound as a colorless oil (776 mg, 24% yield over 4 steps). R_f = 0.21, $KMnO_4$ (3% Et_2O/hexanes); IR (film) 2968, 1770, 1562, 1162 cm^{-1}; ^1H NMR (500 MHz, $CDCl_3$) δ 7.27 (dd, *J* = 7.5, 7.0 Hz, 1H), 7.20 (d, *J* = 7.5 Hz, 2H), 4.57 (d, *J* = 10.5 Hz, 1H), 3.01-2.89

[139] Dai, X.; Strotman, N. A.; Fu, G. C. *J. Am. Chem. Soc.* **2008**, *130*, 3302.
[140] The acyl bromide and acyl chloride were obtained from this reaction.

(br m, 2H), 1.97-1.86 (br m, 1H), 1.21 (br d, *J* = 6.7 Hz, 12H), 1.05-0.95 (br m, 2H), 0.80-0.74 (br m, 1H), 0.73-0.68 (br m, 1H); ^{13}C NMR (125 MHz, $CDCl_3$) ppm 163.0, 144.8, 140.1, 127.4, 124.2, 92.5, 27.4 (2C), 23.7, 22.6,

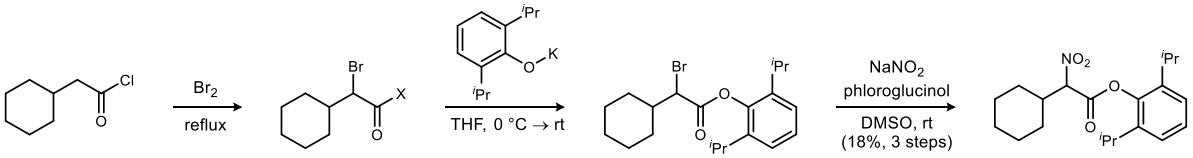

22.5 (2C), 11.8, 5.06, 4.39; HRMS (CI): Exact mass calcd for $C_{17}H_{24}NO_4$ $[M+H]^+$ 306.1700, found 306.1694.

2,6-Diisopropylphenyl 2-cyclohexyl-2-nitroacetate (127l). Bromine (845 µL, 16.5 mmol) was added to the acid chloride (2.30 mL, 15.0 mmol), and the mixture was refluxed for 6 h. Short path distillation (oil bath temperature = 75 °C), to remove excess bromine, left behind a mixture of acid halides140 which were subsequently esterified without further purification or analysis.

A flame-dried flask was charged with KHMDS (3.30 g, 16.6 mmol) and THF (40 mL) and chilled to 0 °C. Propofol (1.40 mL, 7.50 mmol) was added, and the mixture was stirred at temperature for 1 h. The crude mixture of acid halides in THF (40 mL) was added dropwise to the resulting phenolate solution, warmed to ambient temperature, and stirred for 16 h. The resulting brown mixture was poured into H_2O, and extracted with CH_2Cl_2. The combined organic layers were washed with satd aq $Na_2S_2O_3$, 1 N NaOH, H_2O, and brine. The organic layer was then dried and concentrated. The crude residue was subjected to MPLC (SiO_2, 0-3% ethyl acetate in hexanes, 80 mL/min) to afford a mixture of desired bromoester and phenol (1.35 g).138

The bromoester was dissolved in DMSO (15.0 mL), treated with $NaNO_2$ (428 mg, 6.20 mmol) and phloroglucinol (469 mg, 3.72 mmol), and stirred at ambient temperature for 16 h. The resulting dark red mixture was poured over ice, warmed to room temperature, and extracted with Et_2O. The combined organic layers were washed with brine, dried, and concentrated. The red oil was subjected to flash column chromatography (SiO_2, 0.5-3% diethyl ether in hexanes) to afford the desired α-nitro ester as a colorless oil (469 mg, 18% yield over 3 steps). R_f = 0.33, $KMnO_4$ (3% Et_2O/hexanes); IR (film) 2932, 1769, 1560, 1160, 793 cm^{-1}; ^{1}H NMR (400 MHz, $CDCl_3$) δ 7.28 (br dd, *J* = 7.4, 7.4 Hz, 1H), 7.21 (br d, *J* = 8 Hz, 2H), 5.25 (d, *J* = 8.9 Hz, 1H), 2.93-2.80 (br m, 2H), 2.63-2.48 (br m, 1H), 2.09-1.70 (series of br m, 5H), 1.50-1.28 (series of br m, 5H), 1.22 (br d, *J* = 6.8 Hz, 6H), 1.21 (br d, *J* = 6.8 Hz, 6H); ^{13}C NMR (100 MHz, $CDCl_3$) ppm 162.2, 144.8, 140.3, 127.2, 124.1, 93.1, 38.9, 29.0, 28.7, 27.5, 25.7, 25.5, 25.3, 23.5, 22.8, 22.7; HRMS (CI): Exact mass calcd for $C_{20}H_{30}NO_4$ $[M+H]^+$ 348.2169, found 348.2176.

General Procedure for the Enantioselective aza-Henry Reaction:[141] A flame-dried vial was charged with imine (200 µmol), PBAM•$HNTf_2$ (10 µmol) and toluene (285 µL). The resulting solution was cooled to -20 °C for 30 minutes. The α-nitro ester (220 µmol) was added, and the reaction was stirred at -20 °C for 48 h, then filtered while cold through a short plug of silica gel (ethyl acetate) to remove the catalyst. The filtrate was concentrated and subjected to flash column chromatography which afforded the pure adduct. The diastereomeric ratio was determined by ^{1}H NMR analysis of the crude reaction mixture and the enantiomeric excess was determined by HPLC using a chiral stationary phase.

[141] Racemic standards were prepared in the same manner, at ambient temperature with *rac*-PBAM•$HNTf_2$.

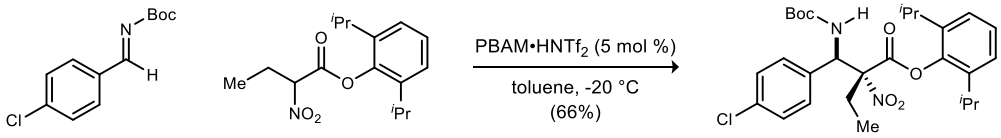

2,6-Diisopropylphenyl (*R*)-2-((*R*)-(4-chlorophenyl)((*tert*-butoxycarbonyl)amino)methyl)-2-nitrobutanoate (128a). Following the general procedure, the imine (48.0 mg, 200 µmol), ester (64.5 mg, 220 µmol), and catalyst (7.9 mg, 10 µmol) in toluene (285 µL) provided, after flash column chromatography (2-5% ethyl acetate in hexanes), the product as a colorless solid (73 mg, 66% yield) in >20:1 dr and 99% ee; (Chiralcel AD-H, 5% ^{i}PrOH/hexanes, 1 mL/min) t_r(*syn*, major) = 4.3 min, t_r(*anti*,minor) = 5.5 min, t_r(*syn*, minor) = 9.2 min, t_r(*anti*, major) = 10.3 min); mp = 77-78 °C; R_f = 0.37 (10% EtOAc/hexanes); $[\alpha]_D^{25}$ +2.8 (*c* 0.40, $CHCl_3$); IR (film) 2972, 2917, 1720, 1562, 1325, 1168, 1130, 668 cm^{-1}; ^{1}H NMR (400 MHz, $CDCl_3$) δ 7.38-7.16 (series of br m, 6H), 7.10 (br d, *J* = 5.3 Hz, 1H), 6.61 (br d, *J* = 9.2 Hz, 1H), 5.69 (br d, *J* = 9.8 Hz, 1H), 3.24-3.10 (br m, 1H), 2.48-2.30 (m, 2H), 1.76 (br s, 1H), 1.39 (s, 9H), 1.26 (br dd, *J* = 7.1, 7.1 Hz, 3H)143, 1.15 (br d, *J* = 6.2 Hz, 3H), 1.04 (br d, *J* = 5.6 Hz, 3H), 0.82 (br d, *J* = 5.5 Hz, 3H); ^{13}C NMR (100 MHz, $CDCl_3$) ppm 164.5, 154.6, 144.6, 134.9, 130.1, 129.2, 129.0, 128.8, 127.5, 124.5, 123.7, 98.8, 80.6, 59.3, 29.8, 28.2, 27.3, 26.6, 24.3, 24.2, 22.7, 21.4, 9.4; HRMS (ESI): Exact mass calcd for $C_{28}H_{37}ClN_2NaO_6$ $[M+Na]^+$ 555.2238, found 555.2248.

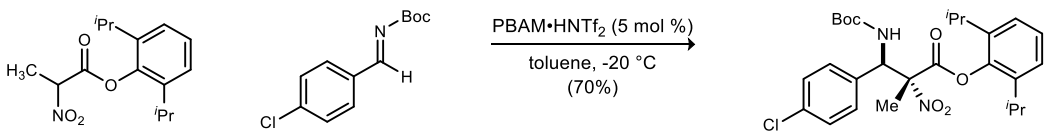

2,6-Diisopropylphenyl (2*R*,3*R*)-3-((*tert*-butoxycarbonyl)amino)-3-(4-chlorophenyl)-2-methyl-2-nitropropanoate (128b). Following the general procedure, the imine (48.0 mg, 200 µmol), ester (61.5 mg, 220 µmol), and catalyst (7.9 mg, 10 µmol) in toluene (285 µL), after flash column chromatography (2-5% ethyl acetate in hexanes) afforded the product as a colorless solid (73 mg, 70% yield) in >20:1 dr and 99% ee; (Chiralcel AD-H, 5% ^{i}PrOH/hexanes, 1 mL/min, t_r(*anti*, minor) = 9.2 min, t_r(*syn*, minor) = 11.2 min, t_r(*anti*, major) = 15.3 min, t_r(*syn*, major) = 28.3 min); mp = 57-60 °C; R_f = 0.42 (10% EtOAc/hexanes); $[\alpha]_D^{25}$ -63 (*c* 1.0, $CHCl_3$); IR (film) 3440, 1751, 1720, 1560, 1491 cm^{-1}; ^{1}H NMR (400 MHz, $CDCl_3$) δ 7.38 (br d, *J* = 8.8 Hz, 2H), 7.35 (br d, *J* = 8.8 Hz, 2H), 7.30-7.18 (br m, 2H), 7.12 (br d, *J* = 6.3 Hz, 1H), 6.47 (br d, *J* = 8.8 Hz, 1H), 5.61 (br d, *J* = 9.6 Hz, 1H), 3.20-3.08 (br m, 1H), 2.04 (s, 3H), 2.00-1.90 (br m, 1H), 1.40 (s, 9H), 1.27 (br d, *J* = 4.4 Hz, 3H), 1.15 (br d, *J* = 6.0 Hz, 3H), 1.02 (br d, *J* = 5.9 Hz, 3H), 0.90 (br d, *J* = 5.9 Hz, 3H); ^{13}C NMR (100 MHz, $CDCl_3$) ppm 164.3, 154.6, 144.7, 140.8, 139.2, 134.9, 133.9, 130.3, 129.1, 127.5, 124.5, 123.8, 94.9, 80.6, 60.0, 28.2, 27.3, 26.6, 24.0, 23.8, 22.8, 22.7, 21.7; HRMS (ESI): Exact mass calcd for $C_{27}H_{35}ClN_2NaO_6$ $[M+Na]^+$ 541.2081, found 541.2085.

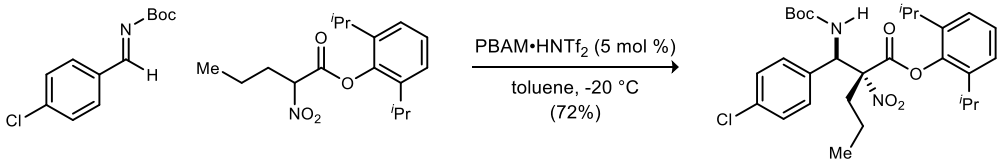

2,6-Diisopropylphenyl (*R*)-2-((*R*)-((*tert*-butoxycarbonyl)amino)(4-chlorophenyl)methyl)-2-nitropentanoate (128c). Following the general procedure, the imine (48.0 mg, 200 µmol), ester (67.6 mg, 220 µmol), and catalyst (7.9 mg, 10 µmol) in toluene (285 µL) provided, after flash column chromatography (2-5% diethyl ether in hexanes), the product as a colorless foamy solid (79 mg, 72% yield) in >20:1 dr and 96% ee; (Chiralpak AD-H, 3% ^{i}PrOH/hexanes, 1 mL/min, t_r(*anti*, minor) = 8.0 min, t_r(*anti*, major) = 9.1 min); mp = 70-72 °C; R_f = 0.39 (10% EtOAc/hexanes); $[\alpha]_D^{25}$ +5.4 (*c* 0.17, $CHCl_3$); IR (film) 3439, 2968, 1745, 1720, 1560, 1491, 1159 cm^{-1}; ^{1}H NMR (400 MHz, $CDCl_3$) δ 7.39-7.30 (br m, 4H), 7.30-7.16 (series of br m, 2H), 7.10 (br d, *J* = 5.6 Hz, 1H), 6.56 (br d, *J* = 9.4 Hz, 1H), 5.69 (br d, *J* = 9.4 Hz, 1H), 3.21-3.07 (br m, 1H), 2.34-2.17 (br m, 1H), 1.94-1.70 (br m, 2H), 1.39 (s, 9H), 1.31-1.18 (br m, 5H), 1.15 (br d, *J* = 5.9 Hz, 3H), 1.04 (br d, *J* = 4.6 Hz, 3H), 1.00 (dd, *J* = 7.3 Hz, 3H), 0.84 (br d, *J* = 5.0 Hz, 3H); ^{13}C NMR (100 MHz, $CDCl_3$) ppm 164.4, 154.5, 144.6, 140.9, 139.0, 134.9, 134.1, 130.1, 128.9, 128.8, 127.5, 124.6, 123.7, 98.4, 80.6, 59.4, 38.4, 30.3, 29.7, 28.2, 27.2, 26.6, 24.2, 22.7, 21.4, 18.2, 14.1; HRMS (ESI): Exact mass calcd for $C_{29}H_{39}ClN_2NaO_6$ $[M+Na]^+$ 569.2394, found 569.2372.

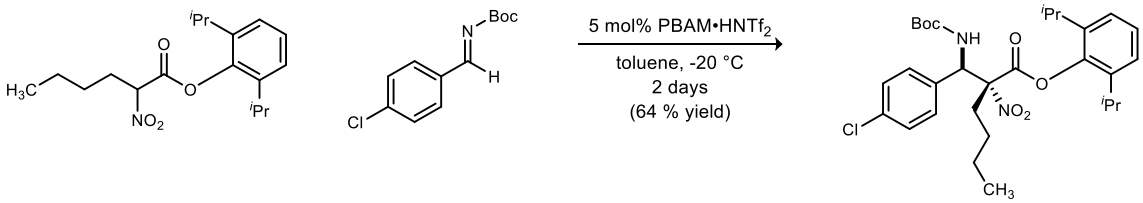

2,6-Diisopropylphenyl (*R*)-2-((*R*)-((*tert*-butoxycarbonyl)amino)(4-chlorophenyl)methyl)-2-nitrohexanoate (128d). Following the general procedure, the imine (48.0 mg, 200 µmol), ester (70.7 mg, 220 µmol), and catalyst (7.9 mg, 10 µmol) in toluene (285 µL), after flash column chromatography (2-5% ethyl acetate in hexanes) afforded the product as a colorless solid (79 mg, 64% yield) in 11:1 dr and 97% ee; (Chiralcel IA, 3% ^{i}PrOH/hexanes, 1 mL/min, tr(anti, major) = 6.5 min, tr(anti, minor) = 5.9 min); mp = 57-60 °C; Rf = 0.13 (3% EtOAc/Hexanes); $[\alpha]_D^{25}$ -63 (c 1.0, CHCl3); IR (film) 3440, 2968, 1720, 1560, 1491, 1159, 1091 cm^{-1}; 1H NMR (500 MHz, CDCl3) δ 7.40-7.30 (m, 4H), 7.28-7.20 (m, 2H), 7.13-7.06 (m, 1H), 6.60-6.45 (m, 1H), 5.69 (d, J = 9.5 Hz, 1H), 3.20-3.10 (m, 1H), 2.40-2.20 (m, 2H), 1.90-1.70 (m, 1H), 1.40-1.30 (m, 4H), 1.38 (s, 9H), 1.30-1.19 (m, 3H), 1.20-1.15 (m, 3H), 1.10-1.00 (m, 3H), 0.91 (t, J = 7.0 Hz, 3H), 0.85-0.75 (m, 3H); 13C NMR (125 MHz, CDCl3) ppm 164.5, 154.5, 144.6, 140.9, 139.1, 134.9, 134.1, 130.1, 128.8, 127.5, 124.6, 123.7, 98.5, 80.6, 59.3, 36.1, 28.2, 27.2, 26.7, 26.6, 24.3, 22.8, 22.7, 21.5, 13.7; HRMS (ESI): Exact mass calcd for C30H41N2O6NaCl [M+Na] 583.2551, found 583.2575.

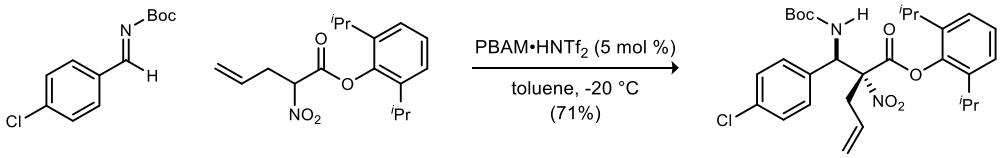

2,6-Diisopropylphenyl (*R*)-2-((*R*)-((*tert*-butoxycarbonyl)amino)(4-chlorophenyl)methyl)-2-nitropent-4-enoate (128e). Following the general procedure, the imine (48.0 mg, 200 µmol), ester (67.2 mg, 220 µmol), and catalyst (7.9 mg, 10 µmol) in toluene (285 µL) provided, after flash column chromatography (3-5% diethyl ether in hexanes), the product as a colorless solid (77 mg, 71% yield) in 9:1 dr and 97% ee; (Chiralpak AD-H, 3% ^{i}PrOH/hexanes, 1 mL/min, t_r(*syn*, major) = 7.6 min, t_r(*anti*, minor) = 10.8 min, t_r(*anti*, major) = 14.2 min, t_r(*syn*,

minor) = 24.7 min); mp = 72-74 °C; R_f = 0.56 (10% EtOAc/hexanes); $[\alpha]_D^{25}$ +2.9 (*c* 0.30, $CHCl_3$); IR (film) 3442, 2969, 2932, 1766, 1723, 1562, 1490, 1366, 1340, 1211, 1160, 1093, 1015 cm^{-1}; ^1H NMR (400 MHz, $CDCl_3$) δ 7.36 (s, 4H), 7.29-7.16 (series of br m, 2H), 7.10 (br d, *J* = 5.8 Hz, 1H), 6.59 (br d, *J* = 9.2 Hz, 1H), 6.01 (dddd, *J* = 14.0, 10.2, 7.2, 7.2 Hz, 1H), 5.71 (br d, *J* = 9.8 Hz, 1H), 5.30 (br dd, *J* = 17.2 Hz, 0.88 Hz, 1H), 5.29 (br dd, *J* = 9.8 Hz, 0.6 Hz, 1H), 3.24-3.10 (br m, 1H), 3.05 (br d, *J* = 6.6 Hz, 2H), 1.77 (br s, 1H), 1.38 (s, 9H), 1.26 (br d, *J* = 6.5 Hz, 3H), 1.15 (br d, *J* = 5.8 Hz, 3H), 1.04 (br d, *J* = 5.6 Hz, 3H), 0.82 (br d, *J* = 5.5 Hz, 3H); ^{13}C NMR (100 MHz, $CDCl_3$) ppm 164.1, 154.5, 144.6, 140.8, 139.0, 135.0, 133.8, 130.2, 129.5, 129.3, 129.2, 128.9, 127.5, 124.6, 123.7, 122.2, 98.3, 80.6, 59.3, 40.6, 28.2, 27.3, 26.6, 24.3, 24.2, 22.7, 21.4; HRMS (ESI): Exact mass calcd for $C_{29}H_{37}ClN_2NaO_6$ $[M+Na]^+$ 567.2238, found 567.2224.

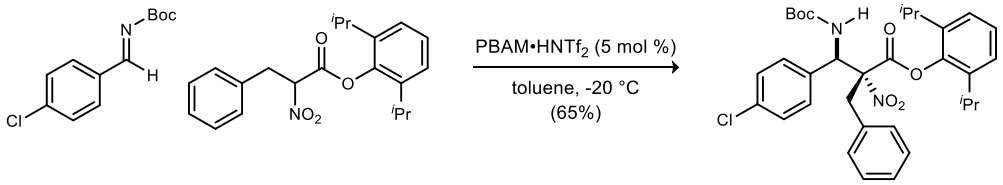

2,6-Diisopropylphenyl (2*R*,3*R*)-2-benzyl-3-((*tert*-butoxycarbonyl)amino)-3-(4-chlorophenyl)-2-nitropropanoate (128f). Following the general procedure, the imine (47.9 mg, 200 µmol), ester (78.2 mg, 220 µmol), and catalyst (7.9 mg, 10 µmol) in toluene (285 µL) provided, after flash column chromatography (2-5% diethyl ether in hexanes), the product as a viscous oil (77 mg, 65% yield)[142] in 4:1 dr and 83% ee; (Chiralcel OD-H, 3% ^{i}PrOH/hexanes, 1 mL/min, t_r(*syn*, major) = 5.2 min, t_r(*anti*, major) = 6.0 min, t_r(*syn*, minor) = 7.7 min, t_r(*anti*, minor) = 9.0 min); R_f = 0.42 (10% EtOAc/hexanes); IR (film) 3432, 2968, 1720, 1561, 1491, 1366, 1160, 1093, 698 cm^{-1}; ^1H NMR (400 MHz, $CDCl_3$) δ 7.46-7.06 (series of br m, 12H), 6.66 (br d, *J* = 8.4 Hz, 1H), 5.85 (br d, *J* = 9.2 Hz, 1H), 3.70 (d, *J* = 14.6 Hz, 1H), 3.62 (d, *J* = 14.2 Hz, 1H), 2.46 (br s, 1H), 1.96-1.79 (br m, 1H), 1.41 (s, 9H), 1.36-0.70 (series of br m, 12H);^{13}C NMR (100 MHz, $CDCl_3$) ppm 169.1, 154.4, 144.0, 135.0, 132.6, 130.3, 130.2, 129.6, 129.1, 129.0, 128.9, 128.5, 128.1, 127.5, 99.0, 80.7, 60.3, 42.0, 28.2, 27.3, 27.1, 26.2, 24.7, 23.8, 21.7; HRMS (ESI): Exact mass calcd for $C_{33}H_{39}ClN_2NaO_6$ $[M+Na]^+$ 617.2394, found 617.2420.

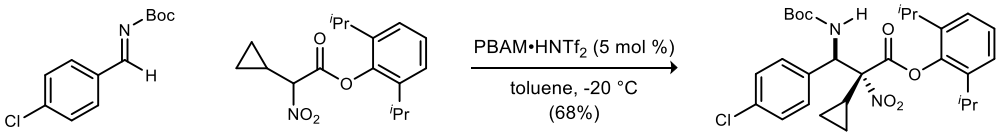

2,6-Diisopropylphenyl (2*R*,3*R*)-3-((*tert*-butoxycarbonyl)amino)-3-(4-chlorophenyl)-2-cyclopropyl-2-nitropropanoate (128g). Following the general procedure, the imine (24.0 mg, 100 µmol), ester (34.0 mg, 110 µmol), and catalyst (4.0 mg, 5 µmol) in toluene (145 µL) provided, after flash column chromatography (SiO_2, 2-5% diethyl ether in hexanes), the product as a colorless viscous oil (37 mg, 68% yield) in 11:1 dr and 98% ee; (Chiralcel OD-H, 2% ^{i}PrOH/hexanes, 0.4 mL/min, t_r(*syn*, minor) = 4.7 min, t_r(*anti*, major) = 5.0 min, t_r(*syn*, major) = 5.5 min, t_r(*anti*, minor) = 7.9 min); R_f = 0.39 (10% EtOAc/hexanes); $[\alpha]_D^{25}$ -6.1 (*c* 0.28, $CHCl_3$); IR

[142] Unable to separate the desired adduct from a small amount of residual starting material α-nitro ester.

(film) 2969, 2929, 1722, 1644, 1561, 1491, 1225, 1161, 1094 cm^{-1}; ^1H NMR (500 MHz, $CDCl_3$) δ 7.44 (br d, *J* = 8.3 Hz, 2H), 7.35 (br d, *J* = 8.6 Hz, 3H), 7.25-7.16 (series of br m, 2H), 7.09 (br d, *J* = 6.5 Hz, 1H), 6.73 (br d, *J* = 9.9 Hz, 1H), 5.76 (br d, *J* = 10.0 Hz, 1H), 3.34-3.23 (br m, 1H), 1.82-1.71 (br m, 1H), 1.26 (br s, 9H), 1.21 (br d, *J* = 6.8 Hz, 2H), 1.16 (br d, *J* = 6.5 Hz, 5H), 1.02 (br d, *J* = 6.2 Hz, 3H), 0.93-0.85 (br m, 2H), 0.76 (br d, *J* = 5.7 Hz, 3H), 0.59-0.50 (br m, 1H); ^{13}C NMR (125 MHz, $CDCl_3$) ppm 164.5, 154.6, 145.2, 140.8, 139.0, 134.8, 134.0, 130.3, 129.8, 128.9, 128.7, 127.4, 124.4, 123.7, 98.5, 80.5, 59.8, 30.3, 29.7, 28.2, 27.4, 26.6, 24.3, 24.0, 22.6, 21.4, 16.5, 5.92, 3.44; HRMS (ESI): Exact mass calcd for $C_{29}H_{37}ClN_2NaO_6$ $[M+Na]^+$ 567.2238, found 567.2224.

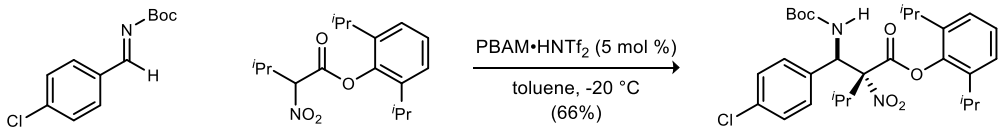

2,6-Diisopropylphenyl (*R*)-2-((*R*)-((*tert*-butoxycarbonyl)amino)(4-chlorophenyl)methyl)-3-methyl-2-nitrobutanoate (128h). Following the general procedure, the imine (48.0 mg, 200 µmol), ester (67.6 mg, 220 µmol), and catalyst (7.9 mg, 10 µmol) in toluene (285 µmol) provided, after flash column chromatography (SiO_2, 1-3% diethyl ether in hexanes), the product as a colorless oil which solidified upon standing (73 mg, 66% yield) in >20:1 dr and 93% ee; (Chiralpak IA, 3% ^{i}PrOH/hexanes, 1 mL/min, t_r(*anti*, major) = 5.1 min, t_r(*anti*, minor) = 6.9 min); mp = 137-138 °C; R_f = 0.61 (10% EtOAc/hexanes); $[\alpha]_D^{25}$ +2.8 (*c* 0.75, $CHCl_3$); IR (film) 2970, 2930, 2871, 1743, 1720, 1556, 1492, 1226, 1160, 1143, 1092 cm^{-1}; ^1H NMR (400 MHz, $CDCl_3$) δ 7.30-7.19 (series of br m, 5H), 7.15 (br d, *J* = 6.2 Hz, 2H), 6.00 (br s, 1H), 5.88 (br d, *J* = 9.0 Hz, 1H), 3.16-3.00 (br m, 1H), 2.86 (br s, 1H), 2.46-2.28 (br m, 1H), 1.41 (s, 9H), 1.36 (d, *J* = 6.8 Hz, 3H), 1.21 (d, *J* = 6.8 Hz, 3H), 1.12 (br d, *J* = 6.5 Hz, 6H), 1.00 (br s, 3H), 0.99 (br s, 3H); ^{13}C NMR (100 MHz, $CDCl_3$) ppm 164.5, 154.6, 144.6, 134.9, 130.1, 129.2, 129.0, 128.8, 127.5, 124.5, 123.7, 98.8, 80.6, 59.3, 29.8, 28.2, 27.3, 26.6, 24.3, 24.2, 22.7, 21.4, 9.4; HRMS (ESI): Exact mass calcd for $C_{29}H_{39}ClN_2NaO_6$ $[M+Na]^+$ 569.2394, found 569.2398.

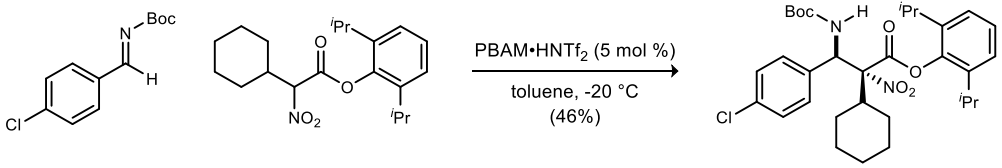

2,6-Diisopropylphenyl (2*R*,3*R*)-3-((*tert*-butoxycarbonyl)amino)-3-(4-chlorophenyl)-2-cyclohexyl-2-nitropropanoate (128i). Following the general procedure, the imine (108 mg, 450 µmol), ester (172 mg, 495 µmol), and catalyst (18.1 mg, 23 µmol) in toluene (650 µL) provided, after flash column chromatography (1-3% ethyl acetate in hexanes), the product as an off-white viscous oil (121 mg, 46% yield) in >20:1 dr and 87% ee; (Chiralcel OZ-H, 2% ^{i}PrOH/hexanes, 0.4 mL/min, t_r(*anti*, minor) = 8.9 min, t_r(*anti*, major) = 10.3 min); R_f = 0.54 (10% EtOAc/hexanes); $[\alpha]_D^{25}$ +3.2 (*c* 0.34, $CHCl_3$); IR (film) 2966, 2930, 2857, 1743, 1720, 1554, 1492, 1366, 1207, 1161, 1092 cm^{-1}; ^1H NMR (400 MHz, $CDCl_3$) δ 7.22-7.12 (series of br m, 5H), 7.07 (br d, *J* = 7.5 Hz, 2H), 5.95-5.73 (br m, 2H), 2.64 (br s, 2H), 2.48 (br s, 1H), 2.05 (br d, *J* = 10.4 Hz, 1H), 1.89-1.75 (br m, 3H), 1.70 (br dd, *J* = 11.4, 8.9 Hz, 2H), 1.36 (br s, 9H), 1.29-0.98 (series of br m, 10H), 0.92 (br s, 6H); ^{13}C NMR (100 MHz,

$CDCl_3$) ppm 163.6, 144.8, 135.1 (br, 2C). 134.6, 129.7, 128.7, 127.4, 124.4 (br, 2C), 103.3, 80.8, 55.3, 43.7, 29.7, 28.2, 27.4, 27.1, 26.6, 26.5, 26.0, 24.3, 22.7; HRMS (ESI): Exact mass calcd for $C_{32}H_{43}ClN_2NaO_6$ $[M+Na]^+$ 609.2707, found 609.2735.

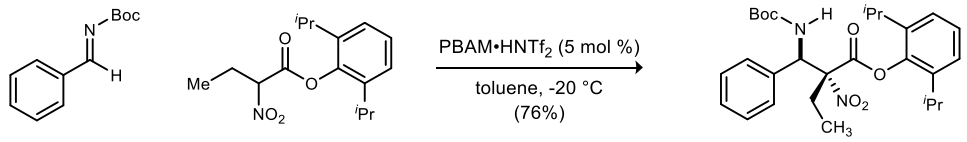

2,6-Diisopropylphenyl (*R*)-2-((*R*)-((*tert*-butoxycarbonyl)amino)(phenyl)methyl)-2-nitrobutanoate (128j). Following the general procedure, the imine (41.1 mg, 200 µmol), ester (64.5 mg, 220 µmol), and catalyst (7.9 mg, 10 µmol) in toluene (285 µmol) provided, after flash column chromatography (2-10% ethyl acetate in hexanes), the product as an amorphous solid (66 mg, 76% yield) in >20:1 dr and 96% ee; (Chiralpak IA, 3% ^{i}PrOH/hexanes, 1 mL/min, t_r(*syn*, minor) = 5.0 min, t_r(*anti*, minor) = 6.5 min, t_r(*syn*, major) = 7.6 min, t_r(*anti*, major) = 9.7 min); mp = 66-68 °C; R_f = 0.44 (10% EtOAc/hexanes); $[\alpha]_D^{25}$ +3.3 (*c* 0.67, $CHCl_3$); IR (film) 2972, 2917, 1720, 1562, 1325, 1168, 1130, 668 cm^{-1}; ^{1}H NMR (500 MHz, DMSO-d_6) δ 7.73 (br d, *J* = 10.5 Hz, 1H), 7.44 (br s, 2H), 7.36 (br s, 3H), 7.31-7.15 (br m, 3H), 5.79 (br d, *J* = 9.5 Hz, 1H), 2.85 (br s, 1H), 2.48-2.39 (br m, 2H), 2.30 (br s, 1H), 1.32 (s, 9H), 1.15-0.97 (br m, 12H), 0.93 (br s, 3H); ^{13}C NMR (125 MHz, DMSO-d_6) ppm 163.4, 154.8, 144.2, 135.9, 128.9, 128.5, 128.2, 127.4, 124.3, 99.6, 79.3, 65.0, 58.2, 28.0, 26.9, 26.5 (2C), 23.9 (2C), 22.6, 22.3, 15.2, 8.7; HRMS (ESI): Exact mass calcd for $C_{28}H_{38}NaN_2O_6$ $[M+Na]^+$ 521.2628, found 521.2609.

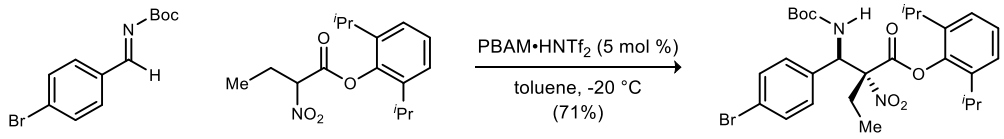

2,6-Diisopropylphenyl (*R*)-2-((*R*)-(4-bromophenyl)((*tert*-butoxycarbonyl)amino)methyl)-2-nitrobutanoate (128k). Following the general procedure, the imine (56.8 mg, 200 µmol), ester (64.5 mg, 220 µmol), and catalyst (7.9 mg, 10 µmol) in toluene (285 µmol) provided, after flash column chromatography (2-5% diethyl ether in hexanes), the product as a colorless solid (82 mg, 71% yield) in >20:1 dr and 99% ee; (Chiralpak IA, 3% ^{i}PrOH/hexanes, 1 mL, /min) t_r(*anti*, major) = 4.7 min, t_r(*syn*, minor) = 10.9, t_r(*anti*, minor) = 17.8 min, t_r(*syn*, major) = 27.3 min); mp = 73-74 °C; R_f = 0.37 (10% EtOAc/hexanes); $[\alpha]_D^{25}$ -3.2 (*c* 0.34, $CHCl_3$); IR (film) 2968, 2929, 1271, 1641, 1561, 1489, 1366, 1225, 1160 cm^{-1}; ^{1}H NMR (400 MHz, $CDCl_3$) δ 7.49 (br d, *J* = 8.5 Hz, 2H), 7.27 (br d, *J* = 5.3 Hz, 2H), 7.24 (br d, *J* = 8.6 Hz, 2H), 7.09 (br d, *J* = 6.0 Hz, 1H), 6.59 (br d, *J* = 9.6 Hz, 1H), 5.66 (br d, *J* = 10.0 Hz, 1H), 3.24-3.08 (br m, 1H), 2.46-2.28 (br m, 2H), 1.75 (br s, 1H), 1.38 (s, 9H), 1.24 (br dd, *J* = 7.2, 7.2 Hz, 3H)[143], 1.14 (br d, *J* = 6.2 Hz, 3H), 1.03 (br d, *J* = 5.5 Hz, 3H), 0.81 (br d, *J* = 5.5 Hz, 3H); ^{13}C NMR (100 MHz, $CDCl_3$) ppm 164.5, 154.5, 144.6, 140.9, 139.1, 134.6, 131.8, 130.4, 127.5. 124.6, 123.7, 123.1, 98.8, 80.6, 59.4, 29.8, 28.2, 27.3, 24.3, 24.2, 22.7, 21.4, 9.4; HRMS (ESI): Exact mass calcd for $C_{28}H_{37}BrN_2NaO_6$ $[M+Na]^+$ 599.1733, found 599.1761.

[143] One methyl signal arising from the aryl ^{i}Pr groups is eclipsed by the dd.

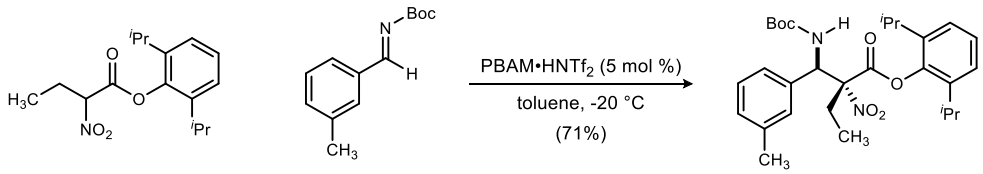

2,6-Diisopropylphenyl (*R*)-2-((*R*)-((*tert*-butoxycarbonyl)amino)(*m*-tolyl)methyl)-2-nitrobutanoate (128l). Following the general procedure, the imine (43.9 mg, 200 µmol), ester (64.5 mg, 220 µmol), and catalyst (7.9 mg, 10 µmol) in toluene (285 µmol), after flash column chromatography (2-5% ethyl acetate in hexanes) afforded the product as a colorless solid (73 mg, 71% yield) in 12:1 dr and 97% ee; (Chiralcel AD-H, 3% ^{i}PrOH/hexanes, 1 mL/min, t_r(*syn*, major) = 4.4 min, t_r(*anti*, minor) = 5.6 min), t_r(*syn*, minor) = 6.4 min, t_r(*anti*, major) = 7.9 min); mp = 48-50 °C; R_f = 0.38 (10% EtOAc/hexanes); $[\alpha]_D^{25}$ -34 (*c* 1.0, $CHCl_3$); IR (film) 3442, 2968, 1747, 1723, 1559, 1490, 1220, 1160 cm^{-1}; ^{1}H NMR (500 MHz, $CDCl_3$) δ 7.30-7.10 (series of m, 6H), 7.10-7.00 (br m, 1H), 6.65 (br d, *J* = 9.1 Hz, 1H), 5.67 (br d, *J* = 9.5 Hz, 1H), 3.30-3.15 (br m, 1H), 2.43-2.36 (br m, 2H), 2.35 (s, 3H), 1.90-1.70 (br s, 1H), 1.39 (s, 9H), 1.35-1.20 (br m, 6H), 1.15 (br d, *J* = 6.1 Hz, 3H), 1.05-0.95 (br s, 3H), 0.80-0.74 (br s, 3H); ^{13}C NMR (125 MHz, $CDCl_3$) ppm 164.5, 154.6, 144.7, 139.2, 138.3, 135.3, 129.5, 128.5, 127.3, 125.6, 124.5, 123.6, 99.2, 80.2, 60.0, 29.9, 28.2, 27.3, 27.1, 26.6, 24.2, 22.7, 21.5, 9.44; HRMS (ESI): Exact mass calcd for $C_{29}H_{40}N_2NaO_6$ $[M+Na]^+$ 535.2784, found 535.2778.

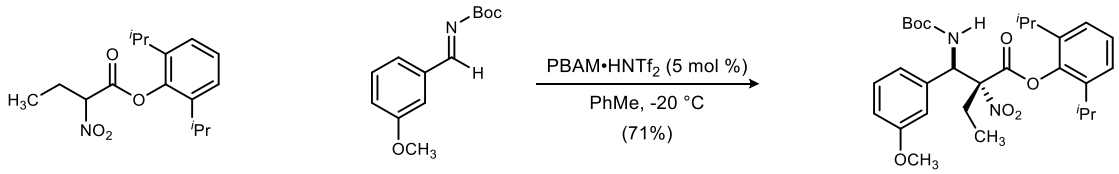

2,6-Diisopropylphenyl (*R*)-2-((*R*)-((*tert*-butoxycarbonyl)amino)(3-methoxyphenyl)methyl)-2-nitrobutanoate (128m). Following the general procedure, the imine (47.1 mg, 200 µmol), ester (64.5 mg, 220 µmol), and catalyst (7.9 mg, 10 µmol) in toluene (285 µmol) provided, after flash column chromatography (3-10% ethyl acetate in hexanes), the product as a colorless viscous oil (75 mg, 71% yield) in 5:1 dr and 96% ee. (Chiralcel AD-H, 5% ^{i}PrOH/hexanes, 1 mL/min, t_r(*syn*, major) = 4.6 min, t_r(*anti*, minor) = 6.3 min, t_r(*syn*, minor) = 6.7 min, t_r(*anti*, major) = 11.2 min); R_f = 0.21 (10% EtOAc/hexanes); $[\alpha]_D^{25}$ +6.9 (*c* 0.35, $CHCl_3$); IR (film) 3441, 2971, 1747, 1722, 1602, 1560, 1489, 1366, 1221, 1159 cm^{-1}; ^{1}H NMR (400 MHz, $CDCl_3$) δ 7.30-7.15 (series of br m, 3H), 7.07 (br d, *J* = 5.6 Hz, 1H), 6.99-6.86 (series of br m, 3H), 6.66 (br d, *J* = 9.8 Hz, 1H), 5.67 (br d, *J* = 9.6 Hz, 1H), 3.77 (s, 3H), 3.28-3.14 (br m, 1H), 2.47-2.30 (br m, 2H), 1.90-1.76 (br m, 1H), 1.38 (s, 9H), 1.32-1.20 (series of m, 6H), 1.15 (br d, *J* = 5.5 Hz, 3H), 0.99 (br d, *J* = 5.9 Hz, 3H), 0.78 (br d, *J* = 5.8 Hz, 3H); ^{13}C NMR (100 MHz, $CDCl_3$) ppm 164.5, 159.7, 159.6, 154.6, 144.8 (2C), 136.9, 129.6, 127.3, 124.5, 123.6, 120.9, 114.8, 113.8, 99.0, 80.3, 59.9, 55.2, 29.9, 28.2 (3C), 27.3 (2C), 26.6, 24.3, 22.8, 21.4, 9.45; HRMS (ESI): Exact mass calcd for $C_{29}H_{40}N_2NaO_7$ $[M+Na]^+$ 551.2733, found 551.2755.

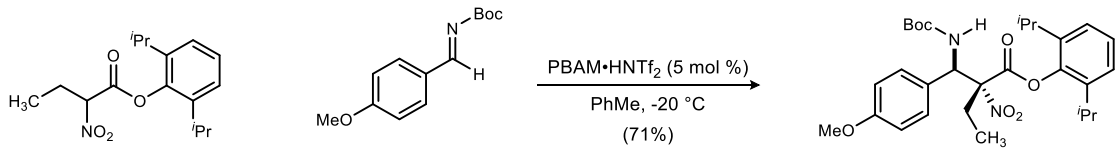

2,6-Diisopropylphenyl (*R*)-2-((*R*)-((*tert*-butoxycarbonyl)amino)(3-methoxyphenyl)methyl)-2-nitrobutanoate (128n). Following the general procedure, the imine (47.1 mg, 200 µmol), ester (64.5 mg, 220 µmol), and catalyst (7.9 mg, 10 µmol) in toluene (285 µmol) provided, after flash column chromatography (3-10% ethyl acetate in hexanes), the product as a colorless viscous oil (75 mg, 71% yield) in 5:1 dr and 96% ee. (Chiralcel AD-H, 5% ^{i}PrOH/hexanes, 1 mL/min, t_r(*syn*, major) = 4.6 min, t_r(*anti*, minor) = 6.3 min, t_r(*syn*, minor) = 6.7 min, t_r(*anti*, major) = 11.2 min); R_f = 0.21 (10% EtOAc/hexanes); $[\alpha]_D^{25}$ +6.9 (*c* 0.35, $CHCl_3$); IR (film) 3441, 2971, 1747, 1722, 1602, 1560, 1489, 1366, 1221, 1159 cm^{-1}; ^{1}H NMR (400 MHz, $CDCl_3$) δ 7.30-7.15 (series of br m, 3H), 7.07 (br d, *J* = 5.6 Hz, 1H), 6.99-6.86 (series of br m, 3H), 6.66 (br d, *J* = 9.8 Hz, 1H), 5.67 (br d, *J* = 9.6 Hz, 1H), 3.77 (s, 3H), 3.28-3.14 (br m, 1H), 2.47-2.30 (br m, 2H), 1.90-1.76 (br m, 1H), 1.38 (s, 9H), 1.32-1.20 (series of m, 6H), 1.15 (br d, *J* = 5.5 Hz, 3H), 0.99 (br d, *J* = 5.9 Hz, 3H), 0.78 (br d, *J* = 5.8 Hz, 3H); ^{13}C NMR (100 MHz, $CDCl_3$) ppm 164.5, 159.7, 159.6, 154.6, 144.8 (2C), 136.9, 129.6, 127.3, 124.5, 123.6, 120.9, 114.8, 113.8, 99.0, 80.3, 59.9, 55.2, 29.9, 28.2 (3C), 27.3 (2C), 26.6, 24.3, 22.8, 21.4, 9.45; HRMS (ESI): Exact mass calcd for $C_{29}H_{40}N_2NaO_7$ $[M+Na]^+$ 551.2733, found 551.2755.

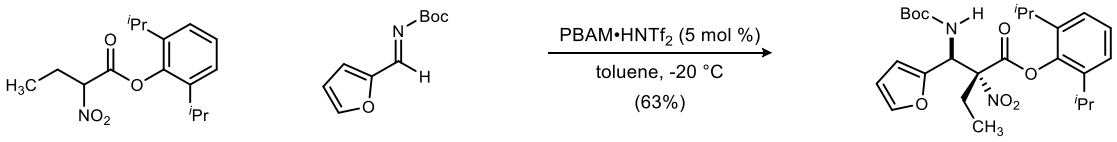

2,6-Diisopropylphenyl (*R*)-2-((*S*)-((*tert*-butoxycarbonyl)amino)(furan-2-yl)methyl)-2-nitrobutanoate (128o). Following the general procedure, the imine (39.0 mg, 200 µmol), ester (64.5 mg, 220 µmol), and catalyst (7.9 mg, 10 µmol) in toluene (285 µL), after flash column chromatography (2-5% ethyl acetate in hexanes) afforded the product as a colorless viscous oil (64 mg, 63% yield) in 4:1 dr and 91% ee; (Chiralcel AD-H, 3% ^{i}PrOH/hexanes, 1 mL/min, t_r(*syn*, minor) = 7.2 min t_r(*anti*, major) = 8.6 min, t_r(*anti*, minor) = 9.1 min, t_r(*syn*, major) = 9.8 min); R_f = 0.42 (10% EtOAc/hexanes); IR (film) 3440, 1724, 1560, 1488, 1226, 1158, 1091 cm^{-1}; ^{1}H NMR (400 MHz, $CDCl_3$) δ 7.41 (s, 1H), 7.30-7.10 (series of br m, 4H), 6.40 (s, 1H), 6.38 (br d, *J* = 10.8 Hz, 1H), 5.87 (br d, *J* = 10.1 Hz, 1H), 3.30-3.16 (br s, 1H), 2.60-2.50 (br m, 1H), 2.48-2.38 (br m, 1H), 2.37-2.28 (br m, 1H), 1.42 (s, 9H), 1.27 (dd, *J* = 4.4, 4.4 Hz, 3H), 1.23-1.10 (series of br m, 9H), 1.04-0.98 (br s, 3H); ^{13}C NMR (100 MHz, $CDCl_3$) ppm 164.4, 154.7, 149.4, 144.7, 142.8, 140.8, 139.7, 127.4, 124.4, 110.8, 110.0, 97.7, 80.5, 53.5, 29.0, 28.2, 27.1, 26.9, 24.3, 22.8, 22.1, 8.84; HRMS (ESI): Exact mass calcd for $C_{26}H_{36}N_2NaO_7$ $[M+Na]^+$ 511.2420, found 511.2444.

2,6-Diisopropylphenyl (*R*)-2-((*S*)-((*tert*-butoxycarbonyl)amino)(thiophen-2-yl)methyl)-2-nitrobutanoate (128p). Following the general procedure, the imine (42.7 mg, 200 µmol), ester (64.5 mg, 220 µmol), and catalyst (7.9 mg, 10 µmol) in toluene (285 µL), after flash column chromatography (1.5-4% ethyl acetate in hexanes) afforded the product as a colorless solid (64 mg, 63% yield) in >20:1 dr and 97% ee; (Chiralcel AD-H, 3% ^{i}PrOH/hexanes, 1 mL/min, t_r (*syn*, minor) = 4.9 min, t_r(*anti*, minor) = 6.5 min, t_r(*syn*, major) = 7.0 min, t_r(*anti*,

major) = 8.1 min); mp = 103-106 °C; R_f = 0.33 (10% EtOAc/hexanes); $[\alpha]_D^{25}$ -17 (*c* 0.51, $CHCl_3$); IR (film) 3433, 1746, 1722, 1560, 1487, 1366, 1225, 1159 cm^{-1}; ^1H NMR (400 MHz, $CDCl_3$) δ 7.32 (dd, *J* = 5.0, 0.72 Hz, 1H), 7.29-7.16 (br m, 2H), 7.11 (br d, *J* = 3.5 Hz, 2H), 7.01 (dd, *J* = 3.7, 1.4 Hz, 1H), 6.51 (br d, *J* = 9.4 Hz, 1H), 5.96 (br d, *J* = 9.8 Hz, 1H), 3.25-3.15 (br m, 1H), 2.50 (m, 2H), 2.05 (br s, 1H), 1.42 (s, 9H), 1.29 (dd, *J* = 7.2, 7.2 Hz, 3H), 1.27-1.20 (br m, 3H), 1.17 (br d, *J* = 4.6 Hz, 3H), 1.06 (br d, *J* = 4.9 Hz, 3H), 0.93 (br d, *J* = 5.3 Hz, 3H); ^{13}C NMR (100 MHz, $CDCl_3$) ppm 164.6, 154.5, 144.7, 140.9, 139.4, 138.5, 127.8, 127.4, 126.9, 126.2, 124.4, 123.8, 98.5, 80.5, 55.9, 29.8, 28.2, 27.2, 26.6, 24.4, 24.1, 22.8, 21.9, 9.15; HRMS (ESI): Exact mass calcd for $C_{26}H_{36}N_2NaO_6S$ $[M+Na]^+$ 527.2192, found 527.2192.

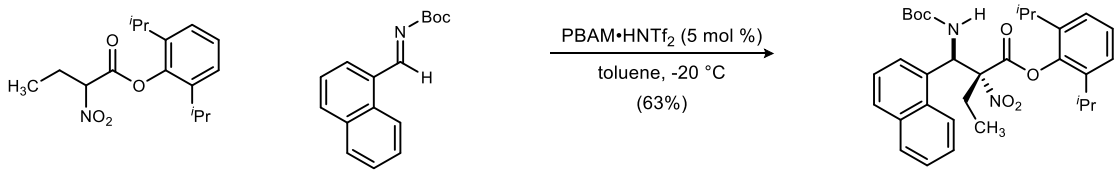

2,6-Diisopropylphenyl (*R*)-2-((*R*)-((*tert*-butoxycarbonyl)amino)(naphthalen-1-yl)methyl)-2-nitrobutanoate (128q). Following the general procedure, the imine (42.7 mg, 200 µmol), ester (64.5 mg, 220 µmol), and catalyst (7.9 mg, 10 µmol) in toluene (285 µL), after flash column chromatography (1.5-4% ethyl acetate in hexanes) afforded the product as a colorless solid (64 mg, 63% yield) in >20:1 dr and 97% ee; (Chiralcel AD-H, 3% ^{i}PrOH/hexanes, 1 mL/min, t_r (*syn*, minor) = 4.9 min, t_r(*anti*, minor) = 6.5 min, t_r(*syn*, major) = 7.0 min, t_r(*anti*, major) = 8.1 min); mp = 103-106 °C; R_f = 0.33 (10% EtOAc/hexanes); $[\alpha]_D^{25}$ -17 (*c* 0.51, $CHCl_3$); IR (film) 3433, 1746, 1722, 1560, 1487, 1366, 1225, 1159 cm^{-1}; ^1H NMR (400 MHz, $CDCl_3$) δ 7.32 (dd, *J* = 5.0, 0.72 Hz, 1H), 7.29-7.16 (br m, 2H), 7.11 (br d, *J* = 3.5 Hz, 2H), 7.01 (dd, *J* = 3.7, 1.4 Hz, 1H), 6.51 (br d, *J* = 9.4 Hz, 1H), 5.96 (br d, *J* = 9.8 Hz, 1H), 3.25-3.15 (br m, 1H), 2.50 (m, 2H), 2.05 (br s, 1H), 1.42 (s, 9H), 1.29 (dd, *J* = 7.2, 7.2 Hz, 3H), 1.27-1.20 (br m, 3H), 1.17 (br d, *J* = 4.6 Hz, 3H), 1.06 (br d, *J* = 4.9 Hz, 3H), 0.93 (br d, *J* = 5.3 Hz, 3H); ^{13}C NMR (100 MHz, $CDCl_3$) ppm 164.6, 154.5, 144.7, 140.9, 139.4, 138.5, 127.8, 127.4, 126.9, 126.2, 124.4, 123.8, 98.5, 80.5, 55.9, 29.8, 28.2, 27.2, 26.6, 24.4, 24.1, 22.8, 21.9, 9.15; HRMS (ESI): Exact mass calcd for $C_{26}H_{36}N_2NaO_6S$ $[M+Na]^+$ 527.2192, found 527.2192.

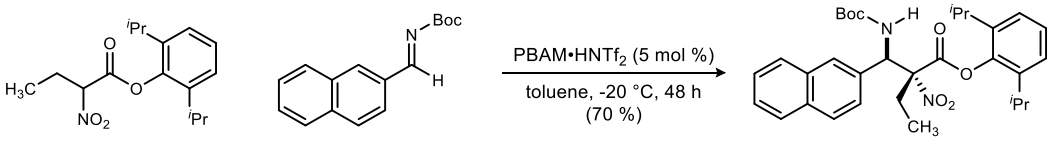

2,6-Diisopropylphenyl (*R*)-2-((*R*)-((*tert*-butoxycarbonyl)amino)(naphthalen-2-yl)methyl)-2-nitrobutanoate (128r). Following the general procedure, the imine (51.1 mg, 200 µmol), ester (64.5 mg, 220 µmol), and catalyst (7.9 mg, 10 µmol) in toluene (285 µmol) provided, after flash column chromatography (2-5% ethyl acetate in hexanes), the product as a colorless solid (76 mg, 70% yield) in >20:1 dr and 96% ee; (Chiralcel IA, 5% ^{i}PrOH/hexanes, 1 mL/min, t_r(*syn*, minor) = 4.8 min), t_r(*anti*, minor) = 5.7 min, t_r(*syn*, major) = 7.4 min, t_r(*anti*, major) = 10.8 min); mp = 66-68 °C; R_f = 0.42 (10% EtOAc/hexanes); $[\alpha]_D^{25}$ -23 (*c* 0.13, $CHCl_3$); IR (film) 3445, 1747, 1720, 1559, 1490, 1160 cm^{-1}; ^1H NMR (400 MHz, $CDCl_3$) δ 7.90-7.80 (series of br m, 4H), 7.56-7.46 (m, 3H), 7.23-7.16 (br m, 2H), 7.02-6.90 (br m, 1H), 6.79 (br d, *J* = 9.6 Hz, 1H), 5.89 (br d, *J* = 9.6 Hz, 1H), 3.30-3.10 (br m, 1H), 2.60-2.35 (br m, 2H), 1.55-1.45 (br m, 1H), 1.39 (s, 9H), 1.28 (dd, *J* = 7.2, 7.2 Hz, 3H), 1.26-

1.21 (m, 3H), 1.13 (d, J = 6.2 Hz, 3H), 0.54 (br d, J = 7.0 Hz, 3H), 0.51 (br d, J = 6.8 Hz, 3H); ^{13}C NMR (100 MHz, $CDCl_3$) ppm 164.6, 154.6, 144.7, 140.9, 139.1, 133.3, 133.0, 133.7, 128.5, 128.4, 128.2, 127.5, 127.3, 126.8, 126.5, 125.9, 124.5, 123.6, 99.2, 80.3, 60.1, 30.1, 28.2, 27.2, 26.6, 24.2, 24.0, 22.7, 20.7, 9.48; HRMS (ESI): Exact mass calcd for $C_{32}H_{40}N_2NaO_6$ $[M+Na]^+$ 571.2784, found 571.2785.

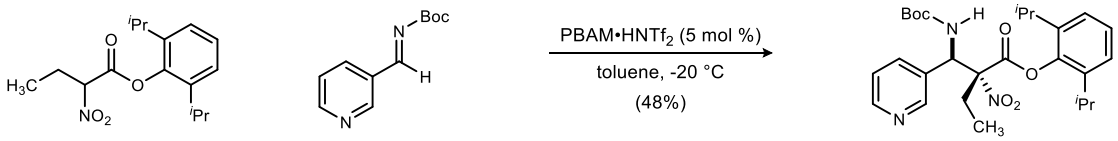

2,6-Diisopropylphenyl (*R*)-2-((*R*)-((*tert*-butoxycarbonyl)amino)(pyridin-3-yl)methyl)-2-nitrobutanoate (128s). Following the general procedure, the imine (20.6 mg, 100 µmol), ester (32.3 mg, 110 µmol), and catalyst (4.0 mg, 5.0 µmol) in toluene (143 µL), after flash column chromatography (20% ethyl acetate in hexanes) afforded the product as a colorless solid (24 mg, 48% yield) in 9:1 dr and 96% ee; (Chiralcel AD-H, 3% ^{i}PrOH/hexanes, 1 mL/min, t_r(*syn*, minor) = 17.6 min , t_r(*anti*, minor) = 23.2 min, t_r(*anti*, major) = 34.8 min, t_r(*syn*, major) = 46.0 min); mp 52-54 °C; R_f = 0.14 (20% EtOAc/hexanes); $[\alpha]_D^{25}$ -18 (*c* 0.45, $CHCl_3$); IR (film) 3442, 1747, 1723, 1559, 1490, 1220, 1160 cm^{-1}; ^{1}H NMR (500 MHz, $CDCl_3$) δ 8.68 (br s, 1H), 8.62 (br d, J = 3.5 Hz, 1H), 7.71 (br d, J = 7.9 Hz, 1H), 7.35-7.20 (series of br m, 3H), 7.10 (br s, 1H), 6.53 (br s, 1H), 5.74 (br d, J = 9.7 Hz, 1H), 3.13 (br s, 1H), 2.50-2.30 (series of br m, 2H), 1.90-1.80 (br s, 1H), 1.39 (s, 9H), 1.30-1.20 (series of m, 6H), 1.18-1.15 (br s, 3H), 1.05-0.95 (br s, 3H), 0.85-0.75 (br s, 3H); ^{13}C NMR (125 MHz, $CDCl_3$) ppm 164.5, 154.5, 150.3, 150.0, 144.5, 140.8, 139.1, 136.1, 131.6, 127.5, 124.6, 123.8, 123.4, 98.8, 80.8, 57.7, 29.6, 28.2, 27.3, 27.2, 24.1, 22.8, 21.9, 9.25; HRMS (ESI): Exact mass calcd for $C_{27}H_{38}N_3O_6$ $[M+H]^+$ 500.2761, found 500.2776.

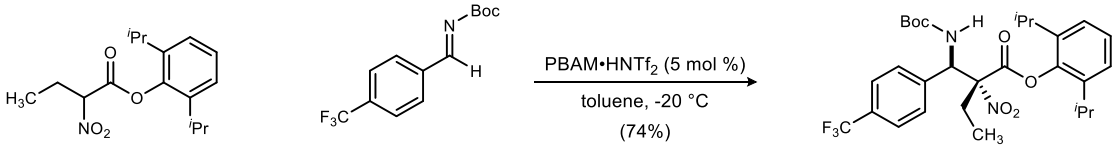

2,6-Diisopropylphenyl (*R*)-2-((*R*)-((*tert*-butoxycarbonyl)amino)(4-(trifluoromethyl)phenyl)methyl)-2-nitrobutanoate (128t). Following the general procedure, the imine (54.7 mg, 200 µmol), ester (64.5 mg, 220 µmol), and catalyst (7.9 mg, 10 µmol) in toluene (285 µmol) provided, after flash column chromatography (2-5% ethyl acetate in hexanes), the product as a colorless solid (84 mg, 74% yield) in 15:1 dr and 99% ee; (Chiralcel AD-H, 5% ^{i}PrOH/hexanes, 1 mL/min, t_r(*anti*, minor) = 5.3 min. t_r(*syn*, major and minor)[144] = 7.3 min, t_r(*anti*, major) = 9.6 min); mp = 55-58 °C; R_f = 0.42 (10% EtOAc/hexanes); $[\alpha]_D^{25}$ +3.3 (*c* 0.67, $CHCl_3$); IR (film) 2972, 2917, 1720, 1562, 1325, 1168, 1130, 668 cm^{-1}; ^{1}H NMR (400 MHz, $CDCl_3$) δ 7.64 (d, J = 8.3 Hz, 2H), 7.55 (d, J = 8.2 Hz, 2H), 7.30-7.15 (series of br m, 2H), 7.11 (br s, 1H), 6.65 (br d, J = 9.3 Hz, 1H), 5.78 (br d, J = 9.6 Hz, 1H), 3.22-3.11 (br m, 1H), 2.49-2.29 (br m, 2H), 1.86-1.76 (br s, 1H), 1.40 (s, 9H), 1.32-1.20 (m, 3H), 1.27 (dd, J = 7.2, 7.2 Hz, 3H), 1.15 (br d, J = 5.4 Hz, 3H), 1.04-0.96 (br m, 3H), 0.79 (br d, J = 4.9 Hz, 3H); ^{13}C NMR (100 MHz, $CDCl_3$) ppm 164.5, 154.5, 144.6, 140.8, 139.7, 139.0, 131.0 ($^2J_{CF}$ = 32 Hz), 129.3, 127.8, 126.5 ($^1J_{CF}$ = 271

[144] The s*yn* diastereomer was inseparable with this assay.

Hz), 125.5 ($^3J_{CF}$ = 3.6 Hz), 98.8, 80.7, 59.5, 29.7, 28.2, 27.3, 26.6, 24.1, 22.7, 21.4, 9.33; HRMS (ESI): Exact mass calcd for $C_{29}H_{37}F_3NaN_2O_6$ $[M+Na]^+$ 589.2501, found 589.2510.

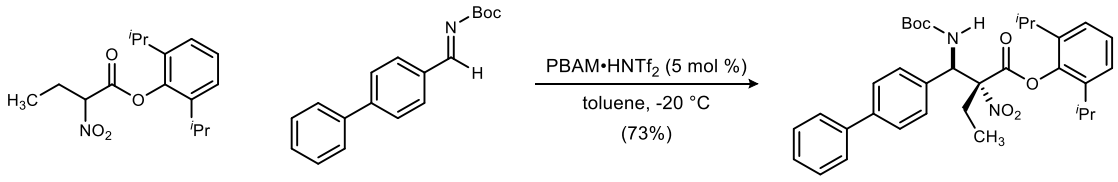

2,6-Diisopropylphenyl (*R*)-2-((*R*)-[1, 1'-biphenyl]-4-yl((*tert*-butoxycarbonyl)amino)methyl)-2-nitrobutanoate (128u). Following the general procedure, the imine (56.3 mg, 200 µmol), ester (64.5 mg, 220 µmol), and catalyst (7.9 mg, 10 µmol) in toluene (285 µmol) provided, after flash column chromatography (2-10% ethyl acetate in hexanes), the product as a colorless solid (84 mg, 73% yield[145]) in >20:1 dr and 99% ee; (Chiralcel AD-H, 5% ^{i}PrOH/hexanes, 1 mL/min, t_r(*anti*, minor) = 6.7 min, t_r(*syn*, major) = 8.4 min, t_r(*syn*, minor) = 8.9 min, t_r(*anti*, major) = 12.9 min); mp = 59-63 °C; R_f = 0.33 (10% EtOAc/hexanes); $[\alpha]_D^{25}$ -18.3 (*c* 1.0, $CHCl_3$); IR (film) 3441, 2967, 1747, 1720, 1558, 1488, 1366, 1225, 1159 cm^{-1}; ^{1}H NMR (400 MHz, $CDCl_3$) δ 7.61 (d, *J* = 8.0 Hz, 4H), 7.53-7.45 (br m, 4H), 7.40 (br dd, *J* = 7.4, 7.4 Hz, 1H), 7.30-7.20 (br m, 2H), 7.09 (br d, *J* = 4.2 Hz, 1H), 6.73 (br d, *J* = 9.6 Hz, 1H), 5.79 (br d, *J* = 9.7 Hz, 1H), 3.35-3.20 (br m, 1H), 2.60-2.35 (br m, 2H), 1.97-1.82 (br m, 1H), 1.42 (s, 9H), 1.30 (br dd, *J* = 7.1, 7.1 Hz, 3H), 1.31-1.25 (br m, 3H), 1.18 (br d, *J* = 7.1 Hz, 3H), 0.96 (br d, *J* = 5.8 Hz, 3H), 0.80 (br d, *J* = 5.7 Hz, 3H); ^{13}C NMR (100 MHz, $CDCl_3$) ppm 165.6, 154.6, 144.7, 141.5, 140.1, 134.3, 130.2, 129.2, 128.9, 127.7, 127.4, 127.2, 127.0, 99.0, 80.3, 59.7, 29.9, 28.2, 27.2, 26.6, 24.2 (2C), 22.8, 21.6, 9.42; HRMS (ESI): Exact mass calcd for $C_{34}H_{42}N_2NaO_6$ $[M+Na]^+$ 597.2941, found 597.2944.

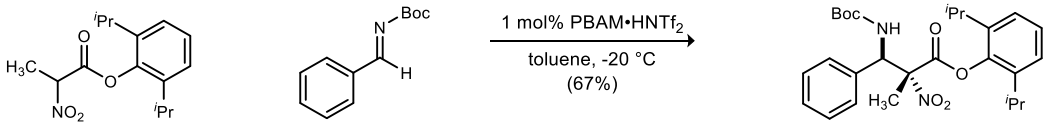

2,6-Diisopropylphenyl (2*R*,3*R*)-3-((*tert*-butoxycarbonyl)amino)-2-methyl-2-nitro-3-phenylpropanoate (129). In a flame-dried, round bottom flask the imine (3.00 g, 14.6 mmol) and catalyst (115 mg, 146 µmol), were dissolved in toluene and chilled to -20 °C. The nitroester (5.00 g, 17.5 mmol) was added and the resulting mixture was allowed to stir at -20 °C for 3 days. To remove the catalyst, the solution was filtered cold through a small pad of silica using ethyl acetate and concentrated to a brown oil. Flash column chromatography (SiO_2, 1.5%-5% ethyl acetate in hexanes) afforded the product as a white foam (4.72 g, 67% yield) in >20:1 dr and 99% ee (Chiralcel IA, 3% ^{i}PrOH/hexanes, 1 mL/min) t_r(*anti*, minor) = 7.8 min, t_r(*syn*, major) = 10.0 min t_r(*anti*, major) = 12. 7 min, t_r(*syn*, minor) = 17.5 min; mp = 48.0-50.0 °C; $[\alpha]_D^{25}$ +3.1 (*c* 0.55, $CHCl_3$); R_f = 0.15 (3% EtOAc/hexanes); IR (film) 3444, 1753, 1723, 1560, 1163 cm^{-1}; ^{1}H NMR (500 MHz, DMSO-d_6) δ 8.01 (br d, *J* = 10.5 Hz, 1H), 7.44-7.33 (series of br m, 5H), 7.31-7.20 (series of m, 3H), 5.93 (br d, *J* = 10.0 Hz, 1H), 2.85-2.68 (br m, 2H), 1.97 (s, 3H), 1.34 (s, 9H), 1.12 (br d, *J* = 7.0 Hz, 6H), 1.10 (br d, *J* = 7.5 Hz, 6H); ^{13}C NMR (125 MHz, DMSO-d_6) ppm

[145] Contaminated with the parent aldehyde.

164.2, 154.8, 144.5, 139.8, 135.8, 128.6, 128.5, 128.4, 127.4, 124.2, 95.7, 79.0, 57.8, 28.1, 26.4, 23.5, 22.5, 17.3; HRMS (ESI): Exact mass calcd for $C_{27}H_{36}N_2NaO_6$ $[M+Na]^+$ 507.2471, found 507.2464.

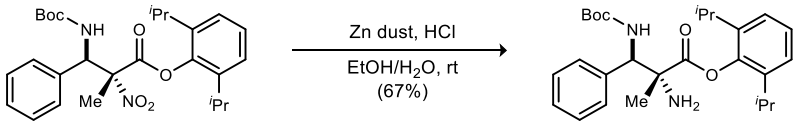

2,6-Diisopropylphenyl (2*R*,3*R*)-2-amino-3-((*tert*-butoxycarbonyl)amino)-2-methyl-3-phenylpropanoate (130). To a solution of nitroester (3.2 g, 6.60 mmol) in ethanol (66 mL) was added aq 2 M HCl (132 mL) followed by freshly purified zinc dust[146] (17.3 g, 264 mmol). The resulting suspension was stirred at room temperature for 6 h. Satd aq $NaHCO_3$ was added until the reaction mixture was basic, and the ethanol was removed *in vacuo*. The residue was redissolved in EtOAc, and washed with satd aq $NaHCO_3$, and then dried and concentrated. Flash column chromatography (SiO_2, 10%-20% ethyl acetate in hexanes) afforded the desired amine as a colorless solid (2.0 g, 67% yield). Mp = 129-131 °C; $[\alpha]_D^{20}$ -11 (*c* 0.80, $CHCl_3$); R_f = 0.10 (10% EtOAc/hexanes); IR (film) 3391, 1748, 1715, 1162 cm^{-1}; ^1H NMR[147] (400 MHz, $CDCl_3$) δ 7.50-7.41 (br m, 3H), 7.36-7.28 (series of br m, 3H), 7.09 (br s, 2H), 5.99 (br d, *J* = 9.5 Hz, 1H), 5.18 (br d, *J* = 9.7 Hz, 1H), 3.19-2.77 (br m, 1H), 2.61 (br s, 1H), 1.66 (s, 3H), 1.44 (s, 9H), 1.21 (br s, 3H), 1.10 (br s, 3H), 0.98 (br s, 3H), 0.88 (br s, 3H) [N**H**$_2$ not observed]; ^{13}C NMR (100 MHz, $CDCl_3$) ppm 173.9, 155.5, 145.2, 140.0, 139.1, 128.5, 128.3, 128.1, 127.7, 126.6, 123.8, 79.4, 62.3, 59.1, 28.3, 28.0, 26.9, 25.6, 23.9, 22.5, 22.0; HRMS (ESI): Exact mass calcd for $C_{27}H_{39}N_2O_4$ $[M+H]^+$ 455.2910, found 455.2927.

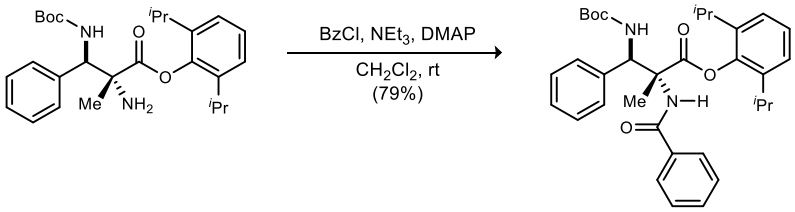

2,6-Diisopropylphenyl (2*R*,3*R*)-2-benzamido-3-((*tert*-butoxycarbonyl)amino)-2-methyl-3-phenylpropanoate (142). The amine (910 mg, 2.00 mmol), NEt_3 (416 µL, 3.00 mmol), and DMAP (25 mg, 200 µmol) were dissolved in CH_2Cl_2 (10 mL). Benzoyl chloride (350 µL, 3.00 mmol) was added slowly, and the reaction was stirred at room temperature for 24 h. The reaction was neutralized with 1 M HCl and the layers were separated. The aqueous layer was extracted with CH_2Cl_2, and the organic layers were combined, washed with 1 M HCl, satd aq $NaHCO_3$, and brine, and then dried and concentrated. Flash column chromatography (SiO_2, 8%-16% ethyl acetate in hexanes) afforded the desired product as a colorless solid (880 mg, 79% yield). Mp = 83-86 °C; $[\alpha]_D^{20}$ -17 (*c* 0.82, $CHCl_3$); R_f = 0.50 (20% EtOAc/hexanes); IR (film) 3328, 2968, 1762, 1713, 1665, 1514, 1487, 1160 cm^{-1}; ^1H NMR (500 MHz, $CDCl_3$) δ 7.67 (br d, *J* = 7.6 Hz, 2H), 7.51 (br dd, *J* = 6.9, 6.9 Hz, 2H), 7.47 (br s, 1H), 7.42 (br dd, *J* = 7.5, 7.5 Hz, 2H), 7.36 (br d, *J* = 6.3 Hz, 2H), 7.31-7.23 (br m, 4H), 7.18 (br d, *J*

[146] Purified according to: Armarego, W.L.F, and Perrin, D.D., *Purification of Laboratory Chemicals*, 4th ed.; Butterworth-Heinemann: Boston, 1998.
[147] Hindered rotation is confirmed by variable temperature ^1H NMR. Data is reported for major rotamer.

= 7.5 Hz, 2H), 5.76 (br d, *J* = 8.6 Hz, 1H), 2.74 (br s, 2H), 2.14 (s, 3H), 1.45 (s, 9H), 1.17 (br d, *J* = 6.7 Hz, 6H), 1.11 (br s, 6H); ^{13}C NMR (125 MHz, $CDCl_3$) ppm 171.8, 168.1, 156.0, 145.0, 140.2, 138.6, 134.5, 131.9, 128.7, 128.2, 127.9, 127.8, 127.2, 126.8, 124.2, 79.5, 66.4, 60.0, 28.5, 27.0, 24.0, 22.6, 21.5; HRMS (ESI): Exact mass calcd for $C_{34}H_{42}N_2NaO_5$ $[M+Na]^+$ 581.2991, found 581.2943.

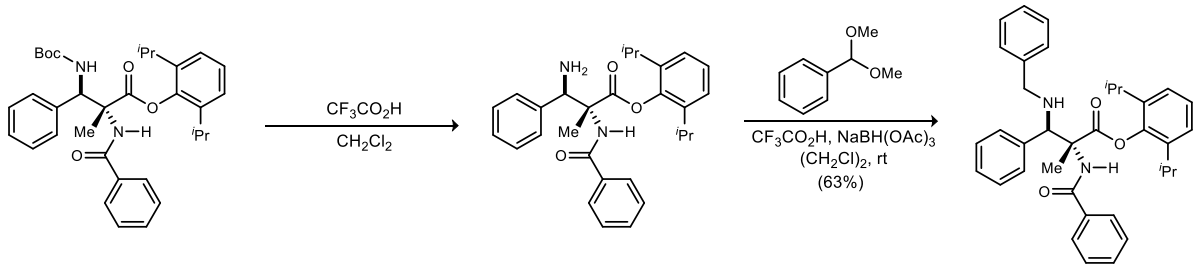

2,6-Diisopropylphenyl (2*R*,3*R*)-3-amino-2-benzamido-2-methyl-3-phenylpropanoate (141). To a solution of amide (600 mg, 1.07 mmol) in CH_2Cl_2 (11 mL) at 0 °C was added trifluoroacetic acid (3.3 mL, 43 mmol). The resulting solution was warmed to ambient temperature and stirred for 1 h. The reaction was neutralized with satd aq $NaHCO_3$. The layers were separated and the aqueous layer was extracted with CH_2Cl_2. The organic layers were combined and washed with satd aq $NaHCO_3$ and brine, and then dried and concentrated to a colorless solid (437 mg) which was submitted to the reductive amination without further purification.

To a stirred solution of amine (400 mg, 872 µmol) in 1,2-dichloroethane (5 mL) was added benzaldehyde dimethyl acetal (200 µL, 1.31 mmol), trifluoroacetic acid (70 µL, 916 µmol) and the borohydride (315 mg, 1.48 mmol). The resulting yellow solution was stirred at ambient temperature for 12 h. The reaction was neutralized carefully (due to excessive foaming) with satd aq $NaHCO_3$. The layers were separated and the aqueous layer was extracted with CH_2Cl_2. The combined organic layers were washed with brine, and then dried and concentrated to a yellow oil which solidified upon standing. Flash column chromatography (SiO_2, 10%-20% ethyl acetate in hexanes) afforded the desired amine as a colorless solid (300 mg, 63% yield). Mp = 156-158 °C; $[\alpha]_D^{20}$ +26 (*c* 0.53, $CHCl_3$); R_f = 0.43 (20% EtOAc/hexanes); IR (film) 3331, 1741, 1669, 1511, 1480, 1455 cm^{-1}; ^{1}H NMR (400 MHz, $CDCl_3$) δ 7.66 (d, *J* = 7.1 Hz, 2H), 7.51-7.46 (m, 3H), 7.45-7.32 (m, 7H), 7.31-7.26 (m, 2H), 7.25-7.17 (m, 3H), 7.13 (br d, *J* = 7.0 Hz, 2H), 4.55 (s, 1H), 3.70 (d, *J* = 13.0 Hz, 1H), 3.52 (d, *J* = 13.0 Hz, 1H), 3.06 (br s, 1H), 2.79 (br s, 1H), 1.95 (s, 3H), 1.10 (br d, *J* = 6.9 Hz, 12H) [N*H* not observed];[148] ^{13}C NMR (100 MHz, $CDCl_3$) ppm 172.1, 166.8, 145.5, 140.6, 139.9, 137.5, 134.9, 131.6, 129.4, 128.5, 128.38, 128.37, 128.2, 128.1, 127.1, 126.9, 126.7, 123.9, 66.8, 63.4, 51.6, 26.8, 19.8; HRMS (ESI): Exact mass calcd for $C_{36}H_{41}N_2O_3$ $[M+H]^+$ 549.3117, found 549.3094.

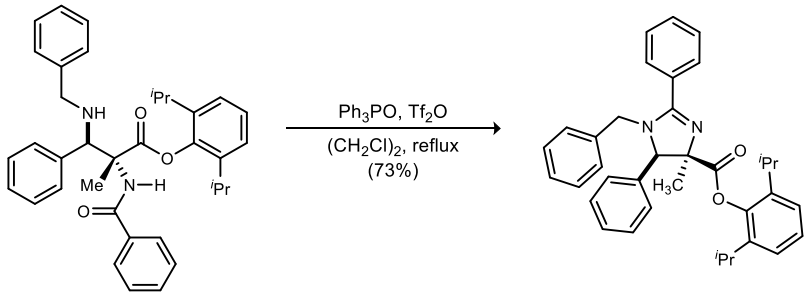

[148] May be hidden underneath the broad singlet at 2.79.

2,6-Diisopropylphenyl (4*R*,5*R)*-1-benzyl-4-methyl-2,5-diphenyl-4,5-dihydro-*1H*-imidazole-4-carboxylate (145). In a flame dried flask, Ph_3PO (473 mg, 1.70 mmol) was dissolved in 1,2-dichloroethane (4.3 mL). At ambient temperature, triflic anhydride (143 µL, 850 µmol) was added dropwise, and the resulting yellow solution was stirred for 30 minutes. The amino amide (233 mg, 425 µmol) was added in one portion, and the reaction was refluxed for 2 h. The reaction was cooled to ambient temperature, and neutralized with satd aq $NaHCO_3$. The layers were separated, and the aqueous layer was extracted with CH_2Cl_2. The organic layers were combined, washed with brine, and then dried and concentrated. Flash column chromatography (SiO_2, 10%-20% ethyl acetate in hexanes) afforded the desired imidazoline as a colorless solid (164 mg, 73% yield). Mp = 62-65 °C; $[\alpha]_D^{20}$ -100 (*c* 0.77, $CHCl_3$); R_f = 0.19 (20% EtOAc/hexanes); IR (film) 2965, 1745, 1451, 1092, 699 cm^{-1}; ^1H NMR (400 MHz, $CDCl_3$) δ 7.68-7.62 (br m, 2H), 7.44-7.38 (br m, 3H), 7.34-7.16 (series of br m, 8H), 7.03-6.89 (m, 5H), 4.58 (br d, *J* = 15.6 Hz, 1H), 4.40 (s, 1H), 3.70 (br d, *J* = 15.6 Hz, 1H), 2.22 (septet, *J* = 6.8 Hz, 2H), 1.74 (s, 3H), 0.85 (br d, *J* = 6.8 Hz, 12H); ^{13}C NMR (100 MHz, $CDCl_3$) ppm 170.9, 165.4, 145.7, 140.4, 136.9, 136.7, 130.9, 130.1, 128.7 (2C), 128.6, 128.4, 128.3, 127.7 (2C), 127.6, 126.1, 123.5, 77.8, 72.8, 48.5, 28.4, 26.5, 23.9, 23.2; HRMS (ESI): Exact mass calcd for $C_{36}H_{39}N_2O_3$ $[M+H]^+$ 531.3012, found 531.2994.

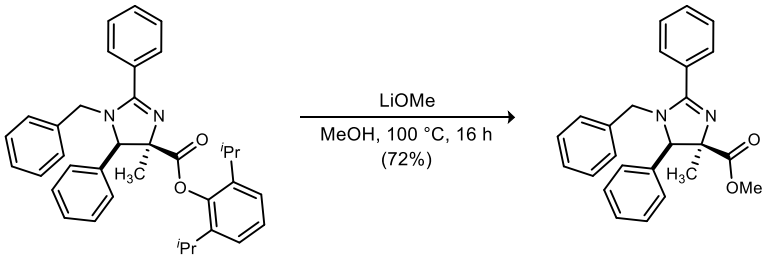

Methyl (4*R*,5*R*)-1-benzyl-4-methyl-2,5-diphenyl-4,5-dihydro-1*H*-imidazole-4-carboxylate (140). A flame dried, sealed tube was charged with anhydrous methanol (1.88 mL). To this was carefully added lithium (17 mg, 2.4 mmol) in portions. After all of the metal dissolved, the imidazoline (50 mg, 94 µmol) was added in one portion, and the mixture was heated[149] at 100 °C for 16 h. The resulting purple solution was cooled to ambient temperature, and the methanol was removed *in vacuo*. The residue was dissolved in EtOAc and neutralized with satd aq NH_4Cl. The layers were separated, and the aqueous layer was extracted with EtOAc. The organic layers were combined, dried, and concentrated. Flash column chromatography afforded the desired methyl ester as a colorless oil (26 mg, 72% yield). Spectral data are identical to those previously reported.[150]

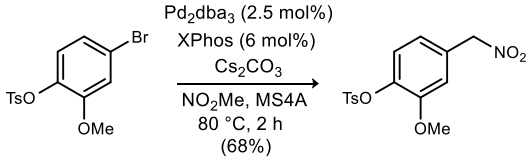

2-Methoxy-4-(nitromethyl)phenyl 4-methylbenzenesulfonate (159). According to Kozlowski's procedure[151], a flask was filled with 4Å molecular sieves (4.90 g, 200 mg/mmol) and Cs_2CO_3 (11.3 g, 32.1 mmol). This flask

[149] This reaction should be carried out behind a blast shield in a high flow fume hood.
[150] Kahlon, D. K.; Lansdell, T. A.; Fisk, J. S.; Hupp, C. D.; Friebe, T. L.; Hovde, S.; Jones, A. D.; Dyer, R. D.; Henry, R. W.; Tepe, J. J. *J. Med. Chem.* **2009**, *52*, 1302.
[151] Walvoord, R. R.; Berritt, S.; Kozlowski, M. C. *Org. Lett.* **2012**, *14*, 4086.

was flame-dried and allowed to cool under argon. The bromobenzene (8.81 g, 24.7 mmol) was added followed by nitromethane (250 mL). This was stirred for 5 minutes at ambient temperature and XPhos (706 mg, 1.48 mmol) was added. To the resulting yellow mixture was quickly added Pd_2dba_3 (566 mg, 618 µmol) under argon. The reaction was stirred at 80 °C for 2 h. After cooling to ambient temperature, the reaction was diluted with CH_2Cl_2, filtered through Celite® and concentrated. The resulting residue was dissolved in CH_2Cl_2 and washed twice with satd aq NH_4Cl. The aqueous layer was extracted with CH_2Cl_2. The combined organic layers were washed with brine, dried, and concentrated to give the crude nitroalkane. Flash column chromatography (SiO_2, 20-50% ethyl acetate in hexanes) afforded the title compound as a colorless to pale yellow oil which solidified upon standing (5.68 g, 68%). Mp = 80.5-82.0 °C; R_f = 0.29 (20% EtOAc/hexanes); IR (film) 2942, 1578, 1424, 1373, 1161 cm^{-1}; ^1H NMR (400 MHz, $CDCl_3$) δ 7.71 (d, *J* = 8.0 Hz, 2H), 7.35 (d, *J* = 8.0 Hz, 2H), 7.22 (d, *J* = 8.0 Hz, 1H), 7.01 (dd, *J* = 8.0, 8.0 Hz, 1H), 7.00 (dd, *J* = 10.0, 10.0 Hz, 1H), 5.42 (s, 2H), 3.62 (s, 3H), 2.48 (s, 3H); ^{13}C NMR (100 MHz, $CDCl_3$) ppm 152.1, 145.3, 139.4, 132.8, 129.41, 129.38, 128.4, 124.3, 122.3, 114.1, 79.4, 55.6, 21.5; HRMS (ESI): Exact mass calcd for $C_{15}H_{15}NNaO_6S$ $[M+Na]^+$ 360.0518, found 360.0509.

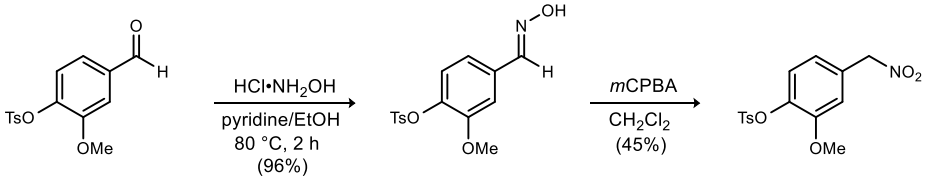

An Alternative Procedure to 159: To a solution of the aldehyde[152] (9.00 g, 29.4 mmol) in pyridine (4.30 mL) was added hydroxylamine hydrochloride (2.45 g, 35.3 mmol) followed by ethanol (10 mL). The resulting solution was stirred at ambient temperature for 24 h and then concentrated *in vacuo*. The residue was dissolved in 1 M HCl and extracted with EtOAc. The combined organics were washed with 1 M HCl and brine, and then dried and concentrated to a colorless solid (9.07 g, 96%) which was oxidized without further purification.

The oxime (9.07 g, 28.2 mmol) was dissolved in dichloromethane (30 mL) and *m*CPBA (19.5 g, 113 mmol) was added in one portion at ambient temperature. The reaction was stirred at ambient temperature for 15 h and then quenched by adding to sat aq $NaHCO_3$. The resulting layers were separated, and the aqueous layer was extracted with CH_2Cl_2. The organic layers were combined and washed with sat aq $NaHCO_3$ and brine, and then dried and concentrated. Flash column chromatography (SiO_2, 20-50% ethyl acetate in hexanes) afforded the title compound as a colorless to pale yellow oil which solidified upon standing (4.28 g, 45%). Analytical data is identical to those reported above.

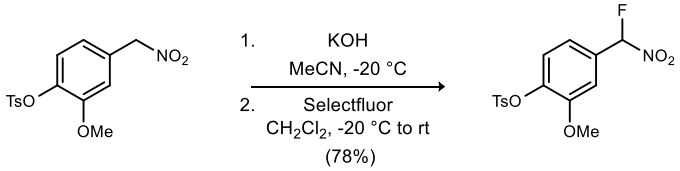

4-(Fluoro(nitro)methyl)-2-methoxyphenyl 4-methylbenzenesulfonate (168). Using the Guo protocol[153], the nitroalkane (710 mg, 2.10 mmol) was dissolved in acetonitrile (1.75 mL) and chilled to 0 °C. KOH (175 mg, 3.15

[152] Carr, J. A.; Bisht, K. S. *Org. Lett.* **2004**, *6*, 3297.
[153] Hu, H.; Huang, Y.; Guo, Y. *J. Fluorine Chem.* **2012**, *133*, 108.

mmol) in H_2O (1.75 mL) was added dropwise. The resulting colored solution was stirred at 0 °C for 1 h, then chilled to -20 °C. To this was added Selectfluor® (1.15 g, 3.15 mmol) in chilled (-78 °C) dichloromethane (1.5 mL). The resulting suspension was gradually warmed to 0 °C over 45 min. The mixture was diluted with hexanes and ether and stirred for 10 minutes, then transferred to a separatory funnel, and the layers were separated. The organic layer was washed with H_2O, dried, and concentrated. Flash column chromatography (SiO_2, 15-50% ethyl acetate in hexanes) afforded the α-fluoro nitroalkane as a colorless solid (585 mg, 78%). Mp = 85.0-86.0 °C; R_f = 0.22 (20% EtOAc/hexanes); IR (film) 2910, 1577, 1424, 1373, 1294, 1272, 1178, 712 cm^{-1}; ^1H NMR (400 MHz, $CDCl_3$) δ 7.77 (d, *J* = 8.4 Hz, 2H), 7.34 (d, *J* = 8.0 Hz, 2H), 7.27 (br dd, *J* = 8.4, 8.4 Hz, 1H), 7.20 (br d, *J* = 8.4 Hz, 1H), 7.11 (br s, 1H), 6.60 (d, $^1J_{HF}$ = 48.4 Hz, 1H), 3.64 (s, 3H), 2.47 (s, 3H); ^{13}C NMR (100 MHz, $CDCl_3$) ppm 152.4, 145.5, 140.9, 132.8, 129.7, 129.5, 128.5, 124.6,[154] 119.3 (d, $^3J_{CF}$ = 6.0 Hz), 110.2 (d, $^3J_{CF}$ = 6.0 Hz), 109.1 (d, $^1J_{CF}$ = 238 Hz), 55.8, 21.6; ^{19}F NMR (376 MHz, $CDCl_3$) δ -140.1; HRMS (ESI): Exact mass calcd for $C_{15}H_{14}FO_4S$ $[M\text{-}NO_2]^+$ 309.0597, found 309.0591.

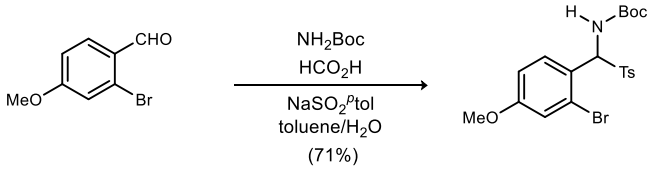

***tert*-Butyl ((2-bromo-4-methoxyphenyl)(tosyl)methyl)carbamate (166).** To a solution of aldehyde (6.00 g, 27.9 mmol) in toluene (52 mL) and H_2O (26 mL) was added NH_2Boc (2.72 g, 23.3 mmol) and $NaSO_2{}^p$tol (8.29 g, 46.5 mmol). To the resulting solution was added formic acid (1.75 mL, 46.5 mmol). The reaction was stirred at ambient temperature for 6 days as a colorless precipitate formed. The solid was filtered, triturated with Et_2O and H_2O, and then dried *in vacuo*. This afforded pure sulfone (7.77 g, 71%) as a fluffy colorless solid. Mp = 169.0-170.5 °C; R_f = 0.11 (5% MeOH/CH_2Cl_2); IR (film) 3431, 1704, 1644, 1146, 657 cm^{-1}; ^1H NMR (400 MHz, DMSO-d_6) δ 8.70 (d, *J* = 10.4 Hz, 1H), 7.86 (d, *J* = 8.8 Hz, 1H), 7.67 (d, *J* = 8.0 Hz, 2H), 7.45 (d, *J* = 7.6 Hz, 2H), 7.23 (d, *J* = 2.0 Hz, 1H), 7.07 (dd, *J* = 8.8, 2.4 Hz, 1H), 6.42 (d, *J* = 10.8 Hz, 1H), 3.81 (s, 3H), 2.39 (s, 3H), 1.20 (s, 9H); ^{13}C NMR (100 MHz, DMSO-d_6) ppm 160.9, 154.4, 145.1, 134.5, 132.4, 130.1, 129.3, 126.2, 122.9, 117.9, 114.5, 76.9, 72.8, 56.2, 28.2, 21.5; HRMS (ESI): Exact mass calcd for $C_{15}H_{17}BrNO_3S$ $[M+H\text{-}Boc]^+$ 370.0113, found 370.0438.

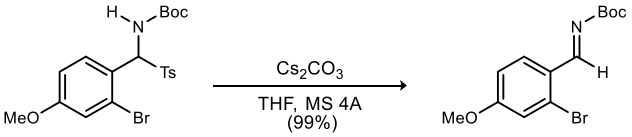

***tert*-Butyl (*E*)-(2-bromo-4-methoxybenzylidene)carbamate (167).** To a solution of sulfone (1.25 g, 2.74 mmol) in THF (50 mL) was added Na_2SO_4 (3.11 g, 21.9 mmol) and molecular sieves (2 g). To the resulting suspension was added Cs_2CO_3 and the reaction was stirred at ambient temperature for 15 h. The reaction was filtered through Celite® and then concentrated to a pure, viscous orange oil (855 mg, 99%). IR (film) 2979, 2935, 2841, 1719,

[154] $^2J_{CF}$ coupling is expected, however, it was not observed in this case.

1598, 1028, 766 cm^{-1}; ^1H NMR (400 MHz, $CDCl_3$) δ 9.19 (s, 1H), 8.16 (d, *J* = 8.8 Hz, 1H), 7.12 (d, *J* = 2.4 Hz, 1H), 6.89 (dd, *J* = 8.0, 2.0 Hz, 1H), 3.85 (s, 3H), 1.58 (s, 9H); ^{13}C NMR (100 MHz, $CDCl_3$) ppm 168.3, 164.0, 162.5, 131.0, 129.4, 125.3, 118.2, 114.2, 82.2, 55.8, 27.9; HRMS (ESI): Exact mass calcd for $C_{14}H_{20}BrNNaO_4$ $[M+MeOH+H]^+$ 368.0473, found 368.0463.

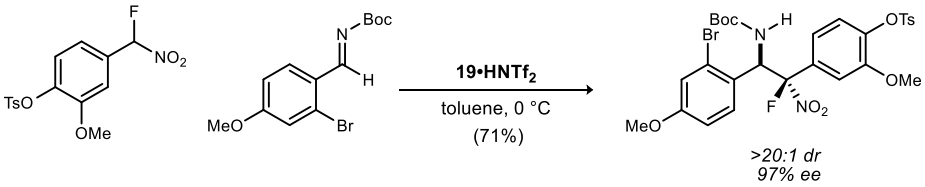

4-((1*R*,2*R*)-2-(2-Bromo-4-methoxyphenyl)-2-((*tert*-butoxycarbonyl)amino)-1-fluoro-1-nitroethyl)-2-methoxyphenyl 4-methylbenzenesulfonate (169). The imine (50 mg, 159μmol) and catalyst (14.4 mg, 15.9 μmol) were dissolved in toluene (230 μL) and chilled to 0 °C. The nitroalkane (62.2 mg, 175 μmol) was added and the reaction was stirred at 0 °C for 48 h. The solution was filtered through a small plug of silica gel (EtOAc) to remove the catalyst, and the resulting eluent was concentrated *in vacuo*. Flash column chromatography (SiO_2, 20-50% ethyl acetate in hexanes) afforded the adduct as a colorless solid (75.3 mg, 71% yield) in >20:1 dr and 97% ee. (Chiralcel OZ-H, 20% ^{i}PrOH/hexanes, 0.6 mL/min, t_r(*anti*, minor) = 17.7 min, t_r(*anti*, major) = 19.8 min, t_r(*syn*, major) = 29.5 min, t_r(*syn*, minor) = 38.2 min); Mp = 79.0-80.5 °C; R_f = 0.27 (30% EtOAc/hexanes); $[\alpha]_D^{25}$ +4.5 (*c* 0.78, $CHCl_3$); IR (film) 3432, 2968, 1720, 1561, 1491, 1366, 1160, 1093, 698 cm^{-1}; ^1H NMR (400 MHz, $CDCl_3$) δ 7.46-7.06 (series of br m, 12H), 6.66 (br d, *J* = 8.4 Hz, 1H), 5.85 (br d, *J* = 9.2 Hz, 1H), 3.70 (d, *J* = 14.6 Hz, 1H), 3.62 (d, *J* = 14.2 Hz, 1H), 2.46 (br s, 1H), 1.96-1.79 (br m, 1H), 1.41 (s, 9H), 1.36-0.70 (series of br m, 12H);^{13}C NMR (100 MHz, $CDCl_3$) ppm 169.1, 154.4, 144.0, 135.0, 132.6, 130.3, 130.2, 129.6, 129.1, 129.0, 128.9, 128.5, 128.1, 127.5, 99.0, 80.7, 60.3, 42.0, 28.2, 27.3, 27.1, 26.2, 24.7, 23.8, 21.7; ^{19}F NMR (376 MHz, $CDCl_3$); HRMS (ESI): Exact mass calcd for $C_{28}H_{39}BrN_2NaO_9$ $[M+Na]^+$ 690.0653, found 690.0659.

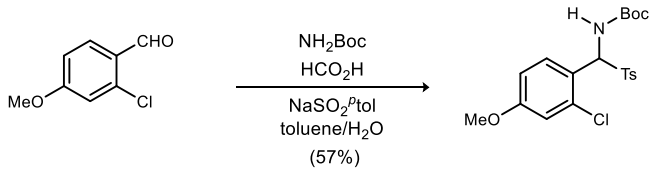

***tert*-Butyl ((2-chloro-4-methoxyphenyl)(tosyl)methyl)carbamate (174).** To a solution of aldehyde (7.50 g, 44.0 mmol) in toluene (82 mL) and H_2O (41 mL) was added $BocNH_2$ (4.30 g, 36.7 mmol) and $NaSO_2{}^pTol$ (13.1 g, 73.4 mmol). To the resulting solution was added formic acid (2.77 mL, 73.4 mmol). The reaction was stirred at ambient temperature for 3 days as a colorless precipitate formed. The solid was filtered, triturated with Et_2O and H_2O, and then dried *in vacuo*. This afforded pure sulfone (8.90 g, 57%) as a fluffy colorless solid. Mp = 168.0-170.0 °C; R_f = 0.11 (5% MeOH/CH_2Cl_2); IR (film) 3438, 1707, 1640, 1145, 587 cm^{-1}; ^1H NMR (400 MHz, DMSO-d_6) δ 8.72 (d, *J* = 10.8 Hz, 1H), 7.88 (d, *J* = 8.8 Hz, 1H), 7.68 (d, *J* = 8.4 Hz, 2H), 7.44 (d, *J* = 8.0 Hz, 2H), 7.08 (d, *J* = 2.4 Hz, 1H), 7.03 (dd, *J* = 8.8, 2.4 Hz, 1H), 6.40 (d, *J* = 10.8 Hz, 1H), 3.81 (s, 3H), 2.38 (s, 3H), 1.20 (s, 9H); ^{13}C NMR (100 MHz, DMSO-d_6) ppm 160.6, 154.1, 144.7, 134.9, 134.1, 132.0, 129.7, 128.9, 120.6, 114.3, 113.6, 79.5, 70.0, 55.8, 27.8, 21.1; HRMS (ESI): Exact mass calcd for $C_{20}H_{24}ClNNaO_5S$ $[M+Na]^+$ 448.0961, found 448.0977.

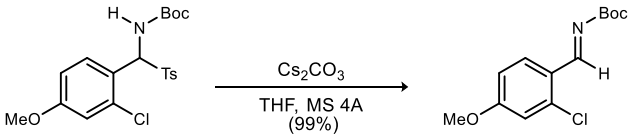

***tert*-Butyl (*E*)-(2-chloro-4-methoxybenzylidene)carbamate (175).** To a solution of sulfone (20.0 g, 46.9 mmol) in THF (470 mL) was added Na_2SO_4 (53.3 g, 375 mmol) and molecular sieves 4A (100 g). To the resulting suspension was added Cs_2CO_3 (33.1 g, 93.8 mmol) and the reaction was stirred at ambient temperature for 15 h. The reaction was filtered through Celite® and then concentrated to a viscous orange oil (12.8 g, 99%), judged to be sufficiently pure for subsequent use. IR (film) 2984, 2918, 2849, 1704, 1603, 1056, 698 cm^{-1}; ^1H NMR (400 MHz, $CDCl_3$) δ 9.27 (s, 1H), 8.18 (d, *J* = 8.8 Hz, 1H), 6.93 (s, 1H), 6.86 (d, *J* = 8.4 Hz, 1H), 3.86 (s, 3H), 1.59 (s, 9H); ^{13}C NMR (100 MHz, $CDCl_3$) ppm 165.8, 164.0, 162.5, 139.5, 130.5, 123.9, 114.8, 113.7, 82.0, 55.7, 27.8; HRMS (CI): Exact mass calcd for $C_{13}H_{17}ClNO_3$ $[M+H]^+$ 270.0891, found 270.0894.

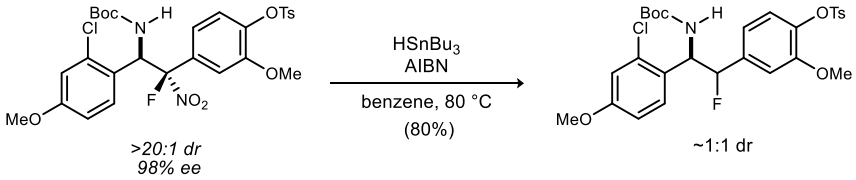

4-((1*R*,2*R*)-2-((*tert*-Butoxycarbonyl)amino)-2-(2-chloro-4-methoxyphenyl)-1-fluoro-1-nitroethyl)-2-methoxyphenyl 4-methylbenzenesulfonate (177). The nitroalkane (6.00 g, 9.60 mmol) and $HSnBu_3$ (7.5 mL, 48 mmol) were dissolved in benzene (100 mL). The solution was degassed (freeze-pump-thaw cycles) and backfilled with argon. The reaction mixture was then heated to 80 °C and AIBN (700 mg, 2.40 mmol) was added in one portion. The reaction was stirred for 1 h at 80 °C and then concentrated *in vacuo*. Flash column chromatography (10% K_2CO_3 in SiO_2, 20-50% ethyl acetate in hexanes) afforded the denitrated product as a colorless solid (4.47 g, 80%) in 1:1 dr. ^1H NMR (400 MHz, $CDCl_3$) δ 7.75 (d, *J* = 10.0 Hz, 2H), 7.70 (d, *J* = 8.4 Hz, 2H), 7.30 (d, *J* = 8.4 Hz, 2H), 7.26 (d, *J* = 10.0 Hz, 2H), 7.20 (d, *J* = 8.0 Hz, 2H), 7.11 (d, *J* = 8.8 Hz, 1H), 7.03 (d, *J* = 8.8 Hz, 2H), 6.86-6.75 (series of m, 5H), 6.60 (dd, *J* = 8.0, 1.6 Hz, 1H), 6.43-6.36 (br s, 1H), 5.91-5.25 (series of br m, 6H), 3.80 (s, 3H), 3.78 (s, 3H), 3.56 (s, 3H), 3.17 (s, 3H), 2.45 (s, 3H), 2.44 (s, 3H), 1.42 (br s, 9H), 1.33 (br s, 9H); ^{13}C NMR (see the spectral image);[155] ^{19}F NMR (376 MHz, $CDCl_3$) δ -189.9, -194.0; HRMS (ESI): Exact mass calcd for $C_{28}H_{31}ClFNNaO_7S$ $[M+Na]^+$ 602.1392, found 602.1370.

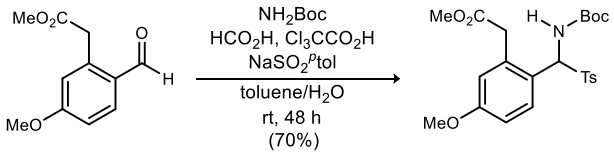

Methyl 2-(2-(((*tert*-butoxycarbonyl)amino)(tosyl)methyl)-5-methoxyphenyl)acetate (187). The aldehyde (8.10 g, 38.9 mmol), *tert*-butyl carbamate (3.03 g, 25.9 mmol), and the sulfinate salt (9.20 g, 51.8 mmol) were

[155] The line listing is not very useful in this case; it is better to compare spectra directly.

suspended in a mixture of water (52 mL) and methanol (26 mL). Formic acid (3.00 mL, 73.4 mmol) and trichloroacetic acid (1.00 g, 6.12 mmol) were added, and the homogeneous solution was stirred at ambient temperature for 48 h. The resulting precipitate was filtered and washed with diethyl ether and water. After drying *in vacuo*, the sulfone was isolated as a colorless fluffy solid (8.37 g, 70%) and was subjected to elimination without further purification. Mp = 148 °C (dec.); R_f = 0.11 (5% MeOH/CH_2Cl_2); IR (film) 3352, 2979, 1721, 1718, 1610, 1503, 1317, 1260, 1162, 1141, 1085 cm^{-1}; ^1H NMR (400 MHz, $CDCl_3$) δ 7.84 (d, *J* = 8.0 Hz, 2H), 7.45 (d, *J* = 8.8 Hz, 1H), 7.35 (d, *J* = 8.0 Hz, 2H), 6.91 (dd, *J* = 8.8, 2.8 Hz, 1H), 6.87 (d, *J* = 2.8 Hz, 1H), 6.19 (d, *J* = 10.8 Hz, 1H), 5.68 (br d, *J* = 10.0 Hz, 1H), 3.92 (d, *J* = 15.6 Hz, 1H), 3.82 (s, 3H), 3.70 (d, *J* = 15.6 Hz, 1H), 3.68 (s, 3H), 2.43 (s, 3H), 1.24 (s, 9H);^{13}C NMR (100 MHz, $CDCl_3$) ppm 170.9, 160.5, 153.2, 144.8, 136.0, 134.3, 129.7 (2C), 129.4, 121.7, 117.0, 113.4, 80.8, 69.7, 55.3, 52.3, 39.4, 27.9, 21.6; HRMS (CI)[156]: Exact mass calcd for $C_{11}H_{14}NO_3$ $[M\text{-}C_{12}H_{15}O_4S]^+$ 208.0968, found 208.0947.

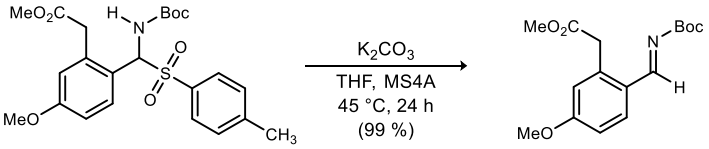

Methyl (*E*)-2-(2-(((*tert*-butoxycarbonyl)imino)methyl)-5-methoxyphenyl)acetate (183). To a solution of sulfone (6.00 g, 12.9 mmol) in THF (80 mL) was added K_2CO_3 (8.75 g, 64.7 mmol) and molecular sieves (13 g). The resulting suspension was stirred at 45 °C for 24 h. After cooling to ambient temperature, the mixture was filtered through a thin layer of Celite® and the filtrate was concentrated to a colorless to pale yellow viscous oil (3.95 g, 99%). IR (film) 2984, 2918, 2849, 1704, 1603, 1056, 698 cm^{-1}; ^1H NMR (400 MHz, $CDCl_3$) δ 9.06 (s, 1H), 7.99 (d, *J* = 8.4 Hz, 1H), 6.90 (dd, *J* = 8.8, 2.4 Hz, 1H), 6.82 (d, *J* = 2.4 Hz, 1H), 3.97 (s, 2H), 3.89 (s, 3H), 3.74 (s, 3H), 1.58 (s, 9H); ^{13}C NMR (100 MHz, $CDCl_3$) ppm 171.1, 168.1, 163.3, 162.7, 138.7, 133.8, 125.3, 117.4, 113.0, 81.6, 67.9, 55.4, 39.1, 27.9; HRMS (CI): Exact mass calcd for $C_{16}H_{22}NO_5$ $[M+H]^+$ 308.1492, found 308.1497.

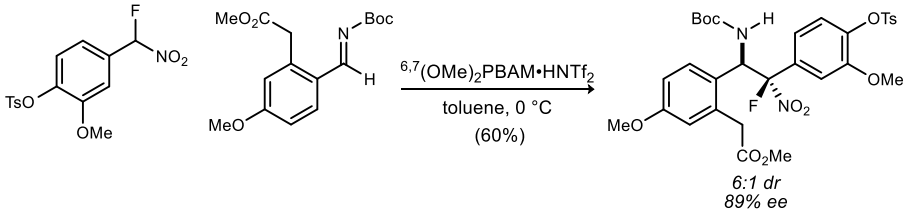

Methyl 2-(2-((1*R*,2*R*)-1-((*tert*-butoxycarbonyl)amino)-2-fluoro-2-(3-methoxy-4-(tosyloxy)phenyl)-2-nitroethyl)-5-methoxyphenyl)acetate (182). The imine (1.52 g, 4.93 mmol) and catalyst (450 mg, 493 µmol) were dissolved in toluene (50 mL) and chilled to 0 °C. The nitroalkane (1.93 g, 5.43 mmol) was added and the reaction was stirred at 0 °C for 48 h. The solution was filtered through a small plug of silica gel (EtOAc) to remove the catalyst, and the resulting filtrate was concentrated *in vacuo*. Flash column chromatography (SiO_2, 20% ethyl acetate in hexanes) afforded the adduct as a colorless solid (1.94 g, 60% yield) in 6:1 dr and 89% ee. (Chiralcel OZ-H, 20% ^{i}PrOH/hexanes, 1 mL/min, t_r(*anti*, minor) = 14.0 min, t_r(*anti*, major) = 16.7 min, t_r(*syn*,

[156] The mass observed corresponds to loss of the Boc-group followed by elimination of the sulfone to yield the iminium ion.

minor) = 23.8 min, t_r(*syn*, major) = 28.9 min); R_f = 0.25 (30% EtOAc/hexanes); IR (film) 3432, 2968, 1720, 1561, 1491, 1366, 1160, 1093, 698 cm^{-1}; ^1H NMR (see the spectral image);[155] ^{13}C NMR (see the spectral image);[155] ^{19}F NMR (376 MHz, $CDCl_3$) -134.4, -135.3; HRMS (ESI): Exact mass calcd for $C_{31}H_{35}FN_2O_{11}S$ $[M+Na]^+$ 685.1843, found 685.1821.

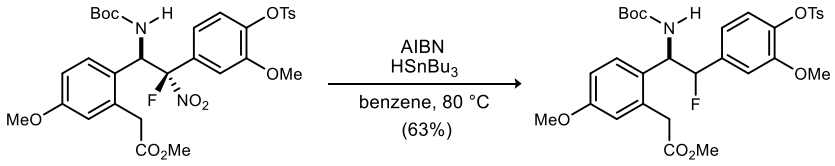

Methyl 2-(2-((1*R*)-1-((*tert*-butoxycarbonyl)amino)-2-fluoro-2-(3-methoxy-4-(tosyloxy)phenyl)ethyl)-5-methoxyphenyl)acetate (181). The nitroalkane (6.00 g, 9.60 mmol) and $HSnBu_3$ (7.5 mL, 48 mmol) were dissolved in benzene (100 mL). The solution was degassed (freeze-pump-thaw cycles) and backfilled with argon. The reaction mixture was then heated to 80 °C and AIBN (700 mg, 2.40 mmol) was added in one portion. The reaction was stirred for 1 h at 80 °C and then concentrated *in vacuo*. Flash column chromatography (10% K_2CO_3 in SiO_2, 20-50% ethyl acetate in hexanes) afforded the denitrated product as a colorless solid (4.47 g, 80%) in ~1.5:1 dr. ^1H NMR (see the spectral image)[155]; ^{13}C NMR (see the spectral image);[155] ^{19}F NMR (376 MHz, $CDCl_3$) δ -189.9, -194.0; HRMS (ESI): Exact mass calcd for $C_{31}H_{36}FNO_9S$ $[M+H]^+$ 617.2089, found 617.2093.

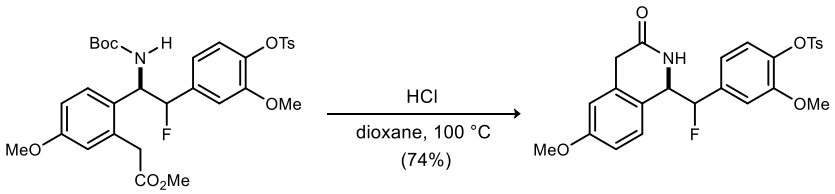

4-(Fluoro((*R*)-6-methoxy-3-oxo-1,2,3,4-tetrahydroisoquinolin-1-yl)methyl)-2-methoxyphenyl 4-methylbenzenesulfonate (180). To a solution of the ester (312 mg, 505 µmol) in dioxane (5 mL) was added a solution of HCl in dioxane (4 M, 1.5 mL, 5.05 mmol). The resulting solution was brought to reflux, stirred for 4 h, and then concentrated *in vacuo*. The residue was dissolved in CH_2Cl_2 and concentrated 3x to remove excess HCl. Flash column chromatography (SiO_2, 60-95% ethyl acetate in hexanes) afforded the desired lactam in ~1.5:1 dr as a colorless solid (180 mg, 74%). R_f = 0.21 (75% EtOAc/hexanes); IR (film) 3352, 2979, 1721, 1718, 1610, 1503, 1317, 1260, 1162, 1141, 1085 cm^{-1}.

Major diastereomer: ^1H NMR (400 MHz, $CDCl_3$) δ 7.74 (br d, *J* = 8.8 Hz, 2H), 7.33 (br d, *J* = 8.0 Hz, 2H), 7.14 (d, *J* = 8.4 Hz, 1H), 6.93 (br d, *J*= 8.4 Hz, 1H), 6.84 (dd, *J* = 8.4, 2.4 Hz, 1H), 6.46 (d, *J* = 2.4 Hz, 1H), 6.39 (d, *J* = 1.6 Hz, 1H), 6.34 (dd, *J* = 8.4, 1.6 Hz, 1H), 6.28 (br s, 1H), 5.57 (dd, *J* = 44.4, 3.6 Hz, 1H), 4.99 (ddd, *J* = 10.4, 3.6, 3.6 Hz, 1H), 3.79 (s, 3H), 3.39 (s, 3H), 3.09 (br d, *J* = 20.4 Hz, 1H), 2.46 (s, 3H), 2.20 (d, *J* = 20.4 Hz, 1H); ^{19}F NMR (376 MHz, $CDCl_3$) δ -180.9.

Minor diastereomer: ^1H NMR (400 MHz, $CDCl_3$) δ 7.76 (br d, *J* = 8.8 Hz, 2H), 7.33 (br d, *J* = 8.2 Hz, 2H), 7.09 (d, *J* = 8.4 Hz, 1H), 6.93 (br d, *J* = 8.4 Hz, 1H), 6.75 (dd, *J* = 8.4, 2.4 Hz, 1H), 6.66 (br dd, *J* = 8.4, 1.6 Hz, 1H), 6.58 (br d, *J* = 2.4 Hz, 1H) 6.51 (br d, *J* = 1.6 Hz, 1H), 6.19 (br s, 1H),5.44 (dd, *J* = 44.8, 4.8 Hz, 1H), 4.69 (ddd, *J* = 16.0, 4.4, 4.4 Hz, 1H), 3.80 (s, 3H), 3.46 (s, 3H), 3.34 (d, *J* = 20.4 Hz, 1H), 3.14 (d, *J* = 20.4 Hz, 1H), 2.46 (s, 3H); ^{19}F NMR (376 MHz, $CDCl_3$) δ -184.4; HRMS (ESI): Exact mass calcd for $C_{25}H_{25}FO_6S$ $[M+H]^+$ 485.1303, found 485.1307.

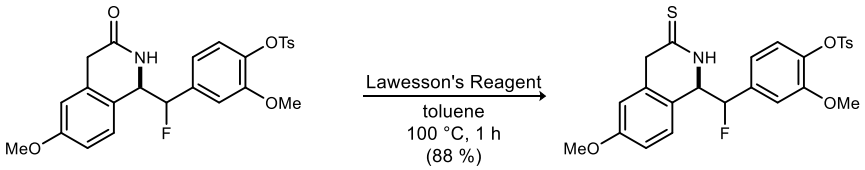

4-(Fluoro((*R*)-6-methoxy-3-thioxo-1,2,3,4-tetrahydroisoquinolin-1-yl)methyl)-2-methoxyphenyl 4-methylbenzenesulfonate (188). To a solution of amide (125 mg, 257 µmol) in toluene (3.0 mL) was added Lawesson's reagent (160 mg, 396 µmol). The resulting suspension was heated to reflux, and stirred for 1 h, during which time the reaction became homogeneous. After cooling to ambient temperature, the solvent was evaporated and the resulting residue was purified *via* flash column chromatography (SiO_2, 40% ethyl acetate in hexanes) to afford the thioamide as a colorless to pale yellow solid in ~1.5:1 dr (114 mg, 88%). R_f = 0.22 (20% EtOAc/hexanes).

Major diastereomer: ^{1}H NMR (400 MHz, $CDCl_3$) δ 8.39 (br s, 1H), 7.51 (d, *J* = 8.0 Hz, 2H), 7.36 (d, *J* = 8.4 Hz, 2H), 7.16 (d, *J* = 8.4 Hz, 1H), 6.93 (d, *J* = 8.4 Hz, 1H), 6.86 (dd, *J* = 8.8, 2.4 Hz, 1H), 6.54 (d, *J* = 1.6 Hz, 1H), 6.44 (d, *J* = 2.0 Hz, 1H), 6.17 (dd, *J* = 8.0, 1.6 Hz, 1H), 5.57 (dd, *J* = 44.4, 3.6 Hz, 1H), 5.12-5.04 (br m, 1H), 3.80 (s, 3H), 3.74 (br d, *J* = 21.6 Hz, 1H), 3.43 (s, 3H), 2.47 (s, 3H), 2.36 (br d, *J* = 21.6 Hz, 1H); ^{19}F NMR (376 MHz, $CDCl_3$) δ -179.2.

Minor diastereomer: ^{1}H NMR (400 MHz, $CDCl_3$) δ 8.25 (br s, 1H), 7.63 (d, *J* = 8.0 Hz, 2H), 7.34 (d, *J* = 8.4 Hz, 2H), 7.11 (d, *J* = 8.0 Hz, 1H), 6.78 (dd, *J* = 8.4, 2.4 Hz, 1H), 6.65-6.54 (br m, 4H), 5.49 (dd, *J* = 44.8, 4.4 Hz, 1H), 4.73 (br ddd, *J* = 20.8, 4.8, 4.8 Hz, 1H), 4.04 (br d, *J* = 21.2 Hz, 1H), 3.80 (s, 3H), 3.80-3.68 (br m, 1H), 3.49 (s, 3H), 2.46 (s, 3H); ^{19}F NMR (376 MHz, $CDCl_3$) δ -179.2.

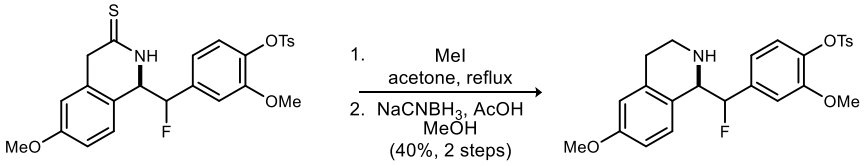

4-(Fluoro((*R*)-6-methoxy-1,2,3,4-tetrahydroisoquinolin-1-yl)methyl)-2-methoxyphenyl 4-methylbenzenesulfonate (179).[157] To a solution of thionamide (145 mg, 289 µmol) in acetone (2 mL) was added methyl iodide (30 µL, 460 µmol) dropwise. The resulting solution was refluxed for 2 h, and then concentrated *in vacuo* to afford the imidate which was reduced without further purification.

To a solution of the salt (196 mg, 305 µmol) in methanol (2.0 mL) was added $NaCNBH_3$ (60.0 mg, 915 µmol) followed by acetic acid (20 µL). The resulting solution was stirred at ambient temperature for 1 h, then concentrated *in vacuo*. The residue was dissolved in CH_2Cl_2 and washed with 1 M NaOH and brine, and then dried and concentrated to a yellow oil. Flash column chromatography (1% methanol in dichloromethane) afforded the amine as a colorless solid in 1.5:1 dr (58 mg, 40%).

Major diastereomer: ^{1}H NMR (400 MHz, $CDCl_3$) δ 7.73 (d, *J* = 8.4 Hz, 2H), 7.28 (d, *J* = 7.6 Hz, 2H), 7.19 (d, *J* = 8.4 Hz, 1H), 7.09 (d, *J* = 8.4 Hz, 1H), 6.79-6.75 (br m, 1H), 6.70-6.66 (br m, 1H), 6.59-6.40 (br m, 1H), 6.38 (br d, *J* = 8.4 Hz, 1H), 5.56 (dd, *J* = 46.0, 6.0 Hz, 1H), 4.41 (dd, *J* = 12.8, 5.6 Hz, 1H), 3.79 (s, 3H), 3.46 (s,

[157] This is an unoptimized procedure.

3H), 2.95-2.89 (m, 1H), 2.88-2.81 (m, 1H), 2.65-2.61 (m, 1H), 2.59-2.56 (m, 1H), 2.44 (s, 3H) [N***H*** not observed]; ^{13}C NMR (see the spectral image);[155] ^{19}F NMR (376 MHz, $CDCl_3$) δ -178.9.

Minor diastereomer: ^{1}H NMR (400 MHz, $CDCl_3$) δ 7.76 (d, *J* = 8.4 Hz, 2H), 7.30 (d, *J* = 7.2 Hz, 2H), 7.13 (d, *J* = 8.0 Hz, 1H), 6.76-6.72 (br m, 1H), 6.70-6.66 (br m, 1H), 6.59-6.40 (br m, 1H), 6.51 (br dd, *J* = 8.8, 2.8 Hz, 1H), 6.38 (br d, *J* = 8.4 Hz, 1H), 5.60 (dd, *J* = 47.2, 6.6 Hz, 1H), 4.22 (dd, *J* = 16.4, 6.4 Hz, 1H), 3.75 (s, 3H), 3.50 (s, 3H), 3.32-3.23 (m, 1H), 3.03-2.97 (m, 1H), 2.78-2.67 (m, 1H), 2.54-2.51 (m, 1H), 2.44 (s, 3H); ^{13}C NMR (see the spectral image);[155] ^{19}F NMR (376 MHz, $CDCl_3$) δ -179.8.

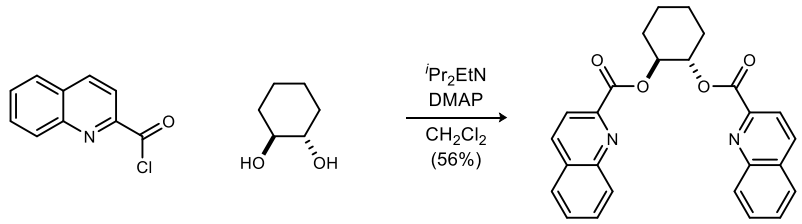

H,QuinBEster To a solution of diol (243 mg, 2.09 mmol) and acid chloride (1.00 g, 5.22 mmol) in CH_2Cl_2 (10 mL) was added DMAP (26 mg, 210 µmol) followed by Hünig's base (1.1 mL, 6.30 mmol). The resulting solution was stirred at ambient temperature for 18 h. The reaction mixture was transferred to a separatory funnel, washed with H_2O, and then dried and concentrated. Flash column chromatography afforded the desired product as a colorless foam (495 mg, 56%). $[\alpha]_D^{25}$ +120 (*c* 0.47, $CHCl_3$); R_f = 0.80 (100% EtOAc); IR (neat) 3283, 3006, 2928, 2858, 1616, 1500 cm^{-1}; ^{1}H NMR (400 MHz, $CDCl_3$) δ 8.19 (d, *J* = 8.8 Hz, 2H), 8.11 (d, *J* = 8.4 Hz, 1H), 7.98 (d, *J* = 8.4 Hz, 2H), 7.71 (d, *J* = 8.4 Hz, 2H), 7.64 (ddd, *J* = 7.2, 7.2, 1.2 Hz, 2H), 7.50 (ddd, *J* = 7.2, 7.2, 1.2 Hz, 2H), 5.41 (ddd, *J* = 9.6, 9.6, 2.8 Hz, 2H), 2.31 (dd, *J* = 13.6, 6.8 Hz, 2H), 1.87-1.79 (br m, 2H), 1.75-1.65 (br m, 2H), 1.48 (ddd, *J* = 7.2, 7.2, 2.8 Hz, 2H); ^{13}C NMR (100 MHz, $CDCl_3$) ppm 147.8, 147.7, 137.2, 130.8, 130.0, 129.1, 128.4, 127.3, 120.9, 75.6, 30.3, 23.6; HRMS (ESI): Exact mass calcd for $C_{26}H_{22}N_2NaO_4$ $[M+Na]^+$ 449.1476, found 449.1477.

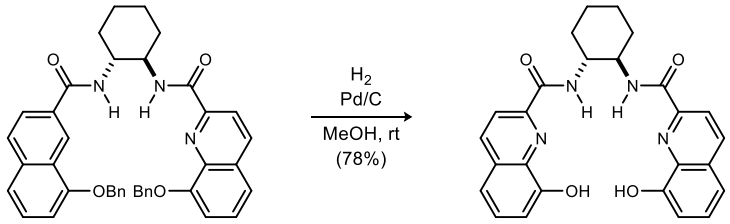

***8*OH-BAMide**. To a solution of the bis(benzyl) ether (350 mg, 550 µmol) in methanol (20 mL) was added Pd/C (10%, 700 mg). The resulting solution was carefully evacuated and refilled with 1 atmosphere of H_2. The resulting solution was stirred for 16 h, then filtered through a pad of Celite®, and the filtrate was concentrated. Flash column chromatography (SiO_2, 1-4% methanol in dichloromethane) afforded the deprotected compound as a yellow solid (195 mg, 78%). Mp = 175.5-176.0 °C; R_f = 0.15 (75% EtOAc/hexanes); $[\alpha]_D^{20}$ -273 (*c* 0.31, $CHCl_3$); IR (film) 3371, 2936, 1669, 1563, 1521, 1501 cm^{-1}; ^{1}H NMR (400 MHz, $CDCl_3$) δ 9.22 (br s, 2H), 8.89 (br d, *J* = 7.2 Hz, 2H), 8.28 (d, *J* = 8.4 Hz, 2H), 8.24 (d, *J* = 8.4 Hz, 2H), 7.52 (dd, *J* = 8.0, 8.0 Hz, 2H), 7.34 (br dd, *J* = 7.6, 0.4

Hz, 2H), 7.29 (br dd, *J* = 7.6, 0.8 Hz, 2H), 4.05-3.90 (br m, 2H), 2.18-2.01 (br m, 2H), 1.42-1.36 (br m, 2H), 1.21-1.15 (br m, 2H), 0.80 (br dd, *J* = 9.6, 9.6 Hz, 2H); ^{13}C NMR (100 MHz, $CDCl_3$) ppm 165.5, 153.1, 147.3, 137.8, 136.7, 129.8, 129.6, 119.4, 117.9, 111.8, 54.3, 31.7, 24.2; HRMS (ESI): Exact mass calcd for $C_{26}H_{24}N_4NaO_4$ $[M+Na]^+$ 479.1695, found 479.1700.

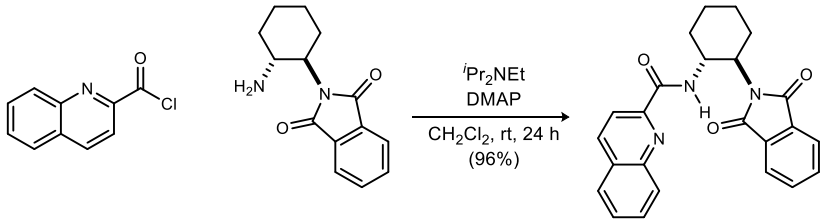

***N*-((1*R*,2*R*)-2-(1,3-Dioxoisoindolin-2-yl)cyclohexyl)quinoline-2-carboxamide**. To a solution of the protected diamine (344 mg, 1.41 mmol) in dichloromethane (14 mL) was added Hünig's base (280 µL, 1.69 mmol), the acid chloride (324 mg, 1.69 mmol) and DMAP (17.0 mg, 141 µmol). The resulting solution was stirred at ambient temperature for 24 h and then quenched with 1 M HCl. The aqueous layer was extracted with CH_2Cl_2, and the combined organic layers were washed with satd aq $NaHCO_3$ and then dried and concentrated to yield the product as a colorless to pale yellow solid (541 mg, 96% yield). Mp = 159.0-160.5 °C; $[\alpha]_D^{20}$ -269.1 (*c* 1.58, $CHCl_3$); R_f = 0.64, $KMnO_4$ (10% MeOH/CH_2Cl_2); IR (film) 3360, 2936, 2858, 1771, 1712, 1679, 1526, 1502, 1427, 1378, 1362, 1161 cm^{-1}; ^{1}H NMR (400 MHz, $CDCl_3$) δ 8.15 (d, *J* = 8.4 Hz, 1H), 8.10 (d, *J* = 8.4 Hz, 1H), 8.03 (d, *J* = 8.4 Hz, 1H), 7.79 (d, *J* = 8.0 Hz, 1H), 7.73 (m, 3H), 7.59 (m, 3H), 4.83 (dddd, *J* = 10.8, 10.2, 10.2, 4.4 Hz, 1H), 4.23 (ddd, *J* = 11.6, 11.6, 4.0 Hz, 1H), 2.58 (dddd, *J* = 13.6, 13.0, 12.8, 4.4 Hz, 1H), 2.29 (br m, 1H), 1.91 (br m, 3H), 1.54 (br m, 3H) [N*H* not observed]; ^{13}C NMR (100 MHz, $CDCl_3$) ppm 168.4, 164.1, 149.4, 146.3, 137.1, 133.6, 131.8, 129.8, 129.1, 127.7, 127.4, 123.1, 118.6, 54.7, 49.6, 33.2, 28.9, 25.4, 24.6 [two aryl carbons (methines) are coincidental][158]; HRMS (ESI): Exact mass calcd for $C_{24}H_{21}N_3NaO_3$ $[M+Na]^+$ 422.1481, found 422.1474.

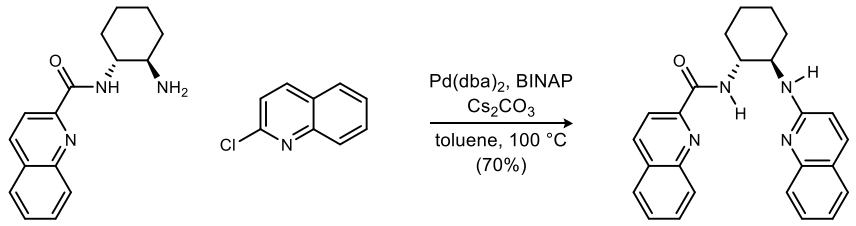

***N*-((1*R*,2*R*)-2-(Quinolin-2-ylamino)cyclohexyl)quinoline-2-carboxamide.** A flask was charged with the amine (70 mg, 260 µmol), 2-chloroquinoline (43 mg, 260 µmol), BINAP (6 mg, 10 µmol), $Pd(dba)_2$ (3 mg, 5 µmol), Cs_2CO_3 (254 mg, 780 µmol), and toluene (1 mL). The reaction mixture was heated at reflux for 24 h, and the orange solution was filtered through a pad of Celite and concentrated. The resulting residue was subjected to flash column chromatography (SiO_2, 10-35% ethyl acetate in hexanes) to afford the title compound as a yellow solid (72 mg, 70%). Mp = 171 °C (decomp.); $[\alpha]_D^{20}$ -27.8 (*c* 0.14, $CHCl_3$); R_f = 0.19, $KMnO_4$ (40% EtOAc/hexanes); IR (film) 3313, 2931, 1649, 1618, 1535, 1502 cm^{-1}; ^{1}H NMR (400 MHz, $CDCl_3$) δ 8.82 (d, *J* = 8.0 Hz, 1H), 8.15

[158] It is not clear which peak (among the 2C peaks at 133.6, 129.8, 123.1) is actually two coincidental methines.

(s, 2H), 7.78 (d, *J* = 8.4 Hz, 1H), 7.73 (d, *J* = 7.2 Hz, 1H), 7.60 (d, *J* = 8.8 Hz, 1H), 7.53-7.38 (m, 5H), 7.13 (dd, *J* = 7.6, 7.2 Hz, 1H), 6.49 (d, *J* = 8.8 Hz, 1H), 4.97 (d, *J* = 7.2 Hz, 1H), 4.45 (dddd, *J* = 14.8, 11.2, 4.0, 4.0 Hz, 1H), 4.01 (dddd, *J* = 14.4, 11.2, 4.0, 3.6 Hz, 1H), 2.33 (br m, 2H), 1.82 (br m, 2H), 1.68-1.39 (m, 4H); ^{13}C NMR (125 MHz, $CDCl_3$) ppm 165.3, 156.8, 149.6, 147.91, 147.86, 146.3, 136.9, 129.8, 129.5, 129.3, 129.0, 127.5, 127.3 (2C), 126.4, 123.3, 121.7, 118.6, 112.7, 55.7, 54.0, 32.9, 32.5, 25.0, 24.9; HRMS (ESI): Exact mass calcd for $C_{25}H_{25}N_4O$ $[M+H]^+$ 397.2028, found 397.2019.

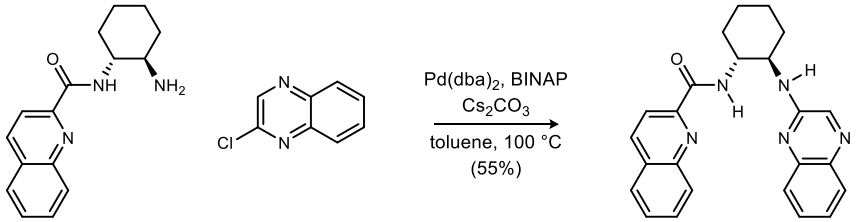

***N*-((1*R*,2*R*)-2-(Quinoxalin-2-ylamino)cyclohexyl)quinoline-2-carboxamide.** A flask was charged with the amine (70 mg, 260 µmol), 2-chloroquinoxaline (43 mg, 260 µmol), BINAP (6.0 mg, 10 µmol), $Pd(dba)_2$ (3.0 mg, 5 µmol), Cs_2CO_3 (254 mg, 780 µmol), and toluene (1 mL) and the solution was heated at reflux for 24 h. The resulting orange solution was filtered through a pad of Celite and concentrated. The residue was subjected to flash column chromatography (SiO_2, 30-50% ethyl acetate in hexanes) to afford the title compound as a pale tan solid (57 mg, 55%). Mp = 152.0-153.0 °C; $[\alpha]_D^{20}$ +86.7 (*c* 0.27, $CHCl_3$); R_f = 0.25, PIP (50% EtOAc/hexanes); IR (film) 3310, 3058, 2928, 2854, 1657, 1585, 1541, 1500, 1413, 759 cm^{-1}; ^{1}H NMR (500 MHz, $CDCl_3$) δ 8.55 (d, *J* = 8.0 Hz, 1H), 8.17 (s, 2H), 8.07 (s, 1H), 7.75 (d, *J* = 8.0 Hz, 1H), 7.70 (br m, 2H) 7.67 (d, *J* = 8.5 Hz, 1H), 7.59 (dd, *J* = 7.5, 7.5 Hz, 1H), 7.51 (dd, 8.0, 7.5 Hz, 1H). 7.48 (dd, *J* = *8*.0, 7.0 Hz, 1H) 7.24 (dd, *J* = 7.0, 7.0 Hz, 1H), 5.72 (d, *J* = 7.0 Hz, 1H), 4.29 (dddd, *J* = 13.0, 10.7, 9.3, 4.3 Hz, 1H), 4.12 (br m, 1H), 2.41 (d, *J* = 11.0 Hz, 1H), 2.27 (d, *J* = 12.5 Hz, 1H), 1.88 (br m, 2H), 1.67 (br m, 1H), 1.53 (br m, 2H), 1.42 (br m, 1H); ^{13}C NMR (125 MHz, $CDCl_3$) ppm 165.5, 151.9, 149.2, 146.3, 141.7, 139.2, 137.3, 137.0, 129.8, 129.7 (2C), 129.1, 128.7, 127.7, 127.5, 126.2, 123.8, 118.7, 55.3, 54.5, 32.5, 32.4, 25.0, 24.8; HRMS (ESI): Exact mass calcd for $C_{24}H_{24}N_5O$ $[M+H]^+$ 398.1981, found 398.1987.

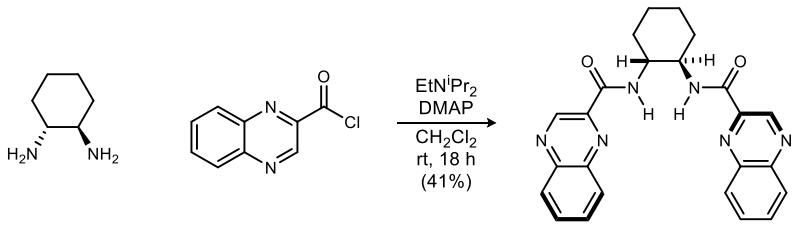

H,Quinox-BAMide. A flask was charged with (1*R*,2*R*)-cyclohexane-1,2-diamine (15.0 mg, 131 µmol), 2-quinoxaloyl chloride (55.0 mg, 288 µmol), Hünig's base (50.0 µL, 288 µmol), and CH_2Cl_2. DMAP (2.0 mg , 29 µmol) was added, and the resulting solution was allowed to stir at room temperature overnight. The reaction was quenched with 1 M HCl, washed with water and satd aq $NaHCO_3$, dried and concentrated to a bright yellow solid. The residue was subjected to flash column chromatography (SiO_2, 20-40% ethyl acetate in CH_2Cl_2) to afford the title compound as a white solid (23 mg, 41%). Mp = 192 °C (decomp.); $[\alpha]_D^{20}$ -206.6 (*c* 0.06, $CHCl_3$); R_f = 0.18,

PIP (40% EtOAc/hexanes); IR (film) 3301, 2931, 2857, 1657, 1532, 1493, 1085 cm^{-1}; ^1H NMR (400 MHz, $CDCl_3$) δ 9.53 (s, 2H), 8.26 (d, *J* = 7.2 Hz, 2H), 8.18-8.13 (m, 2H), 8.12-8.07 (m, 2H), 7.82 (d, *J* = 6.4 Hz, 2H), 7.81 (d *J* = 6.4 Hz, 2H), 4.21 (br m, 2H), 2.31 (d, *J* = 11.6 Hz, 2H), 1.93 (d, *J* = 7.6 Hz, 2H), 1.67-1.50 (m, 4H); ^{13}C NMR (125 MHz, $CDCl_3$) ppm 163.7, 143.8, 143.7, 143.2, 140.3, 131.5, 130.8, 129.9, 129.3, 53.6, 32.6, 24.8; HRMS (ESI): Exact mass calcd for $C_{24}H_{22}N_6NaO_2$ $[M+Na]^+$ 449.1702, found 449.1710

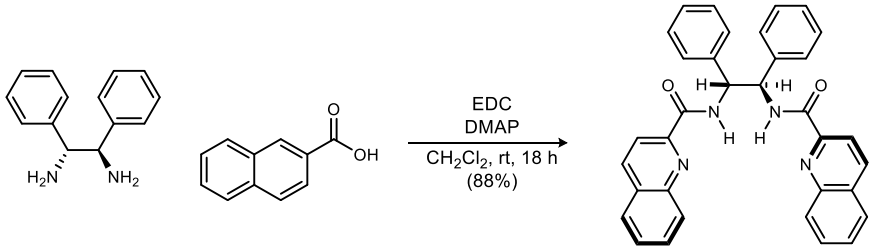

StilbBAMide. A flask was charged with the diamine (59 mg, 277 µmol), acid (144 mg, 831 µmol) and CH_2Cl_2 (1.5 mL). The resulting solution was chilled to 0 °C, and 1-ethyl-3-(3-dimethylaminopropyl) carbodiimide hydrochloride (213 mg, 1.11 mmol) and DMAP (3.5 mg, 28 µmol) were added. The solution was gradually warmed to room temperature and stirred for 16 h, quenched with 1 M HCl, and extracted with CH_2Cl_2. The organic layers were washed with 1 M NaOH, brine, dried and concentrated. The resulting residue was subjected to flash column chromatography (SiO_2, 2-5% methanol in CH_2Cl_2) to afford the desired product as a fluffy white solid (127 mg, 88%). Mp = 212.0-213.5 °C; $[\alpha]_D^{20}$ -16.9 (0.13, $CHCl_3$); R_f = 0.67, $KMnO_4$ (75% EtOAc/hexanes); IR (film) 3341, 3060, 3033, 1649, 1523, 1498 cm^{-1}; ^1H NMR (400 MHz, $CDCl_3$) δ 9.23 (dd, *J* = 8.0, 2.0 Hz, 1H), 8.22 (d, *J* = 8.4 Hz, 1H), 8.17 (d, *J* = 3.2 Hz, 1H), 8.15 (d, *J* = 3.2 Hz, 1H), 7.78 (d, *J* = 8.8 Hz, 1H), 7.75 (ddd, *J* = 8.4, 7.2, 1.6 Hz, 1H), 7.57 (ddd, *J* = 8.4, 6.8, 0.8 Hz, 1H), 7.37 (dt, *J* = 6.8, 1.6 Hz, 2H), 7.32–7.22 (m, 3H), 5.76 (dd, *J* = 6.0, 2.8 Hz, 1H); ^{13}C NMR (100 MHz, $CDCl_3$) ppm 164.7, 149.3, 146.4, 138.7, 137.2, 130.0, 129.9, 129.2, 128.5, 127.9, 127.8, 127.5, 118.7, 58.9; HRMS (ESI): Exact mass calcd for $C_{34}H_{26}NaN_4O_2$ $[M+Na]^+$ 545.1953, found 545.1945.

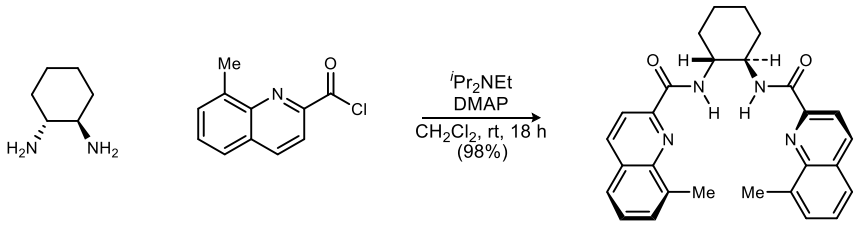

***8*Me-BAMide (XX)**. A flask was charged with the diamine (243 mg, 2.13 mmol), acid chloride (1.10 g, 5.32 mmol), Hünig's base (3.00 mL, 12.8 mmol), and CH_2Cl_2 (11 mL). DMAP (26 mg, 213 µmol) was added, and the resulting solution was allowed to stir at room temperature overnight. The reaction was quenched with 1 M HCl, washed with water and satd aq $NaHCO_3$, dried and concentrated to a pale yellow solid. The residue was subjected to flash column chromatography (SiO_2, 20-50% ethyl acetate in hexanes) to afford the title compound as a colorless solid (552 mg, 57%). Mp = 87.0-89.0 °C; $[\alpha]_D^{20}$ -350 (0.24, $CHCl_3$); R_f = 0.14 (20% EtOAc/hexanes); IR (film) 3359, 2932, 1668, 1525, 1495, 1162, 770 cm^{-1}; ^1H NMR (400 MHz, $CDCl_3$) δ 8.60 (br d, *J* = 6.8 Hz, 2H), 8.19 (d, *J* = 8.4 Hz, 2H), 8.15 (d, *J* = 8.8 Hz, 2H), 7.62 (d, *J* = 8.4 Hz, 2H), 7.58 (d, *J* = 7.2 Hz, 2H), 7.45 (dd, *J* = 7.6, 7.2 Hz, 2H), 4.21-4.16 (br m, 2H), 2.90 (s, 6H), 2.36 (br d, *J* = 9.6 Hz, 2H), 1.90 (br d, *J* = 6.4 Hz,

2H), 1.60-1.53 (br m, 4H); ^{13}C NMR (100 MHz, $CDCl_3$) ppm 165.1, 148.2, 145.5, 138.0, 137.4, 129.9, 129.2, 127.6, 125.4, 118.4, 53.7, 32.5, 24.9, 17.9; HRMS (ESI): Exact mass calcd for $C_{28}H_{28}NaN_4O_2$ $[M+Na]^+$ 475.2110, found 475.2124.

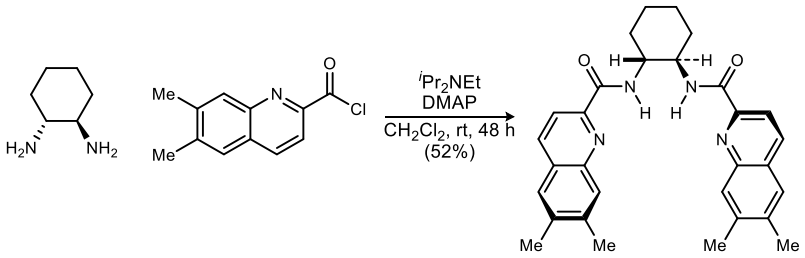

[6,7](Me)$_2$-BAMide. A flask was charged with the diamine (100 mg, 880 µmol), acid chloride (483 mg, 2.20 mmol), Hünig's base (900 µL, 5.30 mmol), and CH_2Cl_2 (5 mL). DMAP (10 mg, 80 µmol) was added, and the resulting solution was allowed to stir for 2 days at ambient temperature overnight. The reaction was quenched with 1 M HCl, washed with water and satd aq $NaHCO_3$, dried and concentrated to a dark brown oil. The residue was subjected to flash column chromatography (SiO_2, 20-50% ethyl acetate in hexanes) to afford the title compound as a colorless solid (220 mg, 52%). Mp = 104.0-106.5 °C; $[\alpha]_D^{20}$ -320 (0.24, $CHCl_3$); R_f = 0.42 (50% EtOAc/hexanes); IR (film) 3370, 2935, 1669, 1524, 1493. 878 cm^{-1}; ^{1}H NMR (400 MHz, $CDCl_3$) δ 8.49 (br d, *J* = 7.6 Hz, 2H), 8.06 (d, *J* = 8.4 Hz, 2H), 7.96 (d, *J* = 8.4 Hz, 2H), 7.84 (s, 2H), 7.42 (s, 2H), 4.23-4.14 (br m, 2H), 2.42 (s, 6H), 2.39 (s, 6H), 2.31 (d, *J* = 10.8 Hz, 2H), 1.87 (d, *J* = 6.4 Hz, 2H), 1.60-1.50 (br m, 4H); ^{13}C NMR (100 MHz, $CDCl_3$) ppm 165.1, 148.6, 145.5, 140.1, 137.9, 135.7, 129.1, 127.8, 126.5, 117.9, 53.4, 32.8, 24.9, 20.3, 20.0; HRMS (ESI): Exact mass calcd for $C_{30}H_{33}N_4O_2$ $[M+H]^+$ 481.2604, found 481.2616.

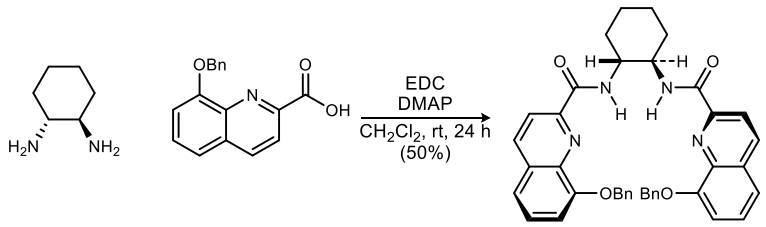

[8]BnO-BAMide. A flask was charged with the diamine (278 mg, 2.44 mmol), acid (1.70 g, 6.09 mmol) and CH_2Cl_2 (12.2 mL). The resulting solution was chilled to 0 °C, and 1-ethyl-3-(3-dimethylaminopropyl) carbodiimide hydrochloride (1.54 g, 8.05 mmol) and DMAP (29.8 mg, 244 µmol) were added. The solution was gradually warmed to room temperature and stirred for 16 h, quenched with 1 M HCl, and extracted with CH_2Cl_2. The organic layers were washed with 1 M NaOH, brine, dried and concentrated. The resulting residue was subjected to flash column chromatography (SiO_2, 50% ethyl acetate in dichloromethane followed by 3% methanol in dichloromethane)[159] to afford the desired product as a colorless solid (766 mg, 50%). Mp = 74.0-76.0 °C; $[\alpha]_D^{20}$ -240 (0.34, $CHCl_3$); R_f = 0.51 (50% EtOAc/hexanes); IR (film) 3361, 2935, 1670, 1500, 1327, 1102, 736 cm^{-1}; ^{1}H NMR (400 MHz, $CDCl_3$) δ 8.59 (br d, *J* = 8.0 Hz, 1H), 8.15 (d, *J* = 8.4 Hz, 1H), 8.09 (d, *J* = 8.4 Hz, 1H), 7.59

[159] The material precipitates on the column, and therefore, a methanol/dichloromethane gradient was needed to flush the compound from the silica gel.

(d, *J* = 7.2 Hz, 3H), 7.44-7.33 (m, 3H), 7.10 (dd, *J* = 7.6, 0.8 Hz, 1H), 5.46 (s, 2H), 4.20-4.16 (br m, 1H), 2.25 (br d, *J* = 10.8 Hz, 1H), 1.84 (br d, *J* = 6.0 Hz, 1H), 1.63 (br m, 1H) 1.55-1.45 (br m, 1H); ^{13}C NMR (100 MHz, $CDCl_3$) ppm 164.6, 154.5, 148.5, 138.8, 137.0, 136.9, 130.3, 128.5, 127.9, 127.7, 127.0, 119.8, 119.2, 111.3, 71.0, 52.9, 32.2, 24.5; HRMS (ESI): Exact mass calcd for $C_{40}H_{36}NaN_4O_4$ $[M+Na]^+$ 659.2634, found 659.2616.

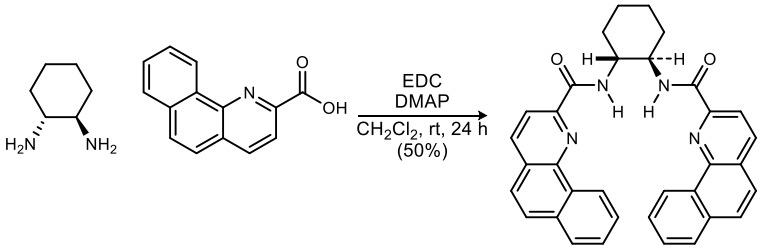

Benzoquin-BAMide. A flask was charged with the diamine (247 mg, 2.16 mmol), acid (1.26 g, 5.40 mmol) and CH_2Cl_2 (10.8 mL). The resulting solution was chilled to 0 °C, and 1-ethyl-3-(3-dimethylaminopropyl) carbodiimide hydrochloride (1.37 g, 7.13 mmol) and DMAP (26.4 mg, 216 µmol) were added. The solution was gradually warmed to room temperature and stirred for 16 h, quenched with 1 M HCl, and extracted with CH_2Cl_2. The organic layers were washed with 1 M NaOH and brine, and then dried and concentrated. The resulting residue was subjected to flash column chromatography (SiO_2, 50% ethyl acetate in hexanes) to afford the desired product as a colorless solid (562 mg, 50%). Mp = 234.0-235.0 °C; $[\alpha]_D^{20}$ -620 (0.46, $CHCl_3$); R_f = 0.27 (50% EtOAc/hexanes); IR (film) 3341, 3049, 2935, 2859, 1656, 1170, 715 cm^{-1}; ^{1}H NMR (400 MHz, $CDCl_3$) δ 9.52 (d, *J* = 8.0 Hz, 1H), 8.90 (d, *J* = 7.2 Hz, 1H), 8.29 (d, *J* = 8.4 Hz, 1H), 7.95 (d, *J* = 8.4 Hz, 1H), 7.84 (ddd, *J* = 7.6, 7.6, 0.8 Hz, 1H), 7.75 (d, *J* = 7.6 Hz, 1H), 7.65 (ddd, *J* = 7.6, 7.6, 0.8 Hz, 1H), 7.61 (d, *J* = 8.8 Hz, 1H), 7.39 (d, *J* = 8.8 Hz, 1H), 4.40-4.30 (br m, 1H), 2.48 (d, *J* = 12.4 Hz, 1H), 1.94 (d, *J* = 8.0 Hz, 1H), 1.71-1.55 (br m, 2H); ^{13}C NMR (100 MHz, $CDCl_3$) ppm 165.2, 147.7, 144.5, 136.6, 133.4, 130.9, 128.9, 128.3, 127.6 (2C), 127.1, 124.7, 124.5, 119.5, 54.0, 32.4, 24.8; HRMS (ESI): Exact mass calcd for $C_{34}H_{29}N_4O_2$ $[M+H]^+$ 525.2291, found 525.2310.

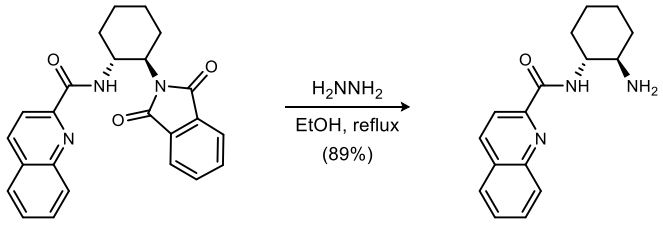

***N*-((1*R*,2*R*)-2-aminocyclohexyl)quinoline-2-carboxamide**. A round-bottom flask was charged with the phthalimide (500 mg, 1.25 mmol) and EtOH (2.5 mL). To the resulting solution was added hydrazine monohydrate (225 µL, 4.63 mmol) and the mixture was heated at reflux overnight. The volatiles were removed under vacuum, the residue was dissolved in a 1:1 mixture of water and CH_2Cl_2, and the aqueous layer was extracted with CH_2Cl_2. The organic layers were dried and concentrated to yield the crude product as a light brown solid, which was filtered through a short pad of silica gel to afford the pure product as a light tan solid (300 mg, 89%). Mp = 158-160 °C; $[\alpha]_D^{20}$ -78.9 (*c* 0.10, $CHCl_3$); R_f = 0.13 (5% MeOH/CH_2Cl_2); IR (film) 3348, 3054, 2928, 2855, 1655, 1563, 1526, 1501 cm^{-1}; ^{1}H NMR (400 MHz, $CDCl_3$) δ 8.30 (s, 2H), 8.20 (d, *J* = 8.4 Hz, 1H),

8.12 (d, *J* = 8.4 Hz, 1H), 7.87 (d, *J* = 8.0 Hz, 1H), 7.77 (br dd, *J* = 8.0, 7.6 Hz, 1H), 7.62 (dd, *J* = 7.6, 7.6 Hz, 1H), 3.80 (dddd, *J* = 13.6, 9.6, 7.2, 3.6 Hz, 1H), 2.69 (ddt, *J* = 10.4, 10.0, 3.6 Hz, 1H), 2.10 (br m, 2H), 1.80 (br m, 4H) 1.36 (m, 4H); ^{13}C NMR (100 MHz, $CDCl_3$) ppm 164.9, 150.1, 146.8, 137.8, 130.4, 130.0, 129.6, 128.2, 128.0, 119.2, 60.7, 58.1, 56.8, 35.4, 32.8, 21.3; HRMS (ESI): Exact mass calcd for $C_{16}H_{20}N_3O$ $[M+H]^+$ 270.1606, found 270.1597.

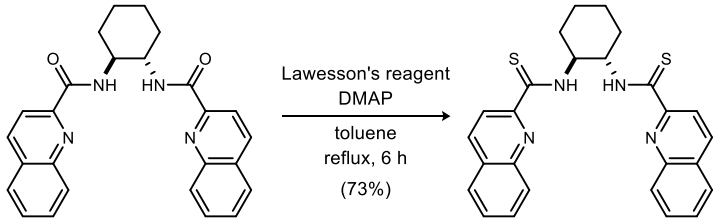

H,Quin-BTAMide. A flask was charged with the bis(amide) (300 mg, 707 µmol) and toluene (14 mL). Lawesson's reagent (1.00 g, 2.47 mmol) was added and the reaction was heated at reflux for 6 h. After cooling to ambient temperature, the reaction was concentrated to a dark brown solid. Flash column chromatography (8-15% ethyl acetate in hexanes) afforded the desired product as a bright yellow solid (237 mg, 73%). Mp = 92.5-95.0 °C; $[\alpha]_D^{20}$ -260 (*c* 0.31, $CHCl_3$); R_f = 0.40 (40% EtOAc/Hexanes); IR (film) 3223, 2856, 1498, 1378, 758 cm^{-1}; ^{1}H NMR (400 MHz, $CDCl_3$) δ 8.69 (d, *J* = 8.4 Hz, 2H), 8.18 (d, *J* = 8.4 Hz, 2H), 8.14 (d, *J* = 8.8 Hz, 2H), 7.78 (d, *J* = 8.4 Hz, 2H), 7.75 (ddd, *J* = 7.4, 7.4, 1.2 Hz, 2H), 7.57 (ddd, *J* = 7.4, 7.4, 1.2 Hz, 2H), 5.15-5.04 (br m, 2H), 2.55 (d, *J* = 12.8 Hz, 2H), 1.97 (d, *J* = 8.0 Hz, 2H), 1.80-1.51 (br m, 4H); ^{13}C NMR (100 MHz, $CDCl_3$) ppm 191.3, 149.7, 145.3, 136.6, 130.1, 130.0, 129.0, 127.9, 127.3, 121.3, 58.8, 31.0, 24.6; HRMS (CI): Exact mass calcd for $C_{26}H_{25}N_4S_2$ $[M+H]^+$ 457.1515, found 457.1525.

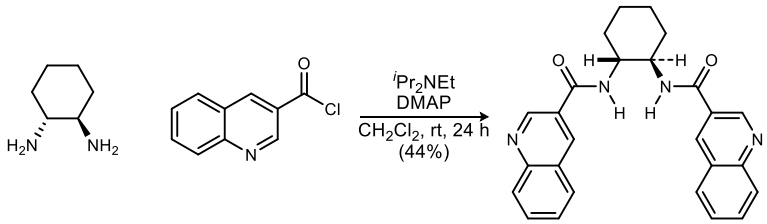

H,^{3}Quin-BAMide. A flask was charged with the diamine (120 mg, 1.04 mmol), acid chloride (500 mg, 2.61 mmol), Hünig's base (450 µL, 2.61 mmol), and CH_2Cl_2 (10 mL). DMAP (12.7 mg, 104 µmol) was added, and the resulting solution was stirred at ambient temperature overnight. The reaction was quenched with 1 M HCl, washed with water and satd aq $NaHCO_3$, and then dried and concentrated to an orange solid. Flash column chromatography (SiO_2, 60-100% ethyl acetate in hexanes) afforded the title compound as a colorless solid (193 mg, 44%). Mp = 207 °C (dec.); $[\alpha]_D^{20}$ -120 (0.14, $CHCl_3$); R_f = 0.30 (3% MeOH/CH_2Cl_2); IR (film) 3281, 1637, 1547, 788 cm^{-1}; ^{1}H NMR (400 MHz, $CDCl_3$) δ 9.29 (d, *J* = 2.4 Hz, 1H), 8.52 (br d, *J* = 1.6 Hz, 1H), 8.02 (d, *J* = 8.4 Hz, 1H), 7.68 (dd, *J* = 8.4, 8.4 Hz, 1H), 7.67 (dd, *J* = 8.4, 4.4 Hz, 1H), 7.47 (d, *J* = 7.2 Hz, 1H), 7.45 (d, *J* = 7.2 Hz, 1H), 4.25-4.14 (br m, 1H), 2.30 (d, *J* = 12.4 Hz, 1H), 1.88 (d, *J* = 8.0 Hz, 1H), 1.60-1.45 (br m, 2H); ^{13}C NMR (100 MHz, $CDCl_3$) ppm 166.5, 149.1, 148.4, 135.4, 131.2, 129.2, 128.7, 127.4, 126.7, 126.5, 54.9, 32.3, 24.8; HRMS (ESI): Exact mass calcd for $C_{26}H_{25}N_4O_2$ $[M+H]^+$ 425.1978, found 425.1965.

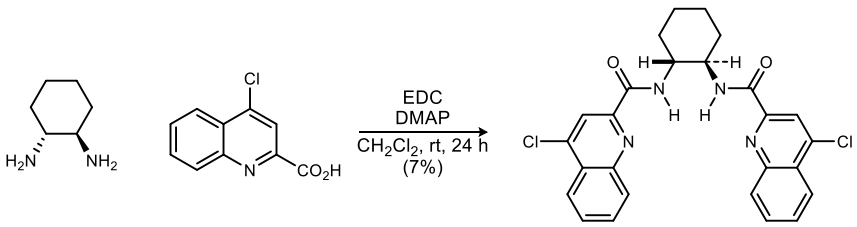

H,^{4}Cl-Quin-BAMide A flask was charged with the diamine (45 mg, 394 µmol), acid (186 mg, 867 µmol) and CH_2Cl_2 (2 mL). The resulting solution was chilled to 0 °C, and 1-ethyl-3-(3-dimethylaminopropyl) carbodiimide hydrochloride (265 mg, 1.38 mmol) and DMAP (5.0 mg, 35 µmol) were added. The solution was gradually warmed to room temperature and stirred for 16 h, quenched with 1 M HCl, and extracted with CH_2Cl_2. The organic layers were washed with 1 M NaOH, brine, dried and concentrated. The resulting residue was subjected to flash column chromatography (SiO_2, 50-100% ethyl acetate in hexanes) to afford the desired product as a colorless solid (30 mg, 7%). Mp = 219.2-221.0 °C; $[\alpha]_D^{20}$ -260 (0.30, $CHCl_3$); R_f = 0.54 (50% EtOAc/hexanes); IR (film) 3317, 2933, 1665, 1494, 760 cm^{-1}; ^{1}H NMR (400 MHz, $CDCl_3$) δ 8.40 (d, *J* = 7.2 Hz, 2H), 8.24 (s, 2H), 8.19 (d, *J* = 8.0 Hz, 2H), 8.17 (d, *J* = 8.4 Hz, 2H), 7.81 (dd, *J* = 7.2, 7.2 Hz, 2H), 7.67 (dd, *J* = 8.0 8.0 Hz, 2H), 4.19-4.15 (br m, 2H), 2.30 (br d, *J* = 10.8 Hz, 2H), 1.90 (br d, *J* = 7.2 Hz, 2H), 1.59-1.52 (br m, 4H); ^{13}C NMR (100 MHz, $CDCl_3$) ppm 163.9, 149.4, 147.2, 143.9, 130.8, 130.3, 128.8, 127.2, 123.4, 119.0, 53.6, 32.7, 24.9; HRMS (ESI): Exact mass calcd for $C_{26}H_{23}Cl_2N_4O_2$ $[M+H]^+$ 493.1198, found 493.1159.

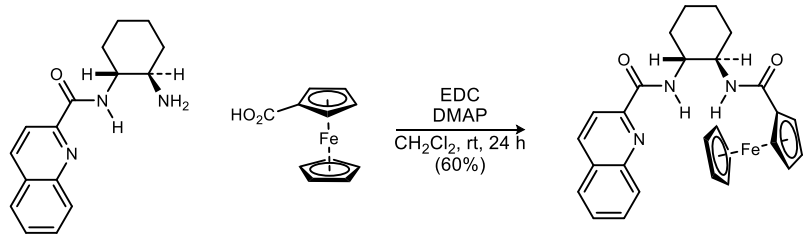

Ferroceneamide. A flask was charged with the amine (121 mg, 450 µmol), acid (124 mg, 540 µmol) and CH_2Cl_2 (2.3 mL). The resulting solution was chilled to 0 °C, and 1-ethyl-3-(3-dimethylaminopropyl) carbodiimide hydrochloride (129 mg, 675 µmol) and DMAP (6.0 mg, 50 µmol) were added. The solution was gradually warmed to room temperature and stirred for 16 h, quenched with 1 M HCl, and extracted with CH_2Cl_2. The organic layers were washed with 1 M NaOH, brine, dried and concentrated. The resulting residue was subjected to flash column chromatography (SiO_2, 30-50% ethyl acetate in hexanes) to afford the desired product as a reddish-orange solid (130 mg, 60%). Mp = 210 °C (dec.); $[\alpha]_D^{20}$ -4.7 (0.40, $CHCl_3$); R_f = 0.20 (40% EtOAc/hexanes); ^{1}H NMR (400 MHz, $CDCl_3$) δ 8.42 (br d, *J* = 8.4 Hz, 1H), 8.35 (d, *J* = 8.4 Hz, 1H), 8.30 (d, *J* = 8.8 Hz, 1H), 8.12 (d, *J* = 8.8 Hz, 1H), 7.84 (d, *J* = 8.0 Hz, 1H), 7.75 (br ddd, *J* = 7.8, 7.8, 1.2 Hz, 1H), 7.59 (br ddd, *J* = 7.2, 7.2, 1.2 Hz, 1H), 4.73 (br dd, *J* = 0.8, 0.8 Hz, 1H), 4.61 (br dd, *J* = 0.8, 0.8 Hz, 1H), 4.28-4.21 (br m, 2H), 4.17-4.02 (br m, 1H), 3.97-3.86 (br m, 6H), 2.40 (br d, *J* = 13.2 Hz, 1H), 2.18 (br d, *J* = 13.2 Hz, 1H), 1.92-1.79 (series of br m, 2H), 1.70-1.50 (series of br m, 1H), 1.50-1.39 (br m, 2H), 1.40-1.23 (br m, 2H); ^{13}C NMR (100 MHz, $CDCl_3$) ppm 170.1,

165.6, 149.0, 146.4, 137.5, 130.2, 129.8, 129.2, 128.0, 127.6, 118.6, 76.2, 70.2, 70.1, 69.4, 68.8, 67.4, 55.7, 52.2, 32.8, 32.3, 25.1, 24.4; HRMS (ESI): Exact mass calcd for $C_{27}H_{28}FeN_3O_2$ $[M+H]^+$ 482.1531, found 482.1511.

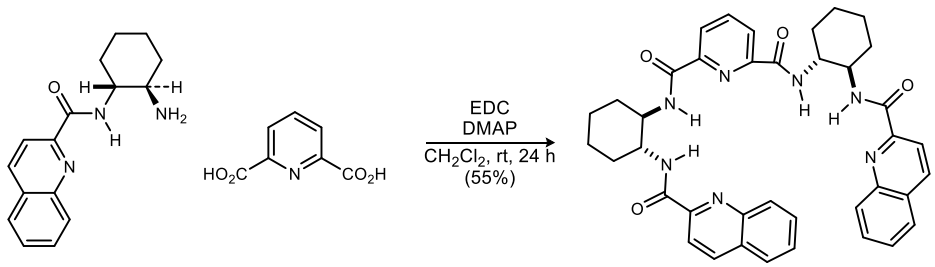

MiracleBAMide. A flask was charged with the amine (231 mg, 858 µmol), acid (48 mg, 290 µmol) and CH_2Cl_2 (3 mL). The resulting solution was chilled to 0 °C, and 1-ethyl-3-(3-dimethylaminopropyl) carbodiimide hydrochloride (274 mg, 1.43 mmol) and DMAP (11 mg, 86 µmol) were added. The solution was gradually warmed to room temperature and stirred for 16 h, quenched with 1 M HCl, and extracted with CH_2Cl_2. The organic layers were washed with 1 M NaOH, brine, dried and concentrated. The resulting residue was subjected to flash column chromatography (SiO_2, 50-80% ethyl acetate in hexanes) to afford the desired product as a colorless solid (110 mg, 55%). Mp = 185-187 °C; $[\alpha]_D^{20}$ -330 (0.90, $CHCl_3$); R_f = 0.14 (50% EtOAc/hexanes); IR (film) 3316, 2935, 1658, 1534, 1052, 775 cm^{-1}; ^1H NMR (400 MHz, $CDCl_3$) δ 9.21 (d, *J* = 8.4 Hz, 2H), 9.40 (d, *J* = 8.8 Hz, 2H), 8.17 (d, *J* = 8.4 Hz, 2H), 8.12 (d, *J* = 8.4 Hz, 2H), 8.08 (d, *J* = 8.8 Hz, 2H), 8.05 (d, *J* = 8.0 Hz, 2H), 7.79 (d, *J* = 8.4 Hz, 2H), 7.72 (br dd, *J* = 6.8, 6.8 Hz, 2H), 7.70 (br dd, *J* = 7.2, 7.2 Hz, 1H), 7.56 (dd, *J* = 7.6 Hz, 2H), 4.50-4.39 (br m, 2H), 4.18-4.04 (br m, 2H), 2.35 (br dd, *J* = 12.0, 12.0 Hz, 4H), 1.98-1.48 (series of br m, 12H); ^{13}C NMR (100 MHz, $CDCl_3$) ppm 165.0, 164.0, 149.6, 148.5, 146.4, 138.2, 137.2, 130.0, 129.9, 129.1, 127.8, 127.5, 123.9, 118.5, 55.1, 52.9, 32.5, 32.2, 24.94, 24.91; HRMS (ESI): Exact mass calcd for $C_{39}H_{39}NaN_7O_4$ $[M+Na]^+$ 692.2961, found 692.2966.

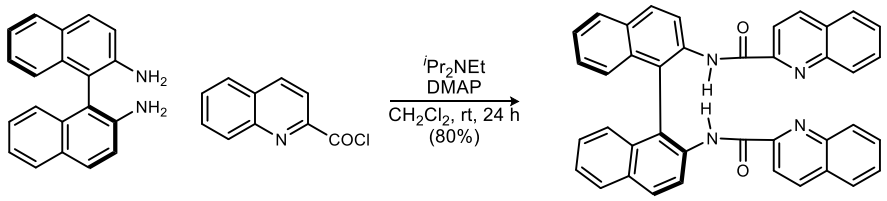

BINAMBAMide. A flask was charged with the (*S*,*S*)-diamine (94 mg, 330 µmol), acid chloride (159 mg, 828 µmol), Hünig's base (137 µL, 828 µmol), and CH_2Cl_2 (3 mL). DMAP (4.0 mg, 33 µmol) was added, and the resulting solution was stirred at ambient temperature overnight. The reaction was quenched with 1 M HCl, washed with water and satd aq $NaHCO_3$, and then dried and concentrated to an orange solid. Flash column chromatography (SiO_2, 10-30% ethyl acetate in hexanes) afforded the title compound as a colorless solid (158 mg, 80%). Mp = 124.0-127.0 °C; $[\alpha]_D^{20}$ +47 (0.40, $CHCl_3$); R_f = 0.52 (50% EtOAc/Hexanes); IR (film) 3281, 1637, 1547, 788 cm^{-1}; ^1H NMR (400 MHz, $CDCl_3$) δ 10.55 (s, 1H), 9.36 (d, *J* = 8.8 Hz, 1H), 8.41 (d, *J* = 8.8 Hz, 1H), 8.15 (d, *J* = 8.4 Hz, 2H), 8.12 (dd, *J* = 8.4, 6.4 Hz, 1H), 7.71-7.61 (br m, 2H), 7.50 (d, *J* = 7.6 Hz, 1H), 7.49 (d, *J* = 7.2 Hz, 1H), 7.45 (d, *J* = 8.4 Hz, 1H), 7.36 (d, *J* = 7.2 Hz, 1H), 7.31 (dd, *J* = 8.8, 8.8 Hz, 1H); ^{13}C NMR (100 MHz, $CDCl_3$) ppm 162.0, 148.9, 145.7, 137.3, 135.6, 132.9, 131.2, 103.1, 129.9, 129.6, 128.9, 128.2, 127.9,

127.3, 127.2, 125.3, 125.2, 119.4, 119.1, 117.9; HRMS (ESI): Exact mass calcd for $C_{40}H_{27}N_4O_2$ $[M+H]^+$ 595.2134, found 595.2130.

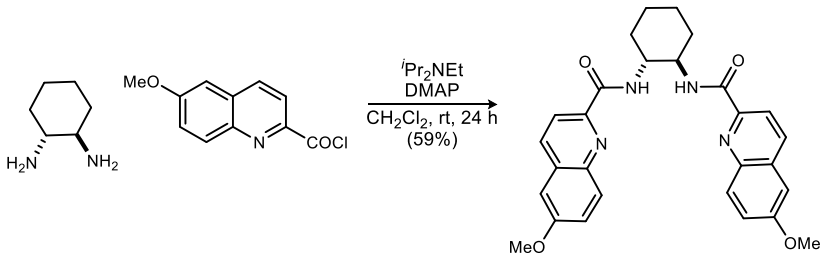

^{6}MeO-QuinBAMide. A flask was charged with the diamine (92.3 mg, 808 µmol), acid chloride (448 mg, 2.02 mmol), Hünig's base (500 µL, 2.02 mmol), and CH_2Cl_2 (8 mL). DMAP (25.0 mg, 202 µmol) was added, and the resulting solution was stirred at ambient temperature overnight. The reaction was quenched with 1 M HCl, washed with water and satd aq $NaHCO_3$, and then dried and concentrated to an orange solid. Flash column chromatography (SiO_2, 3-10% ethyl acetate in dichloromethane) afforded the title compound as a colorless solid (230 mg, 59%). Mp = 239-241 °C; $[\alpha]_D^{20}$ -630 (0.33, $CHCl_3$); R_f = 0.34 (40% EtOAc/hexanes); IR (film) 3317, 2933, 1665, 1494, 760 cm^{-1}; ^{1}H NMR (400 MHz, $CDCl_3$) δ 8.48-8.44 (br m, 1H), 8.10 (d, *J* = 8.4 Hz, 1H), 7.98 (d, *J* = 9.2 Hz, 2H), 7.34 (dd, *J* = 9.2, 2.8 Hz, 1H), 6.96 (d, *J* = 2.8 Hz, 1H), 4.18-4.15 (br m, 1H), 3.86 (s, 3H), 2.29 (br d, *J* = 10.8 Hz, 1H), 1.86 (br d, *J* = 6.8 Hz, 1H), 1.58-1.50 (br m, 2H); ^{13}C NMR (100 MHz, $CDCl_3$) ppm 165.0, 158.7, 147.3, 142.5, 135.5, 131.3, 130.4, 122.9, 119.1, 104.6, 55.5, 53.4, 32.7, 24.9; HRMS (ESI): Exact mass calcd for $C_{28}H_{29}N_4O_4$ $[M+H]^+$ 485.2189, found 485.2202.

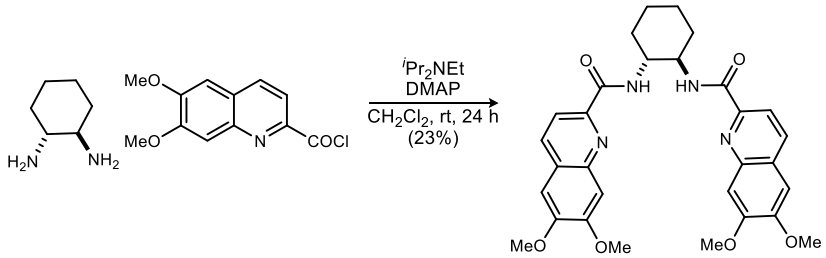

^{6,7}(MeO)$_2$-QuinBAMide. A flask was charged with the diamine (50.0 mg, 437 µmol), acid chloride (310 mg, 1.23 mmol), Hünig's base (245 µL, 1.48 mmol), and CH_2Cl_2 (4 mL). DMAP (6.0 mg, 49 µmol) was added, and the resulting solution was stirred at ambient temperature overnight. The reaction was quenched with 1 M HCl, washed with water and satd aq $NaHCO_3$, and then dried and concentrated to an orange solid. Flash column chromatography (SiO_2, 0.6-2% methanol in dichloromethane) afforded the title compound as a pale yellow solid (55 mg, 23%). Mp = >150 °C (dec.); $[\alpha]_D^{20}$ -350 (0.38, $CHCl_3$); R_f = 0.41 (100% EtOAc); IR (film) 3329, 2934, 1679, 1407, 712 cm^{-1}; ^{1}H NMR (400 MHz, $CDCl_3$) δ 8.02 (d, *J* = 8.4 Hz, 1H), 7.95 (d, *J* = 8.4 Hz, 1H), 7.40 (s, 1H), 6.97 (s, 1H), 4.22-4.10 (br m, 2H), 2.34-2.28 (br m, 2H), 1.90-1.80 (br m, 2H), 1.68-1.45 (br m, 4H); ^{13}C NMR (100 MHz, $CDCl_3$) ppm 165.1, 152.7, 150.8, 147.4, 143.5, 134.8, 125.2, 117.1, 108.1, 104.6, 56.2, 56.0, 53.1, 32.9, 24.9; HRMS (ESI): Exact mass calcd for $C_{30}H_{33}N_4O_6$ $[M+H]^+$ 545.2400, found 545.2405.

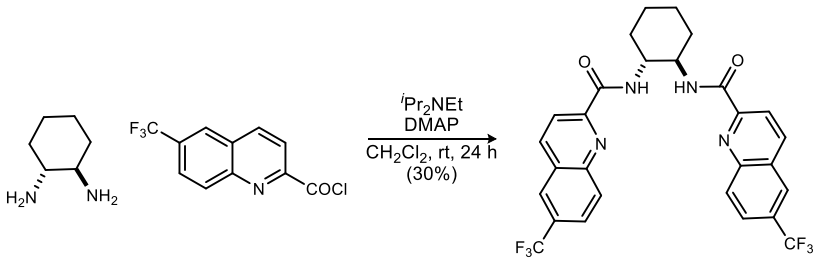

[6]CF3-QuinBAMide. A flask was charged with the diamine (22 mg, 194 µmol), acid chloride (126 mg, 485 µmol), Hünig's base (80 µL, 485 µmol), and CH_2Cl_2 (2.0 mL). DMAP (3 mg, 20 µmol) was added, and the resulting solution was stirred at ambient temperature for 24 h. The reaction was quenched with 1 M HCl, washed with water and satd aq $NaHCO_3$, and then dried and concentrated to a crude residue. Flash column chromatography (0.5-1.0% methanol in dichloromethane) afforded the pure product as a yellow solid (30.1 mg, 30% yield). Mp = 137.3-137.9 °C; $[\alpha]_D^{20}$ -280 (0.20, $CHCl_3$); R_f = 0.24 (25% EtOAc/Hexanes); IR (film) 3316, 2935, 1658, 1052, 775 cm^{-1}; ^1H NMR (400 MHz, $CDCl_3$) δ 8.50 (br d, *J* = 7.2 Hz, 1H), 8.26-8.20 (br m, 3H), 8.09 (app. br s, 1H), 7.88 (dd, *J* = 9.0, 1.6 Hz, 1H), 4.27-4.14 (br m, 1H), 2.32 (br d, *J* = 12.0 Hz, 1H), 1.92 (br d, *J* = 7.2 Hz, 1H), 1.63-1.48 (br series of m, 2H); ^{13}C NMR (100 MHz, $CDCl_3$) ppm 164.2, 151.5, 147.4, 138.1, 131.1, 129.5 (q, $^2J_{CF}$ = 33 Hz), 128.0, 125.6 (q, $^3J_{CF}$ = 3.0 Hz), 125.5 (q, $^3J_{CF}$ = 5.0 Hz), 123.7 (q, $^1J_{CF}$ = 271 Hz), 119.9, 53.7, 32.7, 24.9; HRMS (ESI): Exact mass calcd for $C_{28}H_{22}F_6NaN_4O_2$ $[M+Na]^+$ 583.1545, found 583.1541.

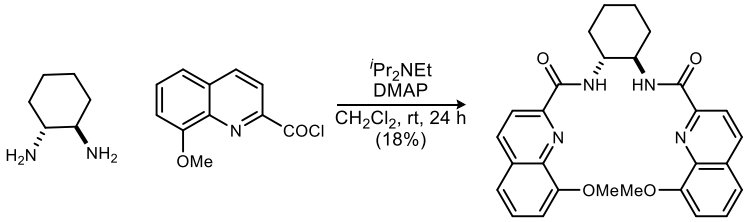

[8]MeO-QuinBAMide. A flask was charged with the diamine (86 mg, 750 µmol), acid chloride (417 mg, 1.88 mmol), Hünig's base (312 µL, 1.88 mmol), and CH_2Cl_2 (6.0 mL). DMAP (10 mg, 75 µmol) was added, and the resulting solution was stirred at ambient temperature for 24 h. The reaction was quenched with 1 M HCl, washed with water and satd aq $NaHCO_3$, and then dried and concentrated to a crude residue. Flash column chromatography (50-80-100% ethyl acetate in hexanes) afforded the pure product as a fluffy, colorless solid (65 mg, 18% yield). Mp = 94.0-96.0 °C; $[\alpha]_D^{20}$ -380 (0.72, $CHCl_3$); R_f = 0.73 (100% EtOAc); IR (film) 3317, 2933, 1665, 1494, 760 cm^{-1}; ^1H NMR (400 MHz, $CDCl_3$) δ 8.81 (br d, *J* = 7.6 Hz, 1H), 8.04 (dd, *J* = 8.4, 1.2 Hz, 1H), 7.97 (dd, *J* = 8.4, 2.0 Hz, 1H), 7.34 (ddd, *J* = 8.0, 8.0, 2.0 Hz, 1H), 7.20 (d, *J* = 9.6 Hz, 1H), 6.93 (d, *J* = 8.0 Hz, 1H), 4.21-4.17 (br m, 1H), 4.09 (s, 3H), 2.13 (br d, *J* = 12.8 Hz, 1H), 1.78 (br d, *J* = 8.4 Hz, 1H), 1.65-1.50 (br m, 1H), 1.48-1.33 (br m, 1H); ^{13}C NMR (100 MHz, $CDCl_3$) ppm 164.7, 155.3, 148.5, 138.3, 136.9, 130.2, 128.0, 119.5, 119.3, 108.2, 55.9, 53.0, 32.8, 24.9; HRMS (ESI): Exact mass calcd for $C_{28}H_{28}NaN_4O_4$ $[M+Na]^+$ 507.2008, found 507.2019.

Appendix C

SI-II

Page

Figure C 1. ^{1}H NMR (400 MHz, $CDCl_3$) of adduct **116**

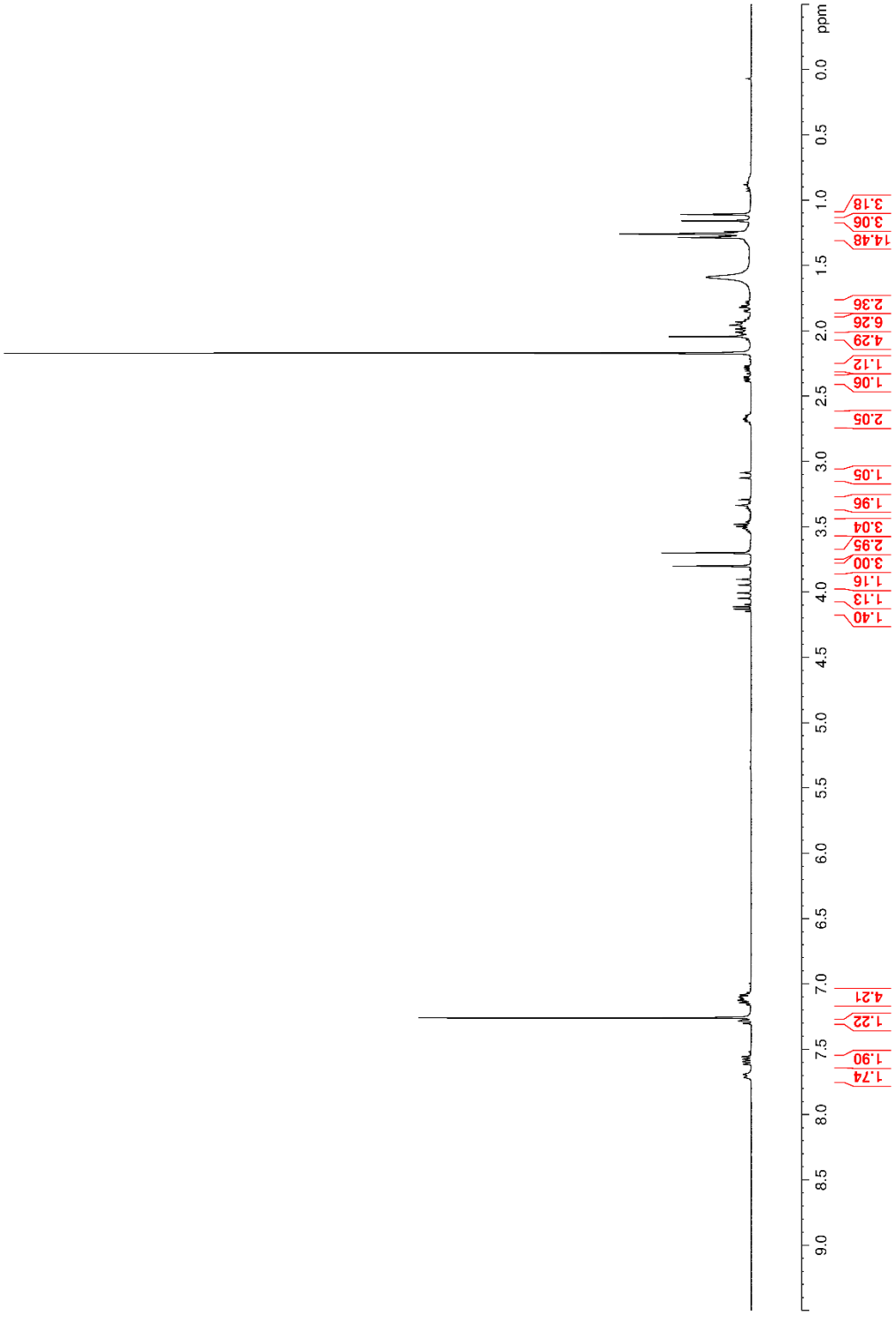

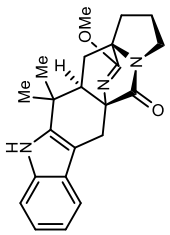

Figure C 2. ^{1}H NMR (400 MHz, $CDCl_3$) of H,$^{4}CF_3$-BAM (**117**)

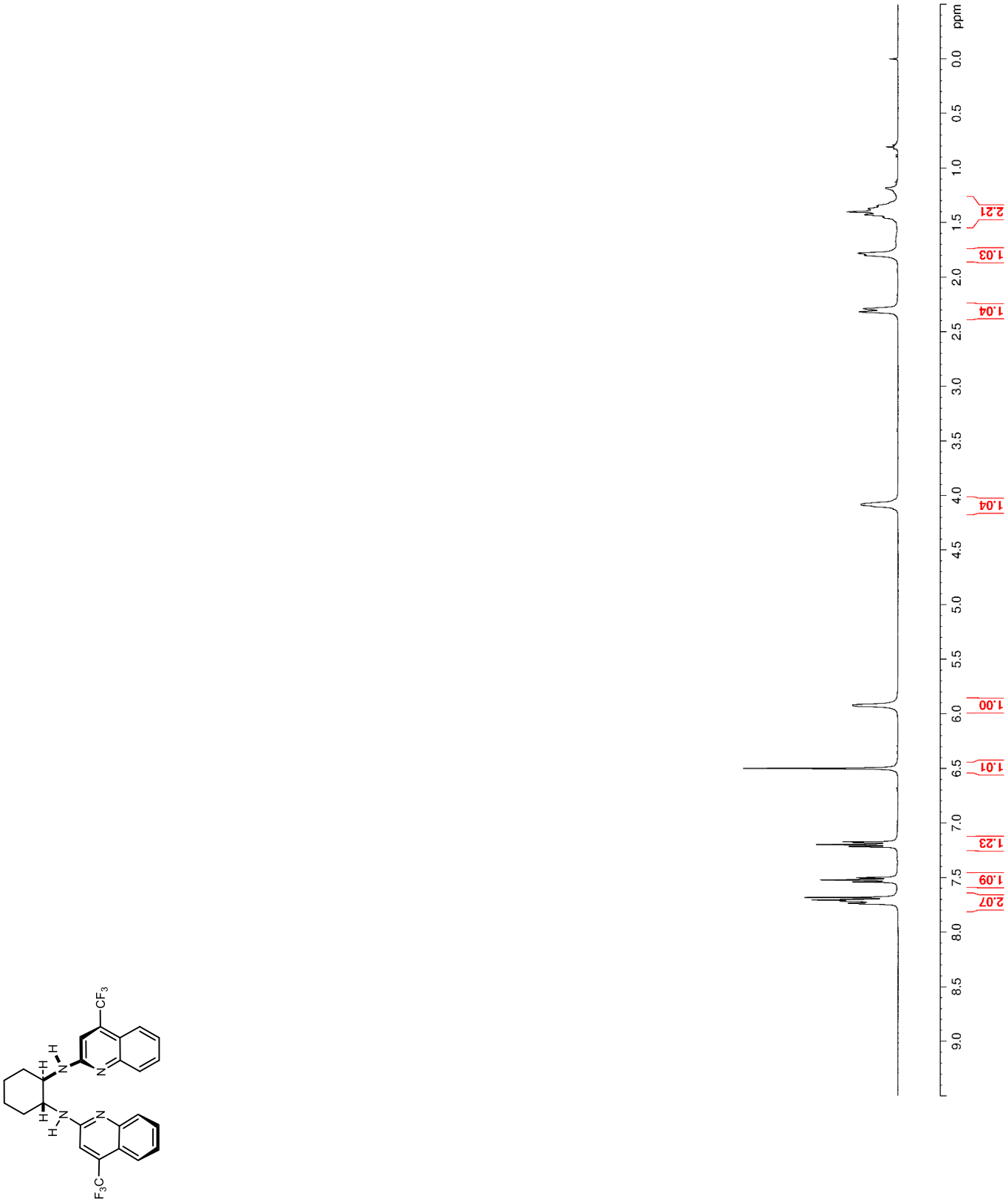

Figure C 3. ^{13}C NMR (100 MHz, $CDCl_3$) of H,$^4CF_3$-BAM (**117**)

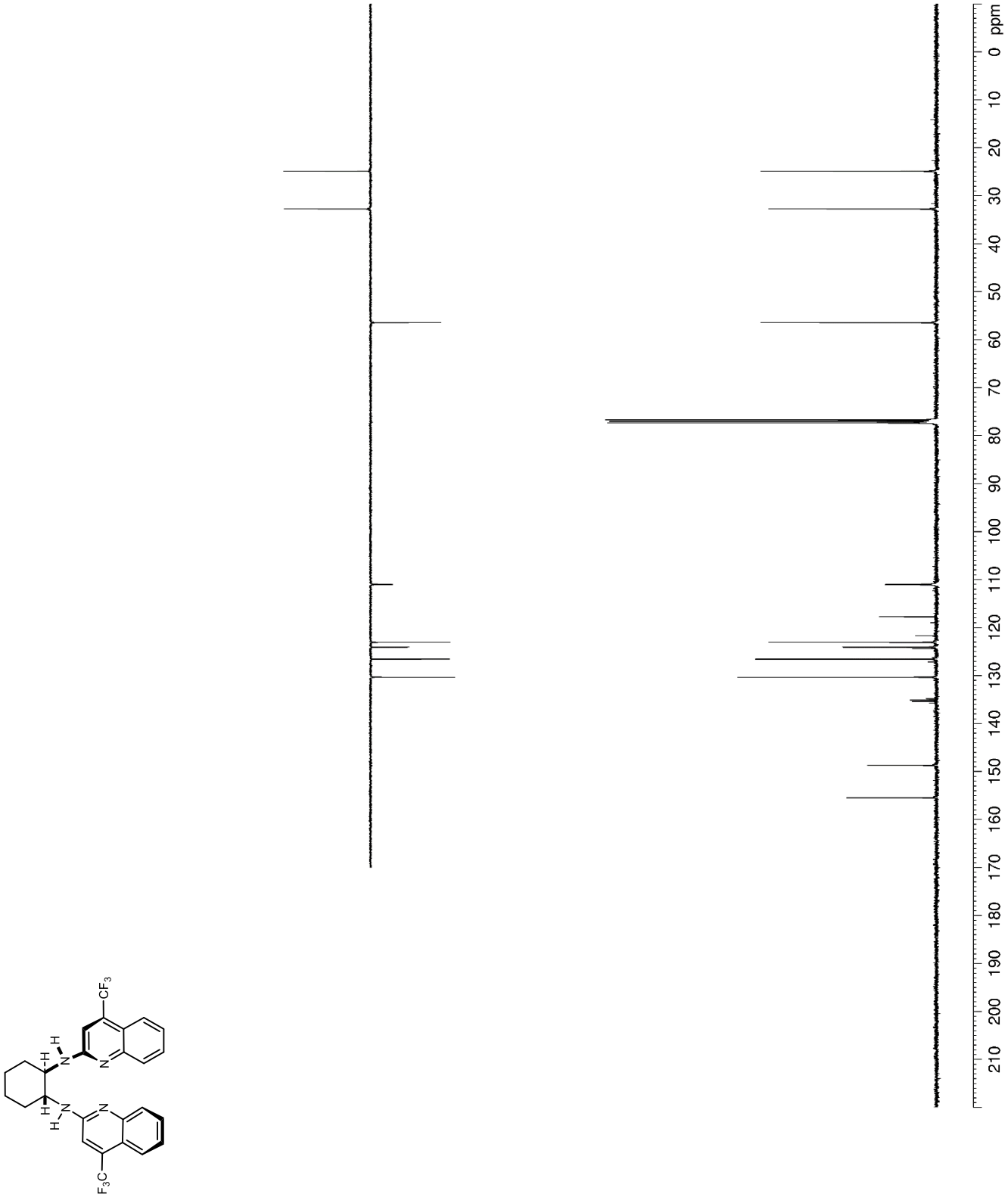

Figure C 4. ^{1}H NMR (400 MHz, $CDCl_3$) of H,^{5}Me-BAM (**119**)

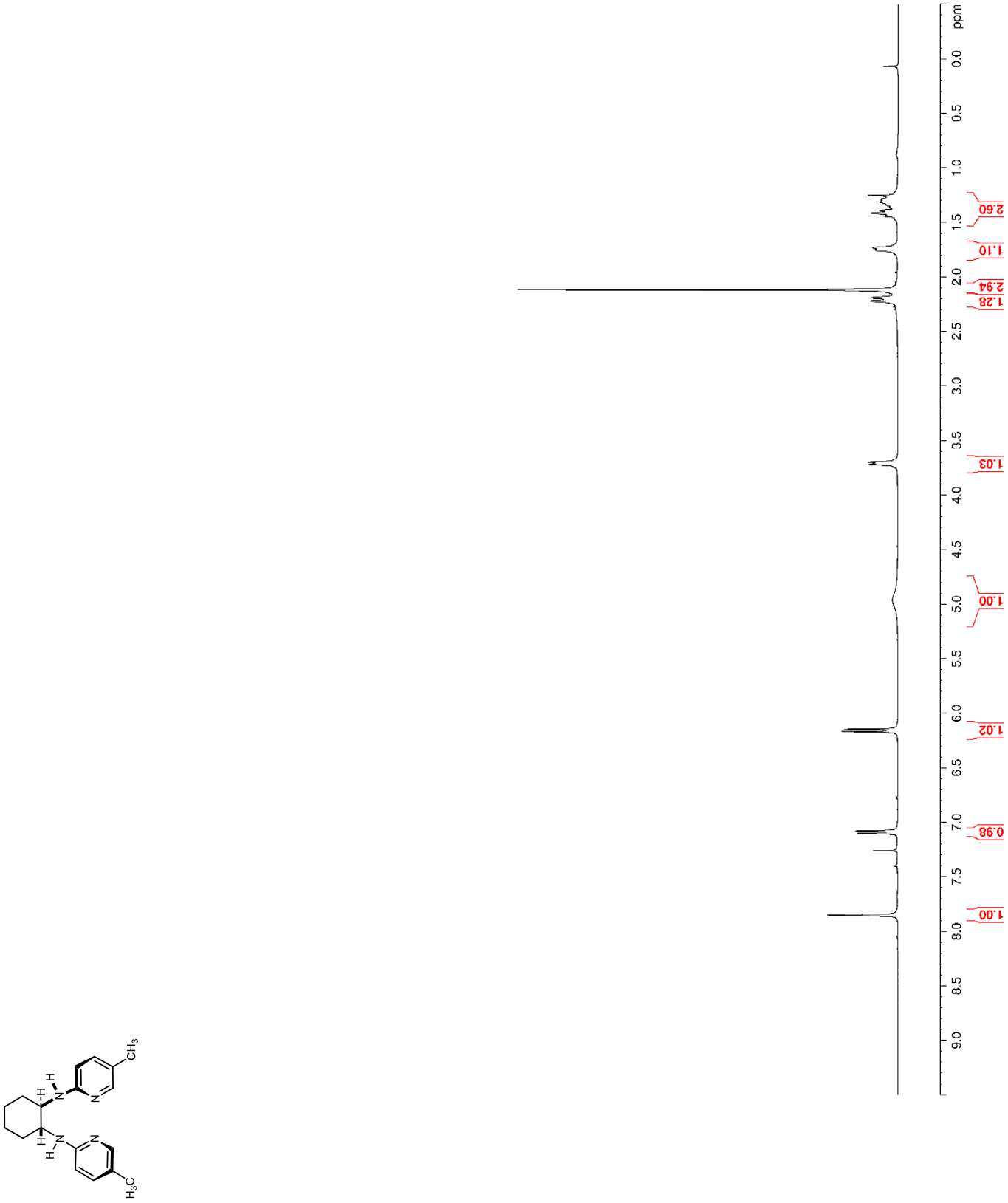

Figure C 5. ^{13}C NMR (100 MHz, $CDCl_3$) of H,^{5}Me-BAM (**119**)

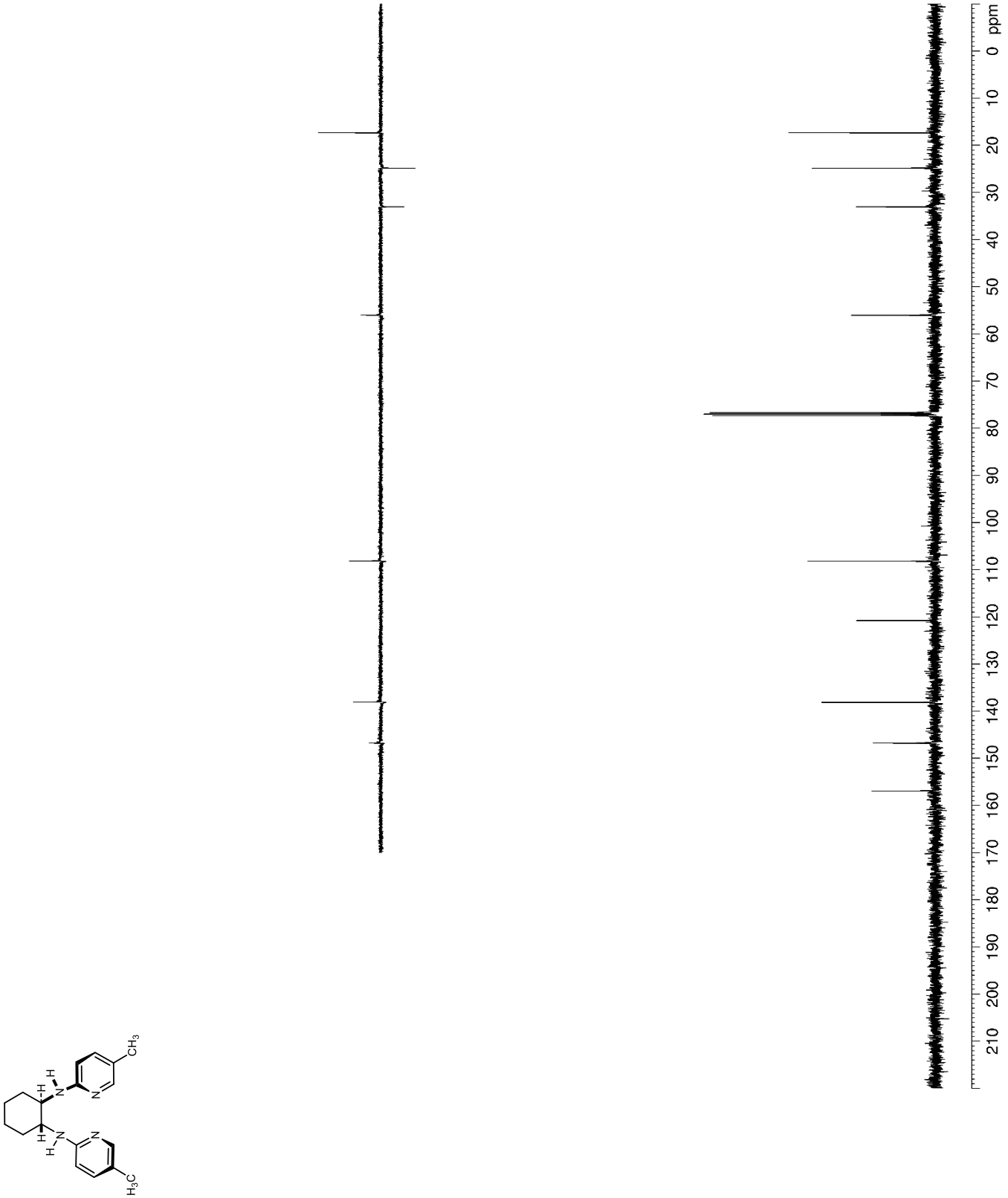

Figure C 6. ^{1}H NMR (400 MHz, $CDCl_3$) of H,^{3}Quin-BAM (**120**)

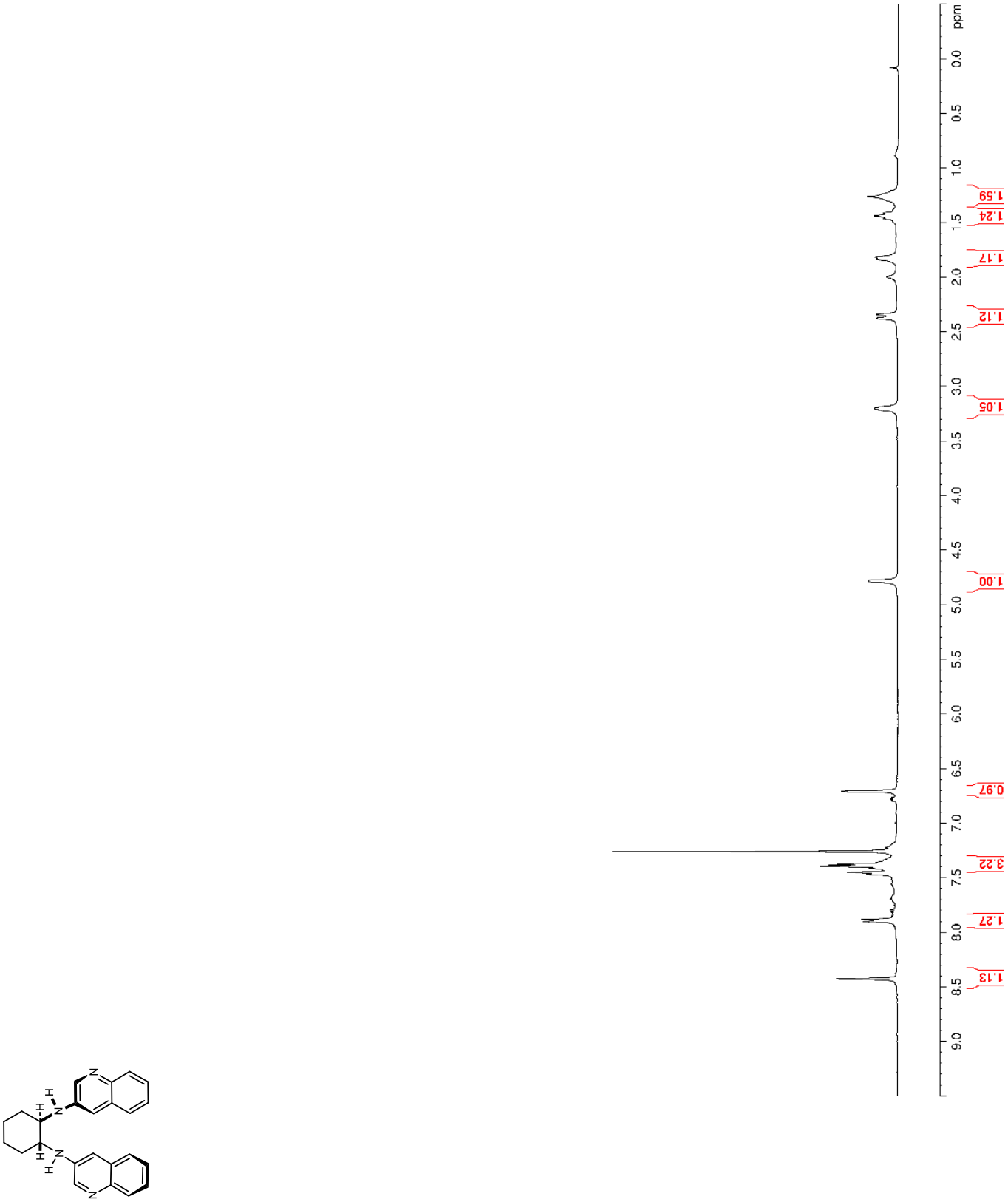

Figure C 7. ^{13}C NMR (100 MHz, $CDCl_3$) of H,^{3}Quin-BAM (**120**)

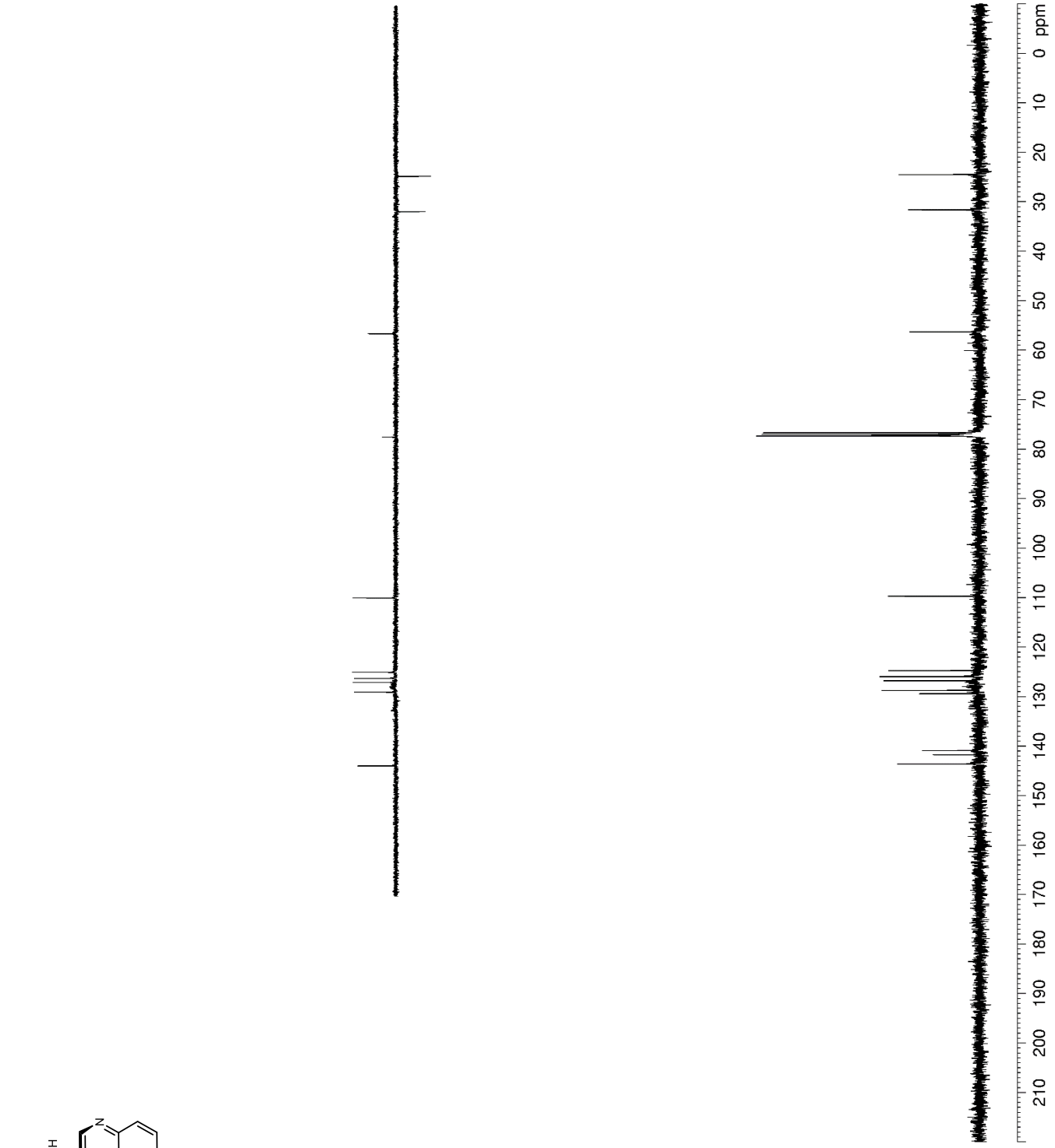

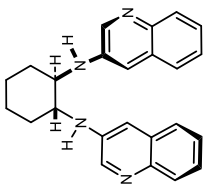

Figure C 8 ^{1}H NMR (500 MHz, $CDCl_3$) of H, Quinox-BAM (**121**)

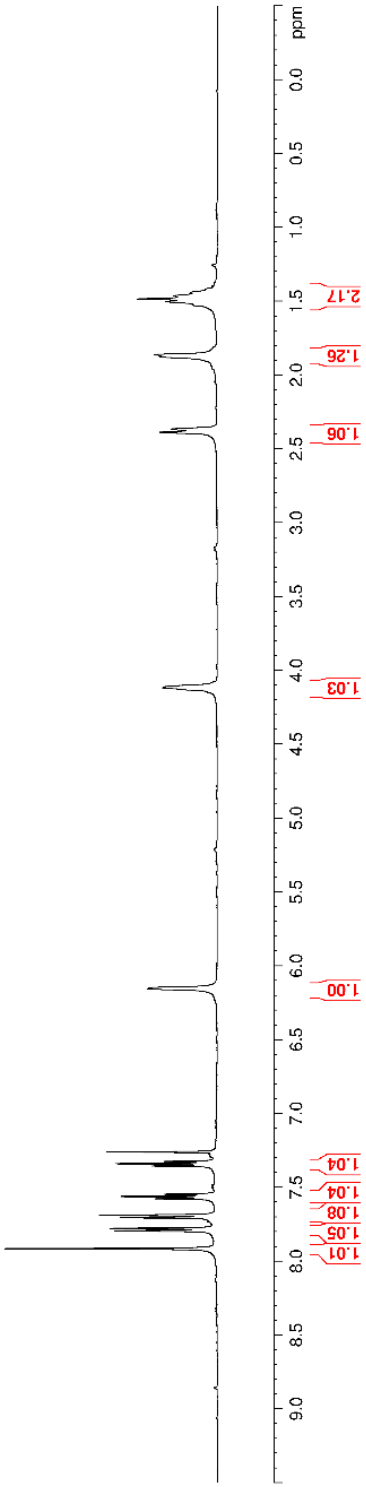

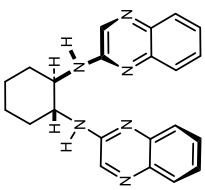

Figure C 9. ^{13}C NMR (125 MHz, $CDCl_3$) of H, Quinox-BAM (**121**)

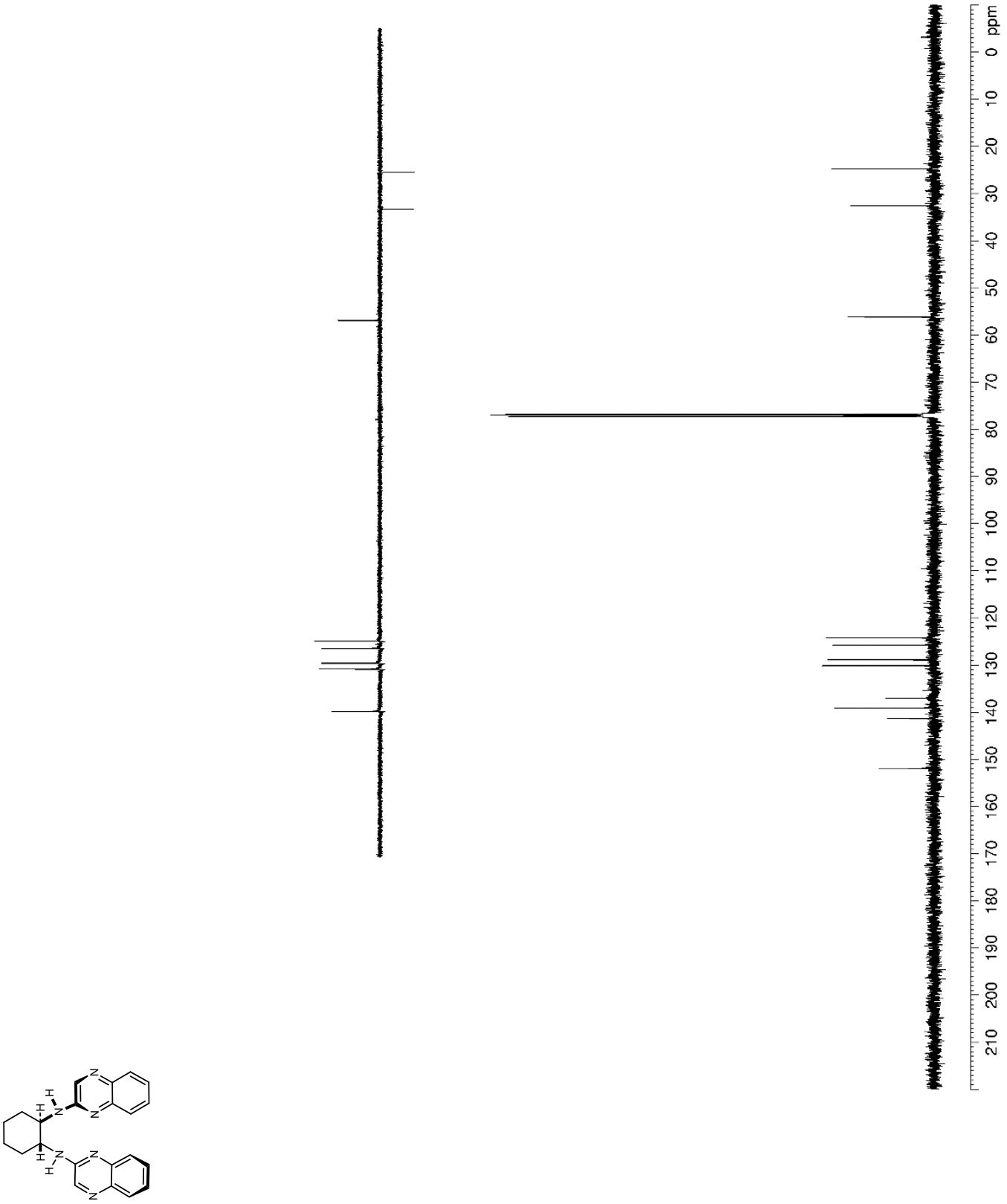

Figure C 10. ^{1}H NMR (600 MHz, $CDCl_3$) of (*S*,*S*)-^{4}MeOStilbBAM (**122**)

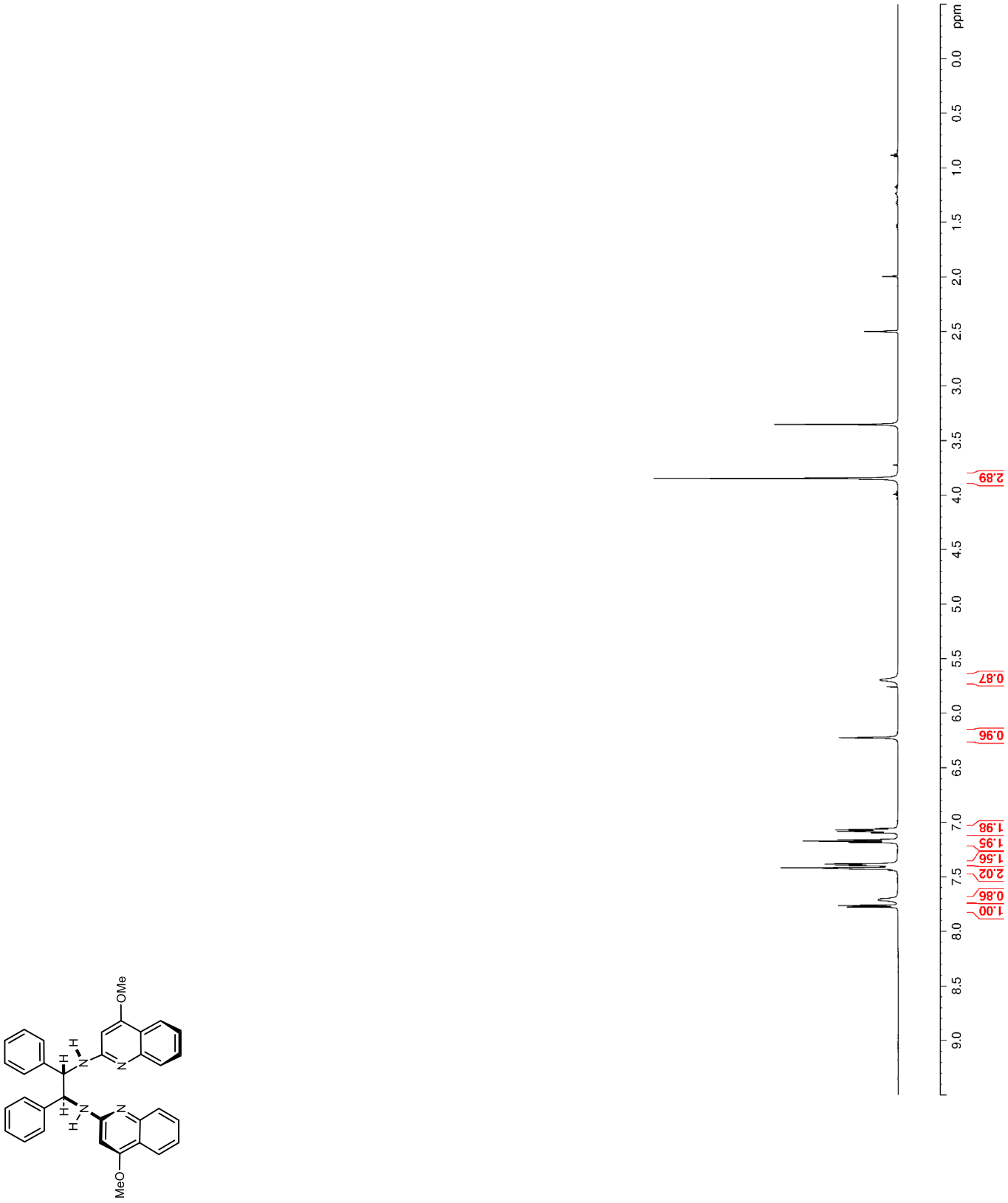

Figure C 11. ^{13}C NMR (150 MHz, $CDCl_3$) of (*S*,*S*)-^{4}MeOStilbBAM (**122**)

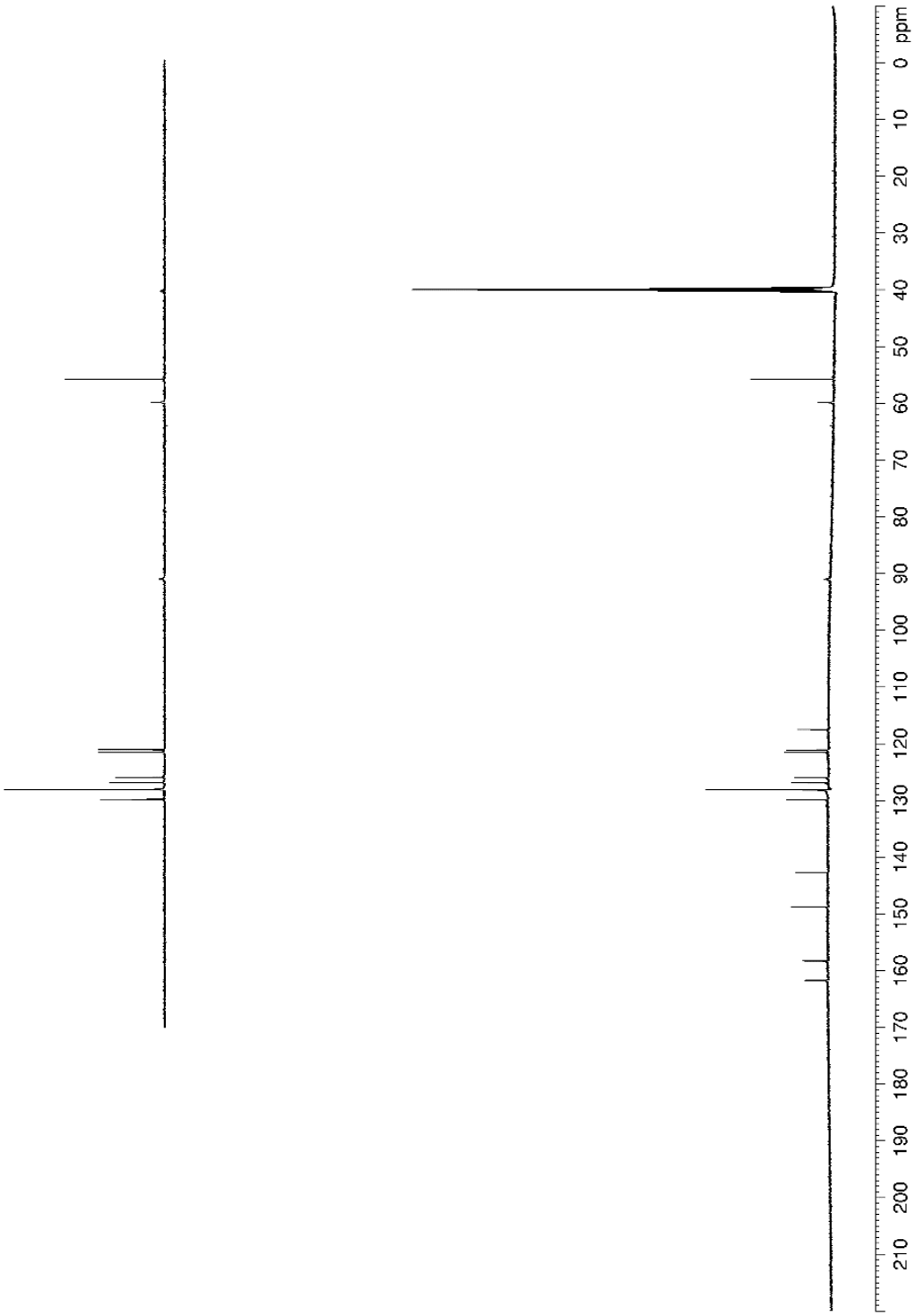

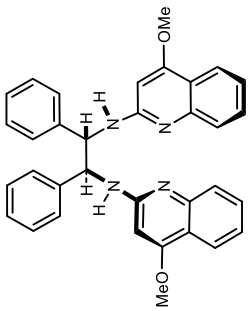

Figure C 12. ^{1}H NMR (400 MHz, $CDCl_3$) of H, Quin-BAMide (**123**)

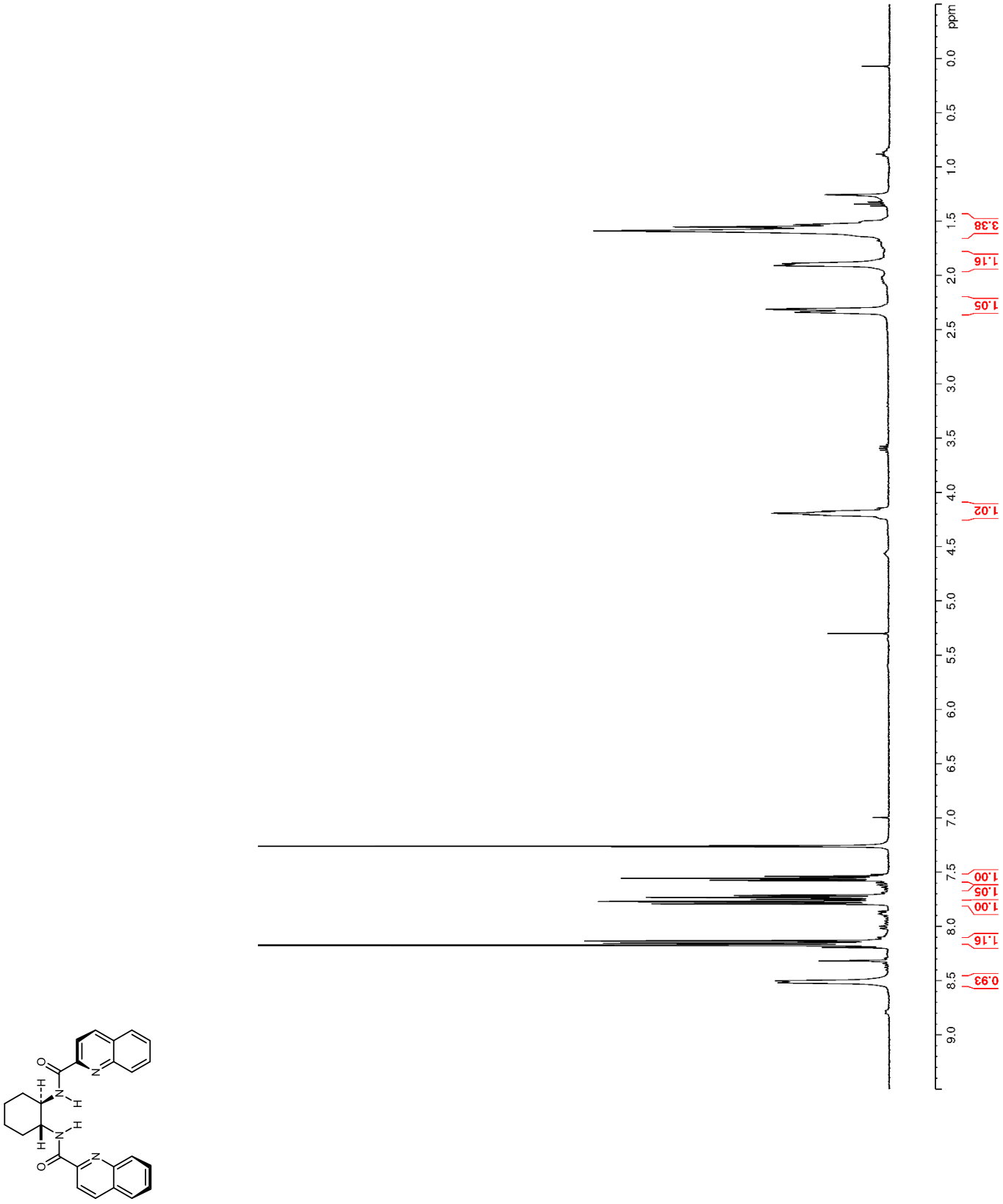

Figure C 13. ^{13}C NMR (100 MHz, $CDCl_3$) of H, Quin-BAMide (**123**)

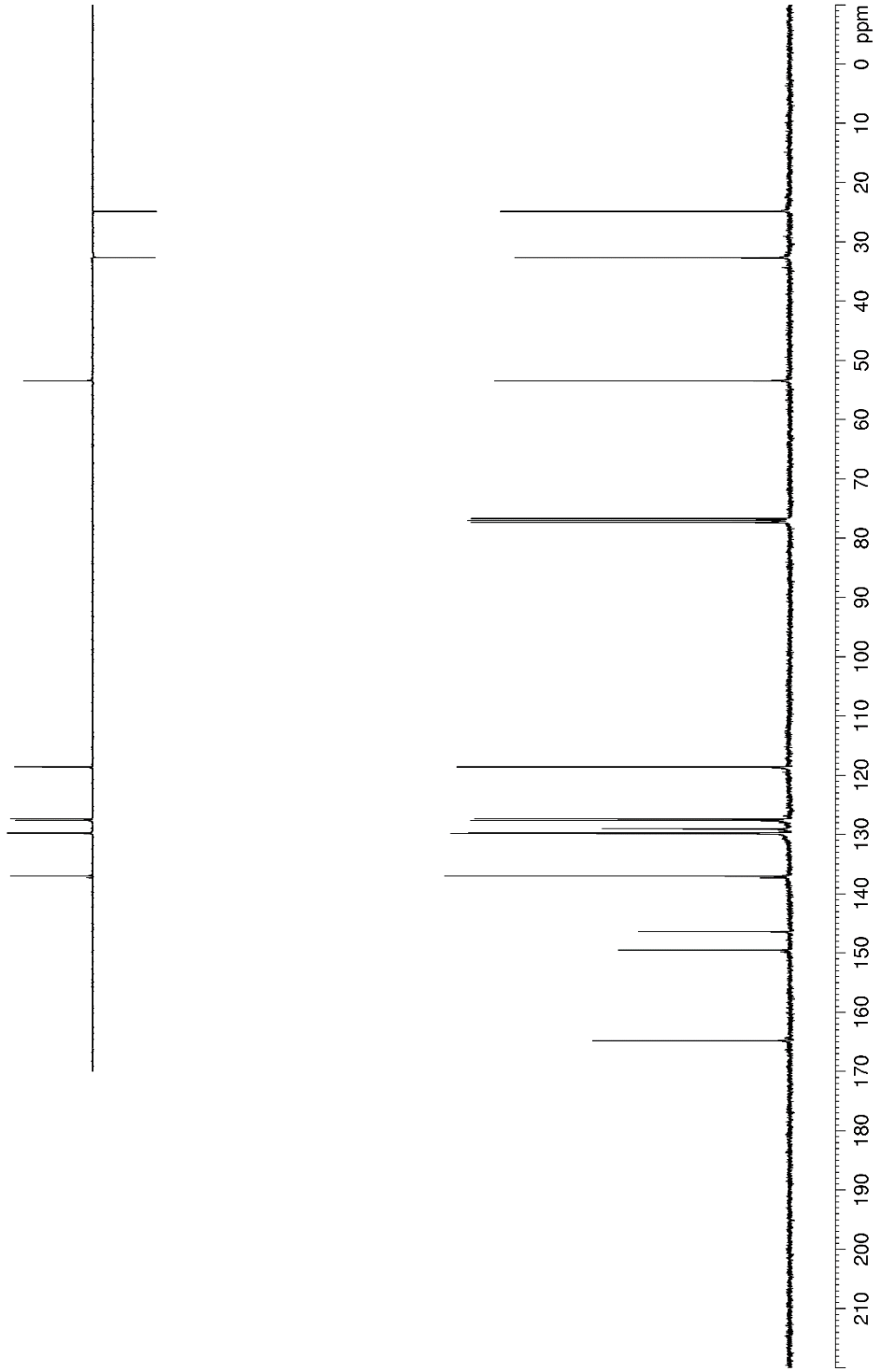

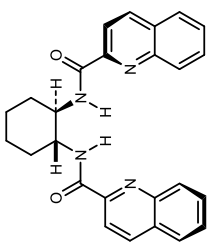

Figure C 14. ^{1}H NMR (400 MHz, $CDCl_3$) of **59h**

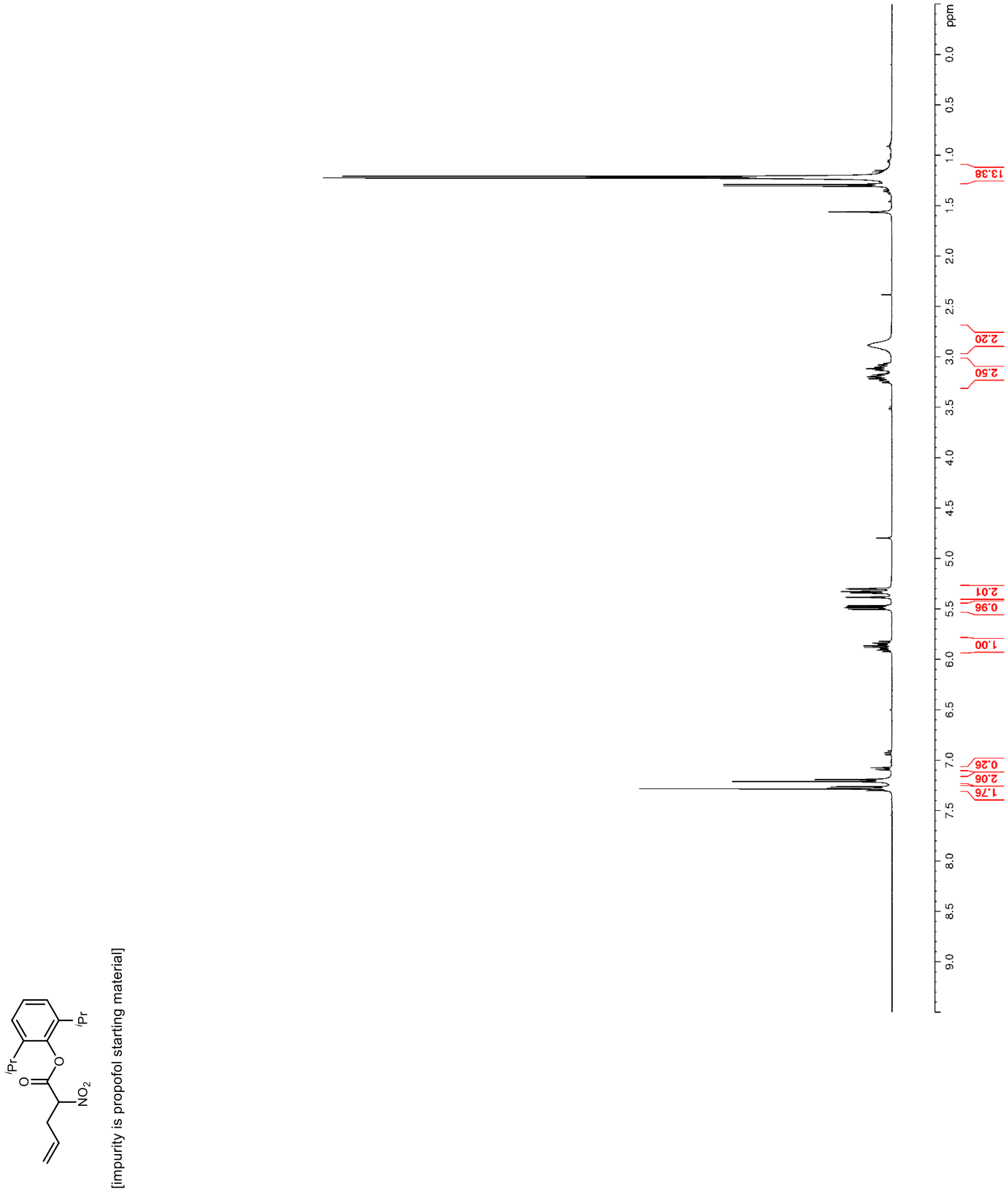

[impurity is propofol starting material]

Figure C 15. ^{13}C NMR (100 MHz, $CDCl_3$) of **59h**

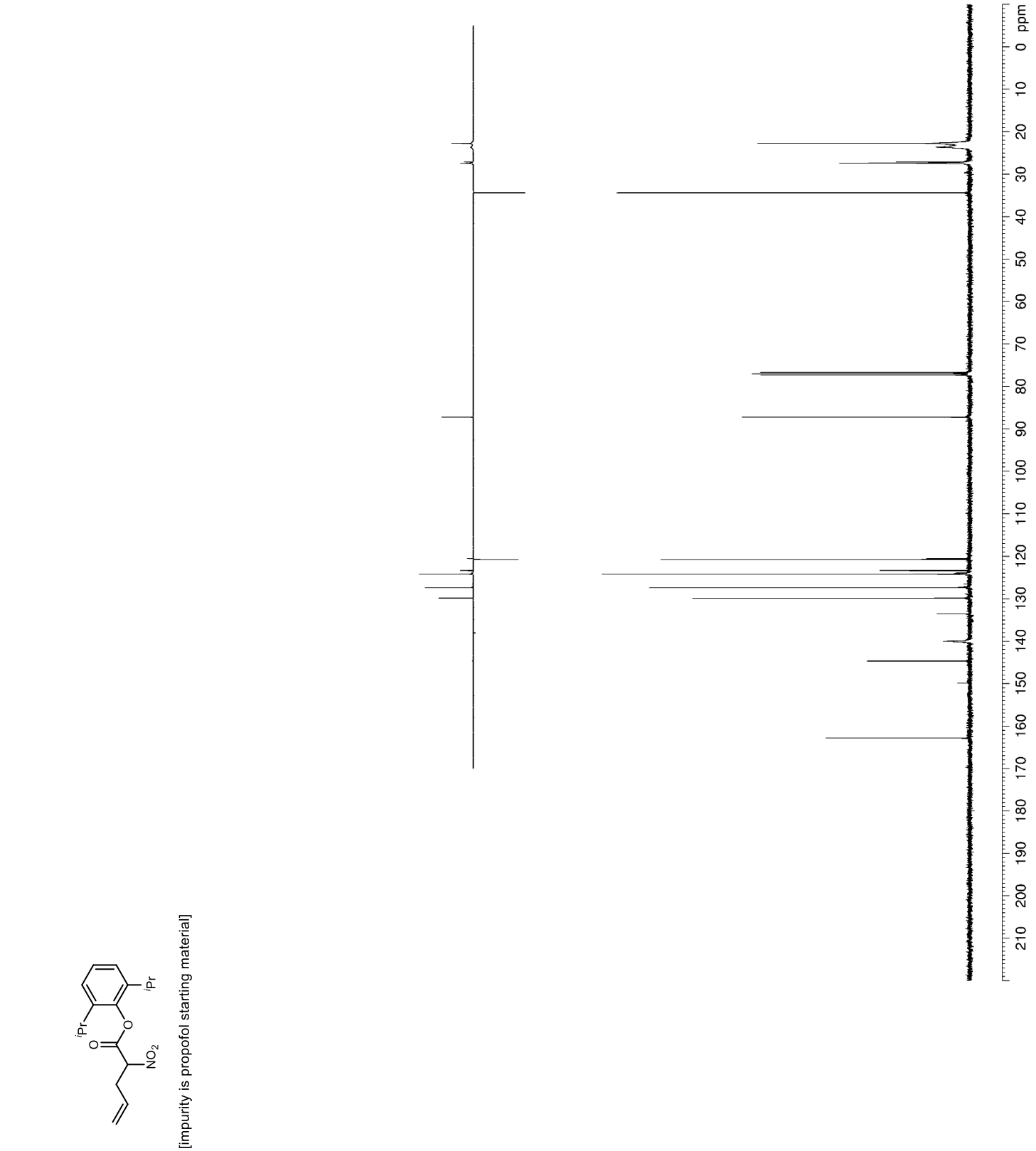

[impurity is propofol starting material]

Figure C 16. ^{1}H NMR (500 MHz, $CDCl_3$) of **59**i

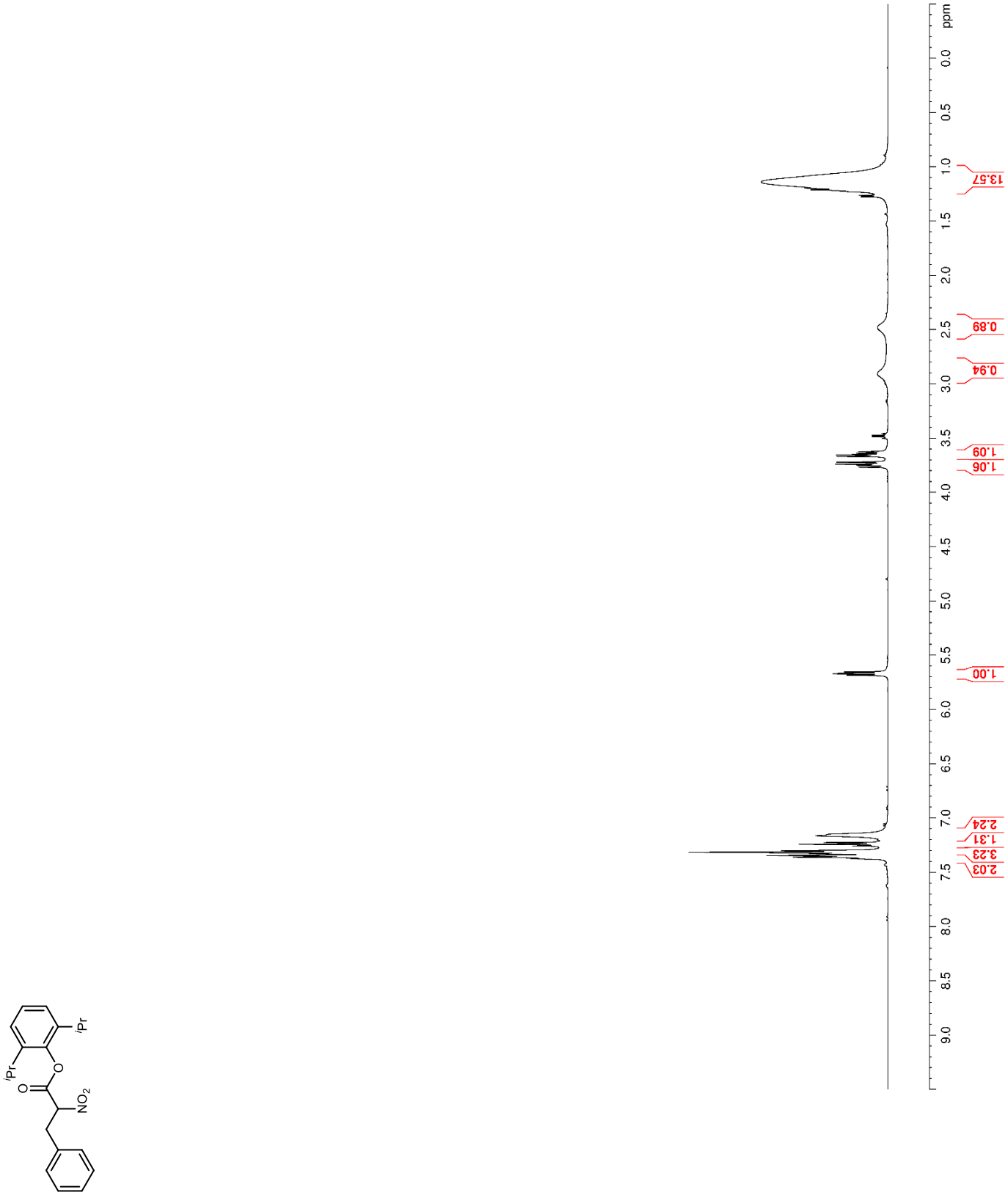

Figure C 17. ^{13}C NMR (125 MHz, $CDCl_3$) of **59i**

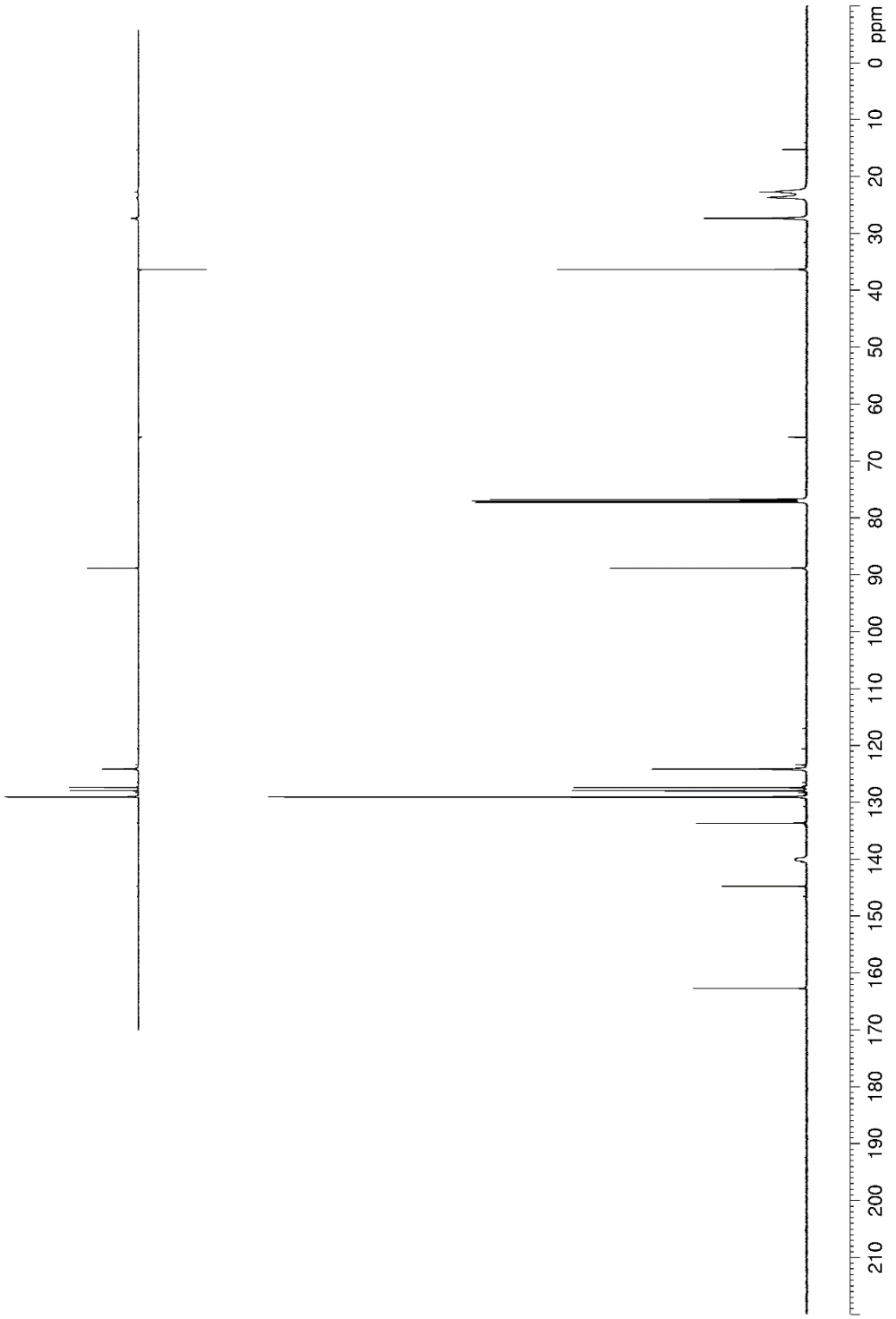

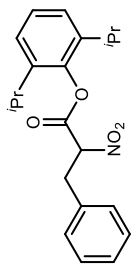

Figure C 18. ^{1}H NMR (500 MHz, $CDCl_3$) of **59j**

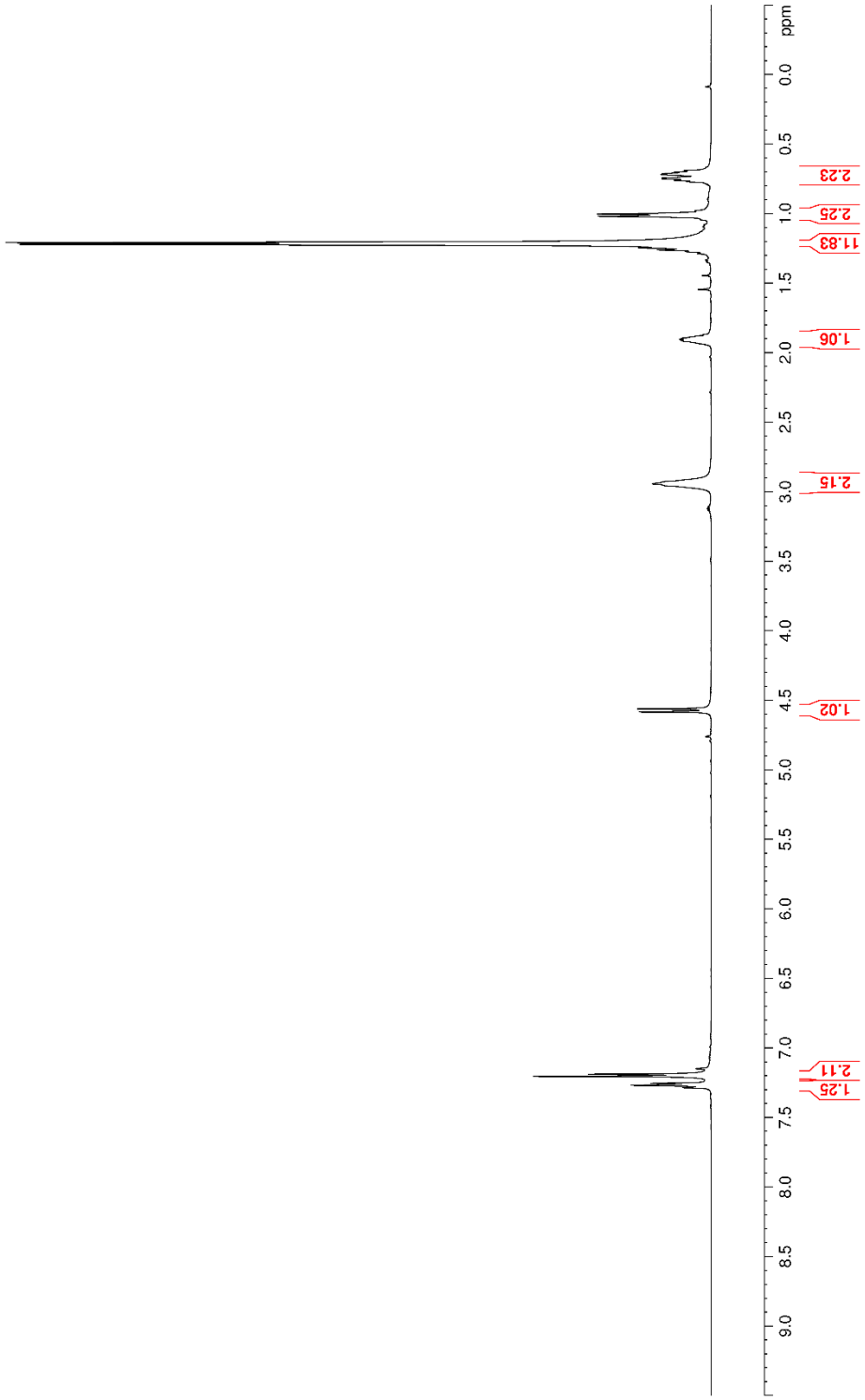

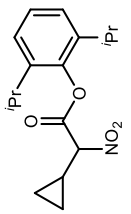

Figure C 19. ^{13}C NMR (125 MHz, $CDCl_3$) of **59j**

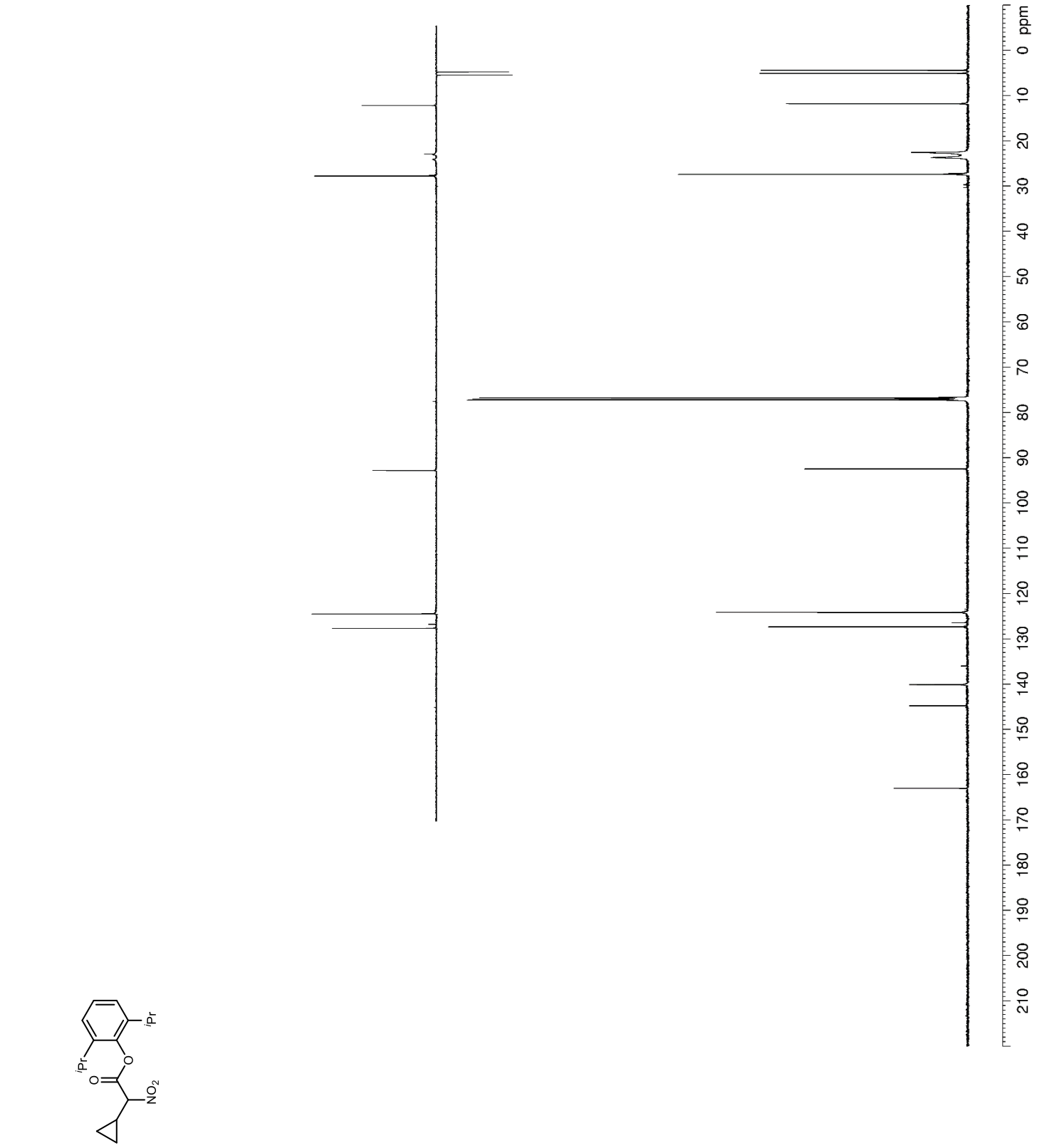

Figure C 20. ^{1}H NMR (400 MHz, $CDCl_3$) of **59l**

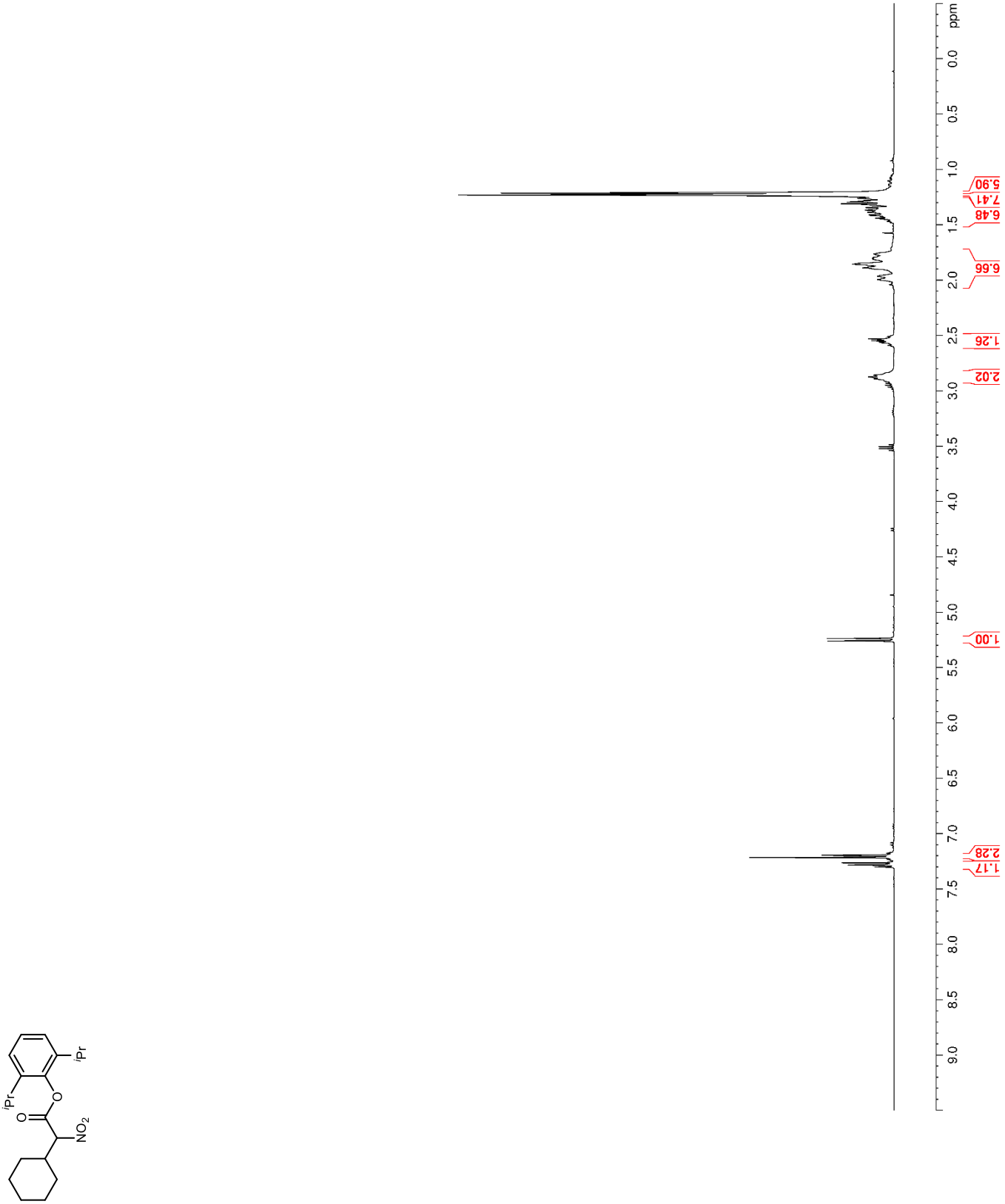

Figure C 21. ^{13}C NMR (100 MHz, $CDCl_3$) of **59l**

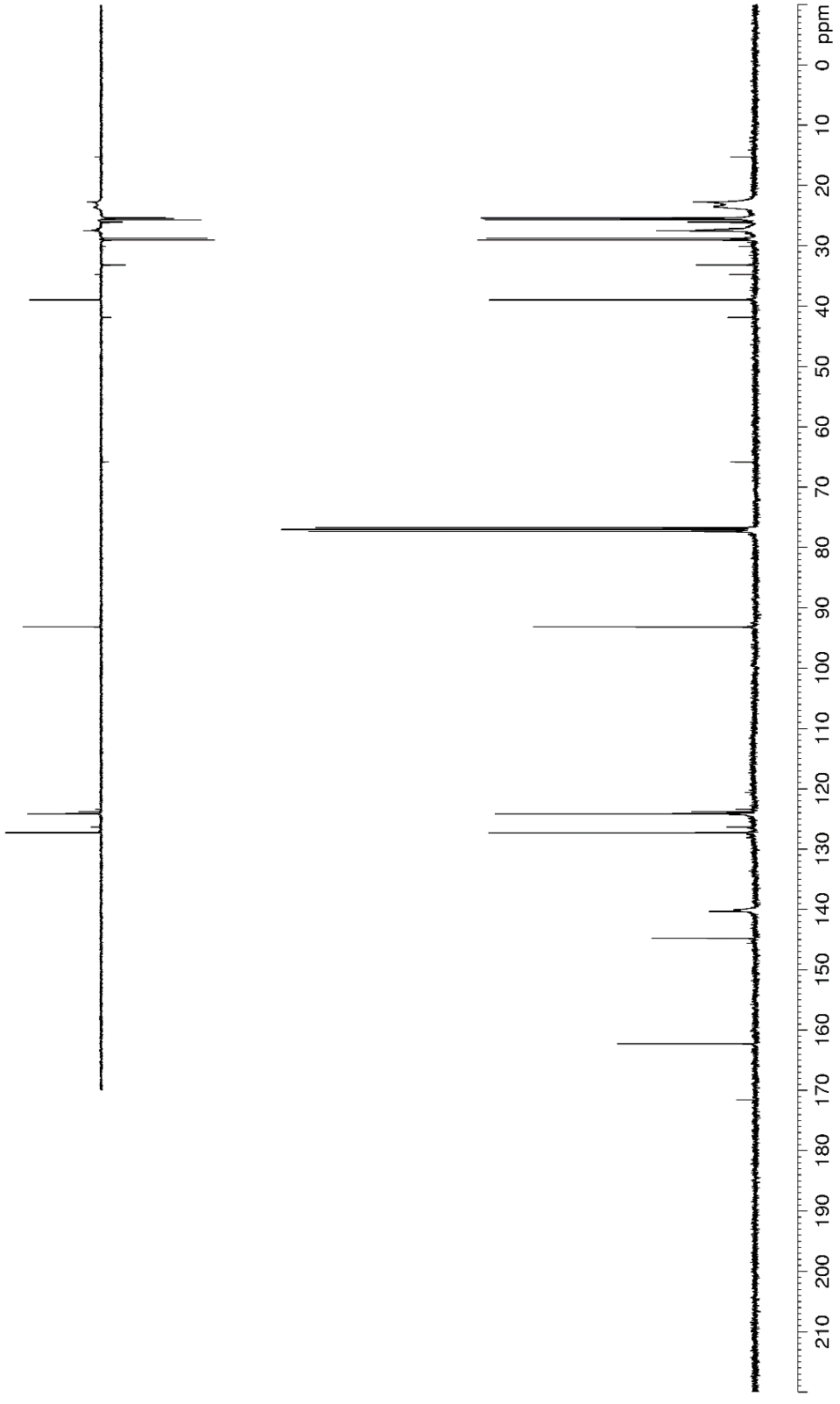

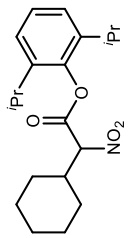

Figure C 22. ^{1}H NMR (400 MHz, $CDCl_3$) of **60a**

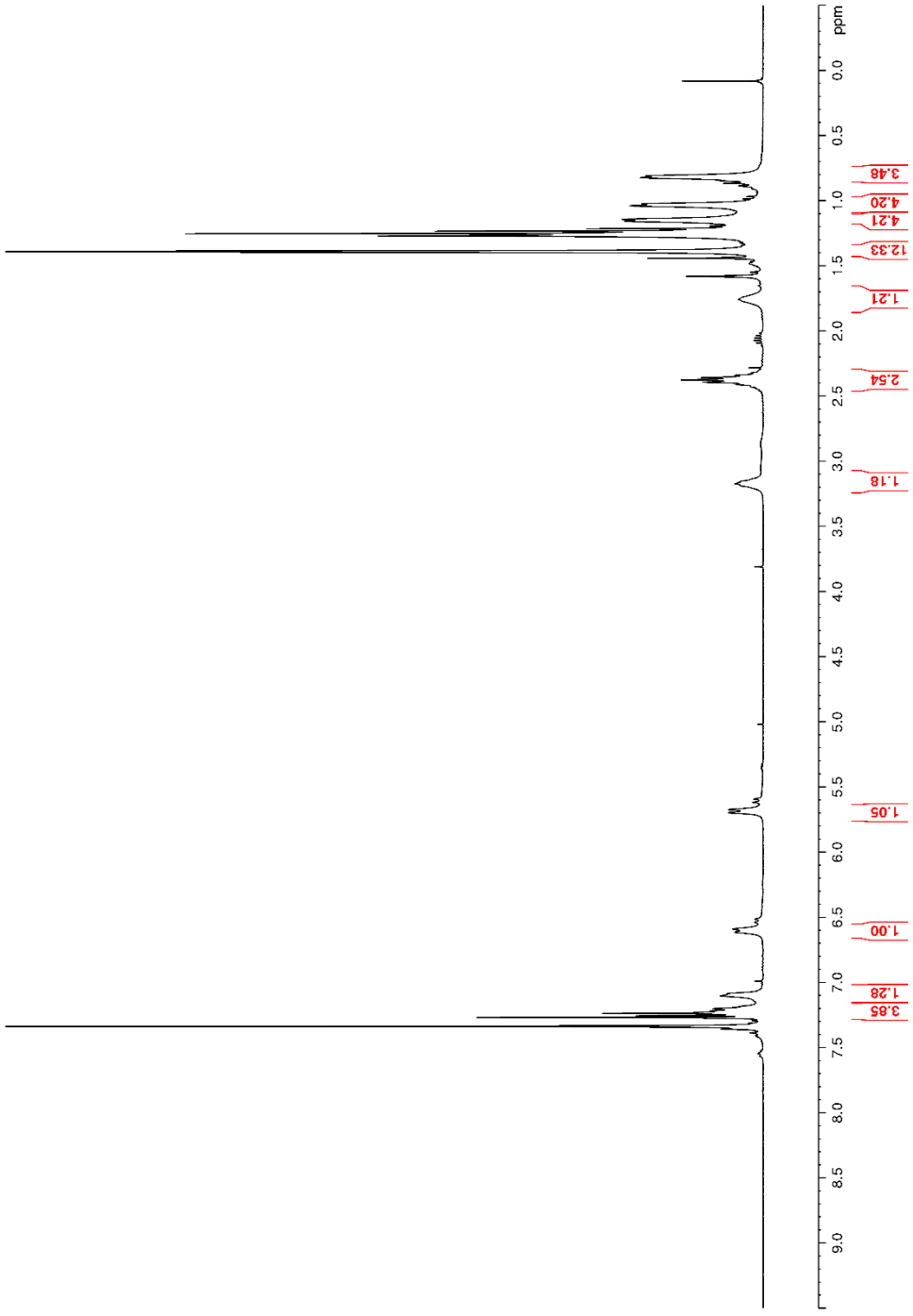

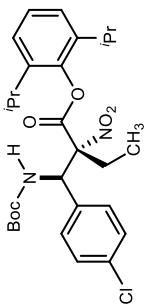

Figure C 23. ^{13}C NMR (100 MHz, $CDCl_3$) of **60a**

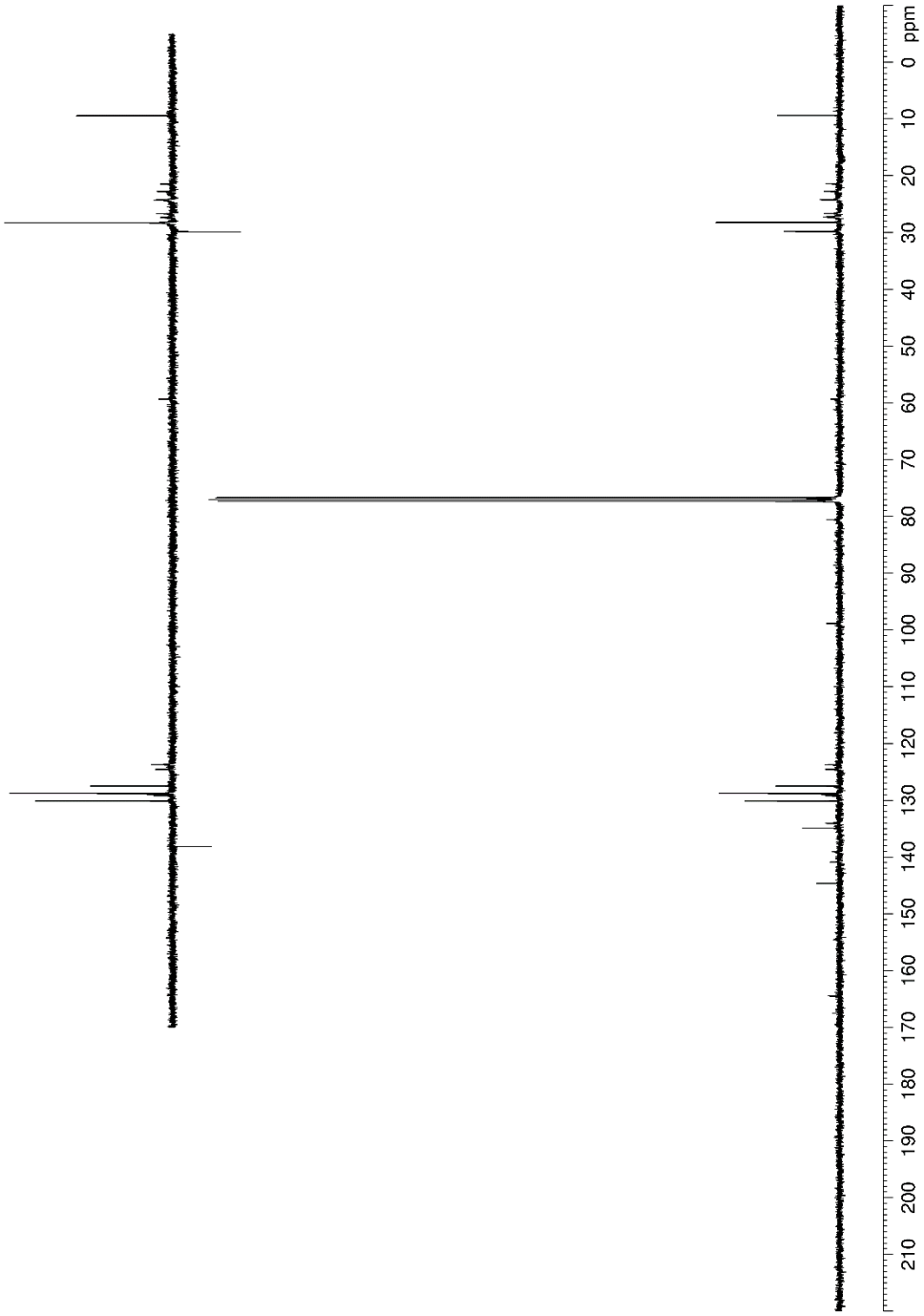

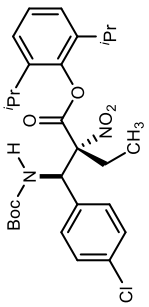

Figure C 24. ^{1}H NMR (400 MHz, $CDCl_3$) of **60b**

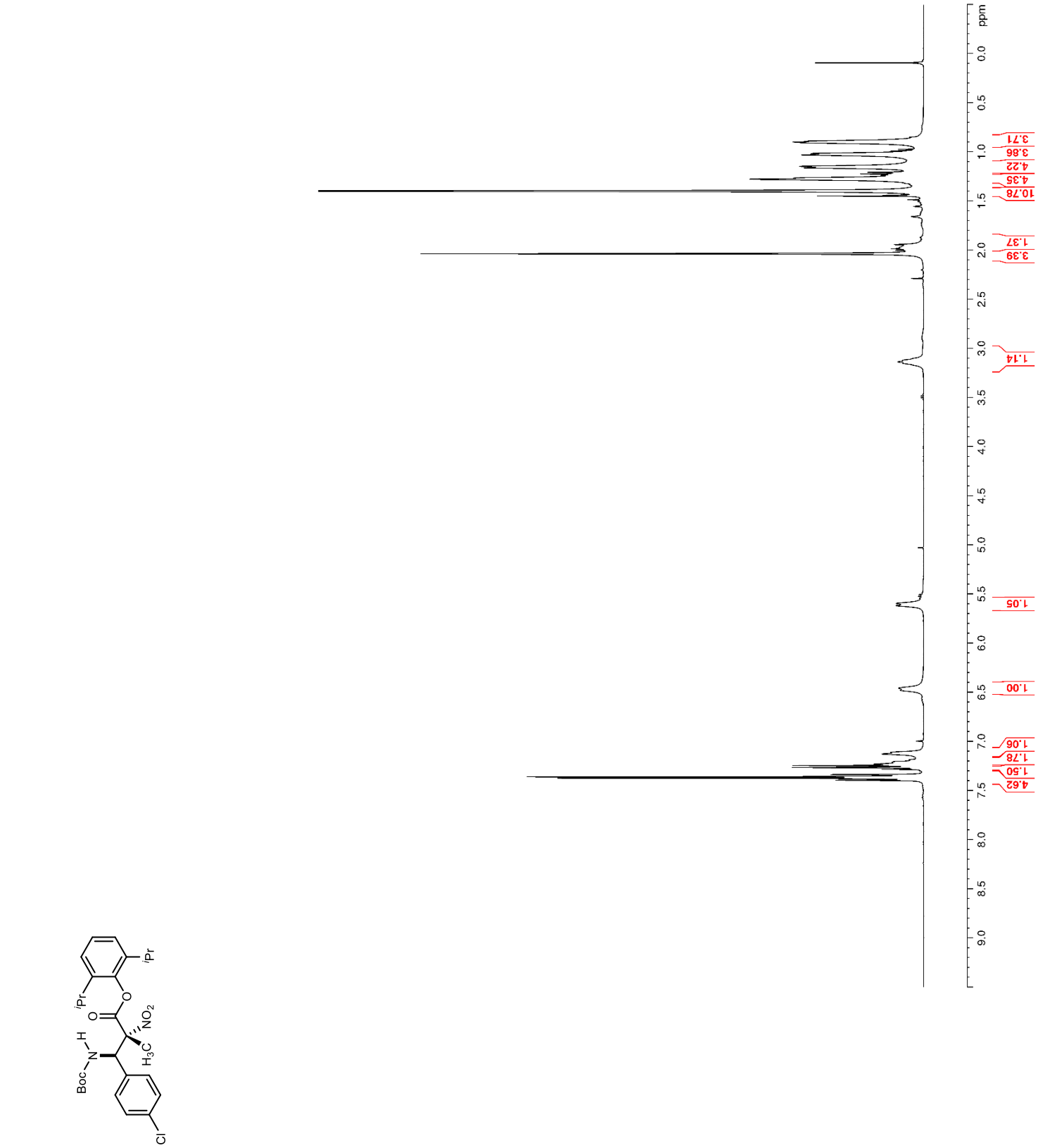

Figure C 25. ^{13}C NMR (100 MHz, $CDCl_3$) of **60b**

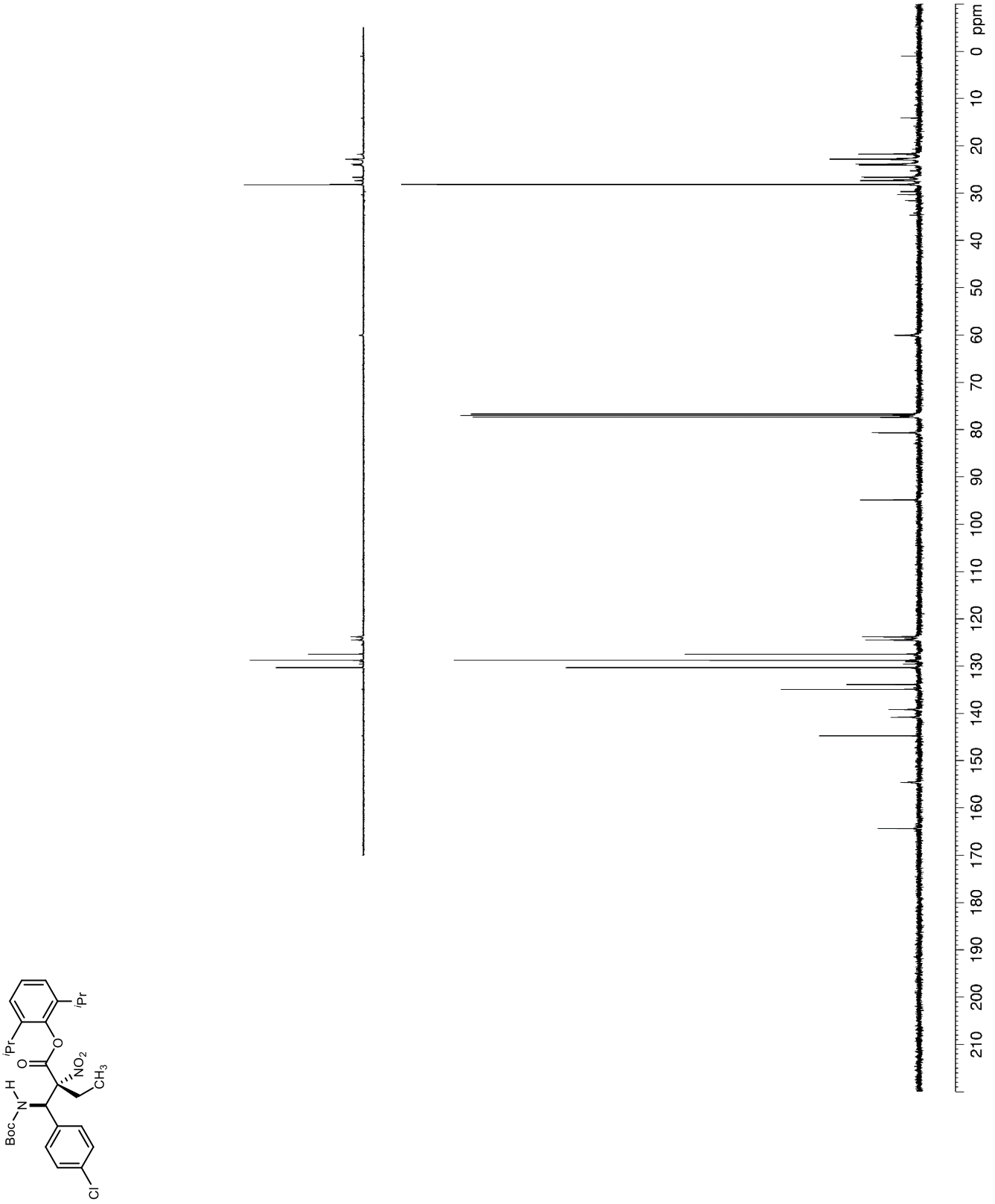

Figure C 26. ^{1}H NMR (400 MHz, $CDCl_3$) of **60c**

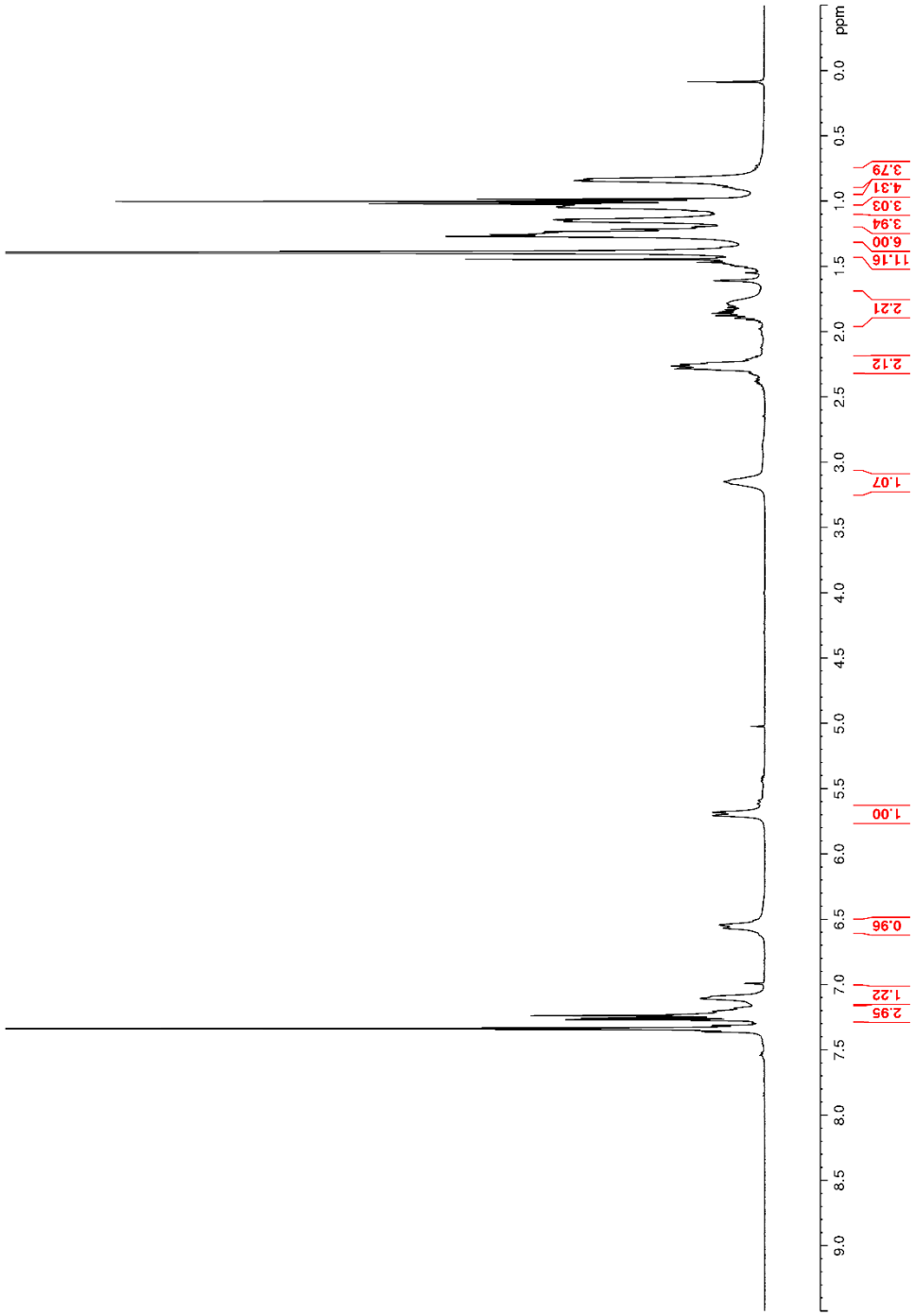

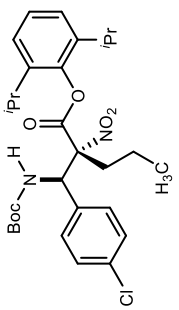

Figure C 27. ^{13}C NMR (100 MHz, $CDCl_3$) of **60c**

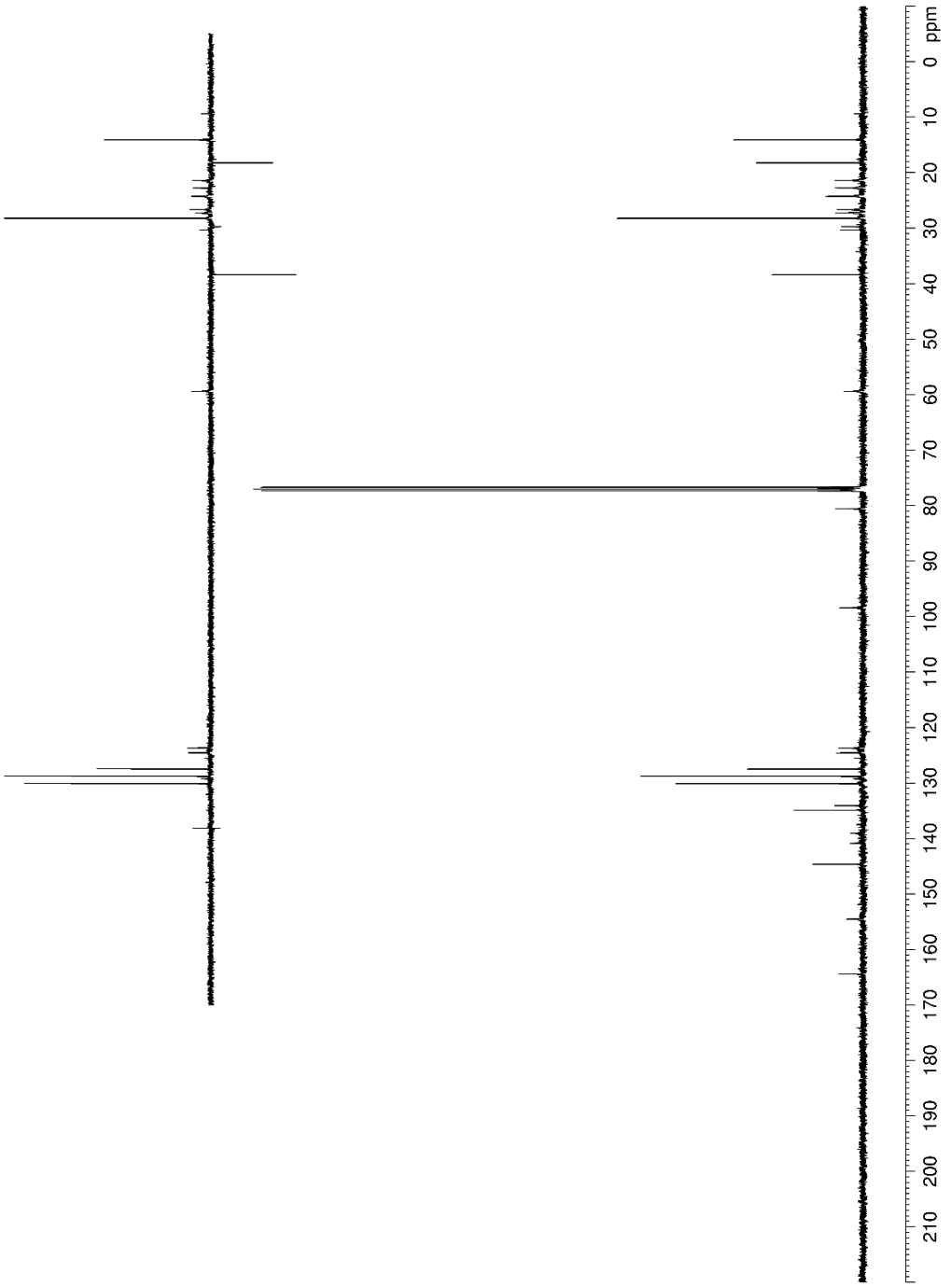

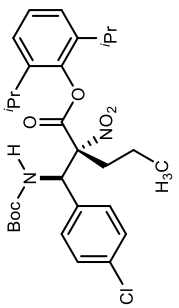

Figure C 28. ^{1}H NMR (500 MHz, $CDCl_3$) of **60d**

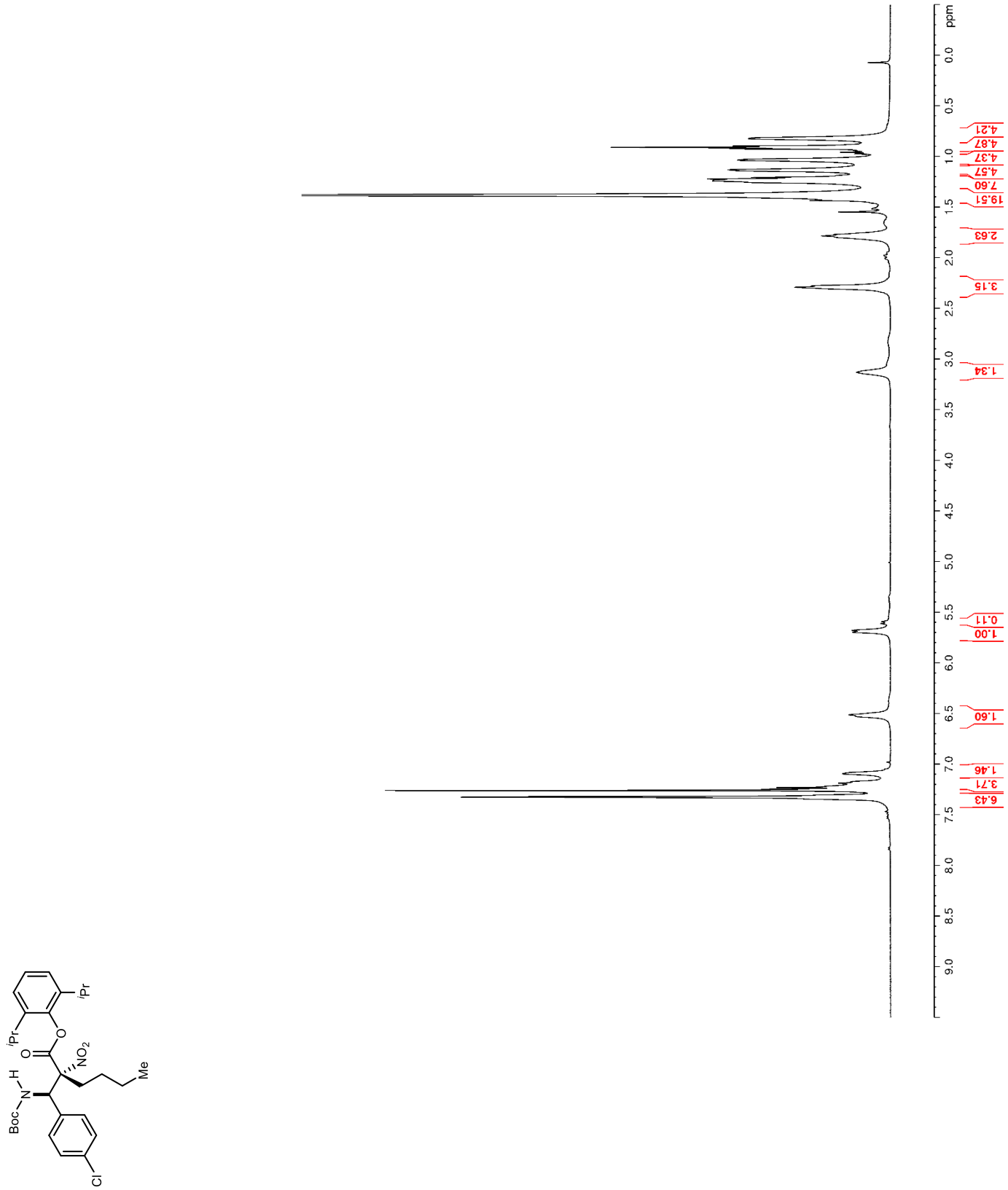

Figure C 29. ^{13}C NMR (125 MHz, $CDCl_3$) of **60d**

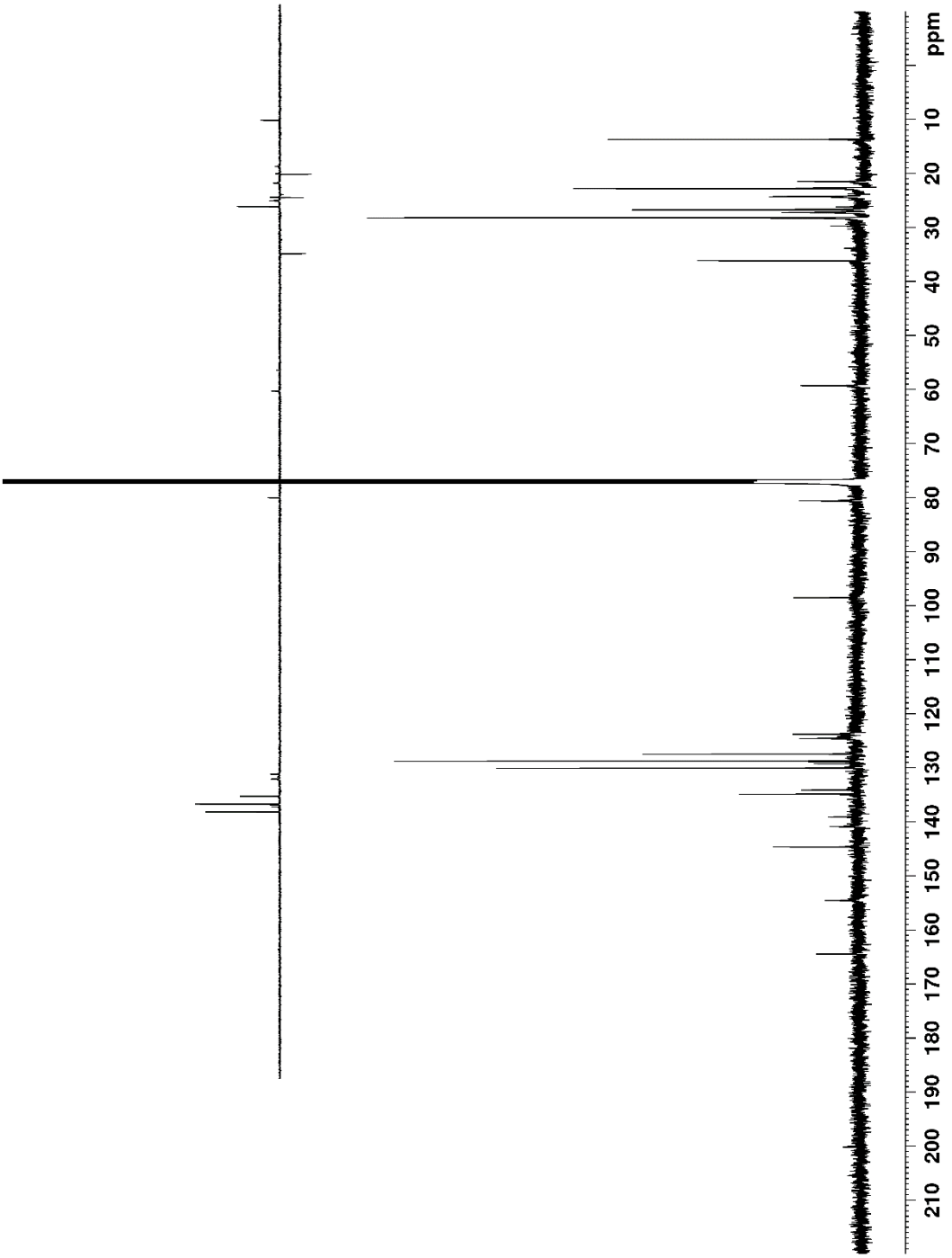

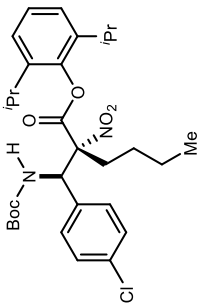

Figure C 30. ^{1}H NMR (400 MHz, $CDCl_3$) of **60e**

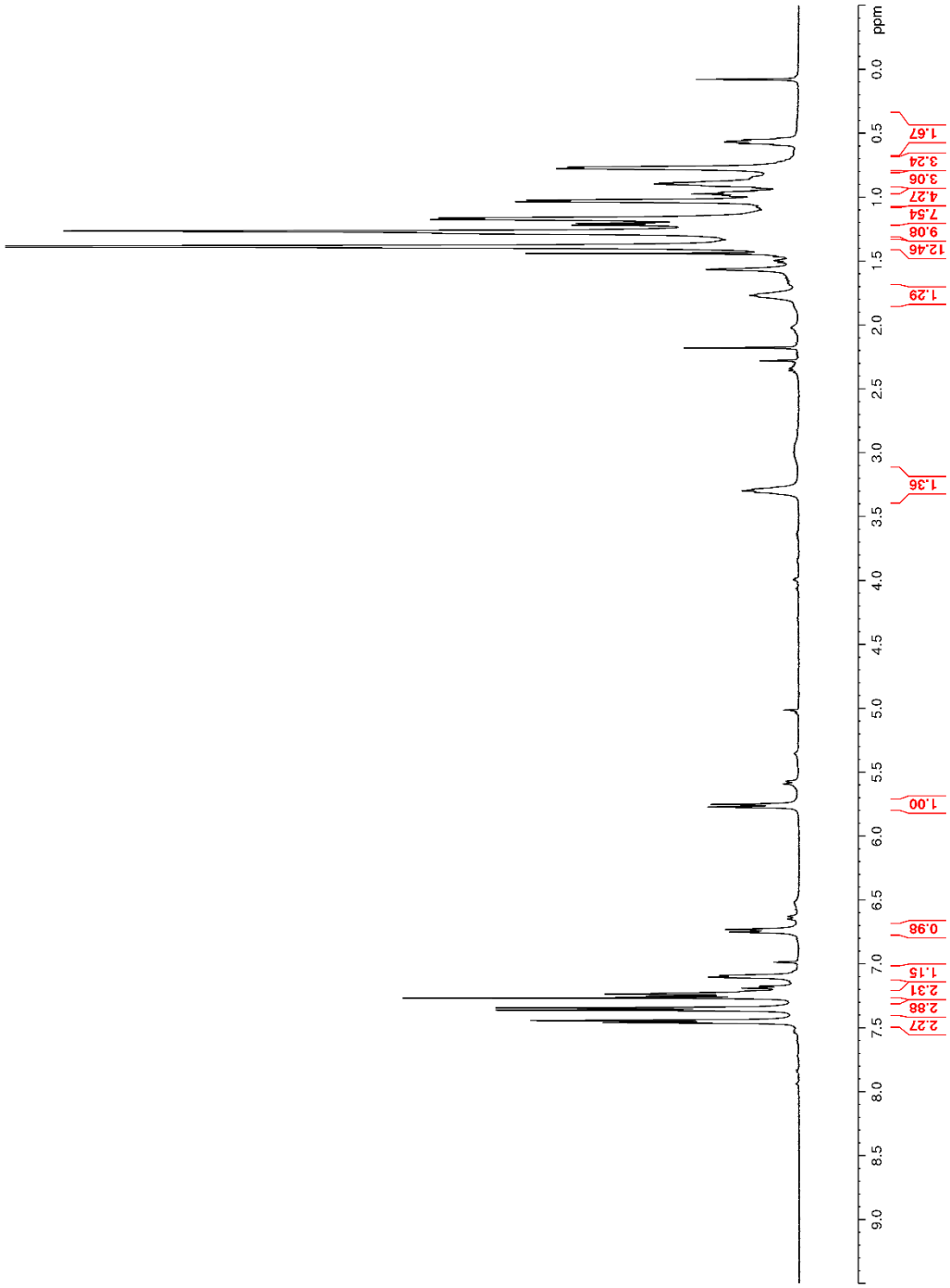

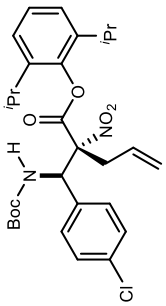

Figure C 31. ^{13}C NMR (100 MHz, $CDCl_3$) of **60e**

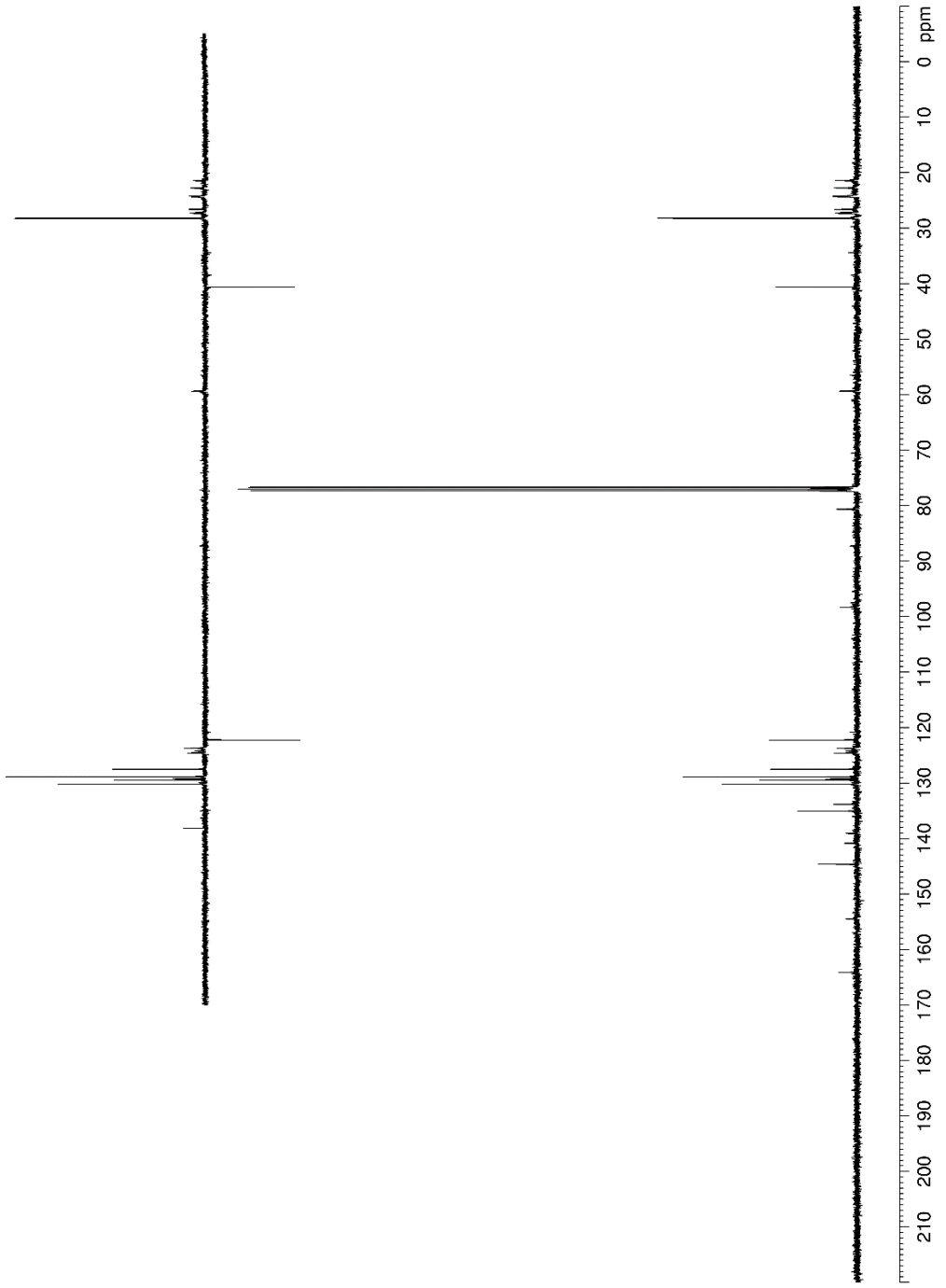

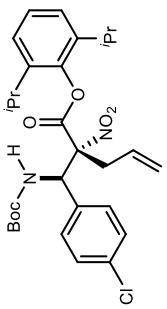

Figure C 32. ^{1}H NMR (400 MHz, $CDCl_3$) of ^{8}MeBAMide.

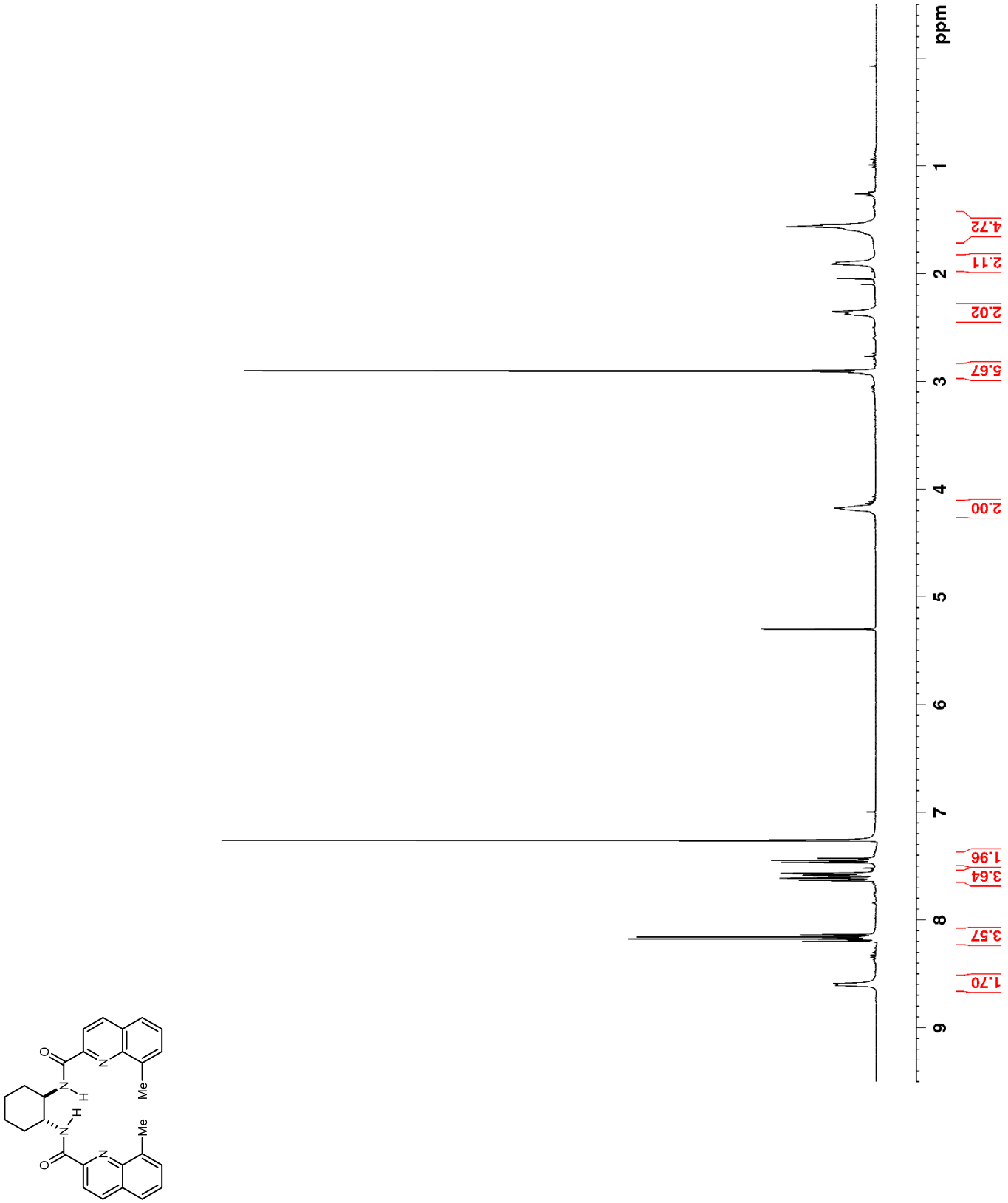

Figure C 33. ^{13}C NMR (100 MHz, $CDCl_3$) of ^{8}MeBAMide

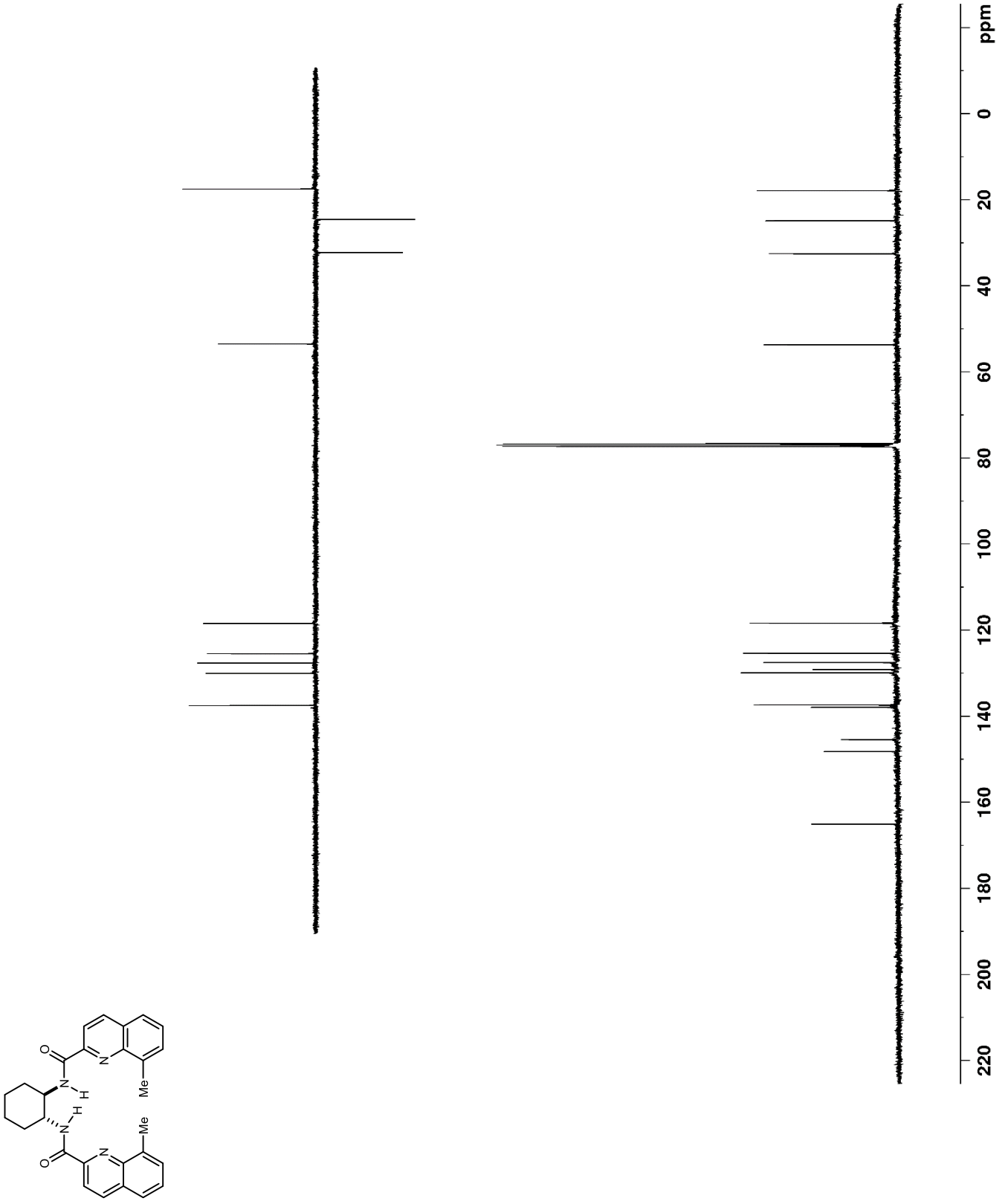

Figure C 34. ^{1}H NMR (400 MHz, $CDCl_3$) of $^{6,7}Me_2$BAMide

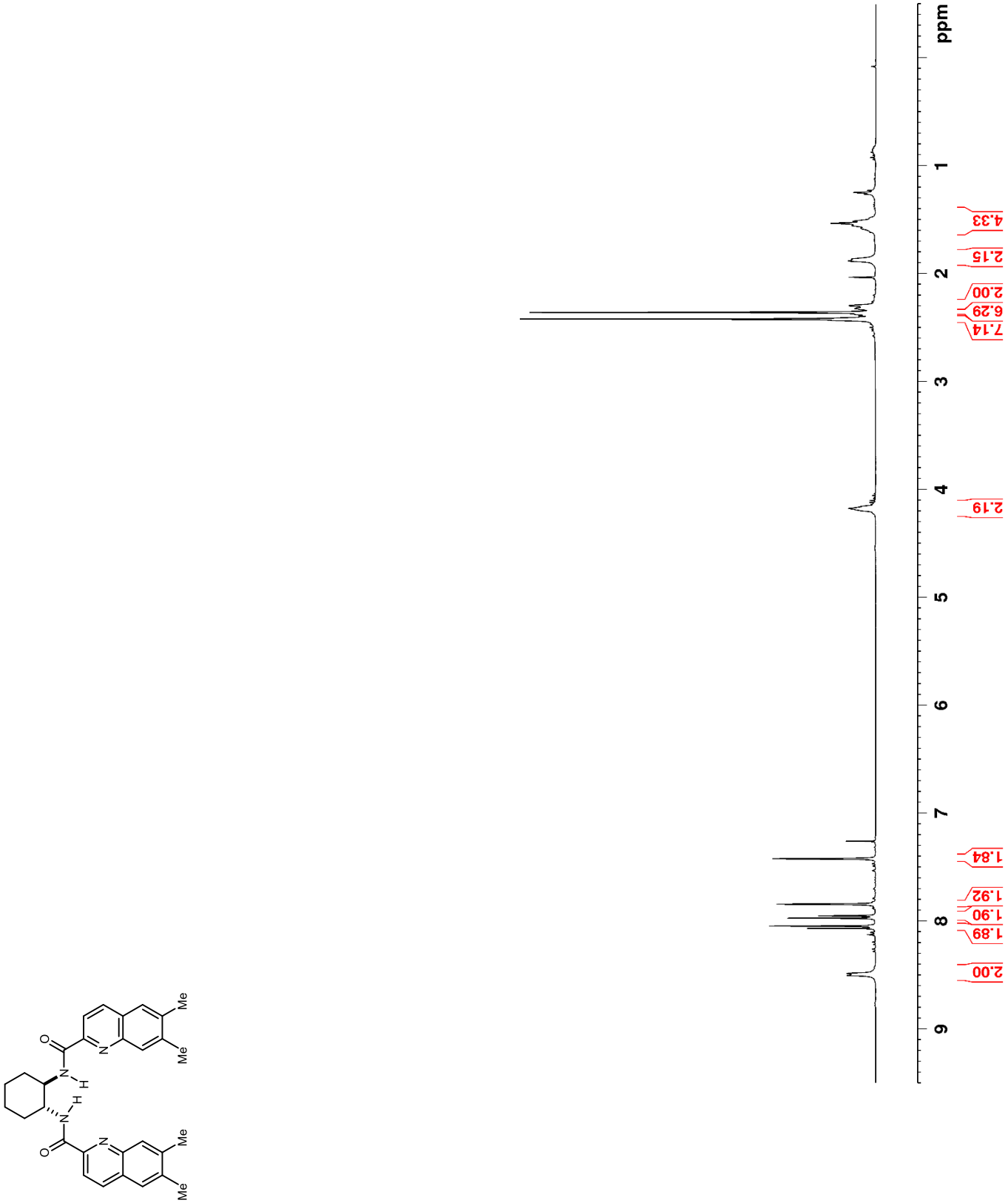

Figure C 35. ^{13}C NMR (100 MHz, $CDCl_3$) of $^{6,7}Me_2$BAMide

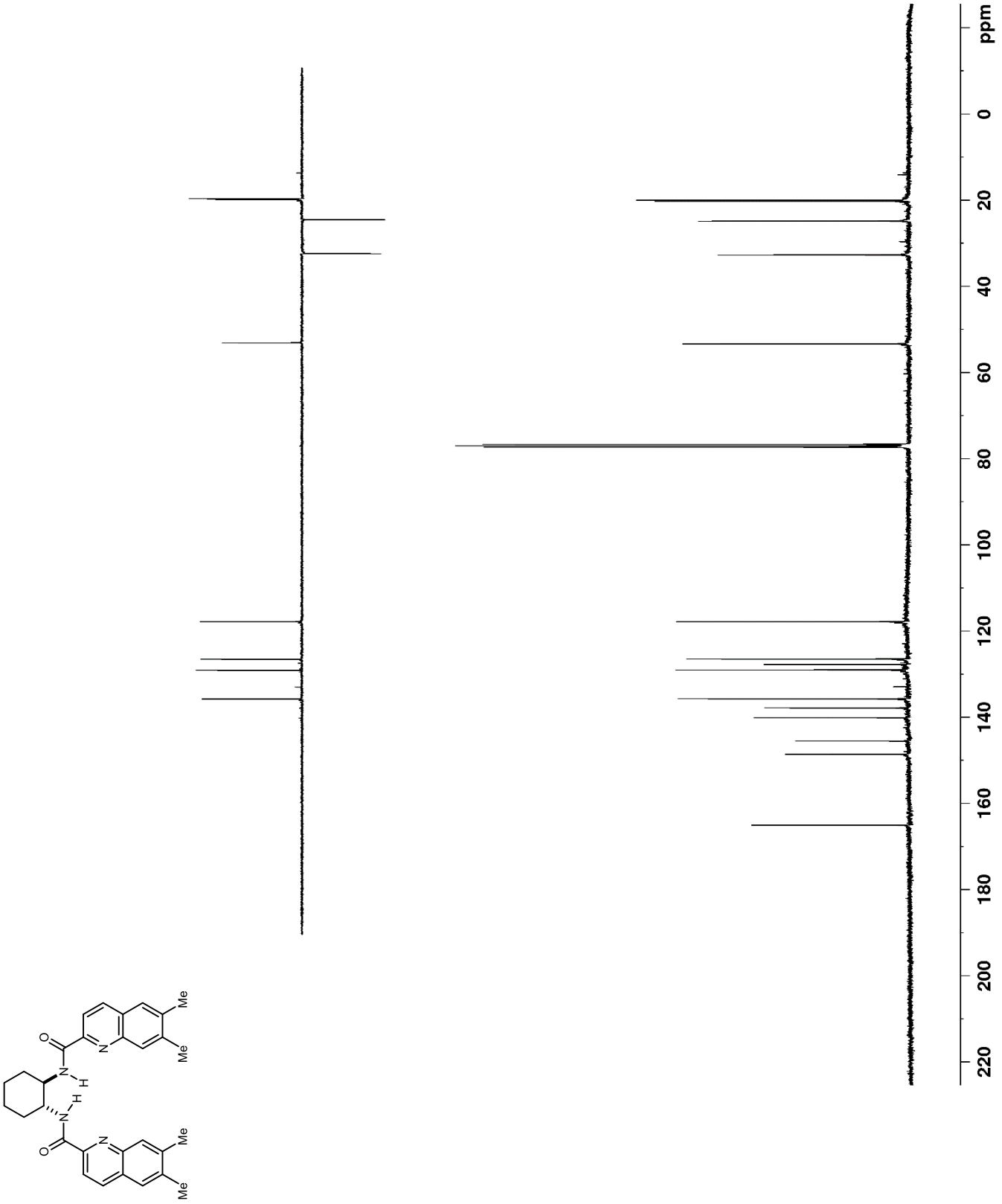

Figure C 36. ^{1}H NMR (400 MHz, $CDCl_3$) of ^{8}OBnBAMide

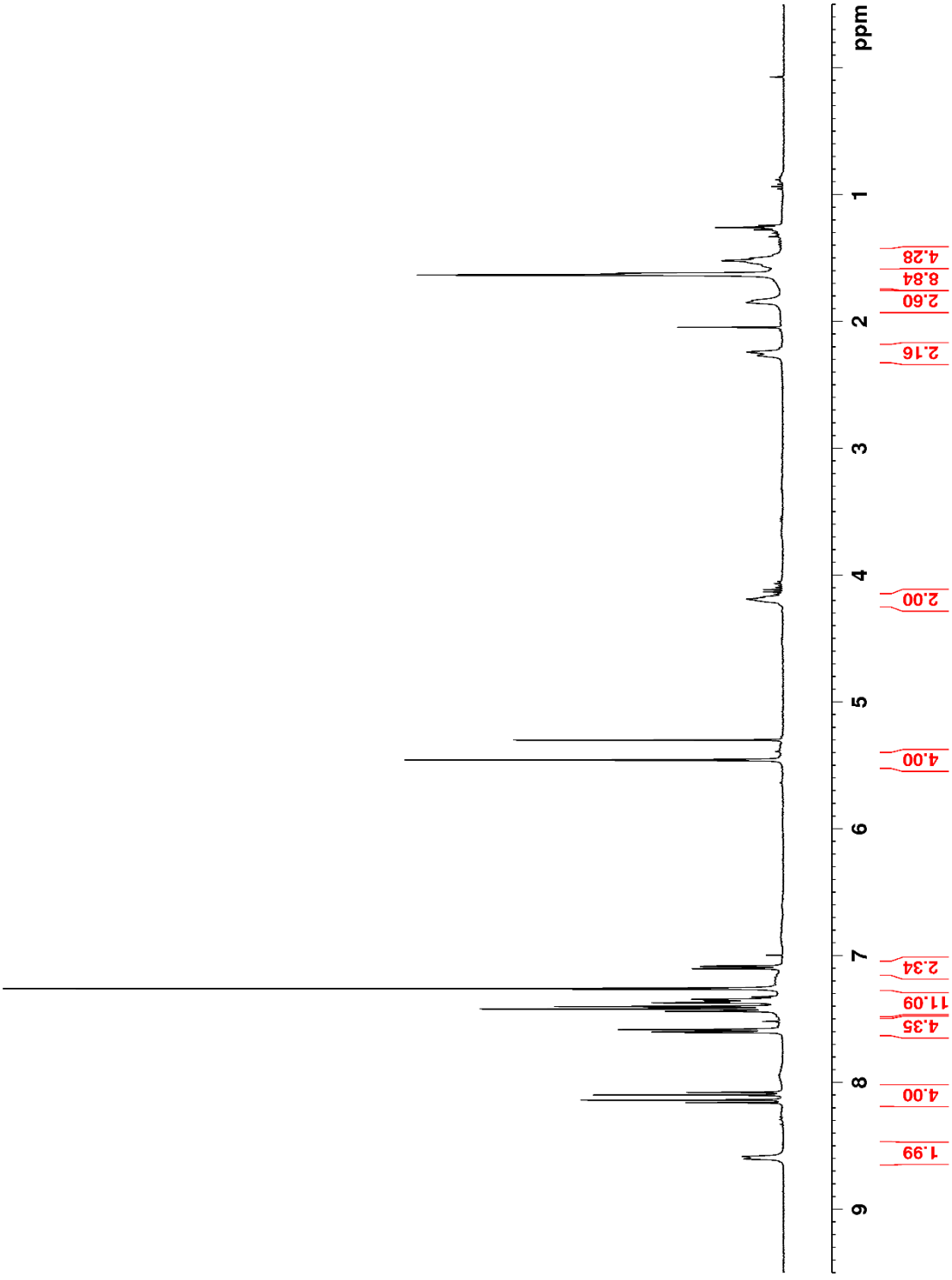

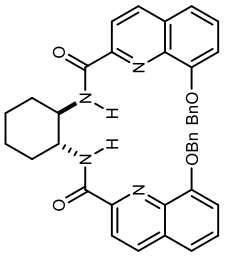

Figure C 37. ^{13}C NMR (100 MHz, $CDCl_3$) of ^{8}OBnBAMide

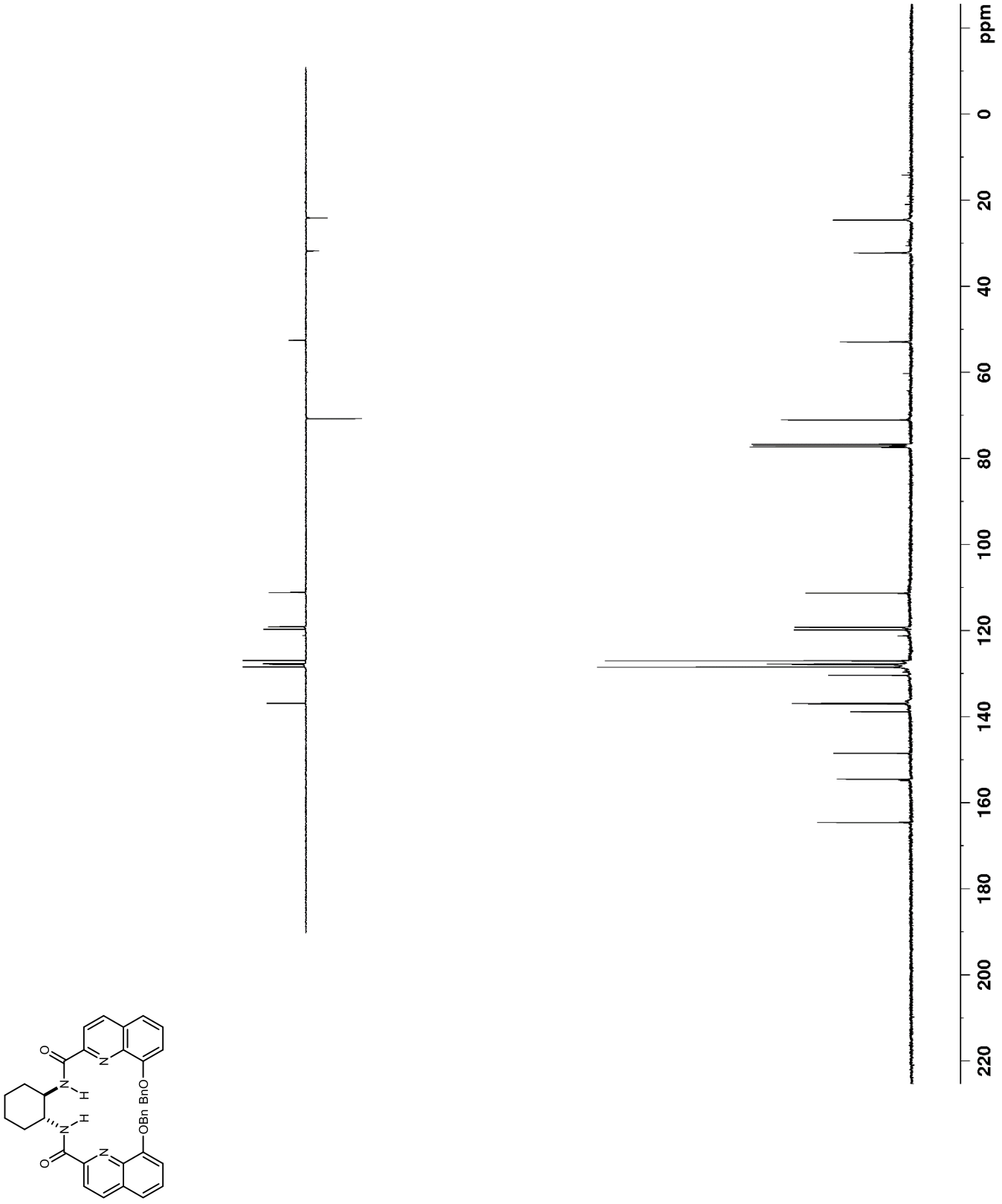

Figure C 38. ^{1}H NMR (400 MHz, $CDCl_3$)

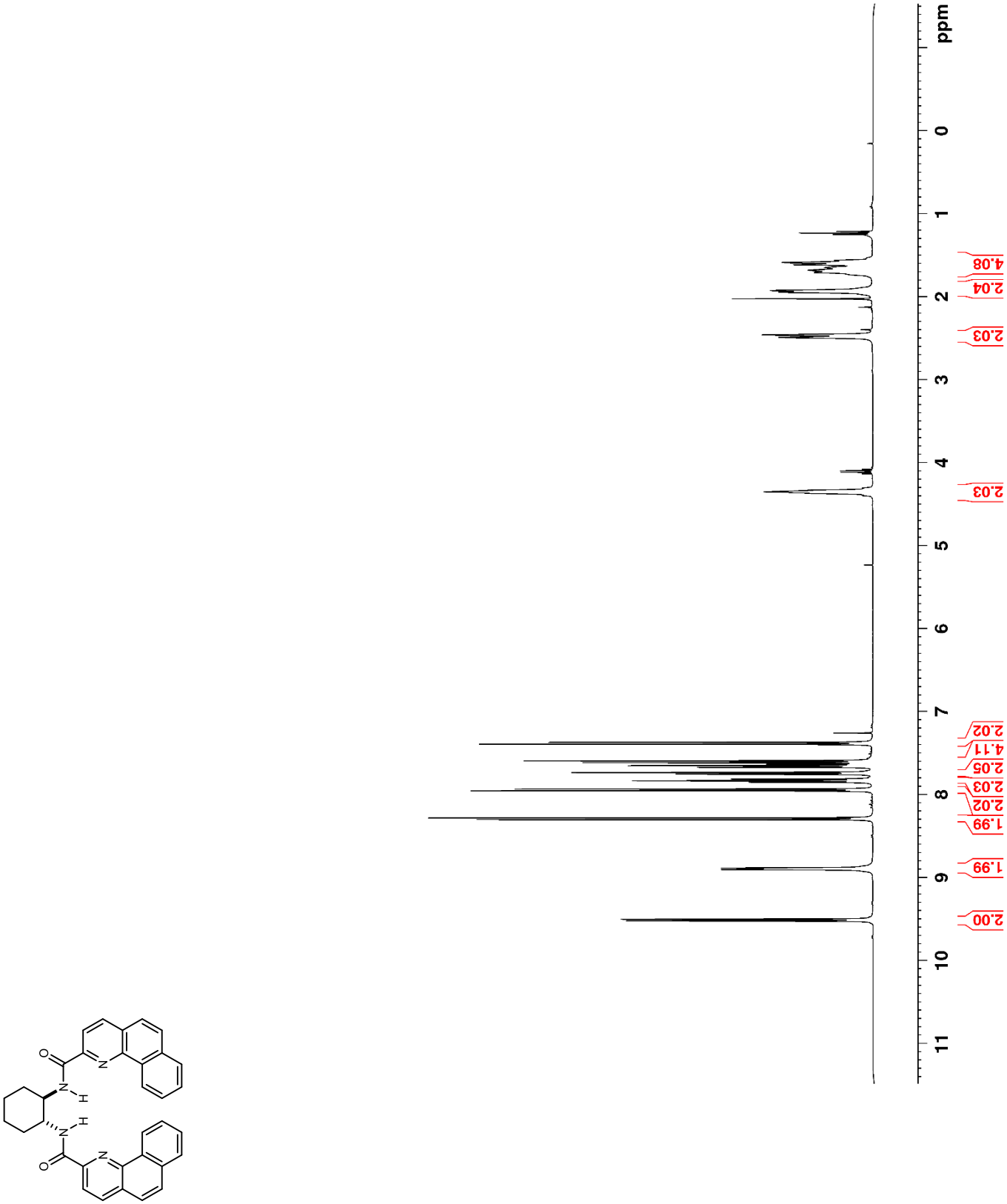

Figure C 39. ^{13}C NMR (100 MHz, $CDCl_3$)

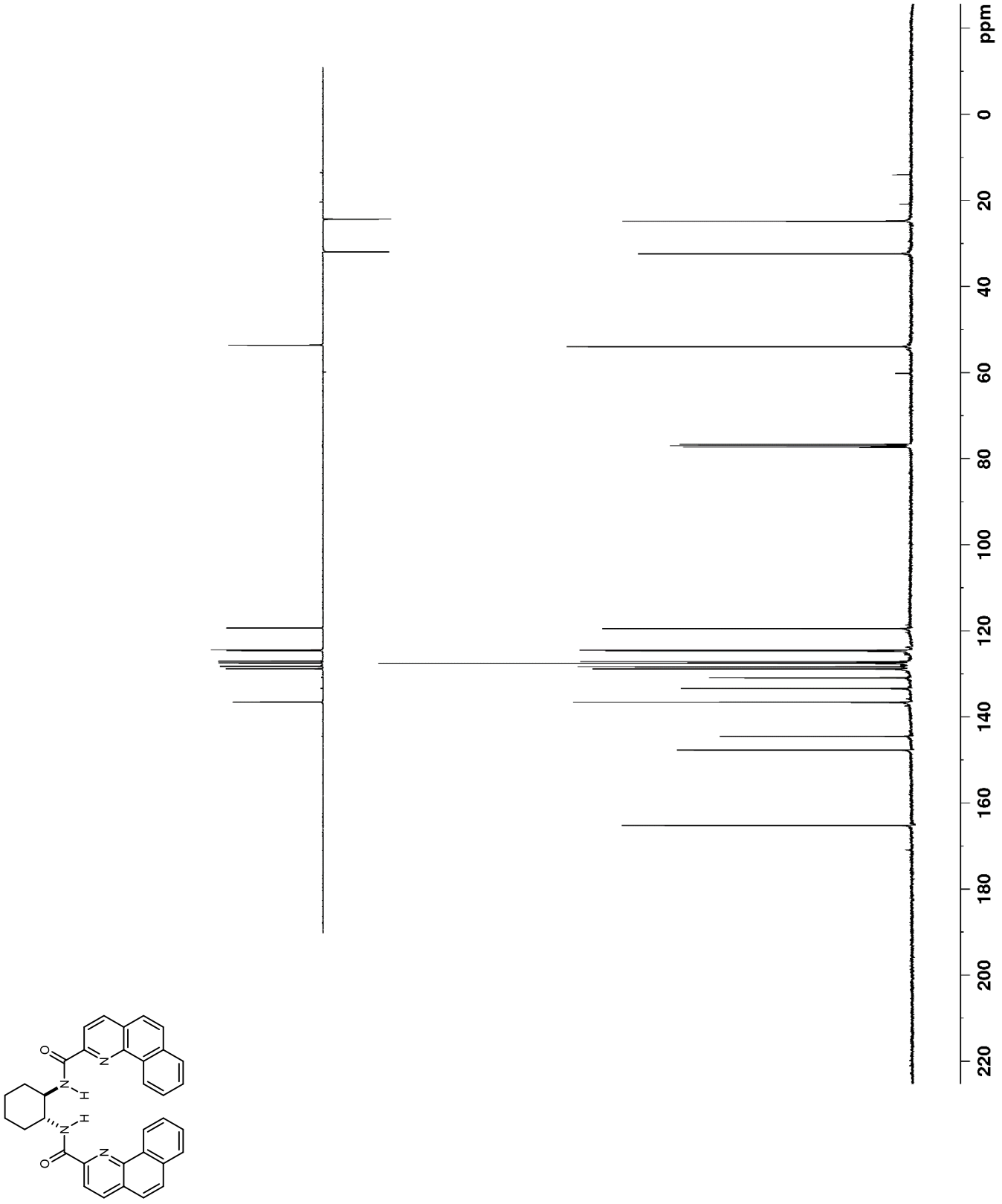

Figure C 40. ^{1}H NMR (400 MHz, $CDCl_3$)

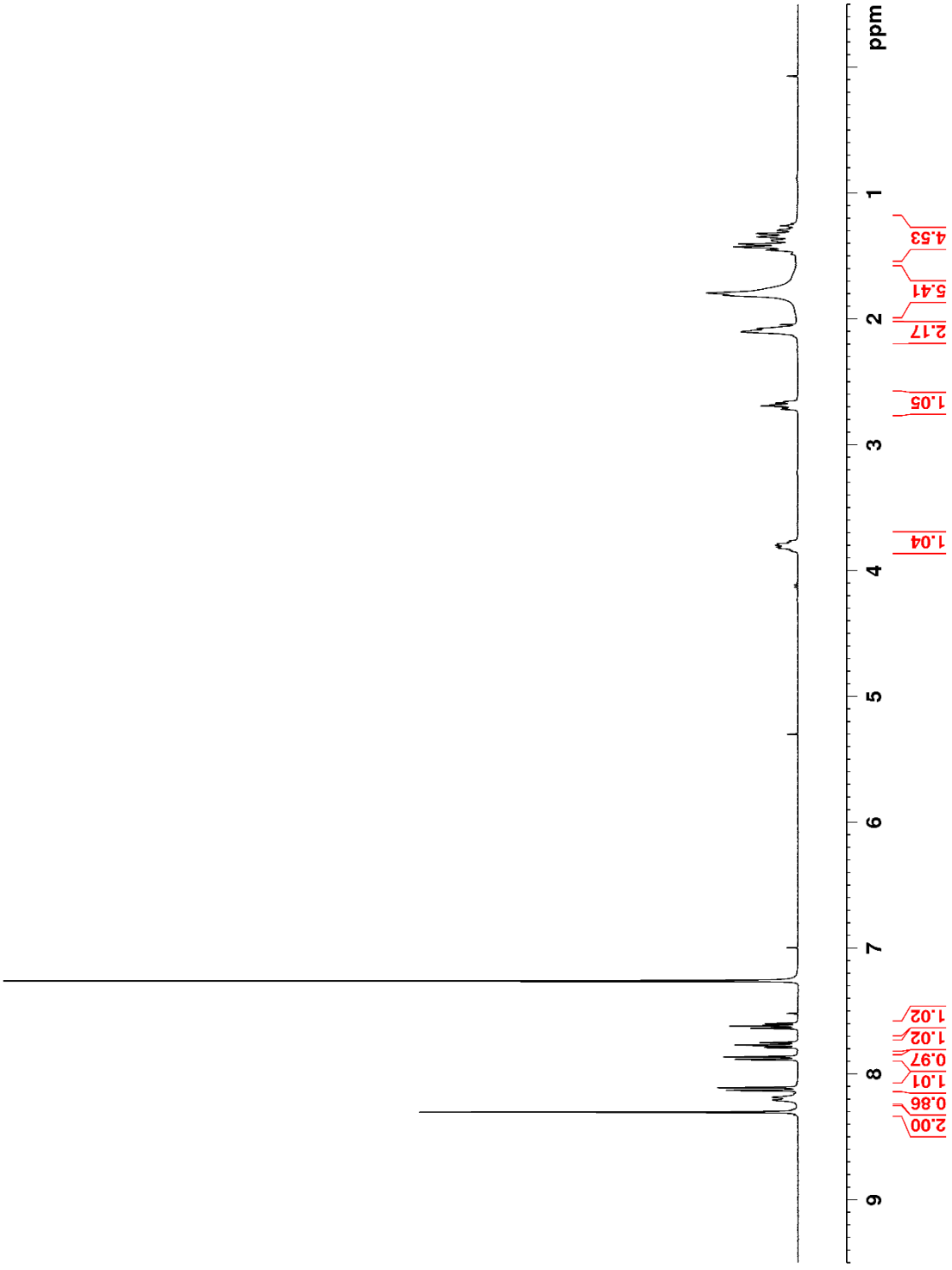

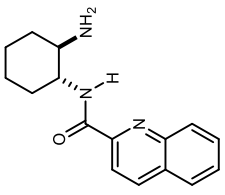

Figure C 41. ^{13}C NMR (100 MHz, $CDCl_3$)

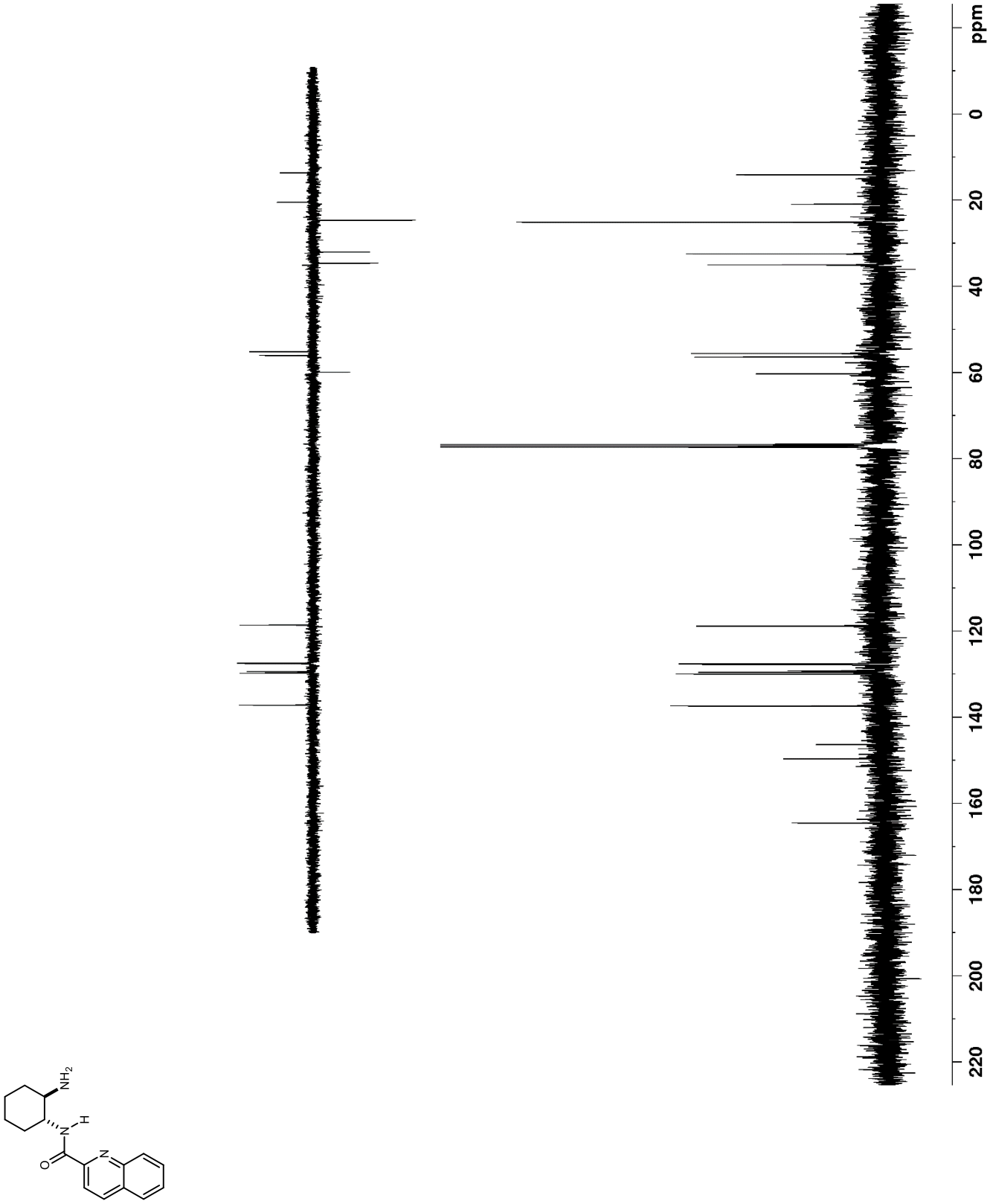

Figure C 42. ^{1}H NMR (400 MHz, $CDCl_3$) of H,ThioBAMide

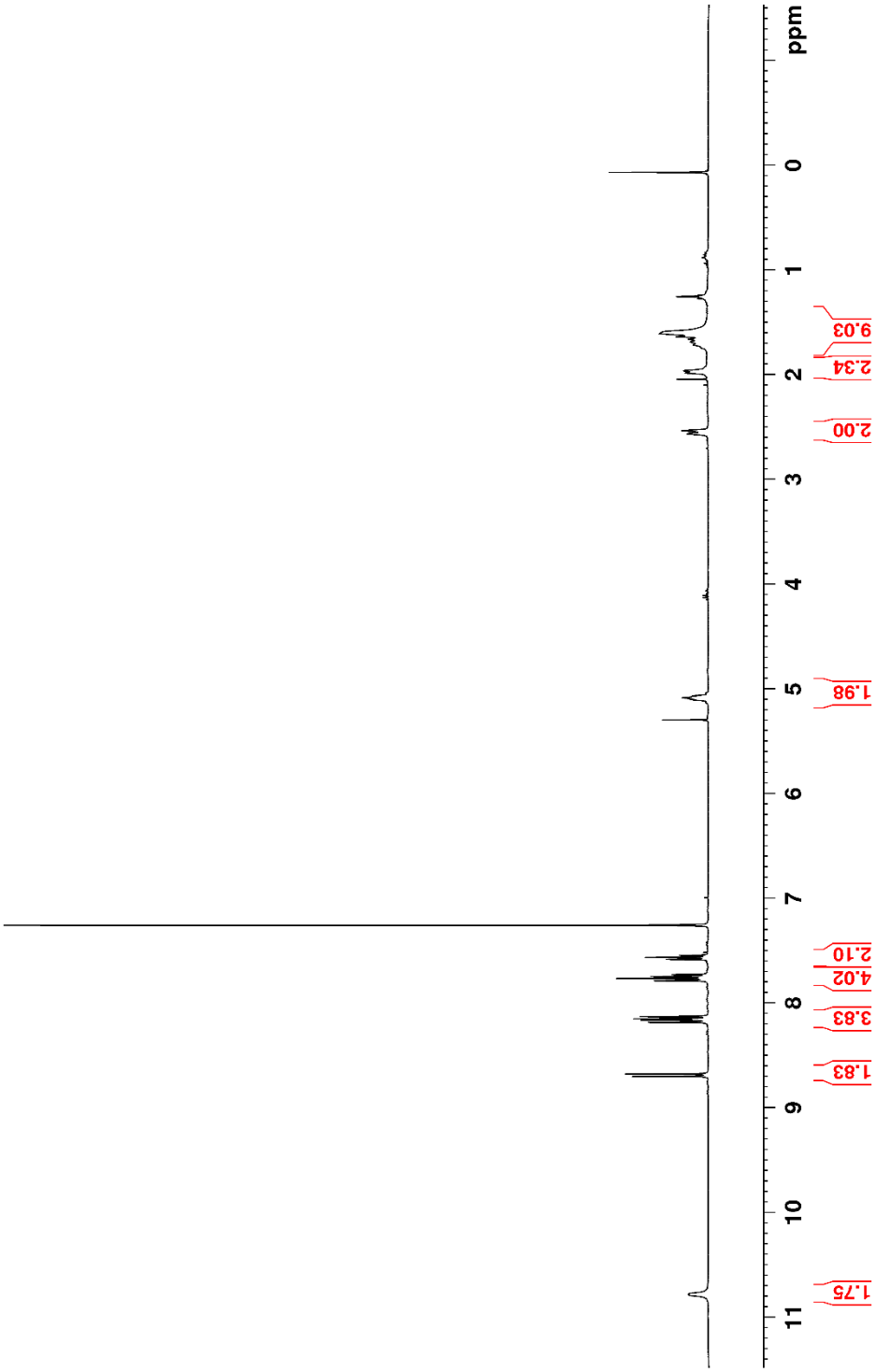

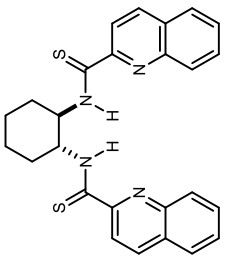

Figure C 43. ^{13}C NMR (100 MHz, $CDCl_3$) of H,ThioBAMide

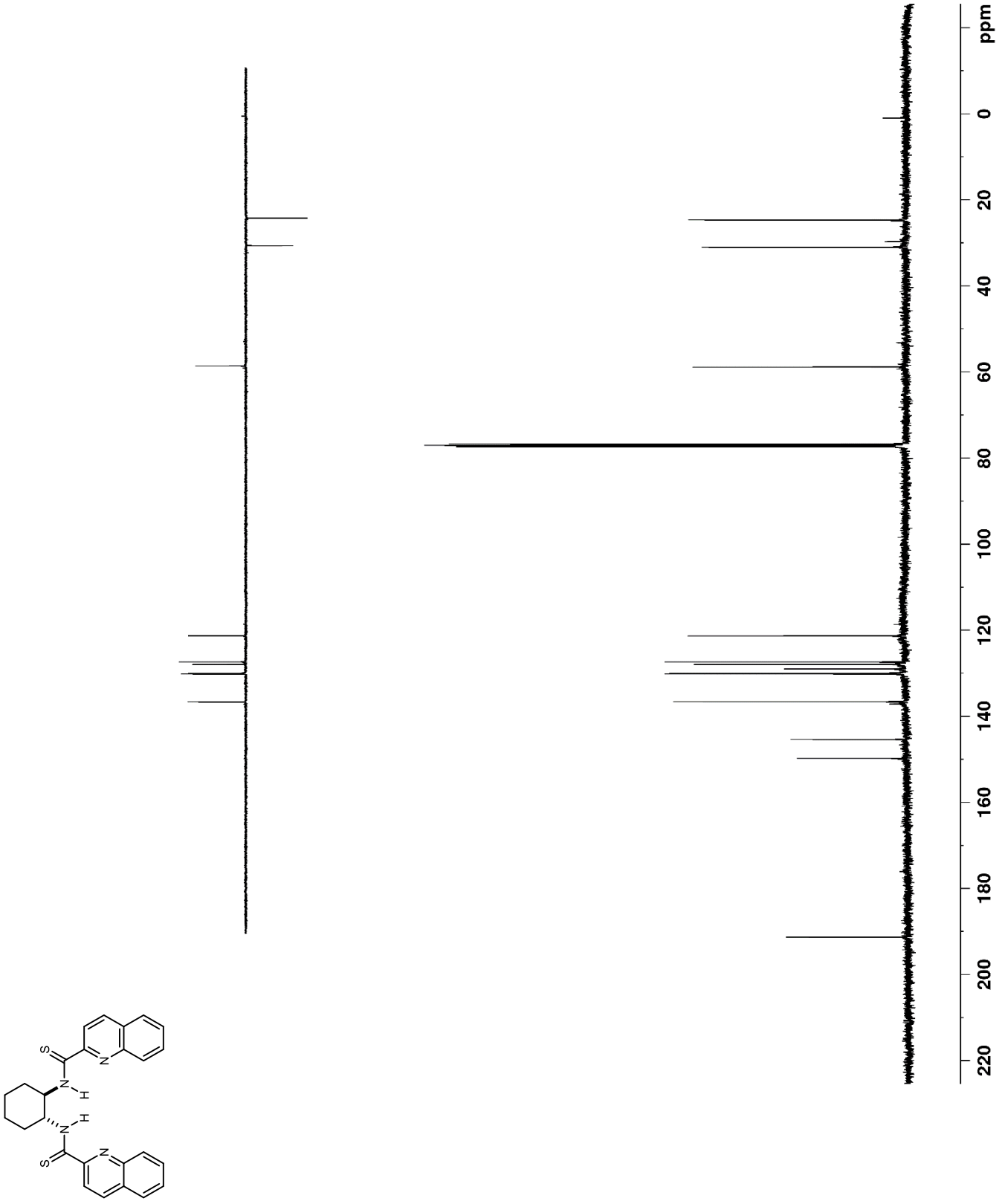

Figure C 44. ^{1}H NMR (400 MHz, $CDCl_3$) of H,^{3}QuinBAMide

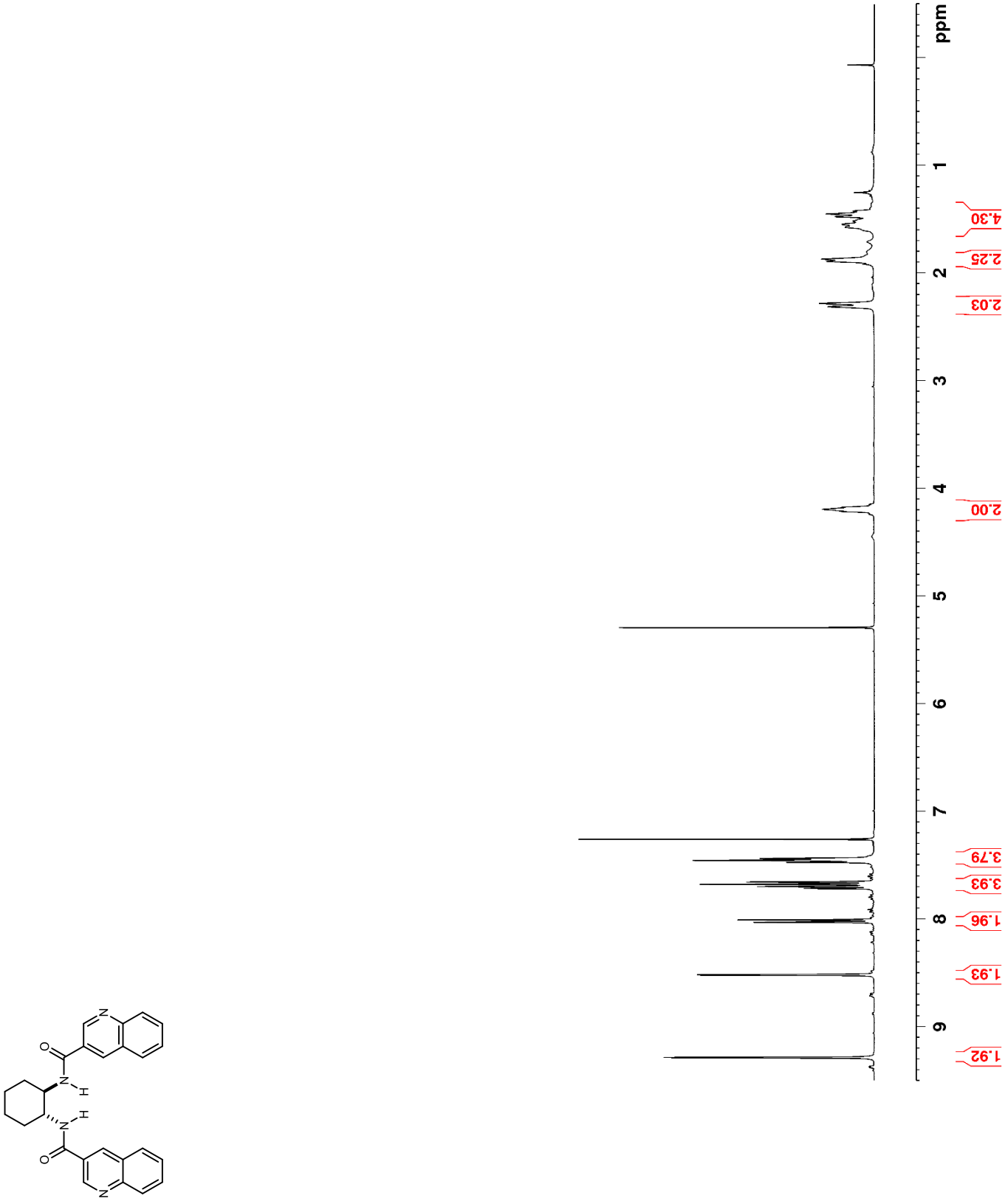

Figure C 45. ^{13}C NMR (100 MHz, $CDCl_3$) of H,^{3}QuinBAMide

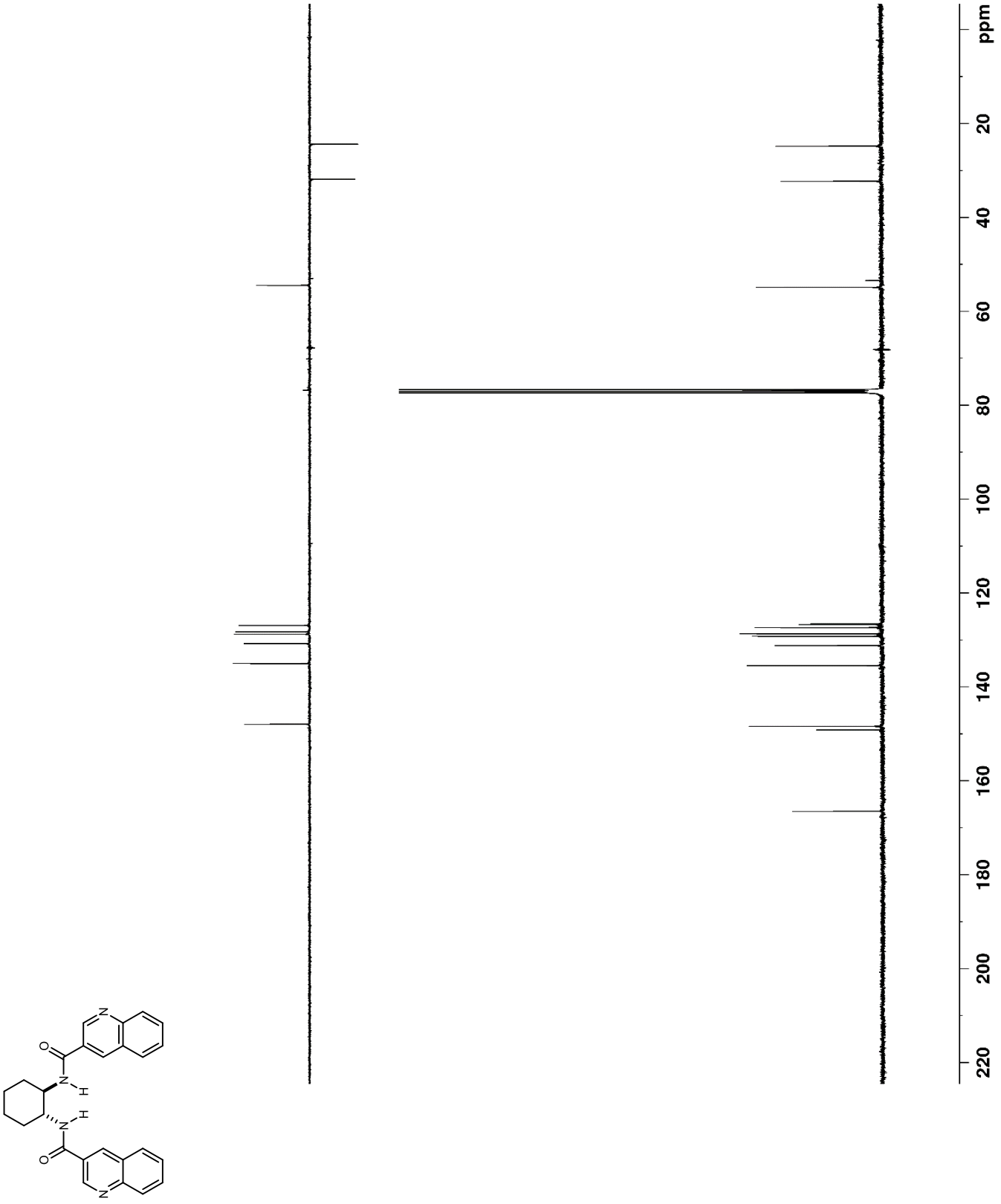

Figure C 46. ^{1}H NMR (400 MHz, $CDCl_3$) of ^{4}Cl-BAMide

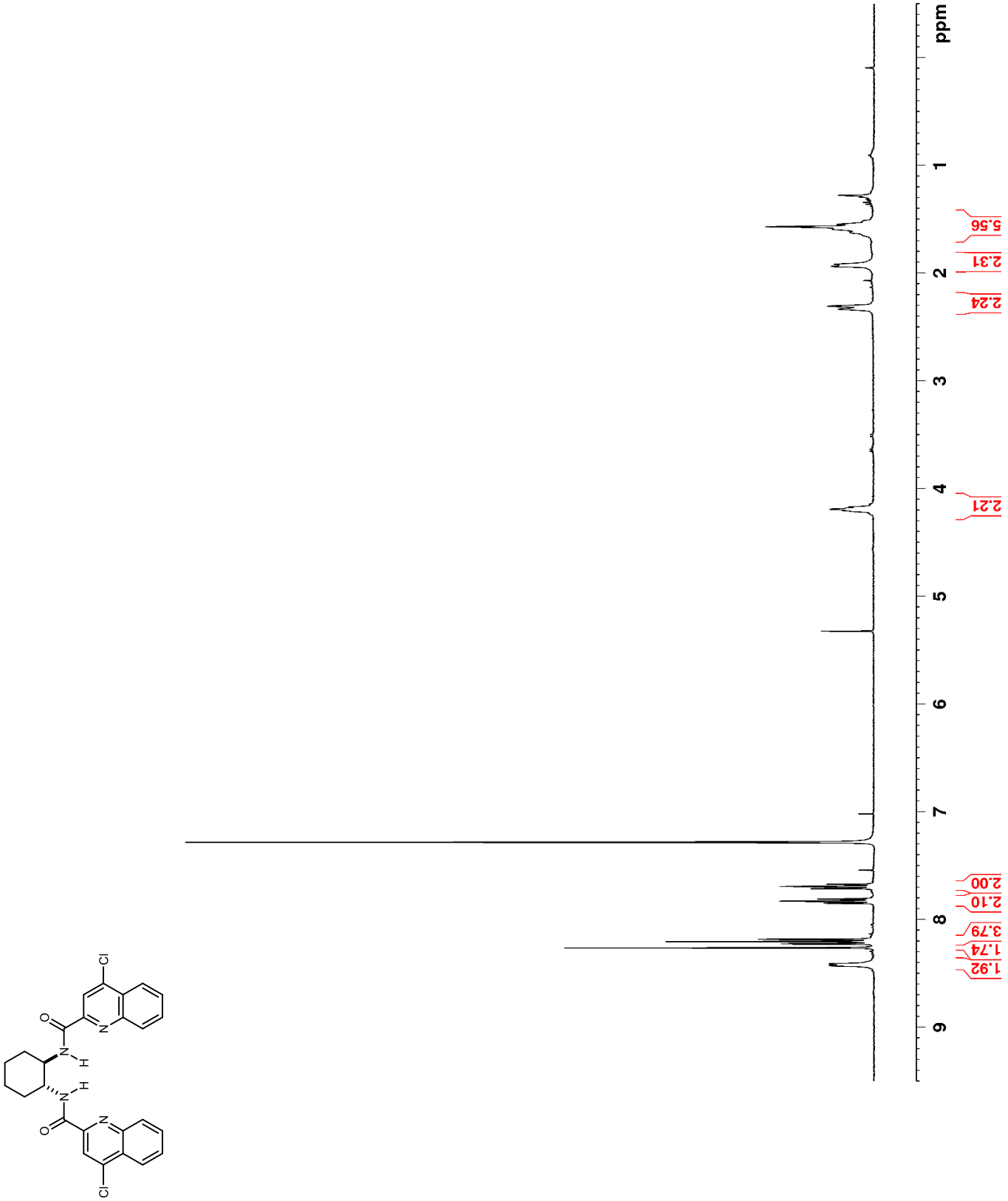

Figure C 47. ^{13}C NMR (100 MHz, $CDCl_3$) ^{4}Cl-BAMide

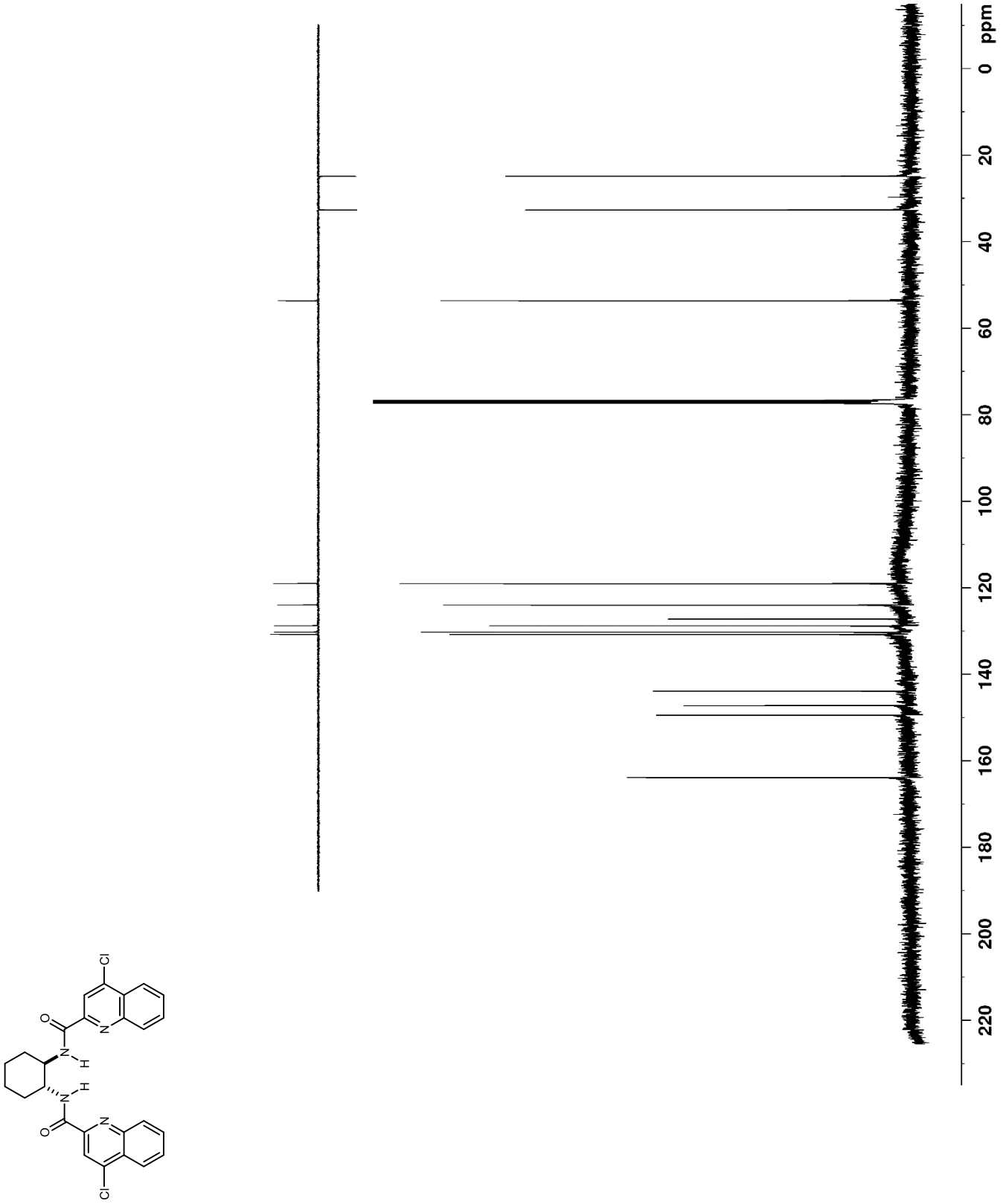

Figure C 48. ^{1}H NMR (400 MHz, $CDCl_3$)

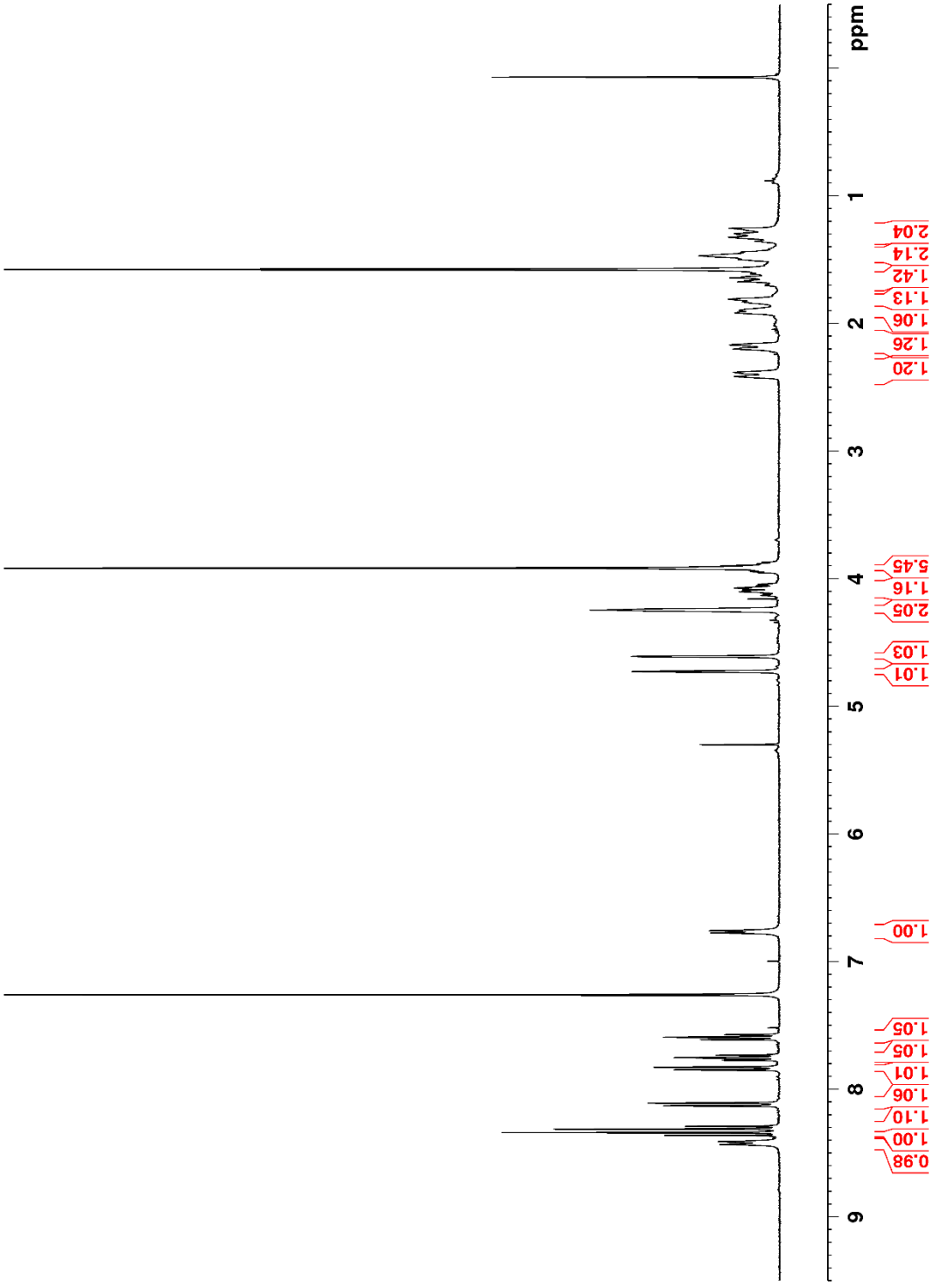

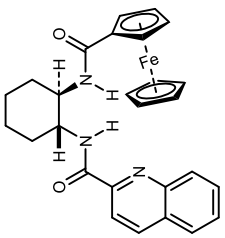

Figure C 49. ^{13}C NMR (100 MHz, $CDCl_3$)

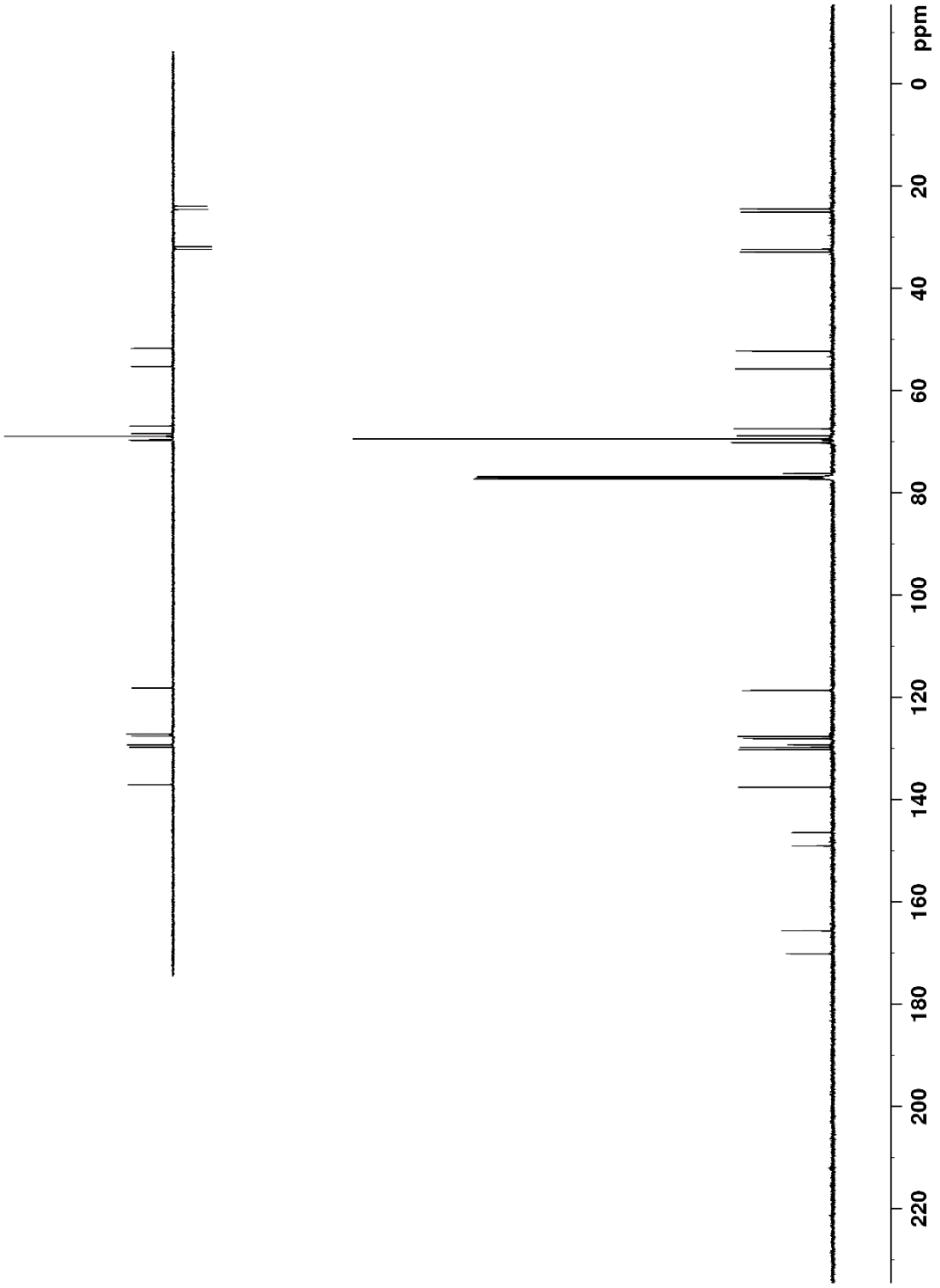

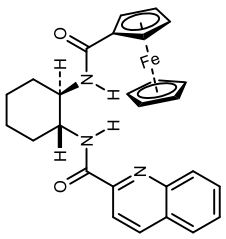

Figure C 50. ^{1}H NMR (400 MHz, $CDCl_3$) of MiracleBAMide

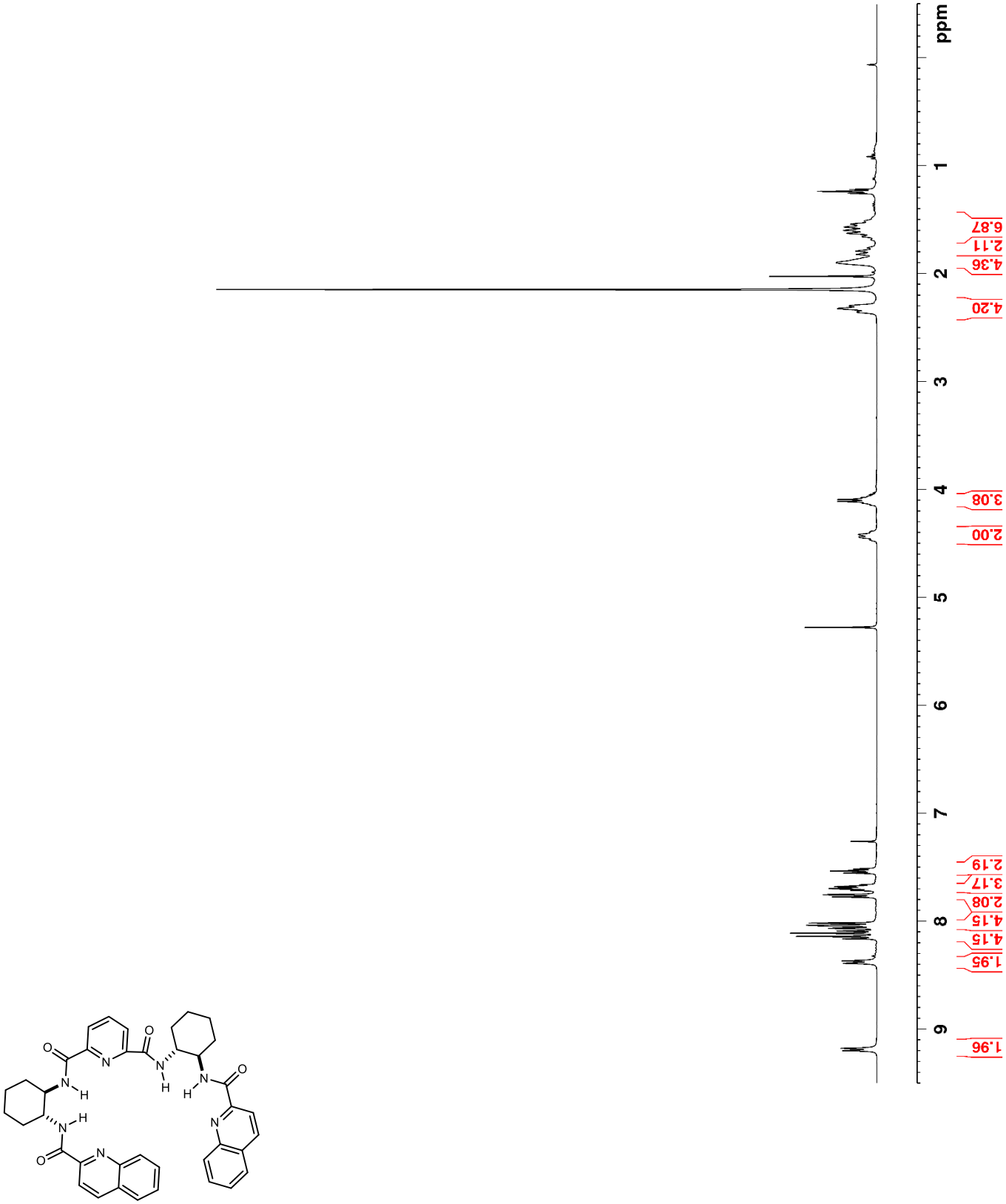

Figure C 51. ^{13}C NMR (100 MHz, $CDCl_3$) of MiracleBAMide

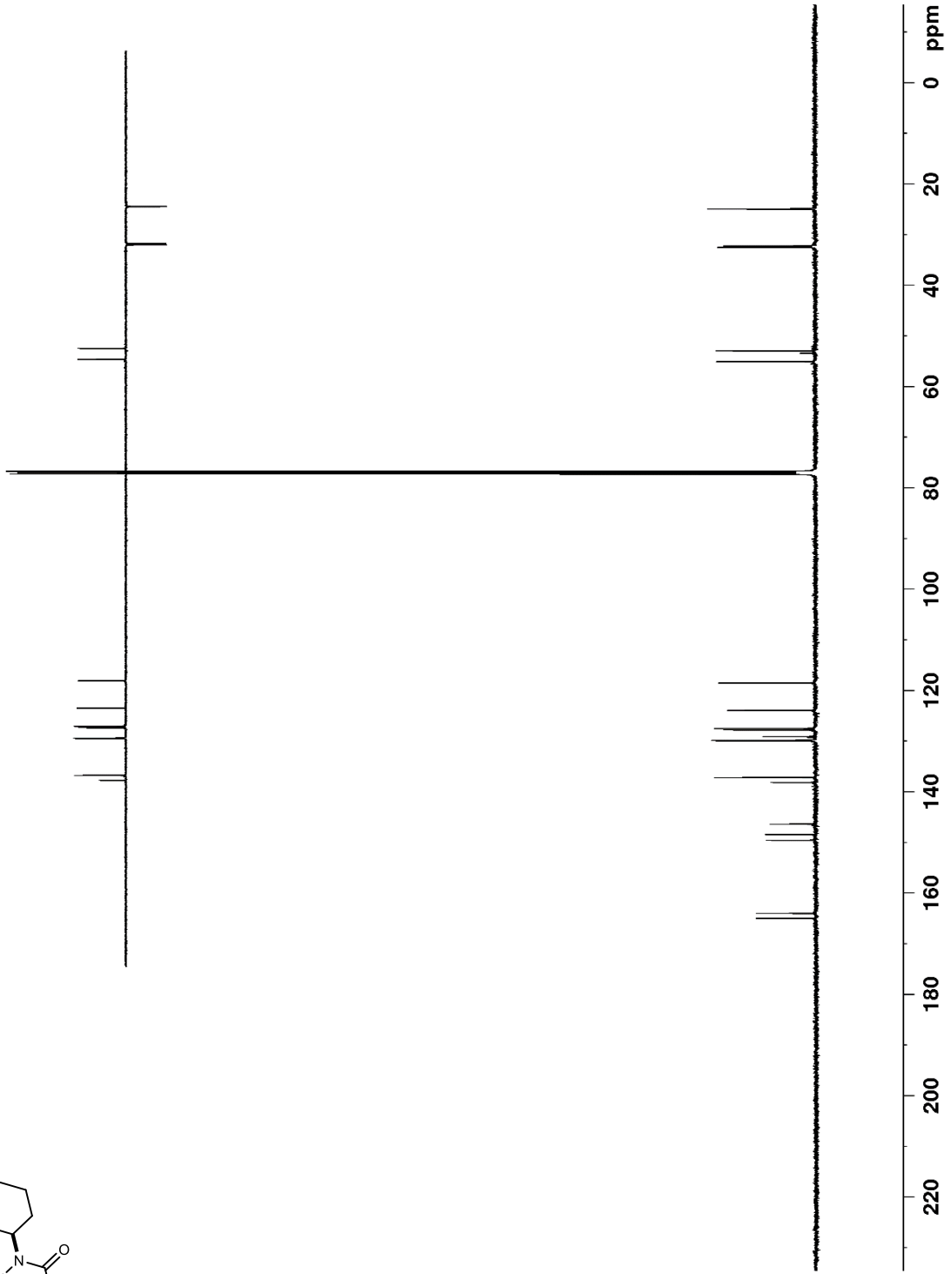

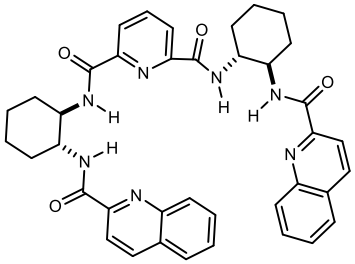

Figure C 52. ^{1}H NMR (400 MHz, $CDCl_3$) of BINAMBAMide

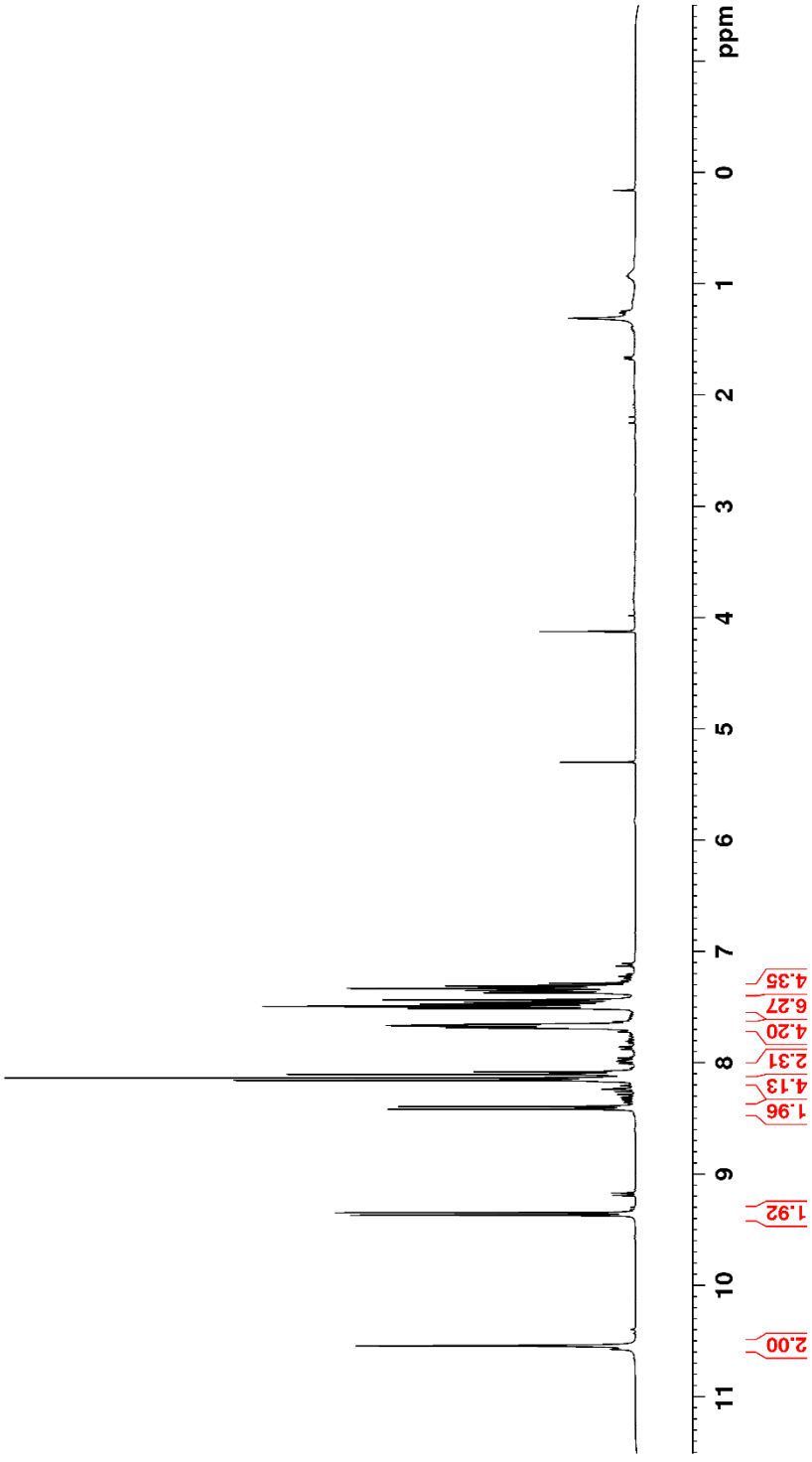

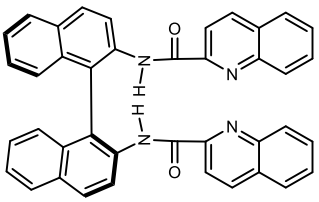

Figure C 53. ^{13}C NMR (100 MHz, $CDCl_3$) of BINAMBAMide

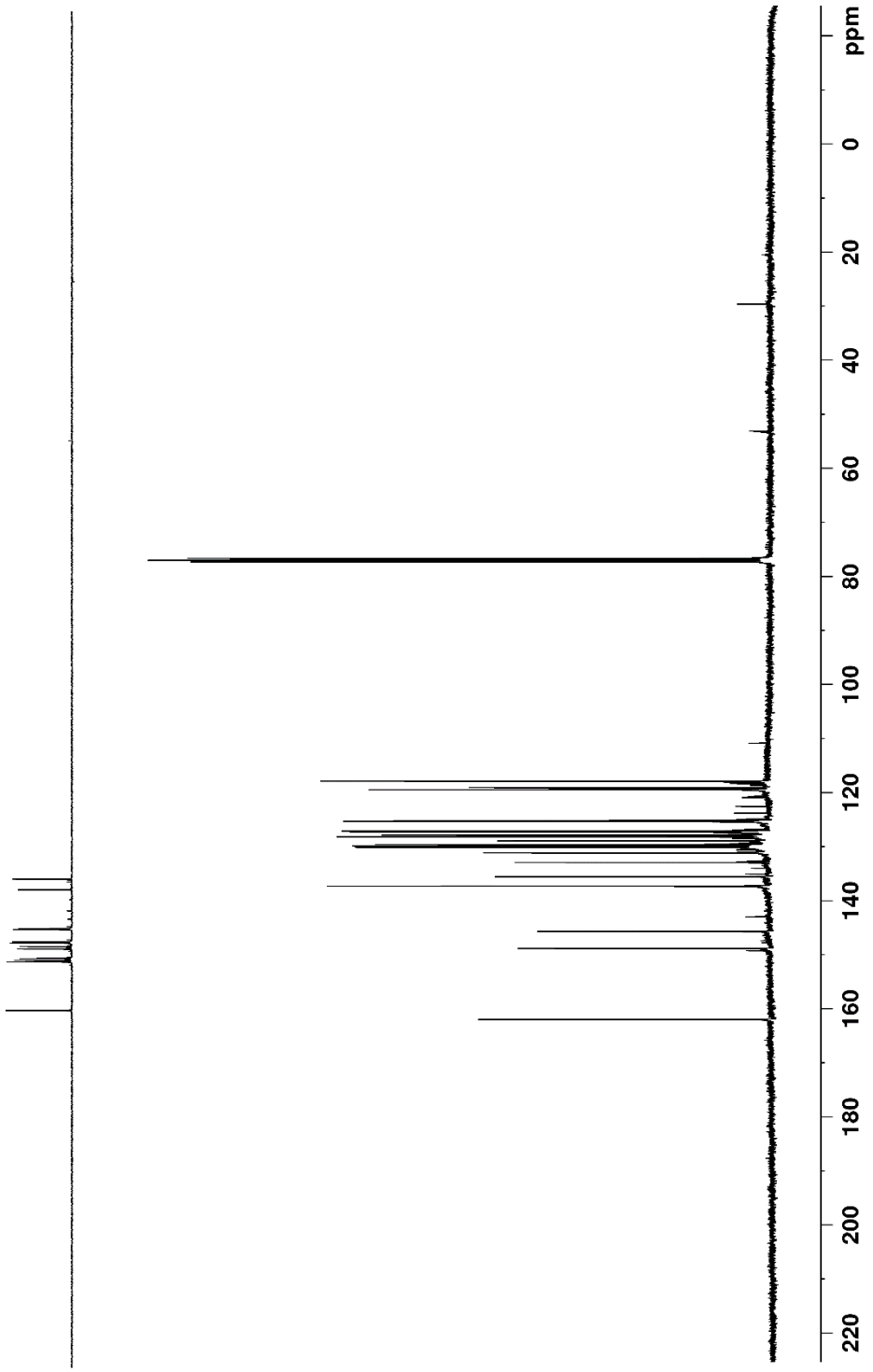

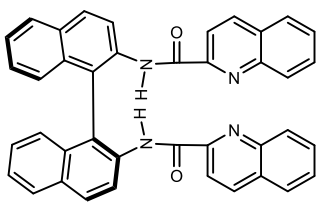

Figure C 54. ^{1}H NMR (400 MHz, $CDCl_3$) of ^{6}OMeBAMide

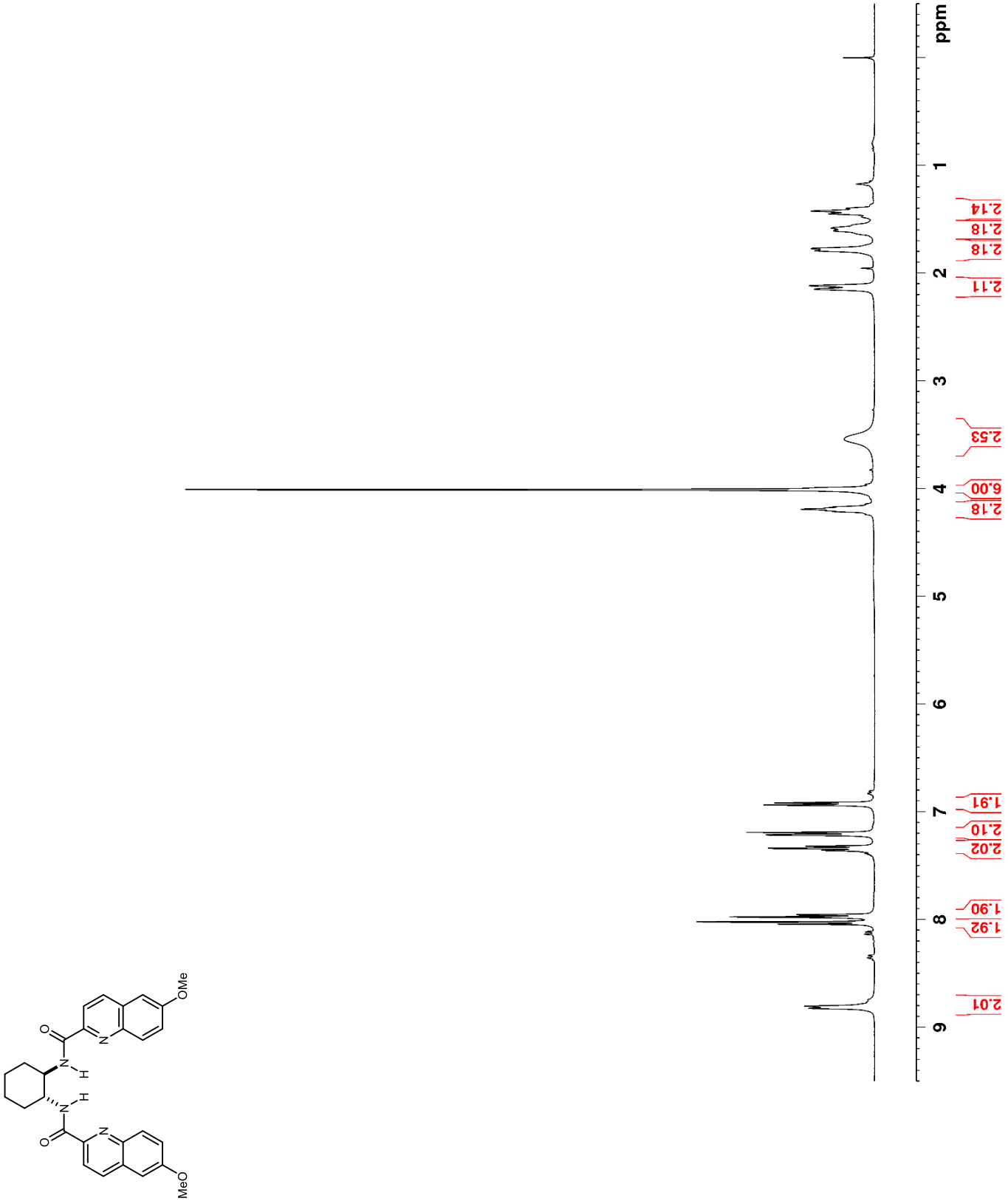

Figure C 55. ^{13}C NMR (100 MHz, $CDCl_3$) of ^{6}OMeBAMide

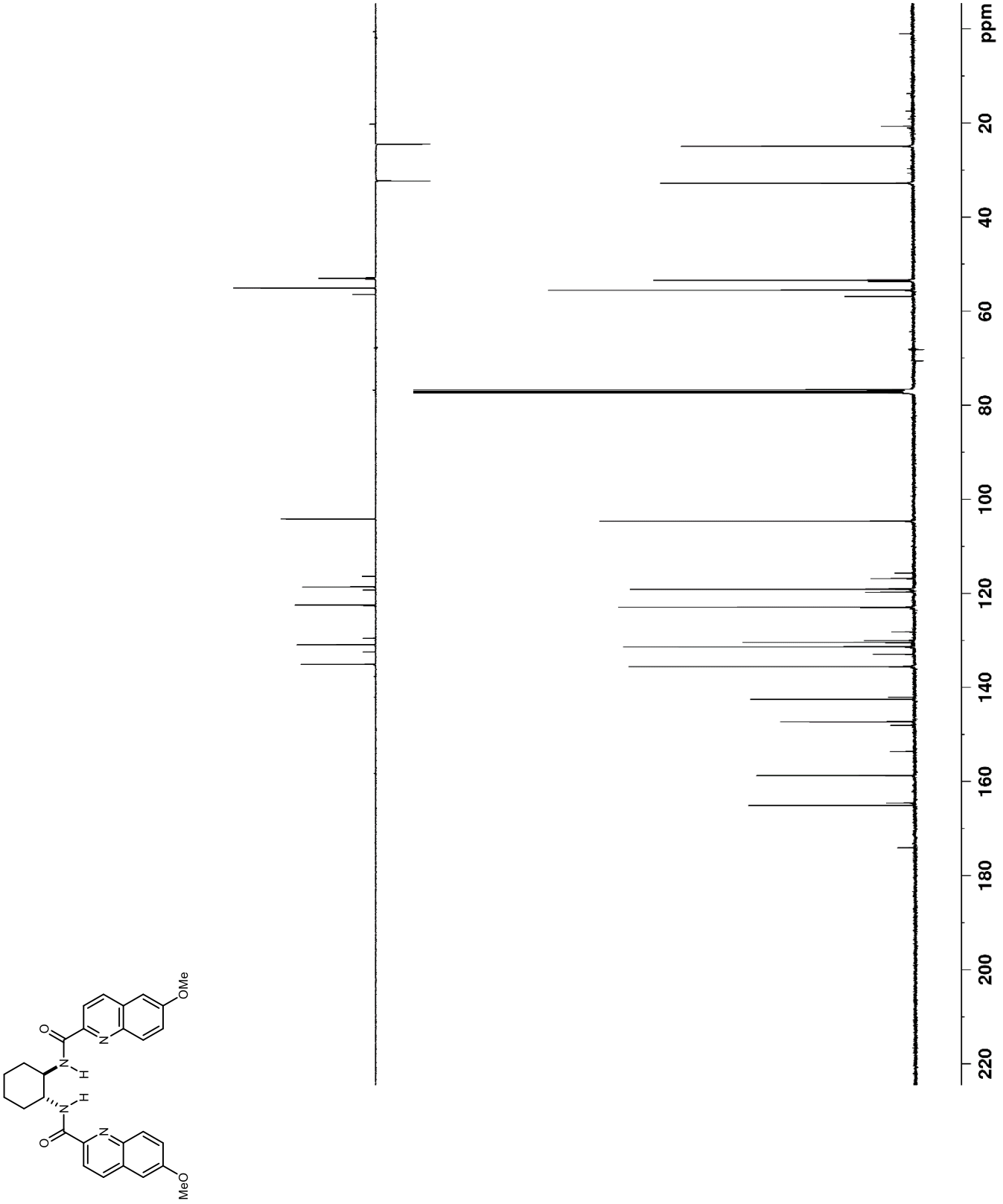

Figure C 56. ^{1}H NMR (400 MHz, $CDCl_3$) of $^{6,7}(OMe)_2$BAMide

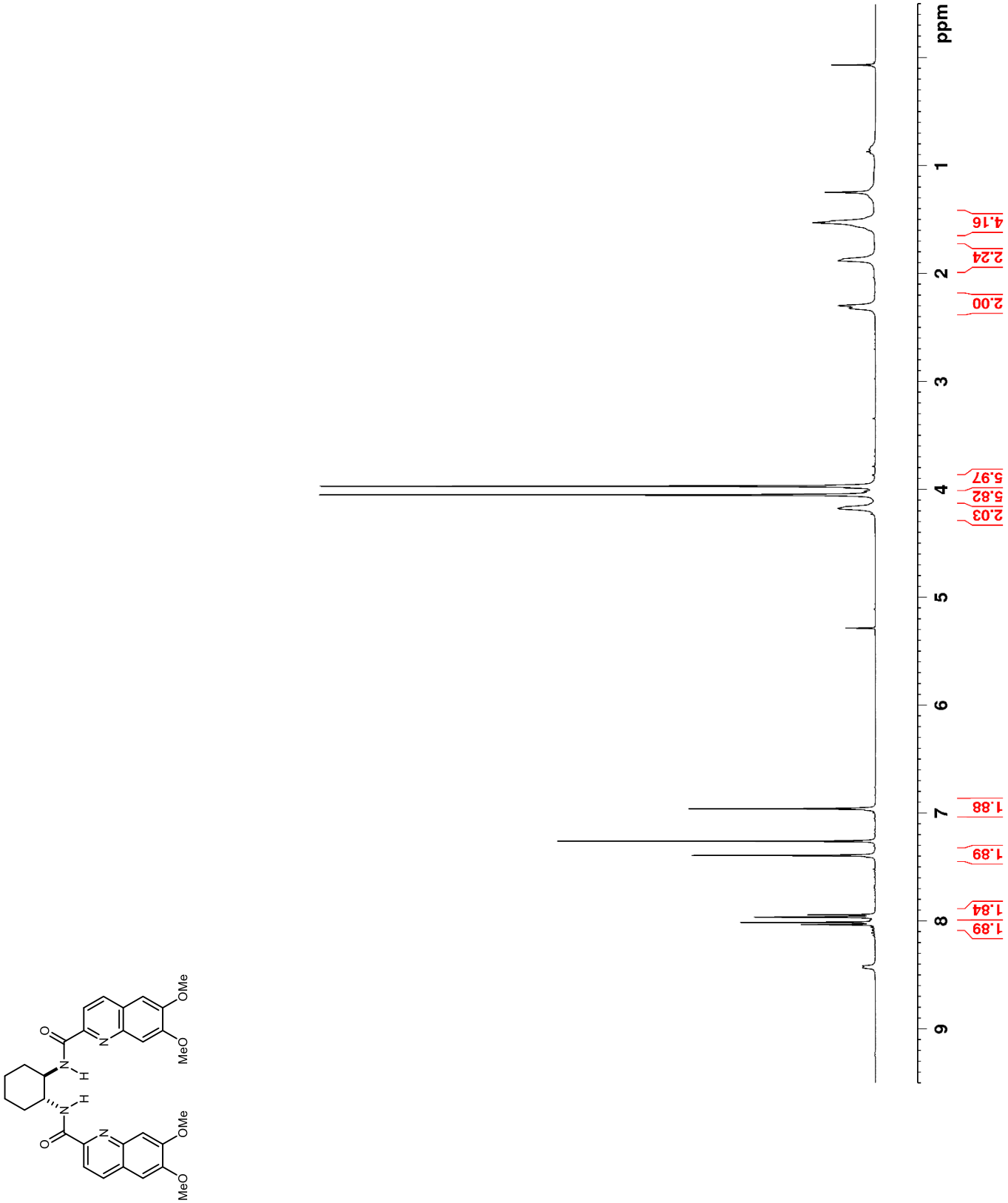

Figure C 57. ^{13}C NMR (100 MHz, $CDCl_3$) of $^{6,7}(OMe)_2$BAMide

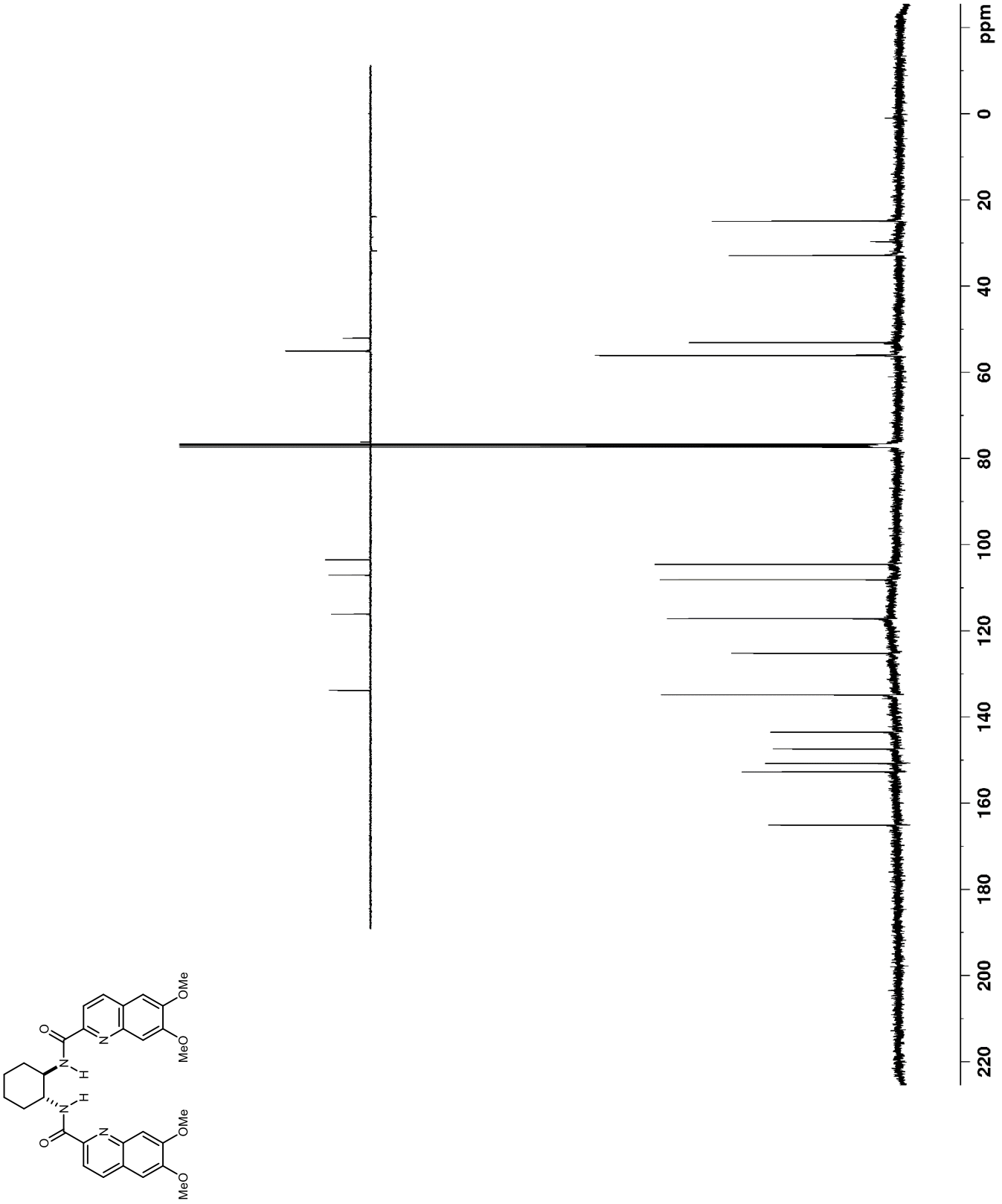

Figure C 58. ^{1}H NMR (500 MHz, $CDCl_3$) of $^{7}MeBAMide$

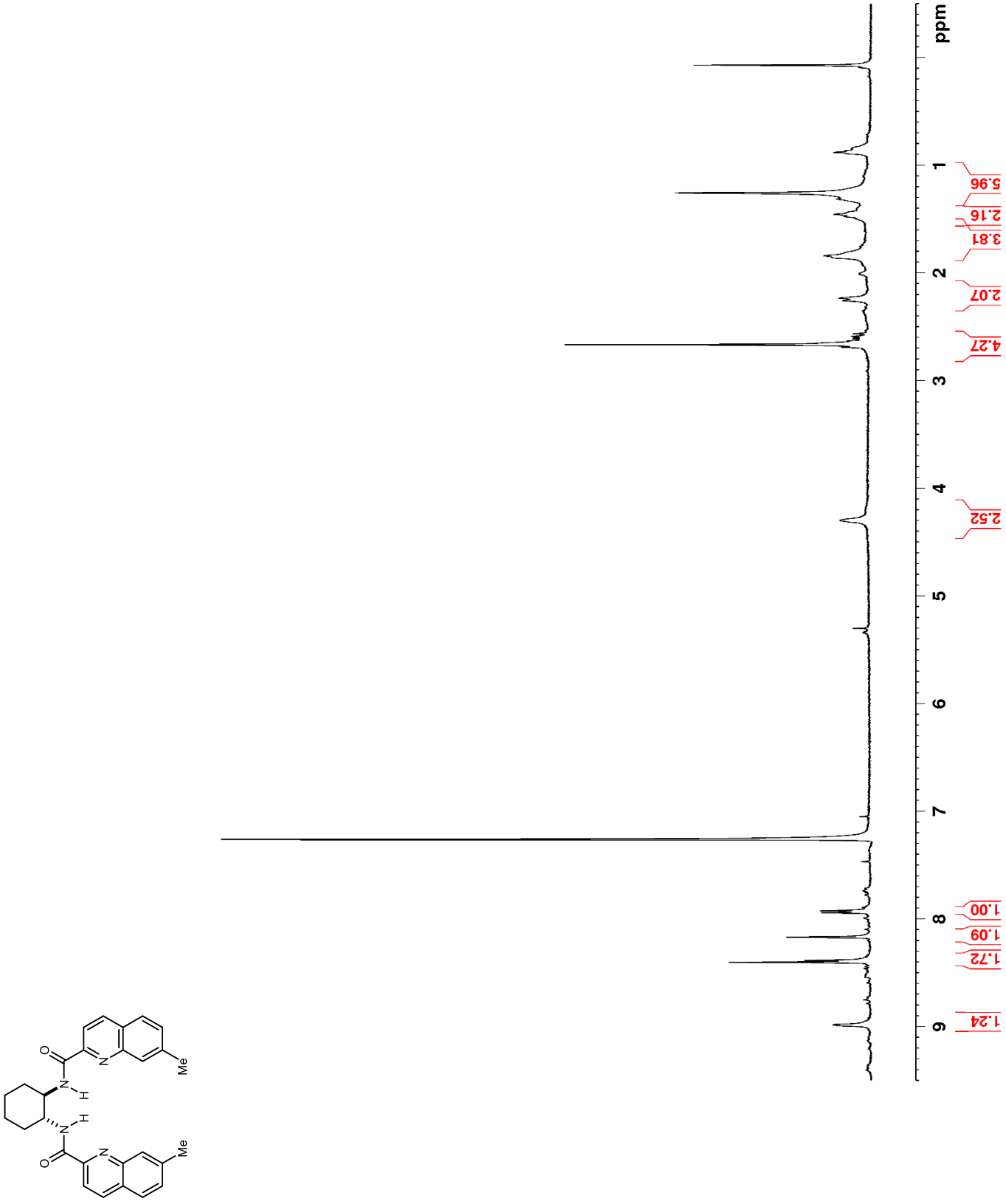

Figure C 59. ^{13}C NMR (125 MHz, $CDCl_3$) of ^{7}MeBAMide

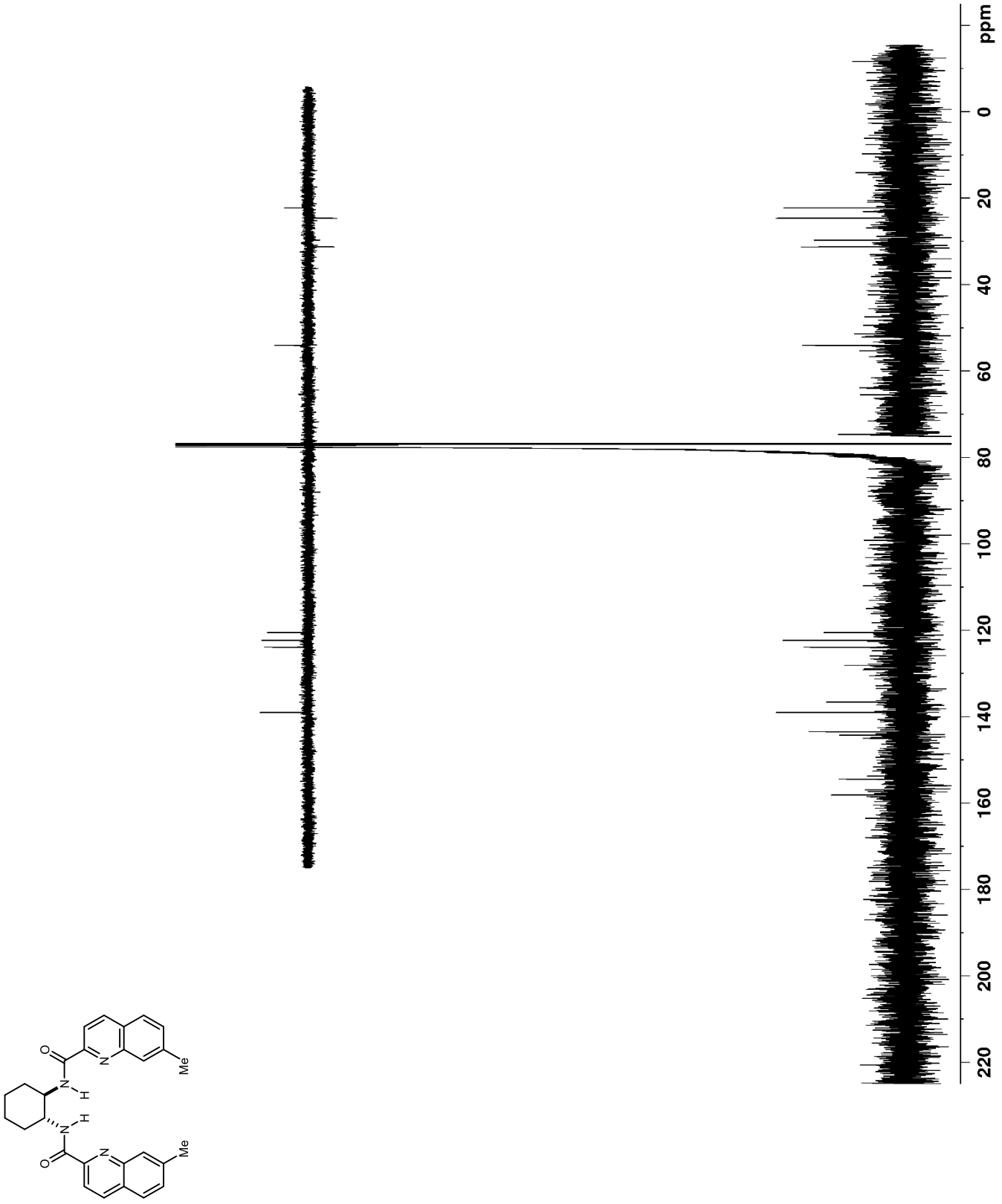

Figure C 60. ^{1}H NMR (400 MHz, $CDCl_3$) of $^{6}CF_3BAMide$

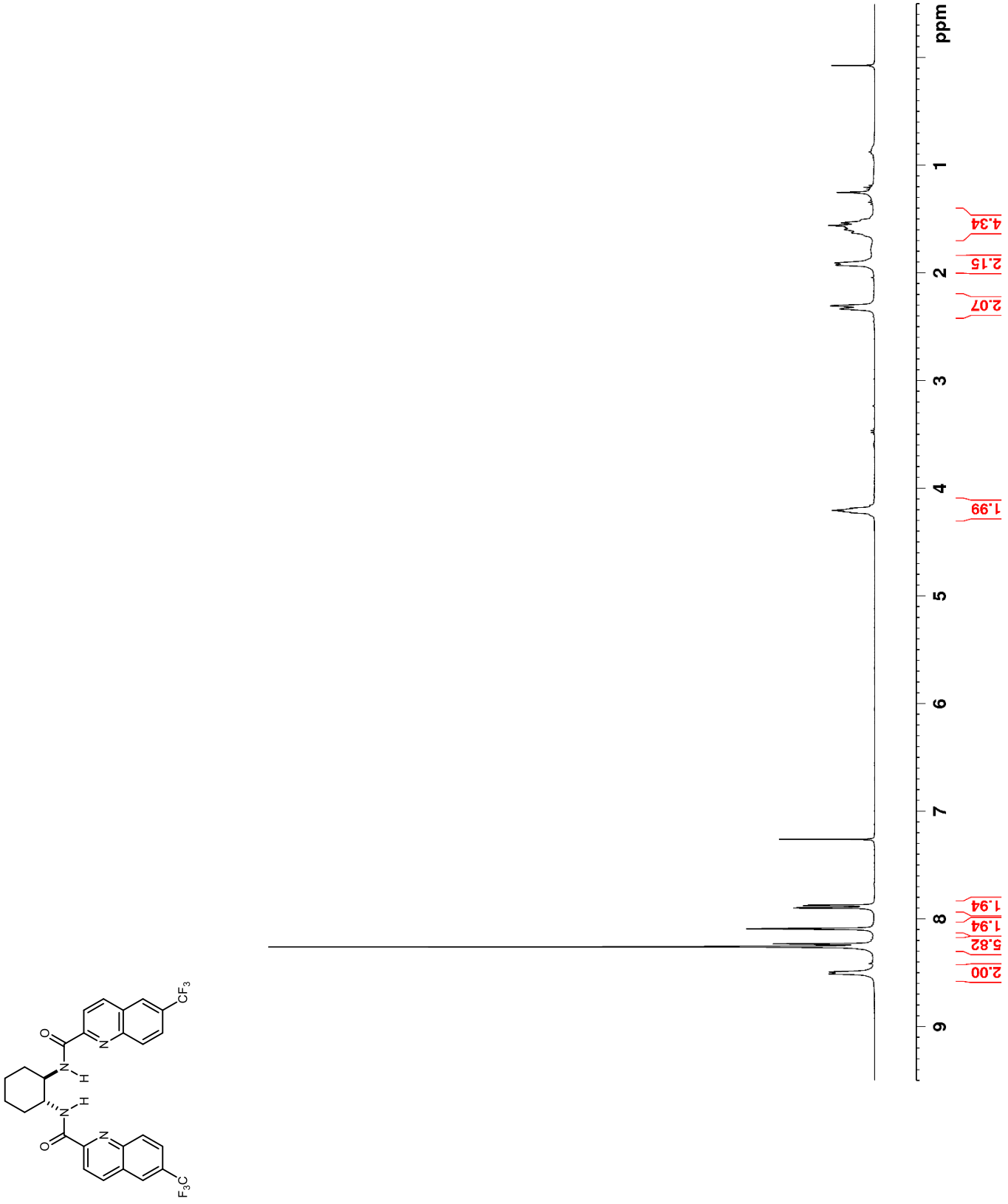

Figure C 61. ^{13}C NMR (100 MHz, $CDCl_3$) of $^{6}CF_3BAMide$

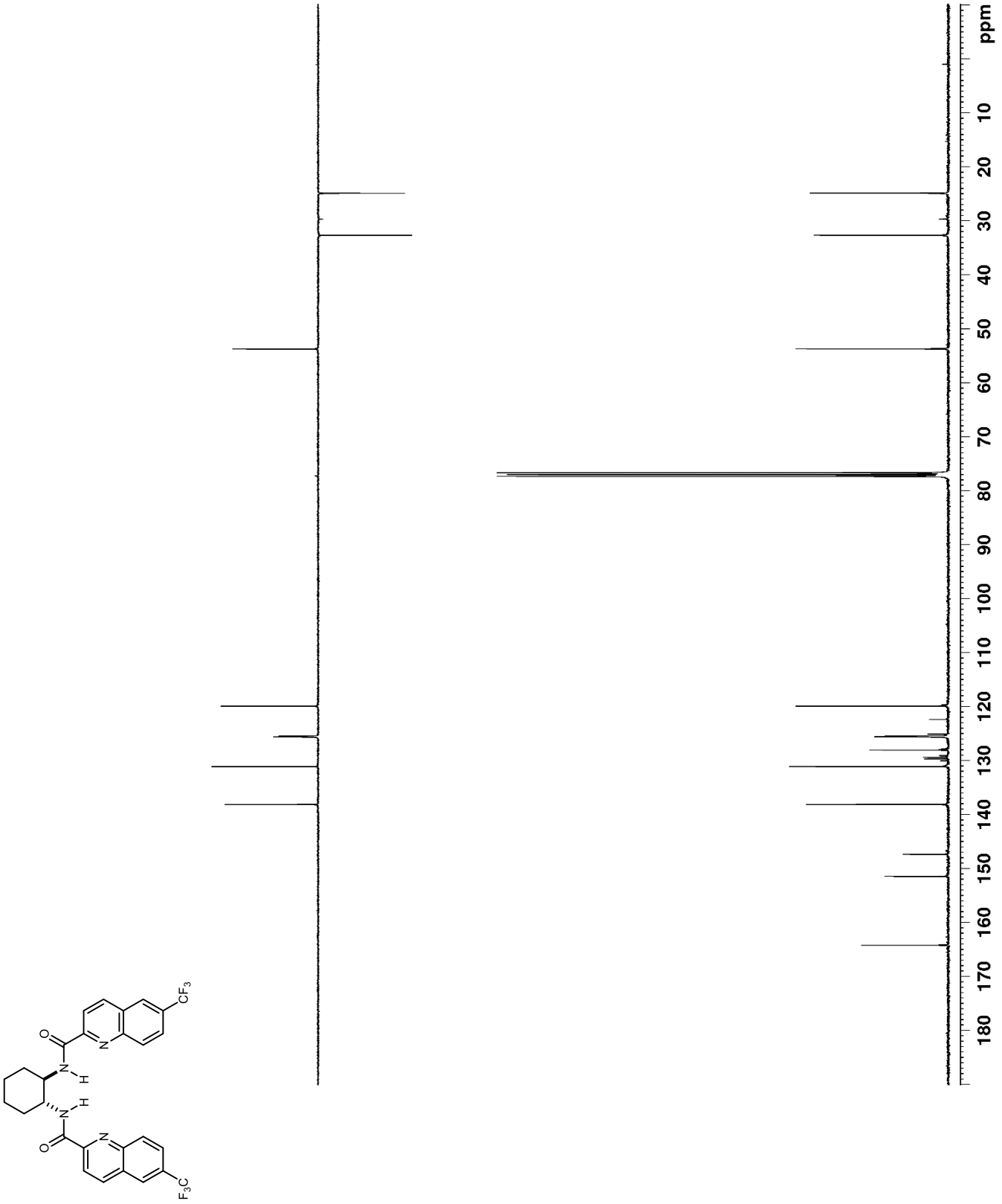

^{19}F NMR (376 MHz, $CDCl_3$) of $^{6}CF_3$BAMide

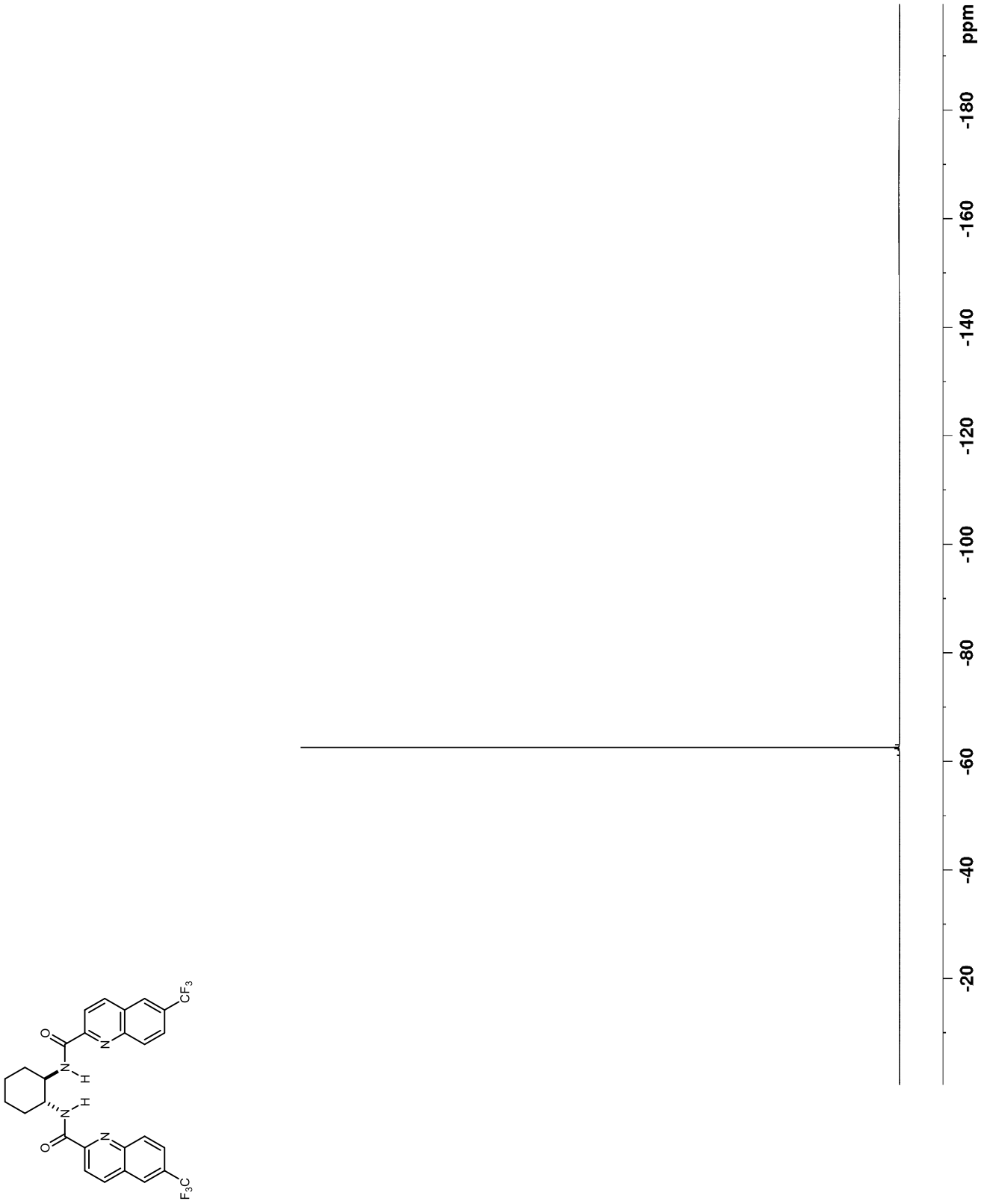

Figure C 62. ^{1}H NMR (400 MHz, $CDCl_3$) of ^{8}OMeBAMide

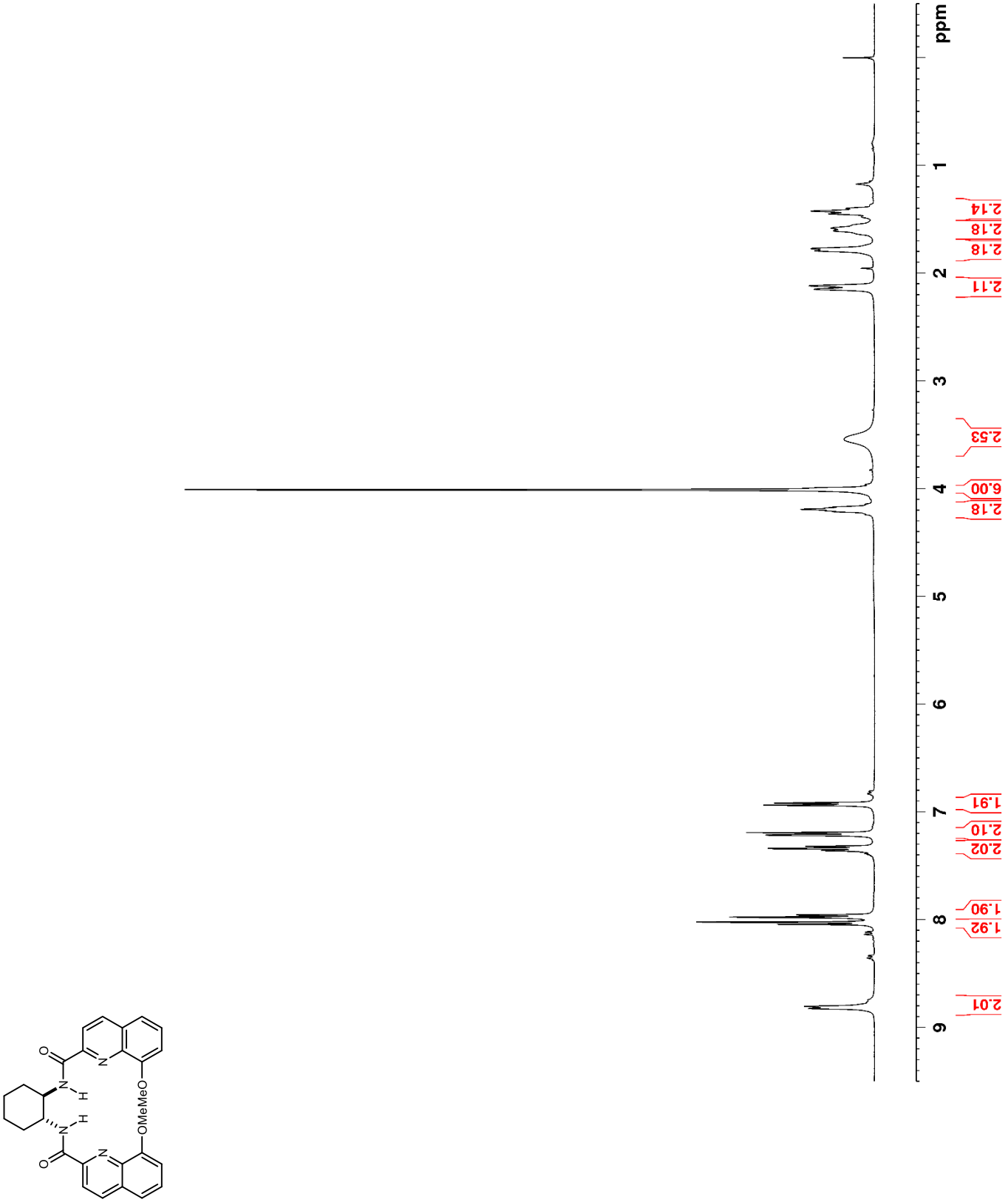

Figure C 63. ^{13}C NMR (100 MHz, $CDCl_3$) of ^{8}OMeBAMide

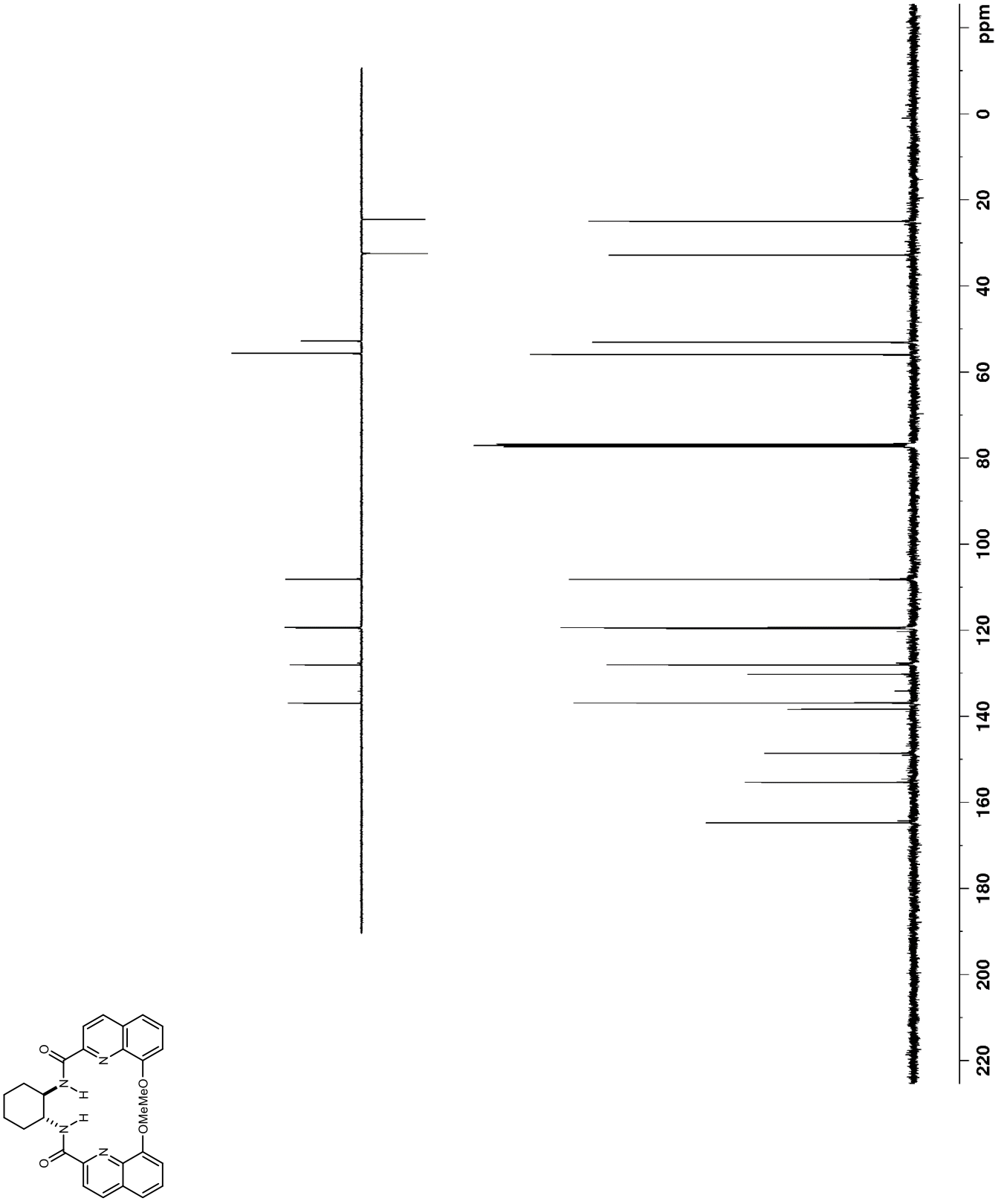

Figure C 64. HPLC trace of **116** (racemic).

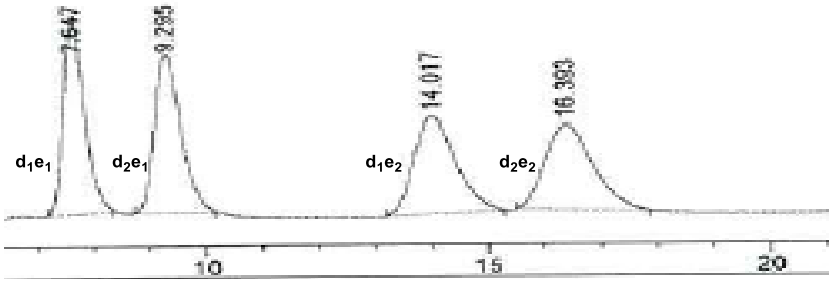

Signal 3: DAD1 D, Sig=230,16 Ref=360,100

Peak #	RetTime [min]	Type	Width [min]	Area [mAU*s]	Height [mAU]	Area %
1	3.029	BV	0.2505	35.87311	1.76933	1.3094
2	3.582	VB	0.0614	30.87045	7.59338	1.1268
3	7.647	BB	0.3870	674.28119	26.31105	24.6123
4	9.295	BB	0.5003	686.33667	20.94360	25.0523
5	14.017	BB	0.7087	651.36517	12.77778	23.7758
6	16.393	BB	0.8060	660.88367	11.23967	24.1233
Totals :				2739.61026	80.63481	

Figure C 65. HPLC trace of **116** using H,^{5}Me-BAM•HOTf (**119**•HOTf).

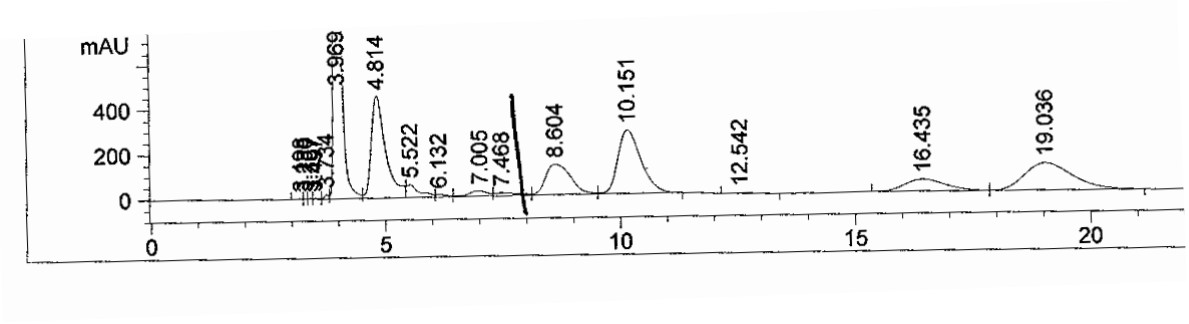

Signal 3: DAD1 D, Sig=230,16 Ref=360,100

Peak #	RetTime [min]	Type	Width [min]	Area [mAU*s]	Height [mAU]	Area %
1	3.198	VV	0.1055	38.23270	4.77273	0.0646
2	3.280	VV	0.0711	21.37368	4.21793	0.0361
3	3.397	VV	0.0799	28.56626	5.21899	0.0483
4	3.497	VV	0.1041	45.27382	5.99604	0.0765
5	3.734	VV	0.0949	124.18613	18.83722	0.2098
6	3.969	VV	0.1703	1.99166e4	1840.18604	33.6406
7	4.814	VV	0.3147	9707.15137	455.35931	16.3961
8	5.522	VV	0.2610	1098.03418	56.92599	1.8547
9	6.132	VV	0.2123	177.28487	11.59710	0.2994
10	7.005	VV	0.3910	677.40808	23.17565	1.1442
11	7.468	VV	0.4473	463.60703	13.47889	0.7831
12	8.604	VV	0.6046	5085.43018	136.50438	8.5897
13	10.151	VB	0.5233	9726.00977	284.17102	16.4280
14	12.542	PP	0.4836	113.47866	3.68185	0.1917
15	16.435	BV	0.9319	3254.18628	53.78373	5.4966
16	19.036	VB	1.0942	8727.22266	121.76282	14.7409
Totals :				5.92040e4	3039.66969	

Figure C 66. HPLC trace of **116** using PBAM•HOTf (**17**•HOTf).

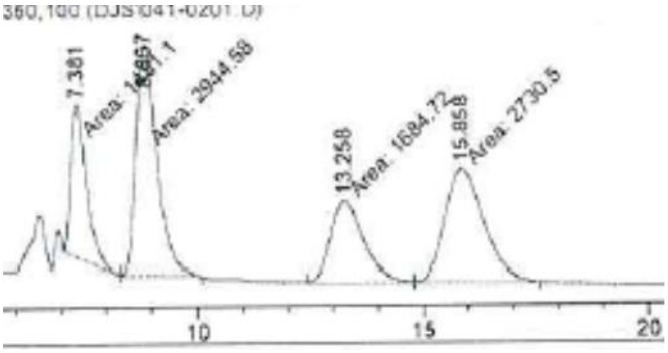

Signal 3: DAD1 D, Sig=230,16 Ref=360,100

Peak #	RetTime [min]	Type	Width [min]	Area [mAU*s]	Height [mAU]	Area %
1	7.381	MM	0.3972	1481.09668	62.15004	16.7528
2	8.867	MM	0.5246	2944.58325	93.55013	33.3064
3	13.258	MM	0.8566	1684.71826	32.77962	19.0560
4	15.858	MM	0.9999	2730.50439	45.51123	30.8849
Totals :				8840.90259	233.99101	

Figure C 67. HPLC trace of **116** using H,^{3}Quin-BAM•HOTf (**120**•HOTf).

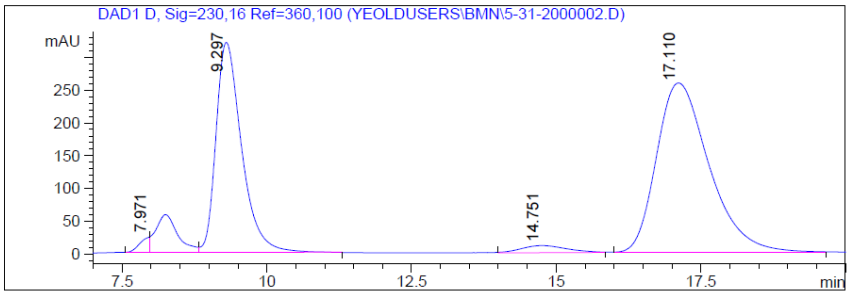

Signal 1: DAD1 D, Sig=230,16 Ref=360,100

Peak #	RT [min]	Width [min]	Area	Area %
1	7.971	0.195	280.599	0.98
2	8.247	0.441	1528.900	5.36
3	9.297	0.514	9877.588	34.64
4	14.751	0.910	599.109	2.10
5	17.110	1.049	16230.839	56.92

Figure C 68. HPLC trace of **116** using H,Quinox-BAM•HOTf (**121**•HOTf).[160]

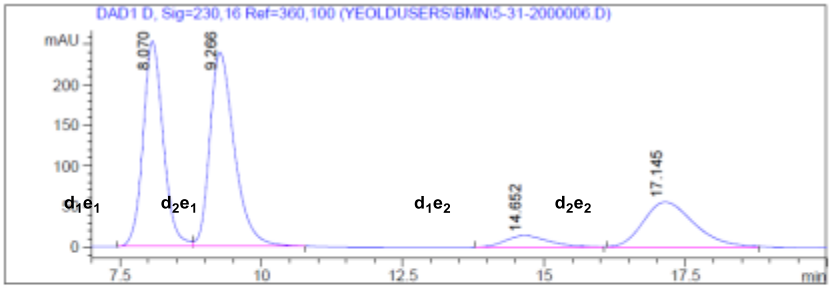

Signal 1: DAD1 D, Sig=230,16 Ref=360,100

Peak #	RT [min]	Width [min]	Area	Area %
1	8.070	0.415	6290.466	35.41
2	9.266	0.504	7234.778	40.72
3	14.652	0.925	784.186	4.41
4	17.145	1.039	3457.315	19.46

Figure C 69. HPLC trace of **116** using H,Quin-BAMide (**123**•HOTf).

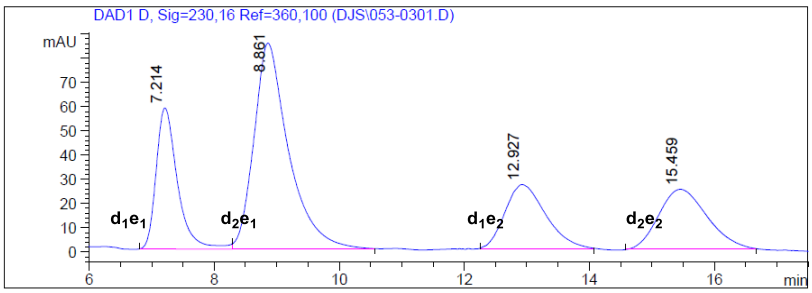

Signal 1: DAD1 D, Sig=230,16 Ref=360,100

Peak #	RT [min]	Width [min]	Area	Area %
1	7.214	0.395	1382.073	19.28
2	8.861	0.644	3283.121	45.81
3	12.927	0.754	1197.117	16.70
4	15.459	0.887	1304.337	18.20

[160] Some chaperone impurity overlaps with the signal at 8.070 and therefore, the er of the minor diastereomers is unable to be determined.

Figure C 70. HPLC trace of **116** using *ent*-H,^{3}Quin-BAM•HOTf (*ent*-**120**•HOTf).

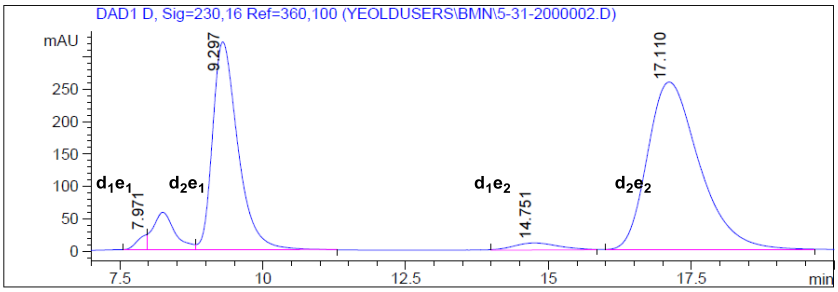

Signal 1: DAD1 D, Sig=230,16 Ref=360,100

Peak #	RT [min]	Width [min]	Area	Area %
1	7.971	0.195	280.599	0.98
2	8.247	0.441	1528.900	5.36
3	9.297	0.514	9877.588	34.64
4	14.751	0.910	599.109	2.10
5	17.110	1.049	16230.839	56.92

Figure C 71. HPLC trace of **60a**

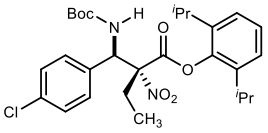

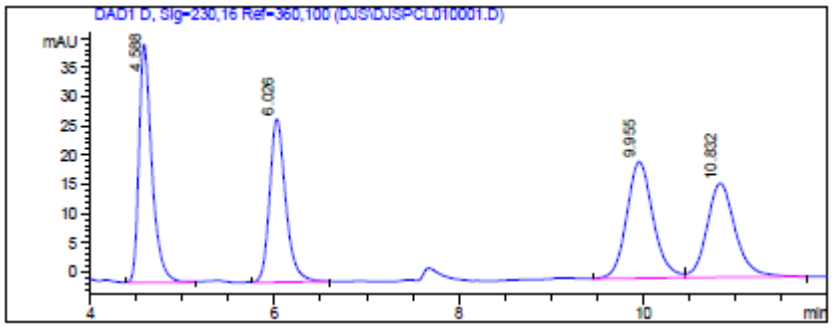

Signal 1: DAD1 D, Sig=230,16 Ref=360,100

Peak #	RT [min]	Width [min]	Area	Area %
1	4.588	0.162	395.129	26.83
2	6.026	0.201	337.076	22.89
3	9.955	0.332	397.256	26.98
4	10.832	0.355	343.018	23.30

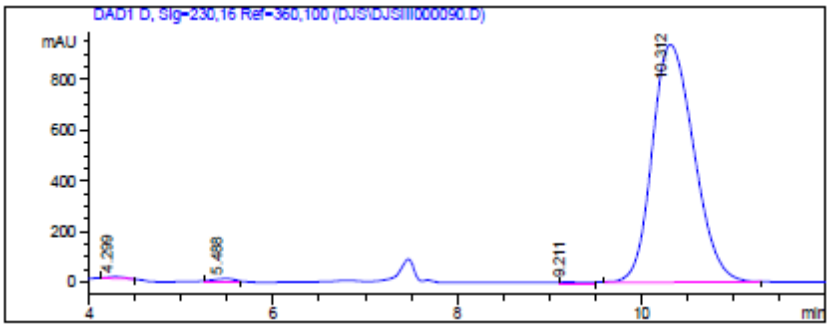

Signal 1: DAD1 D, Sig=230,16 Ref=360,100

Peak #	RT [min]	Width [min]	Area	Area %
1	4.299	0.204	81.523	0.27
2	5.488	0.245	158.381	0.53
3	9.211	0.358	54.916	0.18
4	10.312	0.526	29516.441	99.01

Figure C 72. HPLC trace of **60b**

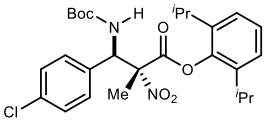

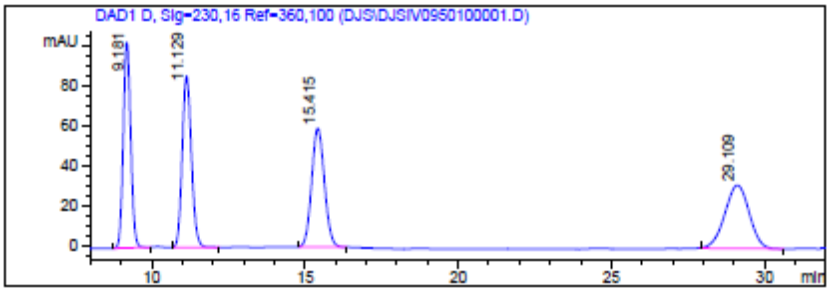

Signal 1: DAD1 D, Sig=230,16 Ref=360,100

Peak #	RT [min]	Width [min]	Area	Area %
1	9.181	0.281	1732.558	24.76
2	11.129	0.350	1797.143	25.68
3	15.415	0.483	1719.821	24.58
4	29.109	0.924	1748.465	24.99

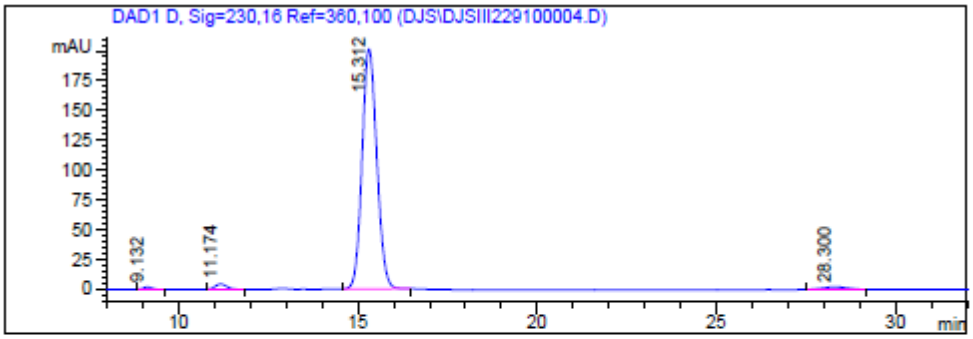

Signal 1: DAD1 D, Sig=230,16 Ref=360,100

Peak #	RT [min]	Width [min]	Area	Area %
1	9.132	0.287	35.665	0.59
2	11.174	0.384	101.297	1.69
3	15.312	0.476	5748.913	95.73
4	28.300	0.881	119.543	1.99

Figure C 73. HPLC trace of **60c**[161]

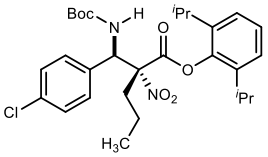

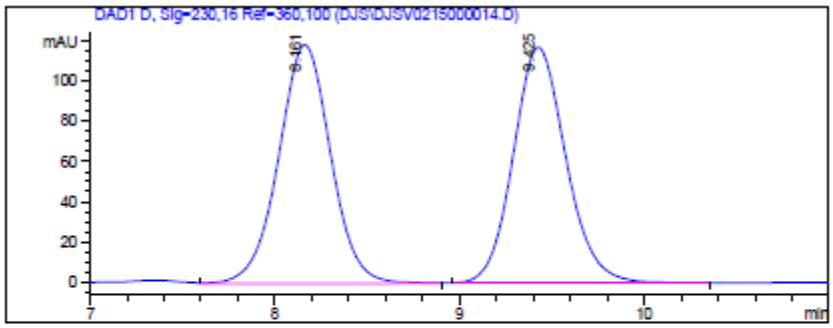

Signal 1: DAD1 D, Sig=230,16 Ref=360,100

Peak #	RT [min]	Width [min]	Area	Area %
1	8.161	0.327	2319.935	49.97
2	9.425	0.331	2322.924	50.03

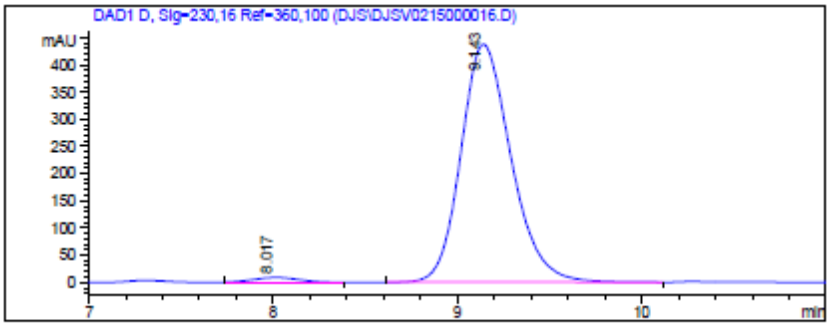

Signal 1: DAD1 D, Sig=230,16 Ref=360,100

Peak #	RT [min]	Width [min]	Area	Area %
1	8.017	0.276	138.022	1.64
2	9.143	0.315	8275.297	98.36

[161] Only 1 diastereomer was seen in the reaction (*rac*-PBAM was used to create the racemate).

Figure C 74. HPLC trace of **60d**

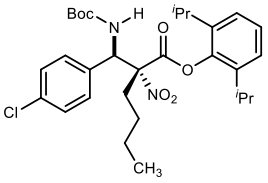

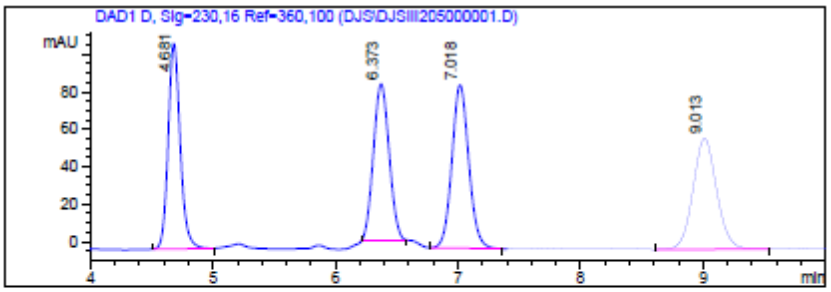

Signal 1: DAD1 D, Sig=230,16 Ref=360,100

Peak #	RT [min]	Width [min]	Area	Area %
1	4.681	0.114	748.867	23.96
2	6.373	0.149	750.449	24.01
3	7.018	0.159	834.238	26.69
4	9.013	0.223	792.462	25.35

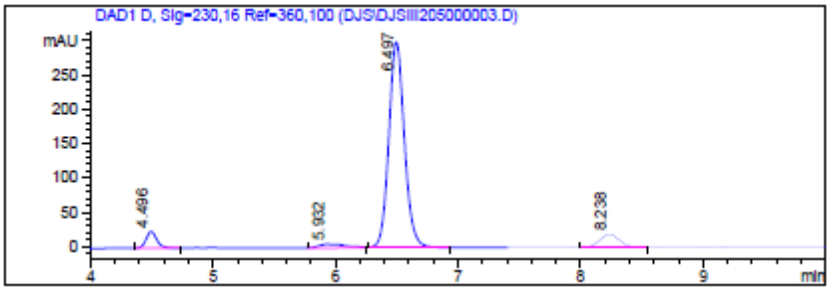

Signal 1: DAD1 D, Sig=230,16 Ref=360,100

Peak #	RT [min]	Width [min]	Area	Area %
1	4.496	0.098	141.020	4.57
2	5.932	0.244	79.387	2.57
3	6.497	0.147	2635.708	85.49
4	8.238	0.195	227.084	7.37

Figure C 75. HPLC trace of **60e**

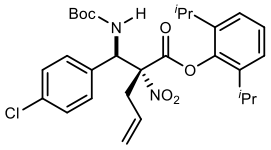

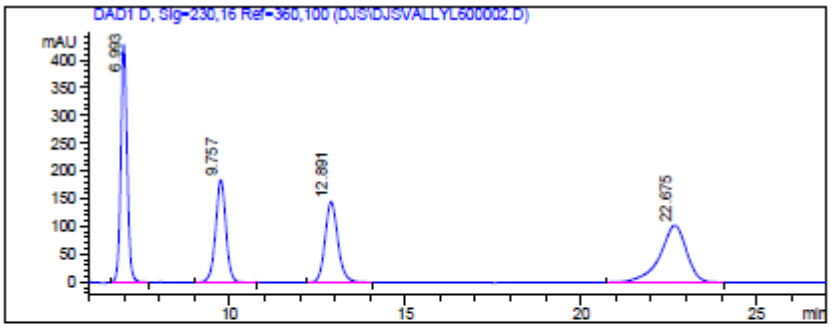

Signal 1: DAD1 D, Sig=230,16 Ref=360,100

Peak #	RT [min]	Width [min]	Area	Area %
1	6.993	0.209	5376.496	29.02
2	9.757	0.343	3800.438	20.51
3	12.891	0.434	3809.733	20.56
4	22.675	0.896	5542.191	29.91

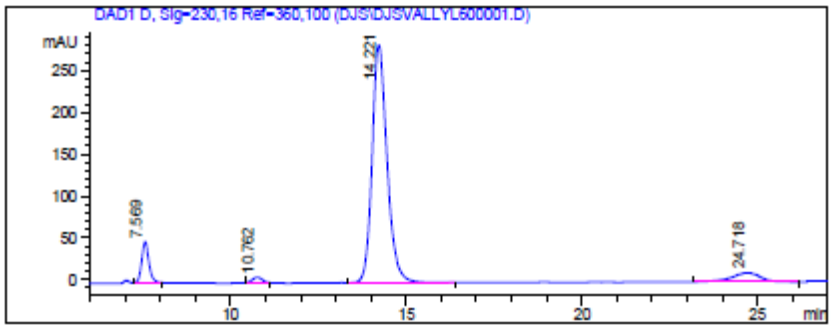

Signal 1: DAD1 D, Sig=230,16 Ref=360,100

Peak #	RT [min]	Width [min]	Area	Area %
1	7.569	0.239	702.016	7.12
2	10.762	0.332	130.307	1.32
3	14.221	0.494	8446.417	85.62
4	24.718	0.907	586.605	5.95

Figure C 76. HPLC trace of **60f**[162]

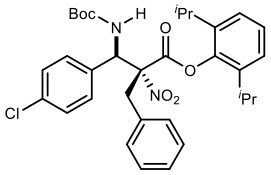

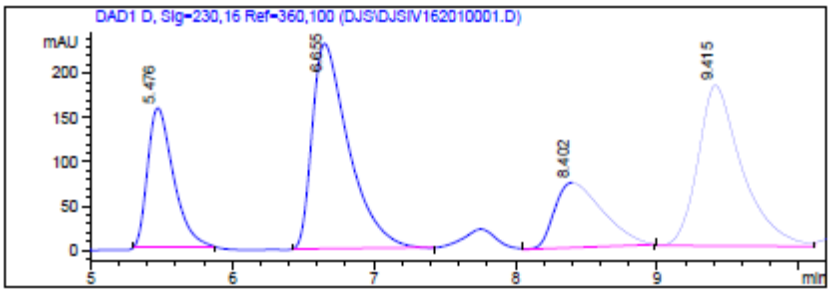

Signal 1: DAD1 D, Sig=230,16 Ref=360,100

Peak #	RT [min]	Width [min]	Area	Area %
1	5.476	0.209	1962.621	16.65
2	6.655	0.299	4154.844	35.24
3	8.402	0.391	1727.450	14.65
4	9.415	0.362	3944.966	33.46

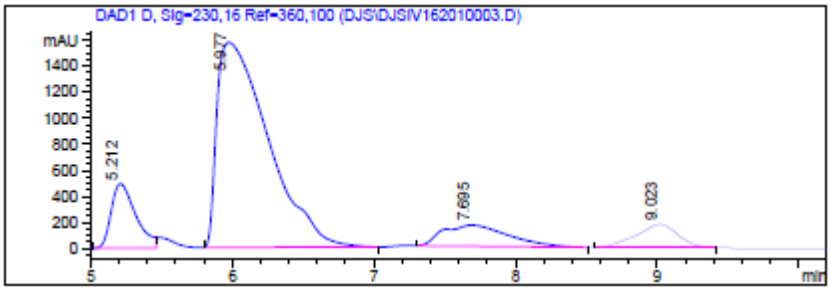

Signal 1: DAD1 D, Sig=230,16 Ref=360,100

Peak #	RT [min]	Width [min]	Area	Area %
1	5.212	0.201	5970.524	10.97
2	5.977	0.420	39633.594	72.81
3	7.695	0.536	5205.801	9.56
4	9.023	0.338	3622.799	6.66

[162] Product was unable to be separated from starting material impurity by column chromatography, however, all 4 peaks of the product are unaffected and visible in the HPLC chromatogram, allowing for determination of selectivity from the reaction.

Figure C 77. HPLC trace of **60g**

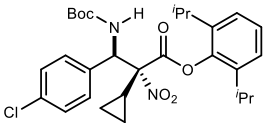

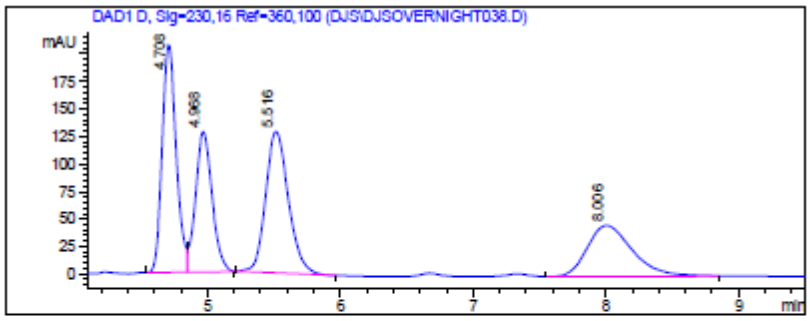

Signal 1: DAD1 D, Sig=230,16 Ref=360,100

Peak #	RT [min]	Width [min]	Area	Area %
1	4.708	0.123	1521.462	29.05
2	4.968	0.144	1101.792	21.04
3	5.516	0.198	1525.785	29.13
4	8.006	0.392	1088.627	20.79

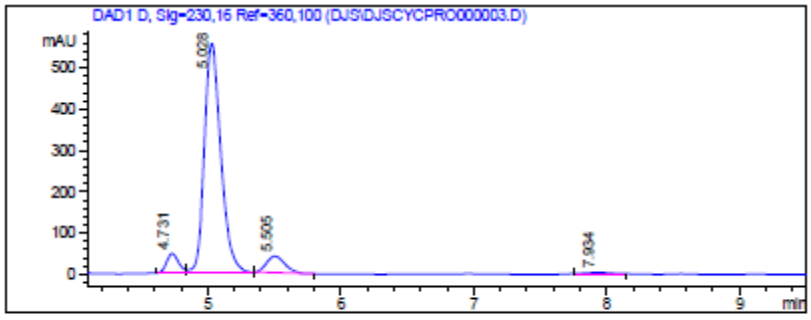

Signal 1: DAD1 D, Sig=230,16 Ref=360,100

Peak #	RT [min]	Width [min]	Area	Area %
1	4.731	0.105	301.070	5.43
2	5.028	0.144	4815.134	86.83
3	5.505	0.162	388.966	7.01
4	7.934	0.226	40.401	0.73

Figure C 78. HPLC trace of **60h**[161]

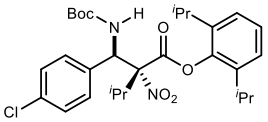

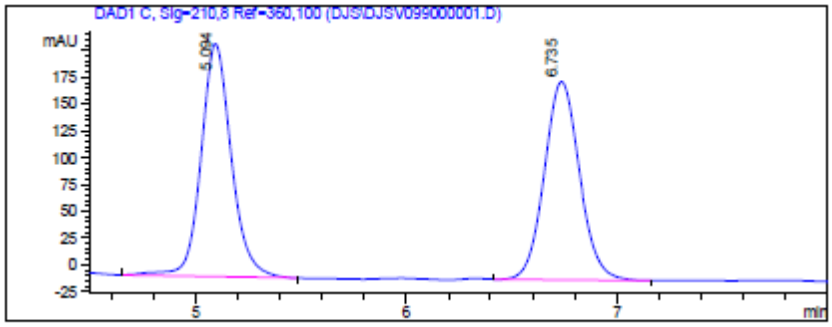

Signal 1: DAD1 C, Sig=210,8 Ref=360,100

Peak #	RT [min]	Width [min]	Area	Area %
1	5.094	0.169	2200.285	50.56
2	6.735	0.194	2151.210	49.44

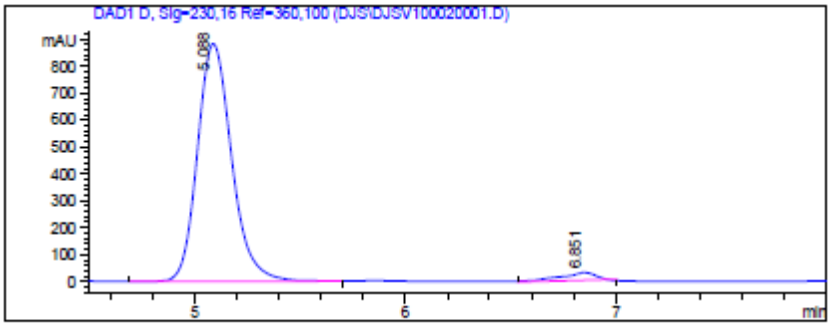

Signal 1: DAD1 D, Sig=230,16 Ref=360,100

Peak #	RT [min]	Width [min]	Area	Area %
1	5.088	0.190	10103.221	96.73
2	6.851	0.205	341.890	3.27

Figure C 79. HPLC trace of **60i**[161]

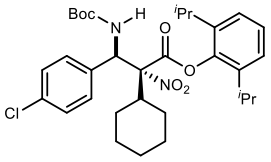

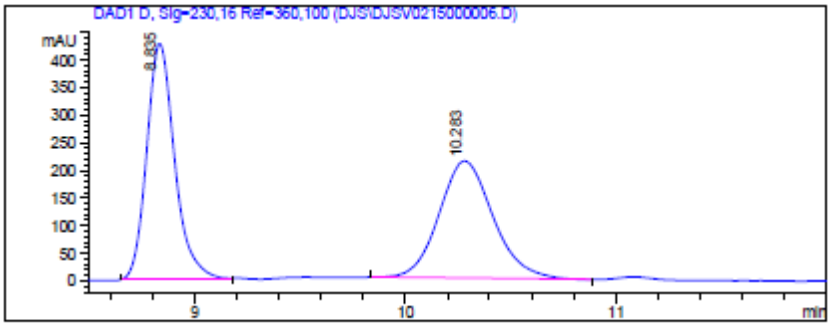

Signal 1: DAD1 D, Sig=230,16 Ref=360,100

Peak #	RT [min]	Width [min]	Area	Area %
1	8.835	0.152	3863.956	50.58
2	10.283	0.298	3795.124	49.42

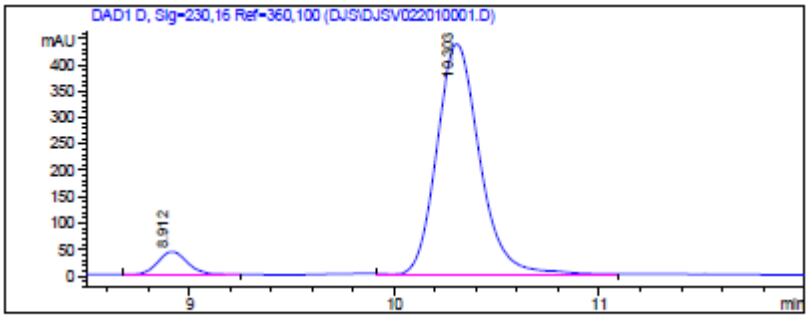

Signal 1: DAD1 D, Sig=230,16 Ref=360,100

Peak #	RT [min]	Width [min]	Area	Area %
1	8.912	0.168	444.695	6.54
2	10.303	0.242	6352.126	93.46

Figure C 80. HPLC trace of **60j**

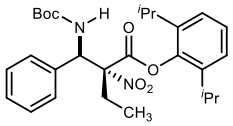

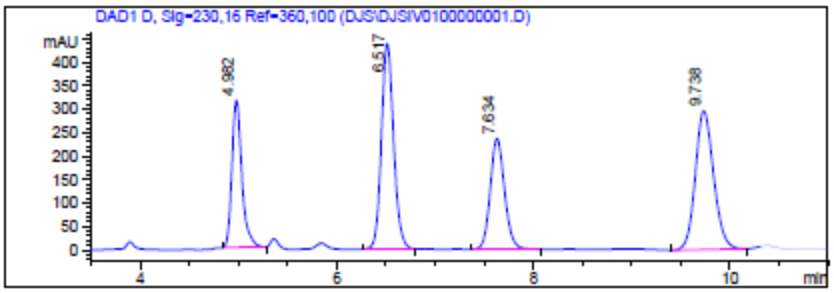

Signal 1: DAD1 D, Sig=230,16 Ref=360,100

Peak #	RT [min]	Width [min]	Area	Area %
1	4.982	0.117	2200.071	18.03
2	6.517	0.144	3777.581	30.95
3	7.634	0.169	2401.456	19.68
4	9.738	0.215	3825.402	31.34

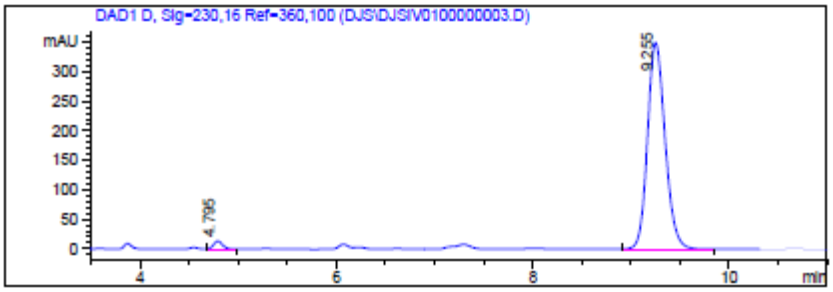

Signal 1: DAD1 D, Sig=230,16 Ref=360,100

Peak #	RT [min]	Width [min]	Area	Area %
1	4.795	0.105	86.437	1.94
2	9.255	0.207	4359.929	98.06

Figure C 81. HPLC trace of **60k**

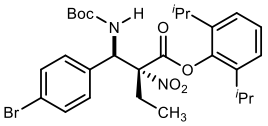

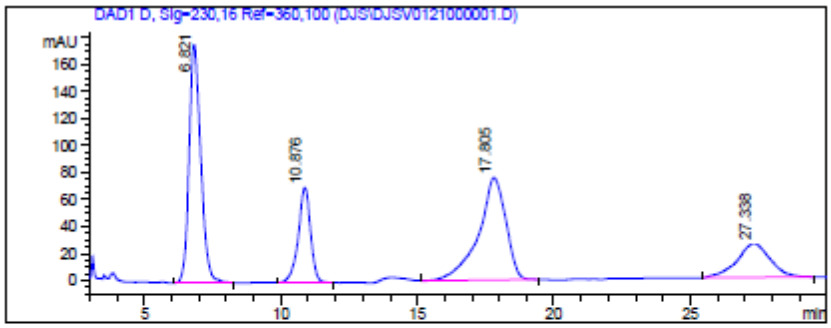

Signal 1: DAD1 D, Sig=230,16 Ref=360,100

Peak #	RT [min]	Width [min]	Area	Area %
1	6.821	0.496	5261.827	35.25
2	10.876	0.525	2226.999	14.92
3	17.805	1.169	5321.908	35.65
4	27.338	1.407	2116.072	14.18

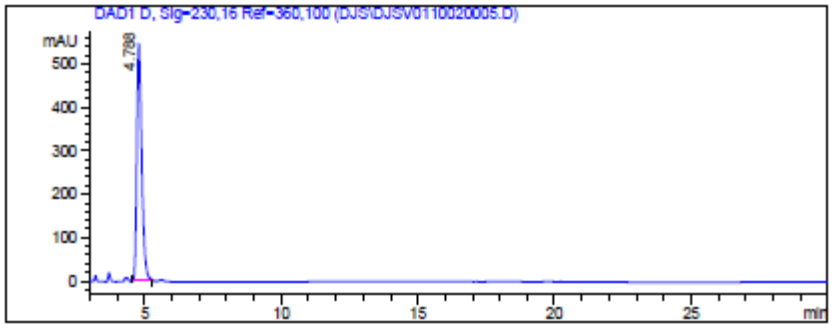

Signal 1: DAD1 D, Sig=230,16 Ref=360,100

Peak #	RT [min]	Width [min]	Area	Area %
1	4.788	0.213	6961.615	100.00

Figure C 82. HPLC trace of **60l**

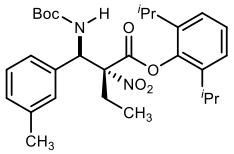

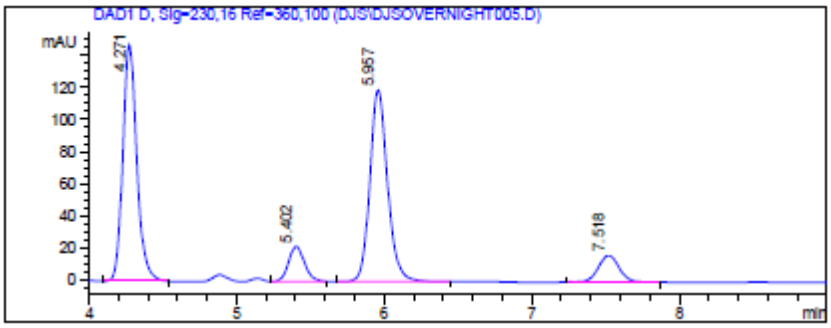

Signal 1: DAD1 D, Sig=230,16 Ref=360,100

Peak #	RT [min]	Width [min]	Area	Area %
1	4.271	0.110	968.415	42.34
2	5.402	0.125	163.946	7.17
3	5.957	0.139	993.731	43.45
4	7.518	0.161	161.119	7.04

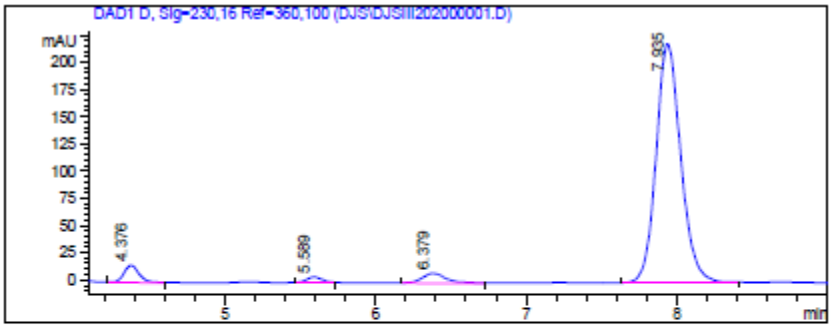

Signal 1: DAD1 D, Sig=230,16 Ref=360,100

Peak #	RT [min]	Width [min]	Area	Area %
1	4.376	0.117	112.484	4.10
2	5.589	0.113	33.327	1.21
3	6.379	0.167	102.333	3.73
4	7.935	0.169	2495.709	90.96

Figure C 83. HPLC trace of **60m**

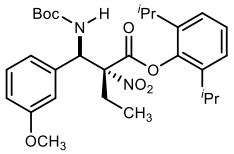

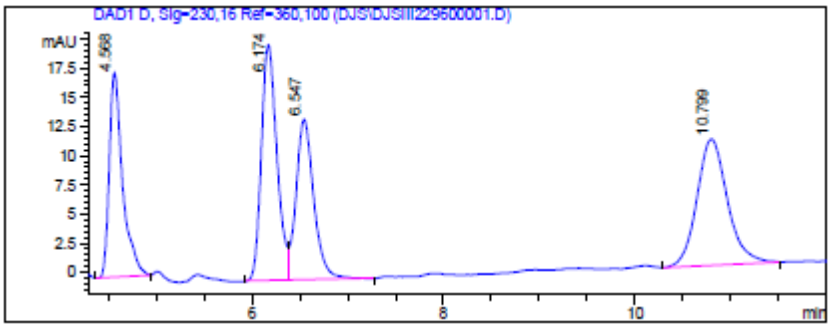

Signal 1: DAD1 D, Sig=230,16 Ref=360,100

Peak #	RT [min]	Width [min]	Area	Area %
1	4.568	0.161	169.195	20.84
2	6.174	0.188	228.191	28.11
3	6.547	0.213	175.896	21.67
4	10.799	0.367	238.463	29.38

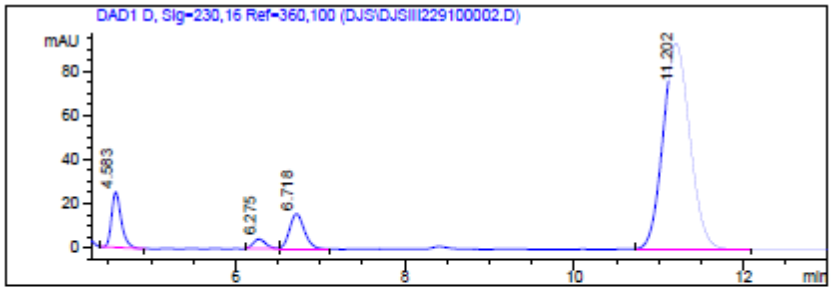

Signal 1: DAD1 D, Sig=230,16 Ref=360,100

Peak #	RT [min]	Width [min]	Area	Area %
1	4.583	0.132	198.499	8.02
2	6.275	0.172	42.868	1.73
3	6.718	0.201	190.837	7.71
4	11.202	0.365	2043.087	82.54

Figure C 84. HPLC trace of **60o**

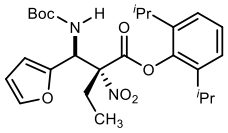

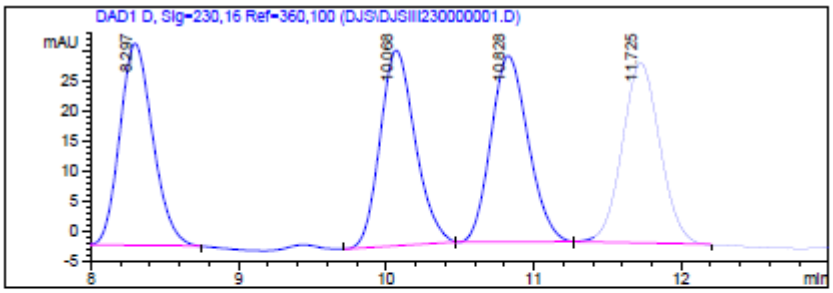

Signal 1: DAD1 D, Sig=230,16 Ref=360,100

Peak #	RT [min]	Width [min]	Area	Area %
1	8.297	0.259	524.881	24.45
2	10.068	0.276	541.293	25.21
3	10.828	0.292	546.372	25.45
4	11.725	0.296	534.589	24.90

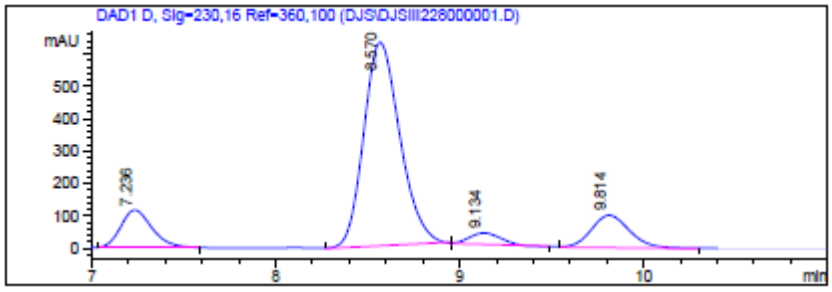

Signal 1: DAD1 D, Sig=230,16 Ref=360,100

Peak #	RT [min]	Width [min]	Area	Area %
1	7.236	0.184	1230.795	10.52
2	8.570	0.227	8585.271	73.42
3	9.134	0.194	405.434	3.47
4	9.814	0.244	1472.593	12.59

Figure C 85, HPLC trace of **60p**

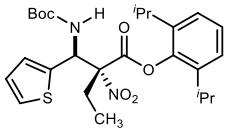

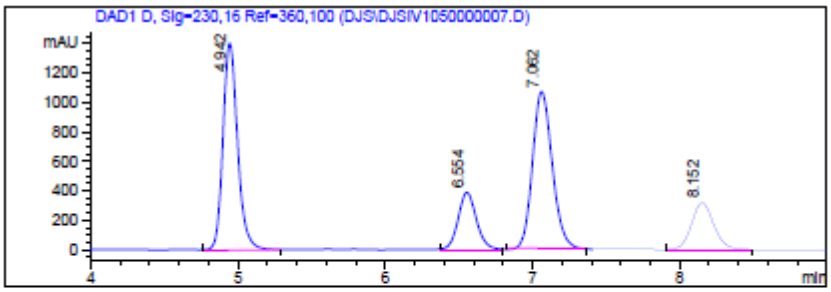

Signal 1: DAD1 D, Sig=230,16 Ref=360,100

Peak #	RT [min]	Width [min]	Area	Area %
1	4.942	0.115	9739.674	37.01
2	6.554	0.144	3361.386	12.77
3	7.062	0.154	9859.396	37.47
4	8.152	0.176	3355.291	12.75

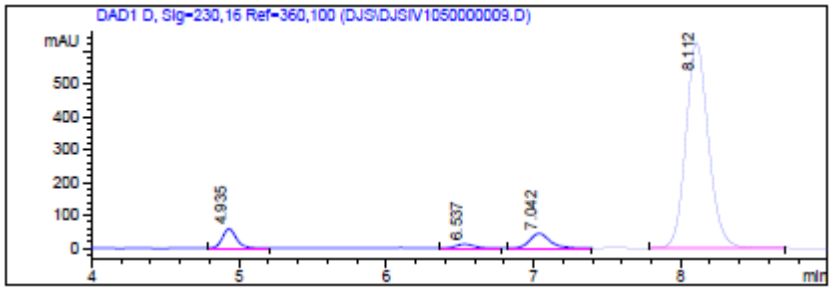

Signal 1: DAD1 D, Sig=230,16 Ref=360,100

Peak #	RT [min]	Width [min]	Area	Area %
1	4.935	0.109	388.537	5.12
2	6.537	0.141	102.983	1.36
3	7.042	0.158	422.848	5.57
4	8.112	0.178	6673.846	87.95

Figure C 86. HPLC trace of **60r**

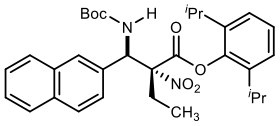

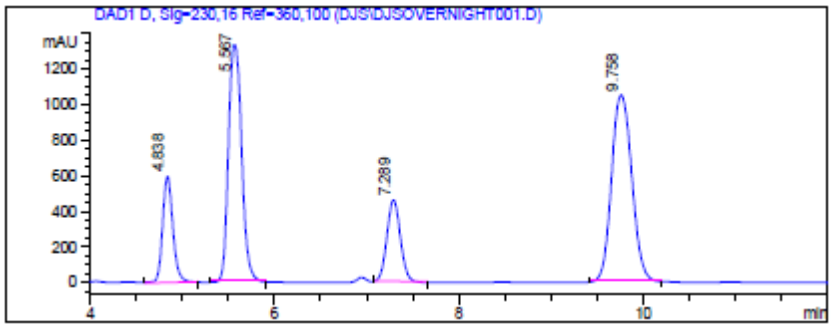

Signal 1: DAD1 D, Sig=230,16 Ref=360,100

Peak #	RT [min]	Width [min]	Area	Area %
1	4.838	0.129	4629.875	12.16
2	5.567	0.164	13068.275	34.32
3	7.289	0.167	4587.058	12.05
4	9.758	0.252	15791.271	41.47

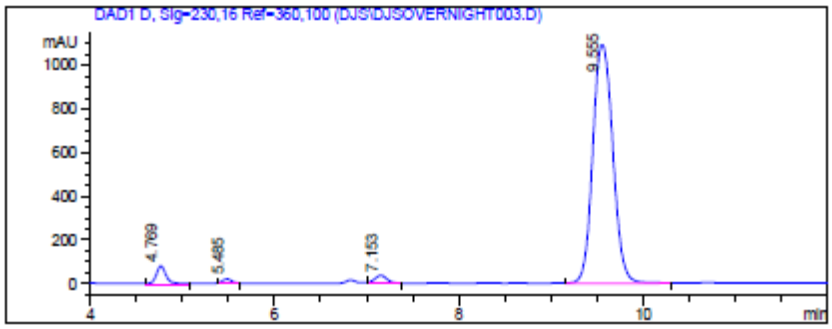

Signal 1: DAD1 D, Sig=230,16 Ref=360,100

Peak #	RT [min]	Width [min]	Area	Area %
1	4.769	0.131	665.205	3.74
2	5.485	0.111	127.301	0.72
3	7.153	0.156	330.658	1.86
4	9.555	0.254	16655.787	93.68

Figure C 87. HPLC trace of **60s**

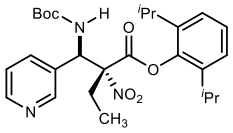

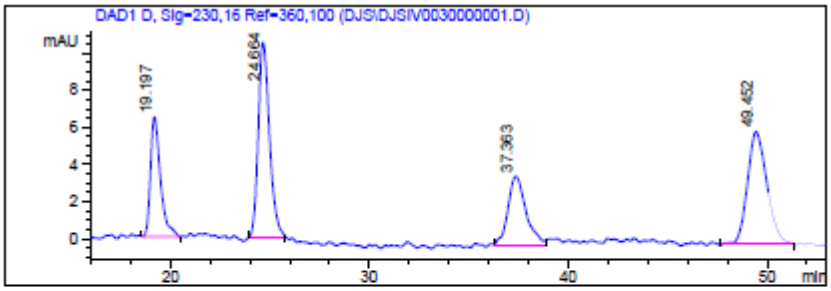

Signal 1: DAD1 D, Sig=230,16 Ref=360,100

Peak #	RT [min]	Width [min]	Area	Area %
1	19.197	0.579	224.281	17.49
2	24.664	0.655	413.658	32.26
3	37.363	1.042	231.462	18.05
4	49.452	1.131	412.803	32.19

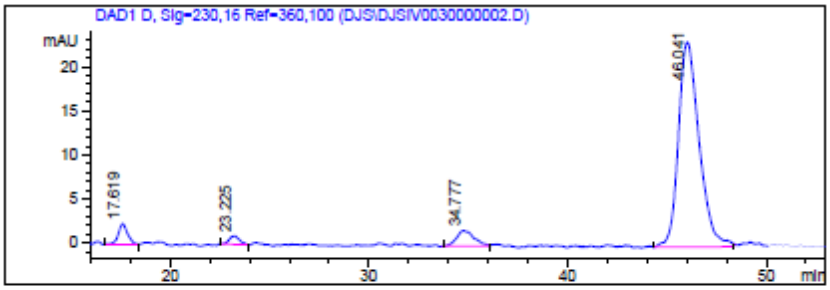

Signal 1: DAD1 D, Sig=230,16 Ref=360,100

Peak #	RT [min]	Width [min]	Area	Area %
1	17.619	0.526	73.799	3.86
2	23.225	0.620	34.850	1.82
3	34.777	1.028	107.879	5.65
4	46.041	1.214	1693.910	88.67

Figure C 88. HPLC trace of **60t**

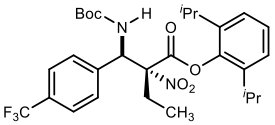

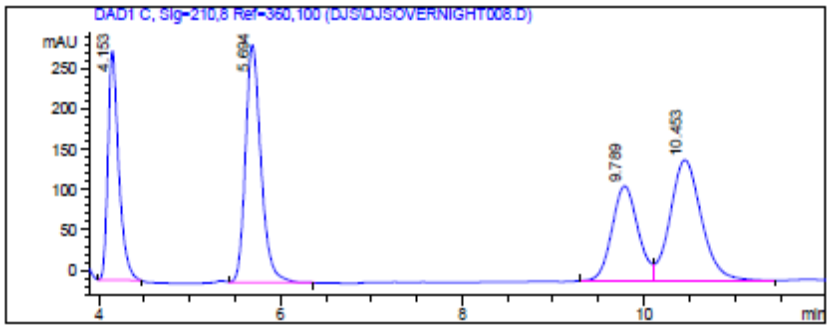

Signal 1: DAD1 C, Sig=210,8 Ref=360,100

Peak #	RT [min]	Width [min]	Area	Area %
1	4.153	0.138	2345.768	19.89
2	5.694	0.198	3497.544	29.65
3	9.789	0.332	2347.997	19.91
4	10.453	0.400	3604.464	30.56

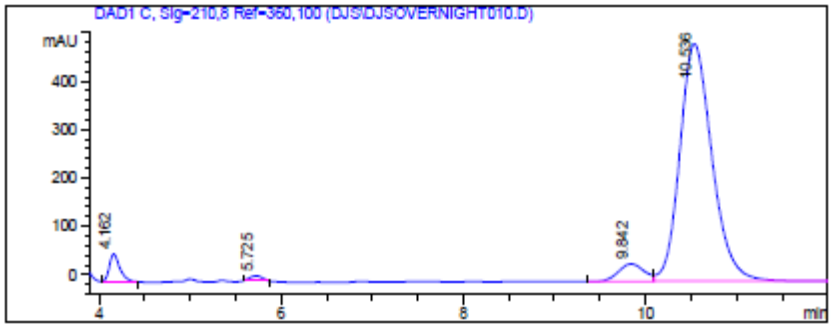

Signal 1: DAD1 C, Sig=210,8 Ref=360,100

Peak #	RT [min]	Width [min]	Area	Area %
1	4.162	0.131	451.034	3.40
2	5.725	0.148	82.500	0.62
3	9.842	0.325	702.720	5.29
4	10.536	0.410	12035.822	90.69

Figure C 89. HPLC trace of **60u**[162]

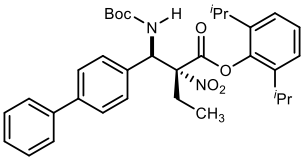

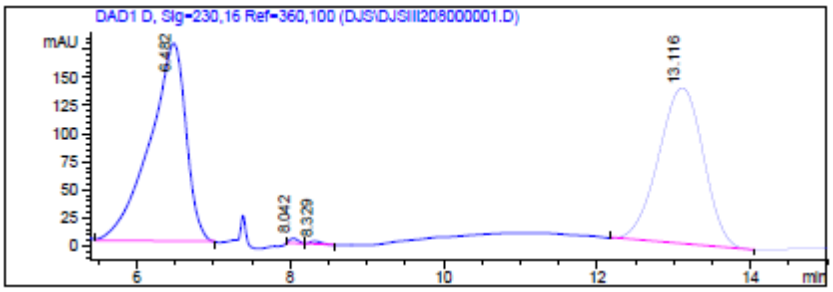

Signal 1: DAD1 D, Sig=230,16 Ref=360,100

Peak #	RT [min]	Width [min]	Area	Area %
1	6.482	0.552	5814.730	50.68
2	8.042	0.126	33.470	0.29
3	8.329	0.166	23.753	0.21
4	13.116	0.675	5602.249	48.82

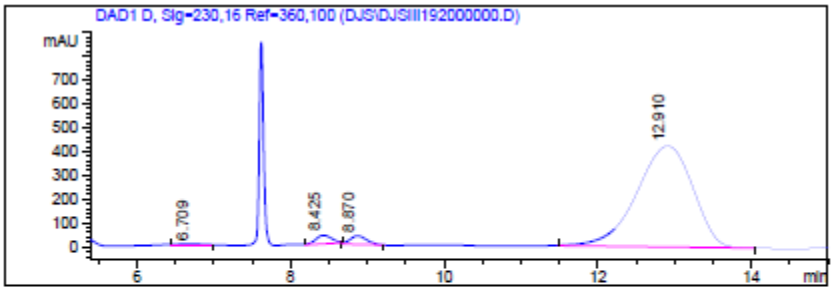

Signal 1: DAD1 D, Sig=230,16 Ref=360,100

Peak #	RT [min]	Width [min]	Area	Area %
1	6.709	0.347	97.340	0.43
2	8.425	0.245	539.446	2.37
3	8.870	0.251	539.384	2.37
4	12.910	0.848	21578.768	94.83

Figure C 90. HPLC trace of **74**

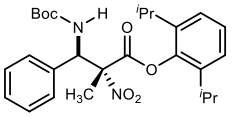

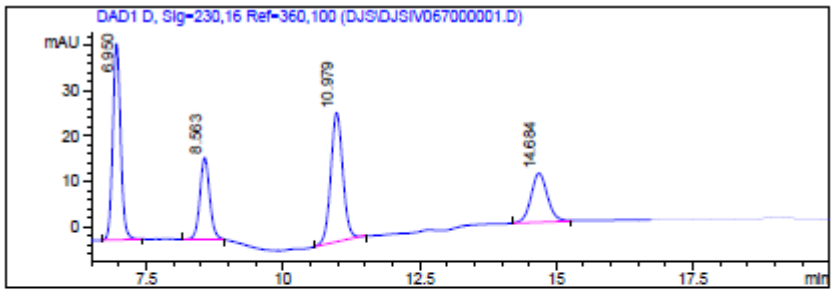

Signal 1: DAD1 D, Sig=230,16 Ref=360,100

Peak #	RT [min]	Width [min]	Area	Area %
1	6.950	0.167	432.810	32.75
2	8.563	0.209	226.393	17.13
3	10.979	0.255	435.921	32.99
4	14.684	0.350	226.234	17.12

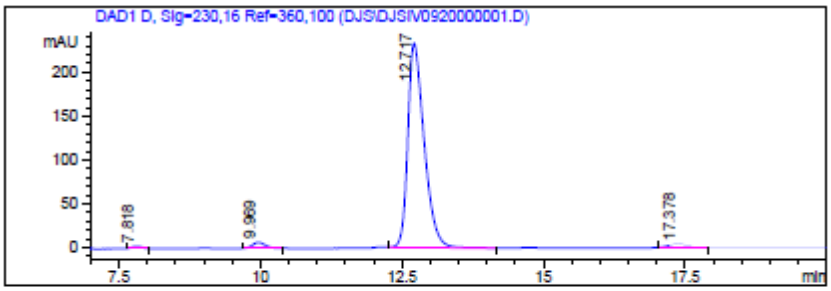

Signal 1: DAD1 D, Sig=230,16 Ref=360,100

Peak #	RT [min]	Width [min]	Area	Area %
1	7.818	0.196	29.793	0.60
2	9.969	0.259	103.128	2.09
3	12.717	0.336	4694.535	95.31
4	17.378	0.388	97.836	1.99

Figure C 91. HPLC trace of **148**

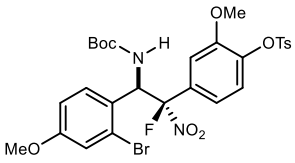

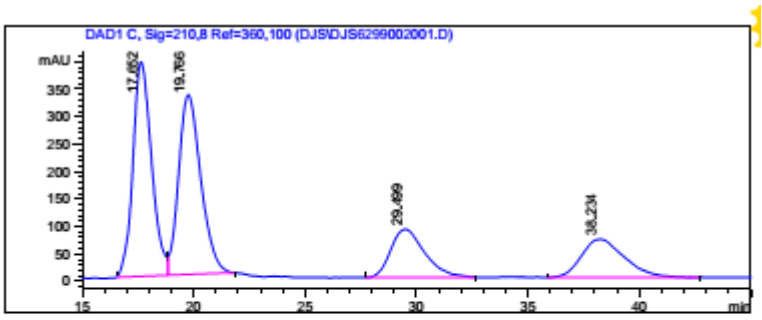

Signal 1: DAD1 C, Sig=210,8 Ref=360,100

Peak #	RT [min]	Width [min]	Area	Area %
1	17.652	0.970	22728.041	35.47
2	19.766	1.154	22667.049	35.37
3	29.499	1.773	9365.907	14.62
4	38.234	2.233	9316.913	14.54

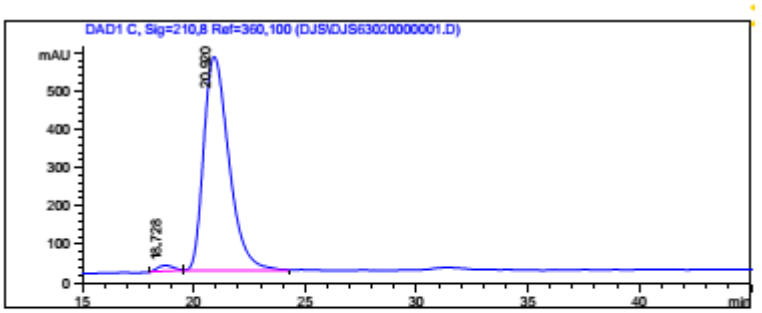

Signal 1: DAD1 C, Sig=210,8 Ref=360,100

Peak #	RT [min]	Width [min]	Area	Area %
1	18.728	0.576	720.180	1.61
2	20.920	1.314	43922.578	98.39

Figure C 92. HPLC trace of **161**

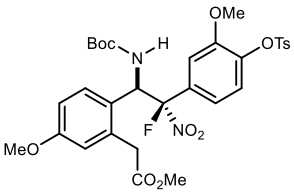

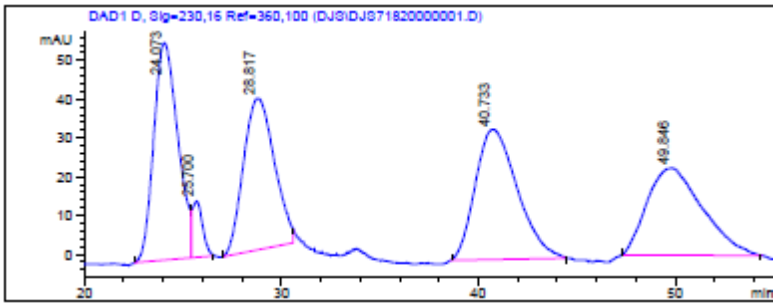

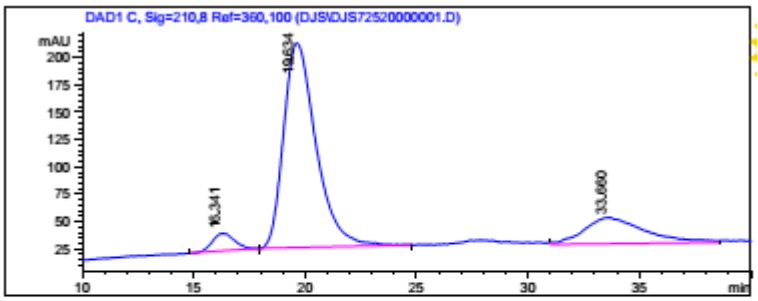

Signal 1: DAD1 C, Sig=210,8 Ref=360,100

Peak #	RT [min]	Width [min]	Area	Area %
1	16.341	1.132	1068.912	4.40
2	19.634	1.684	18818.574	77.47
3	33.660	3.101	4403.132	18.13